EVALUATION OF FOULING IN

A PILOT SCALE MEMBRANE BIOREACTOR

Thesis submitted by

Maneerat Tiranuntakul

BSc (Industrial Chemistry) Srinakarinwirote University (Thailand),

ME (Chemical Engineering) Kasetsart University (Thailand)

March 2011

A thesis submitted in fulfillment of the requirement for the degree of

Doctor of Philosophy

School of Engineering, James Cook University

Queensland, Australia

LIST OF PUBLICATIONS

M. Tiranuntakul, P.A. Schneider and V. Jegatheesan, H.L. Fracchia, “Modelling based design of a pilot-scale membrane bioreactor for combined nutrient removal from domestic wastewater”, Conference proceeding, IWA World Water Congress and Exhibition, Beijing, China. 2006.

M. Tiranuntakul, V. Jegatheesan and P.A. Schneider, “Assessment of critical flux in a pilot scale membrane bioreactor”, Bioresource Technology, Volume 102, Issue 9, May 2011, Pages 5370-5374.

STATEMENT OF ACCESS

I, the undersigned, author of this work, understand that James Cook University will make this thesis available for use within the University Library and, via the Australian Digital Theses network, for use elsewhere.

I understand that, as an unpublished work, a thesis has significant protection under the Copyright Act and;

In consulting this thesis I agree not to copy or closely paraphrase it in whole or in part without the written consent of the author, and to make proper public written acknowledgement for any assistance, which I may have obtained from it.

Beyond this, I do not wish to place any further restriction on access to this work.

_____ _____

Signature Date

STATEMENT OF SOURCES

DECLARATION

I declare that this thesis is my own work and has not been submitted in any form for another degree or diploma at any university or other institution of tertiary education. Information derived from the published or unpublished work of others has been acknowledged in the text and a list of references is given.

_____ _____

Signature Date

ACKNOWLEDGEMENTS

Firstly, I would like to convey my sincere gratitude to my supervisor Dr Philip A. Schneider and my co-supervisor A/Prof. Dr. Jega V. Jegatheesan for their guidance, encouragement, and patience.

Secondly, I would like to thank Thai government, Queensland government, Townsville CitWater, Kubota Company and JCU School of Engineering for the financial support and materials support throughout my entire PhD study.

In regard to my experimental work, my appreciation goes to the following persons:

- Mr. Eric van Prooije and Mr. Cameron Tully, for their assistance related to pilot plant setting-up and commissioning
- Mr. Stuart Peterson and Mr. Curtis Arrowsmith from the JCU workshop for their kind assistance with my experimental apparatus

Finally, I would like to thank my parents, my aunty, my brother and sister for their love and support. And thank you to all my friends in Townsville for their friendship.

DEDICATION

Dedicated to

My parents, my aunty and my husband

ABSTRACT

A 2.4-m^3 pilot plant MBR for wastewater treatment was designed and constructed for membrane biofouling studies. Three categories of membrane fouling study were carried out with this MBR pilot plant in order to obtain a better understanding of MBR performance and fouling. Firstly, critical flux assessment based on various defining concepts and influencing parameters was examined. The results showed small variations of critical flux values obtained from different defining concepts. Decline of critical flux as the step change of fouling air flow rate increased was observed, while step length had no obvious effects on the critical flux. A positive relationship between aeration rate and critical flux is observed, while higher sludge concentration caused lower critical flux. Secondly, fouling mechanisms under different sludge composition and different flux regimes were tested. Under supra-critical flux operation, cake resistance accounted for the main fouling contribution, while pore fouling was marginal in both supra-critical flux and sub-critical flux regimes. EPS carbohydrate in soluble and bound forms has greater impact on both pore fouling and cake fouling than protein. Finally, optimization of the MBR pilot plant was carried out. Based on equivalent permeate yield and equivalent energy consumption for each experimental run, three operational variables showed significant influence in membrane fouling rate increase. They were, in the order of importance, filtration mode > scouring frequency > regular aeration intensity. The optimum operating conditions determined by the proposed methodology were 11 L/m^2.min air intensity with continuous filtration and scouring 24 times per day for the pilot plant MBR.

TABLE OF CONTENTS

LIST OF TABLES

LIST OF FIGURES

CHAPTER 1

INTRODUCTION

1.1 BACKGROUND AND THESIS AIM

Conventional activated sludge process (CASP), using microorganisms for biological degradation of organic pollutions, can be used to treat both municipal and industrial wastewater. However, the CASP requires a large operational area for aeration and sedimentation unit and a big problem of this process is a solid-liquid separation because of excess, bulking and foaming sludge. An advanced technology for wastewater reclamation and reuse that has been widely used to separate pollutants and suspended solids from liquid phase is a membrane bioreactor. Membrane bioreactor (MBR) for wastewater treatment is defined as a combined process between membrane filtration for biomass withholding and biological activated sludge treatment. This membrane bioreactor, integrated bio-treatment and clarification step, is employed in order to replace the clarifier and settlement unit in typical conventional treatment. Organic matter from raw wastewater will be removed by microorganisms and converted into simple products of nitrogen, carbon, hydrogen and oxygen compounds depending on aerobic, anoxic or anaerobic biological process. Then, the final effluent will be separated between suspended solids and clear liquid stream by membrane process. Since late 20^{th} century, MBR technologies have mostly been used in wastewater treatment due to a satisfaction of pathogen removal and permeate clarification. A number of MBR focusing on wastewater research are highly increased about two times from late 1990s to early 2000s (Yang, 2006). Compared

with CASP, submerged membrane technology has many advantages over CASP including: less land requirement (by replacement of clarifier unit), capability to deal with high sludge concentration, giving constant and excellent disinfected treatment. However, MBR process still has a major disadvantage of membrane fouling which affects on operational cost and energy cost for membrane replacement, membrane fouling control and membrane cleaning. Therefore, further studies are required to obtain better understanding of membrane fouling and optimization. Since the MBR system includes living microorganisms, their properties and their relative contributions on membrane fouling problem may also vary with experimental conditions from one study to another. Also, in most previous MBR works, the filtrations were carried out with lab scale and sometimes fed with synthetic sewage which, in fact, has substantially different fouling phenomena compared to those of pilot or full scale operating with real sewage. Based on these considerations, this thesis has the following aims:

- to learn and understand design factors involving in MBR process and to construct a pilot scale submerged MBR for the thesis experiments
- to examine the effect of various parameters such as step heights, step lengths, aerations and sludge concentrations on assessment and variation of critical flux
- to see an interaction among sludge compositions, flux stages of filtration and membrane fouling mechanisms
- to investigate the contribution of controllable parameters including aeration modes, imposed fluxes and scouring frequencies on the membrane

fouling behavior and to evaluate the optimum operational conditions through the these different parameters

1.2 THESIS STRUCTURE

Chapter 2 provides a literature review of various topics related to the submerged membrane bioreactor including background of crossflow filtration, the effect of governing parameters, the filtration behavior, the critical flux concepts as well as measure against membrane fouling.

Chapter 3 describes the details of design and construction of a pilot scale submerged membrane bioreactor as well as details of wastewater treatment performances occurring in the pilot scale submerged MBR.

Chapter 4 presents the determination of membrane critical fluxes using different assessment parameters such as step heights, step lengths and judgment concepts. The effect of aeration and sludge concentration on critical flux is also examined.

Chapter 5 investigates the fouling performances affected by sludge concentration and EPS components in different flux stage operations. The interaction among these parameters and mechanisms of fouling namely pore blocking and cake fouling are also observed.

Chapter 6 studies the possibility of incorporating various aeration modes, flux modes and scouring modes as an alternative approach to improve the filtration performance. The effect of these various operation modes are analyzed and optimized

using analysis of variance (ANOVA) and Sequential Elimination of Level (SEL) technique, respectively.

Chapter 7 summarizes the main finding and provides general conclusion and recommendation for future work.

CHAPTER 2

LITERATURE REVIEW

2.1 MEMBRANE FILTRATION: AN OVERVIEW

There is several membrane systems currently employed. The following sections outline these system details including membrane process, membrane material and categorization, and industrial applications of microfiltration membrane.

2.1.1 Membrane process

Membrane filtration systems have been developed for more than 150 years, starting from preliminary research and development through to modern widespread use (Negaresh 2007). By the 1960s, elements of modern membrane science had been developed and used in laboratories. By the 1980s, the problem of slow permeation rates and the issue of packaging a large membrane surface area into low cost modules had been overcome. One of the principal limitations of membrane processes still remains is selectivity (Baker 2004).

In general a membrane can be defined as a selective barrier between two fluid phases. It has a lateral dimensions much greater than the thickness of the structure through which mass transfer occurs. Membrane processes are driven by differences in a driving force, such as the pressure, concentration, or voltage of the separated phases across the membrane (Pinnua 2004). Membrane-based filtration is becoming a mainstream separation process and competes with conventional processes for various operations, such as separation, concentration and purification of chemical species present in many mixtures. In many cases, membrane separation decreases costs and

offers superior performance, improving a broad range of water quality problems (Stephenson *et al.* 2000). Moreover, membrane-based separation processes are flexible and can be integrated with other techniques.

Membrane filtration can be operated in two configuration extremes: dead-end and crossflow modes as shown in Fig. 2.1. In the dead-end filtration process, feed and permeate streams are pumped in the same flow direction perpendicular to the membrane surface. In contrast, for crossflow filtration mode, only the permeate flow is in the normal direction, while the feed and retentate directions are parallel with the membrane. Compared with the dead-end configuration, crossflow operation gives less cake thickness and lowers fouling resistance due to the occurrence of tangential shear on the membrane surface. Hence, crossflow filtration is more favorable in industrial applications.

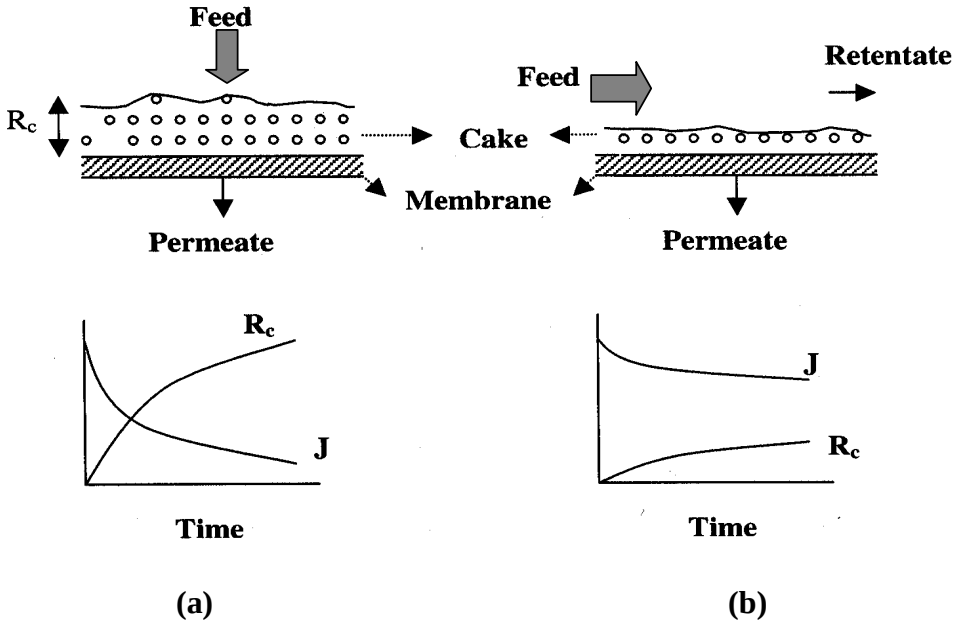

Fig. 2.1 Modes of operation for membrane filtration (Cheryan 1998):

(a) Dead-end; (b) Crossflow

2.1.2 Membrane material and categorization

Proper selection of membrane material is important and can affect the successful use of membrane processes. Ideally, a membrane should have a high permeate flux, high contaminant rejection, durability, good chemical resistance and low cost (Zhou and Smith 2001). Extensive research has been conducted to develop new membrane materials, according to the review by Wiesner and Chellam (1999). A membrane can be homogenous or heterogeneous, symmetric or asymmetric in its structure, and it can consist of organic or inorganic materials. Thickness of membranes can vary between less than 100 nm to more than 10 mm. Membranes can be formed in different physical layouts such as plate and frame, hollow fibre, spiral wound, and tubular modules. A comparison of membrane modules is shown in table 2.1. Two common modules used in MBR are plate and frame, and hollow fibred.

Table 2.1 Comparison of different membrane configurations (Wagner 2001)

Properties	Spiral wound	Tubular		Plate and frame	Hollow wide fibre system	Hollow fine fibre	Ceramic
		high price	low price				
Membrane density	high	Low		average	average	very high	low
Plant investment	low	high	low	high	very high	medium	very high
Tendency to fouling	average	Low		average	Low	very high	medium
Cleanability	good	good		good	Low	non	good
Variable costs	low	high	low	average	average	low	high
Change of membrane only*	no	yes	no	yes	no	no	yes
Flow demand	medium	high	mediu m	medium	High	low	very high
Pre-filter	$\leq$ 50 um no fibres	sieve		$\leq$ 100 um few fibres	$\leq$ 100um few fibres	$\leq$ 5um extreme pretreatment	sieve

Note *: Most tubular and flat sheets are made in such a way that only the membrane is changed, leaving the membrane cartridge unchanged.

One of the most important properties is that of pore size or molecular weight cutoff (MWCO), which specifies the maximum molecular weight of solute to be rejected. Based on membrane pore size, membrane processes can be classified into four categories (see table 2.2): microfiltration (MF), ultrafiltration (UF), nanofiltration (NF) and reverse osmosis (RO).

Table 2.2 Membrane categories based on permeate size (adapted from Osmonics, 1996)

Permeate (µm)	**0.001**	**0.01**	**0.1**	**1**	**10**	**100**	**1000**
Microfiltration			Carbon black		Yeast cells	Human hair	Granular activated carbon
Ultrafiltration			Virus	Bacteria	Flour	Mist	
Nanofiltration	Salts	Sugars	Protein	Paint pigment	Red blood cells	Pin point	Beach sand
Reverse osmosis	Metal Ions		Gelatin	Tobacco smoke			

Microfiltration has a relatively large pore size (around 0.1-10 µm) and commonly used to separate particles greater than 10 µm from other components in a solution or suspension. Minor driving force or a small pressure difference across the membrane is adequate to sustain high flux, since the hydrodynamic flow of the membrane is low. Ultrafiltration has pores in the range of 5 nm to about 50 nm. This membrane resistance and applied pressure is higher than in microfiltration. Nanofiltration has characteristics between UF and RO with a larger membrane pore size than in RO to retain sugars and divalent salts. Reverse osmosis can be considered

as a dewatering technology using a very dense membrane without detectable pores. The hydrodynamic resistance increases from MF, UF, NF to RO.

2.1.3 Industrial applications of microfiltration membranes

Microfiltration is a routinely used for a number of applications. The industrial applications of microfiltration can be summarized as follows: bacteria removal/extended shelf life of milk, clarification of fruit juices, wine and beer, enzyme/cell separation and purification in the pharmaceutical industry, ultra-pure water in the semiconductor industry, metal recovery (separation of colloidal oxides and hydroxides), drinking water and wastewater treatment, etc (Wicaksana 2006).

2.2 DEVELOPMENT OF MBR TECHNOLOGY

The following sections outline the development of MBR technology in wastewater treatment including general wastewater treatment, membrane bioreactors and MBR process configuration.

2.2.1 General wastewater treatment

Wastewater treatment is grouped into primary, secondary, and advanced treatment (Psoch 2005). Primary treatment comprises physical operations, such as screening and sedimentation, to remove floatable and settle-able solids from the water. Secondary treatment uses biological and chemical processes to reduce the load of organic matter in the water. Advanced (tertiary) treatment further aims to remove other constituents like nitrogen and phosphorous (Tchobanoglous and Burton 1991). The conventional activated sludge process, commercialized in 1920 as a continuous process, is the most common biological process able to handle secondary and

advanced treatment (Kraume *et al.* 2004). Although well understood and extensively modeled, the use of activated sludge process is constrained by several factors. Those constraints are, namely, relatively large areas required for the process, large volumes for the aeration and sedimentation tanks, further treatment of excess sludge, required adaptation to fluctuations in loading rates, and frequent problems associated with sludge separation due to bulking and foaming (Le Clech 2002).

2.2.2 Membrane bioreactors (MBR)

An interest in combining membranes with activated sludge processes for wastewater treatment began over 30 years ago (Judd *et al.* 2000). The first time a membrane was combined with biological wastewater treatment was reported by Smith *et al.* (1967). The combination of these two technologies has since led to the development of MBR process, which consists of the presence of a membrane replacing the secondary settling tank in a conventional activated sludge process. A comparison between activated sludge and membrane process is shown in Fig. 2.2.

By using membrane filtration, problems related to poor biomass settling can be eliminated and higher quality of treated water can be achieved, since the biomass is physically retained by the membrane (Muller *et al.* 1995). There are numerous advantages of the MBR technology over conventional biological wastewater treatment process: small footprint, low maintenance, complete solids removal from effluent, easy to scale-up and scale-down by modular extension, and high disinfectant production. For space-restricted areas, such as densely populated urban areas and on-board ships, MBRs are a superior alternative due to its small footprint (Ng and Hermanowics 2004). Because of the above mentioned merits, the application of MBR

has gained vast interest worldwide and over 500 commercial MBR processes in operation worldwide were expected by 200 (Stephenson *et al.* 2000).

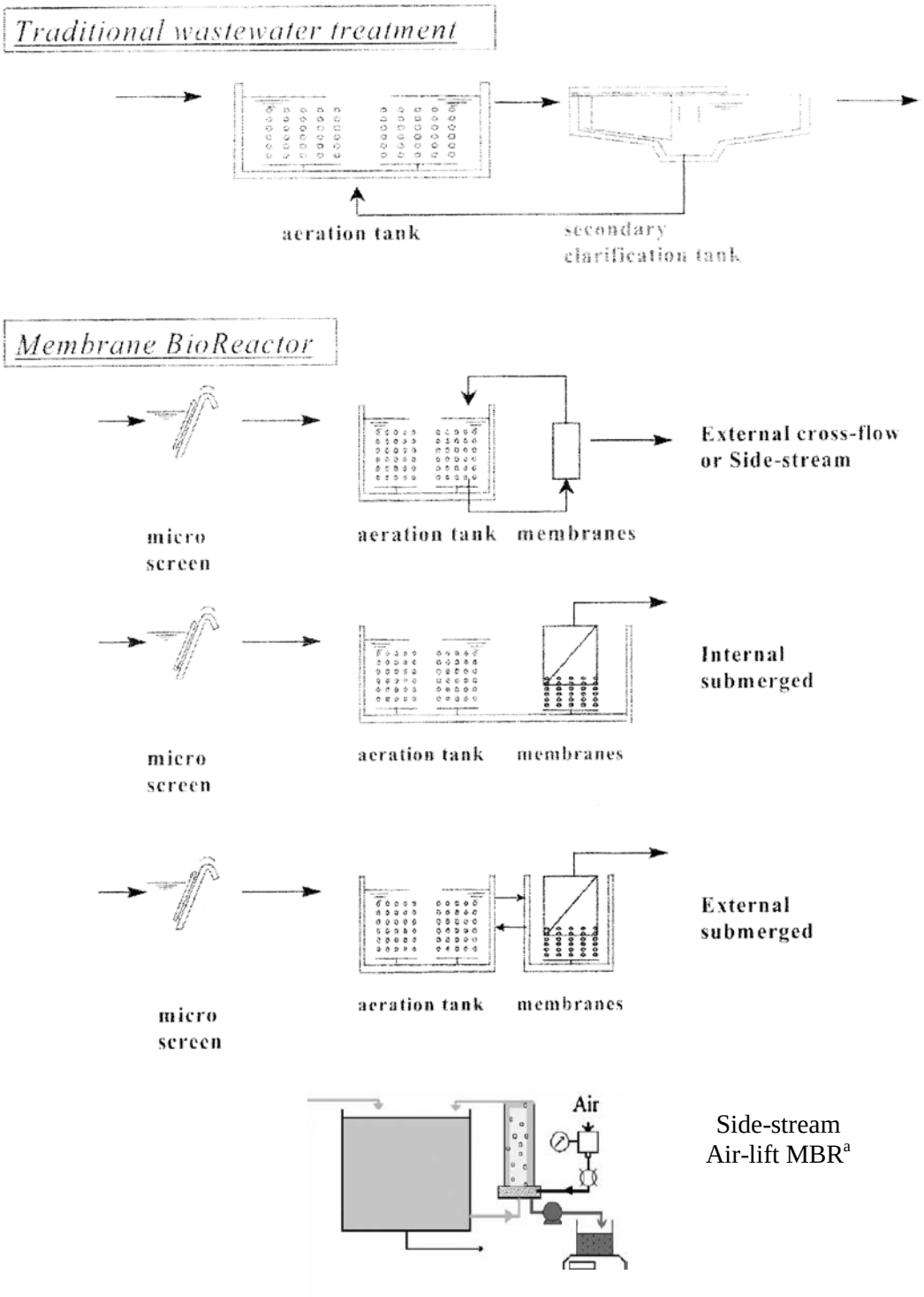

Fig. 2.2 Conventional wastewater treatment and MBR (Lawrence *et al.* 2002; [a]Helan *et al.* 2006)

2.2.3 MBR process configuration

2.2.3.1 Side-stream configuration

For wastewater treatment, the sidestream mode has been applied successfully since the early 1970s. In this configuration (Fig. 2.6), the membrane is placed in a recirculation loop external to the bioreactor. In such a system, the feed is pumped into the membrane module, and part of the feed is withdrawn as permeate, while the other part is forced to flow along the membrane surface. The advantage is a better control of the cake layer build-up resulting in more constant flux. On the other hand, this configuration is a more complex system with high energy consumption. The comparative study performed by Gander *et al.* (2000) showed that the energy consumption for side-stream systems is generally two orders of magnitude higher than for submerged configurations.

2.2.3.2 Submerged configuration

The submerged configuration was introduced at an industrial scale in the mid-1990s. For this configuration, the membrane is directly placed in the aeration tank containing the mixed liquor (Fig. 2.6). The uplifting bubbles generate a scouring effect at the membrane surface and provide oxygen to microorganisms. The advantages of a submerged configuration are simple design, lower energy consumption and high hydraulic efficiencies compared to the sidestream configuration. The submerged configuration membranes are either hollow fibres aligned vertically or horizontally, or flat plates aligned vertically (Fane 2002). Hollow fibre geometry is commercially produced by Zenon and the flat plate is produced by Kubota.

Low flux operation is essential in submerged systems to reduce fouling on the membrane surface. The lower flux involves a larger membrane area resulting in a higher capital cost which is offset by the lower energy demand (Wicaksana *et al.* 2006). As a result, strategies to reduce energy further are important for submerged MBR. For moderate to large scale municipal wastewater treatment, submerged systems are preferable over side-stream configuration due to small footprint and reactor requirement. Even though the submerged type is newer than other, approximately 55% of MBR installations are the submerged type while the remainders are in the side-stream type (Stephenson *et al.* 2000).

2.3 MEMBRANE FOULING

2.3.1 Characterization of membrane fouling

Particle separation and water permeation involve various mass transport steps in the membrane filtration process. Mass transfer can lead to the attachment, accumulation or adsorption of material onto the membrane surface and/or within membrane pores causing an increase in hydraulic resistance over time. This phenomenon is called membrane fouling (Zhou and Smith 2001). Fouling can be classified as (Mulder 2000; Duranceau 2001).

- Crystalline fouling (scaling): deposition of mineral due to the excess of the product being dissolved
- Organic fouling: deposition of dissolved humic acids, oil, grease and lipids
- Particle and colloidal fouling: deposition of clay, particulate humic substances, debris and silica
- Biofouling: adhesion and accumulation of microorganism forming biofilms

Fouling is the key problem in all membrane applications. Fouling changes the pore size and pore size distribution either by deposition of a layer onto the membrane surface or by blockage or partial blockage of the pores (Field *et al.* 1995). Three fouling phenomena were introduced for membrane filtration in general that can be applied to the MBR (Knyazkova and Maynarovich 1999):

- Pore narrowing: when the diameter of particles is smaller than the diameter of pores, particles could enter the pores. As a result, some of the entered particles pass the membrane and some are fouled or adsorbed onto the pore walls and reduce the open cross-section area for flow.
- Pore plugging: for the case when diameters of particles are similar to those of the pores, particles block the pores.
- Cake formation: when diameters of particles are bigger than diameter of pores, particles deposition on the membrane surface and build a cake layer.

2.3.2 Mass transfer in crossflow filtration

Transport phenomena of crossflow filtration are shown in Fig. 2.3, which shows a particle under a number of influences for a vertical plane membrane surface. Particles flow toward the membrane surface by permeate-suction force, while the crossflow forced particles back transport into the bulk by shear-induced migration and diffusion mechanisms (to a lower concentration). If the suction force is higher than other forces, fouling, either gelatinous form or cake form (layer B in Fig. 2.7), will occur on the membrane surface. In the ideal case, only the clean membrane resistance is involved, while, in the real condition, fouling caused by several factors such as concentration polarization, external fouling on the membrane surface, and fouling

inside membrane layer by narrowing and plugging of the pores. Bulk phase is a phase of influent and considered to be less influenced from suction force. Concentration Polarization (CP) is a layer of stagnant solution where the suspension concentration remains higher than the bulk stream concentration due to balance between suction forces and migration/diffusion forces back to the bulk solution.

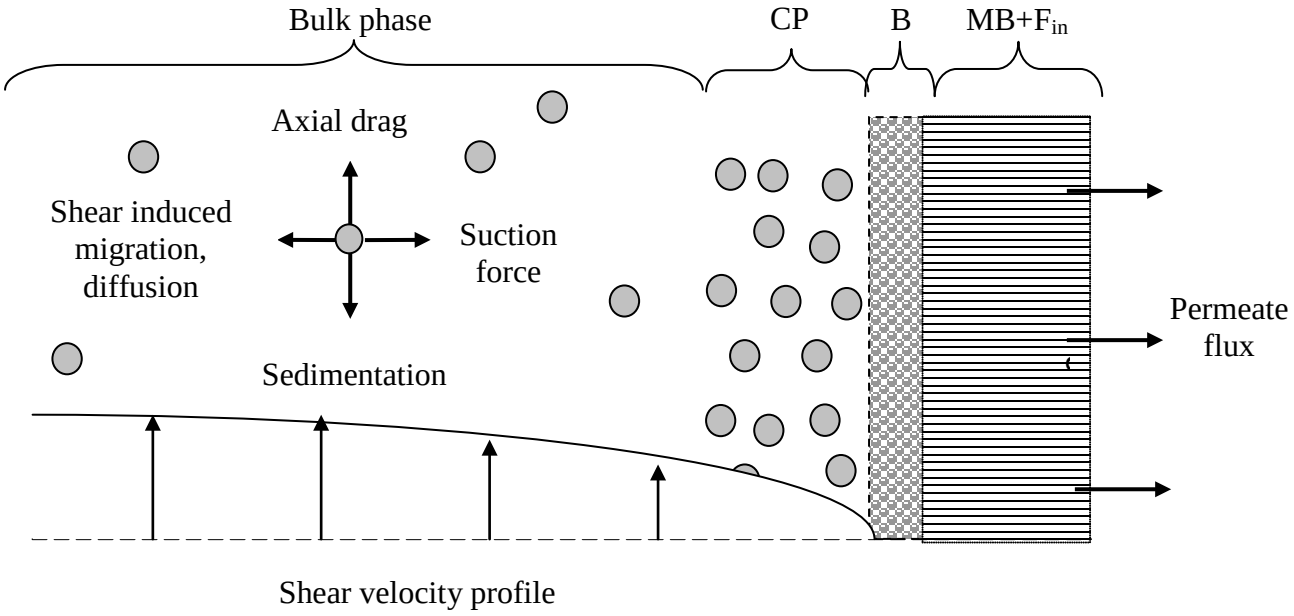

Fig. 2.3 Schematic of submerged membrane filtration display effective force on suspended microorganism particle and fouling phenomena on membrane surface, where CP = concentration polarisation, B = membrane biofouling (gel or cake formation), MB + F_{in} = membrane layer and internal fouling

Fouling of the membrane can occur if concentration polarization progresses too far, leading to irreversible fouling. Cake fouling or biofouling can occur on the membrane surface and extend outward into the feed channel and inward into membrane pores. Generally, the suspended particles in MBR system are small enough to neglect inertial and gravitational forces. Only the shear migration force and suction

force can be considered. As seen in Fig. 2.7, membrane filtration resistance can be divided into three categories;

(1) The natural membrane resistance for pure water (R_m), which depends on pore size, pore density, pore depth, the material's wet-ability, and the hydrodynamic resistance of the device holding the membrane (Ahn *et al.* 1998; Evans and Miller 2002; Zhao *et al.* 2003).

(2) A resistance due to concentration polarization (Rc_p) is caused by convection through the membrane. The thickness of the CP layer depends upon the solution velocity created by the difference between suction force and axial shear force on the membrane surface. The higher the shear force compared with suction pressure, the thinner the CP layer. If the fluid flows through the membrane faster than the retained material can transport back into the bulk fluid, a dense particle layer forms in front of the membrane surface and creates a secondary dynamic membrane.

(3) Resistance due to membrane fouling (R_f) composed of cake resistance (R_c : shown as layer B in Fig. 2.3) and internal plugging resistance (R_i: shown as layer F_{in} in Fig. 2.3). Many studies found that the filtration resistance due to the accumulated cake on the membrane is dominant in the membrane process, compared to the resistance due to the micropore plugging or surface adsorption (Ahn *et al.* 1998; Kimura *et al.* 1998; Zhao *et al.* 2003). Most filtration resistance due to the micro pore plugging or irreversible adherence to the membrane was caused by organic substances (Kimura *et al.* 1998). Masciola *et al.* (2001) reported that the fouling layer resistance, R_f, was 63% of the total filtration resistance; however, concentration polarization was the predominant factor controlling resistance in the tubular UF system.

2.3.3 External and internal fouling resistance

For simplicity and for practical reasons fouling is often separated into internal and external fouling, or cake fouling and internal fouling. This is because it is almost impossible to distinguish between the different types of fouling in practice (Psoch 2005). If the suspension has particulates with diameters larger than the membrane pores, the surface mechanism of sieving occurs. A cake layer grows on the membrane surface based on the retained particles. The cake provides an additional resistance to filtration. For dead-end filtration the cake continuously grows but in the crossflow operation the tangential shear stress may arrest the cake growth and extended operation is possible (Psoch 2005). Under the assumption of an incompressible cake, its porosity and resistance are independent of pressure. The specific cake resistance per unit thickness can be estimated by a variation of the Carman-Kozeny Equation, if further parameters, such as particle diameters, etc., are known (Belfort *et al*. 1994).

Contrary to cake fouling or cake resistance, internal, or actual, fouling resistance (R_{in}) is considered more severe. Cake resistance (R_c) can be more easily removed by shear stress and/or chemicals than the internal fouling. The internal fouling resistance normally happens below the surface level of the membrane, including adsorption and partial pore blocking. It is comparably harder to eliminate internal fouling because it is more difficult to reach micro pores with back-flushing or even with a chemical cleaning agent. If some membrane pore areas cannot be accessed by the cleaning agent, a loss of total membrane capacity, which is expressed as decreasing initial flux, is the result. Thus, the treatment of internal fouling is essential lengthen membrane life expectancy and should be appropriately carried out.

2.4 MEMBRANE FOULING AND INFLUENCING FACTORS

2.4.1 Biofouling mechanism

Unwanted deposition and growth of biofilm are commonly embedded on a membrane surface in a matrix of microbial origin, consisting of extra-cellular polymeric substances (EPS) and microorganisms (Strathmann *et al.* 2002). The formation of a biofilm in an aqueous environment generally proceeds in the following sequence (Fig. 2.4) (Escher and Characklis 1990; Gottenbos *et al.* 1999; Ahmed *et al.* 2000):

(1) When organic matter is presented, a conditioning film of adsorbed components is formed on the membrane surface prior to the arrival of the first microorganisms.

(2) Microorganisms are transported to the surface through diffusion, convection, sedimentation or active movement. This step is the initial step of membrane biofouling.

(3) Initial microbial adhesion occurs when EPS is synthesized to protect and stabilize cell attachment from the outside environmental effects.

(4) Attachment of adhering microorganisms is strengthened through EPS production and unfolding of cell surface structures.

(5) Growth and metabolism of the attached microorganisms and film develop, and continue secretion of exo-polymers.

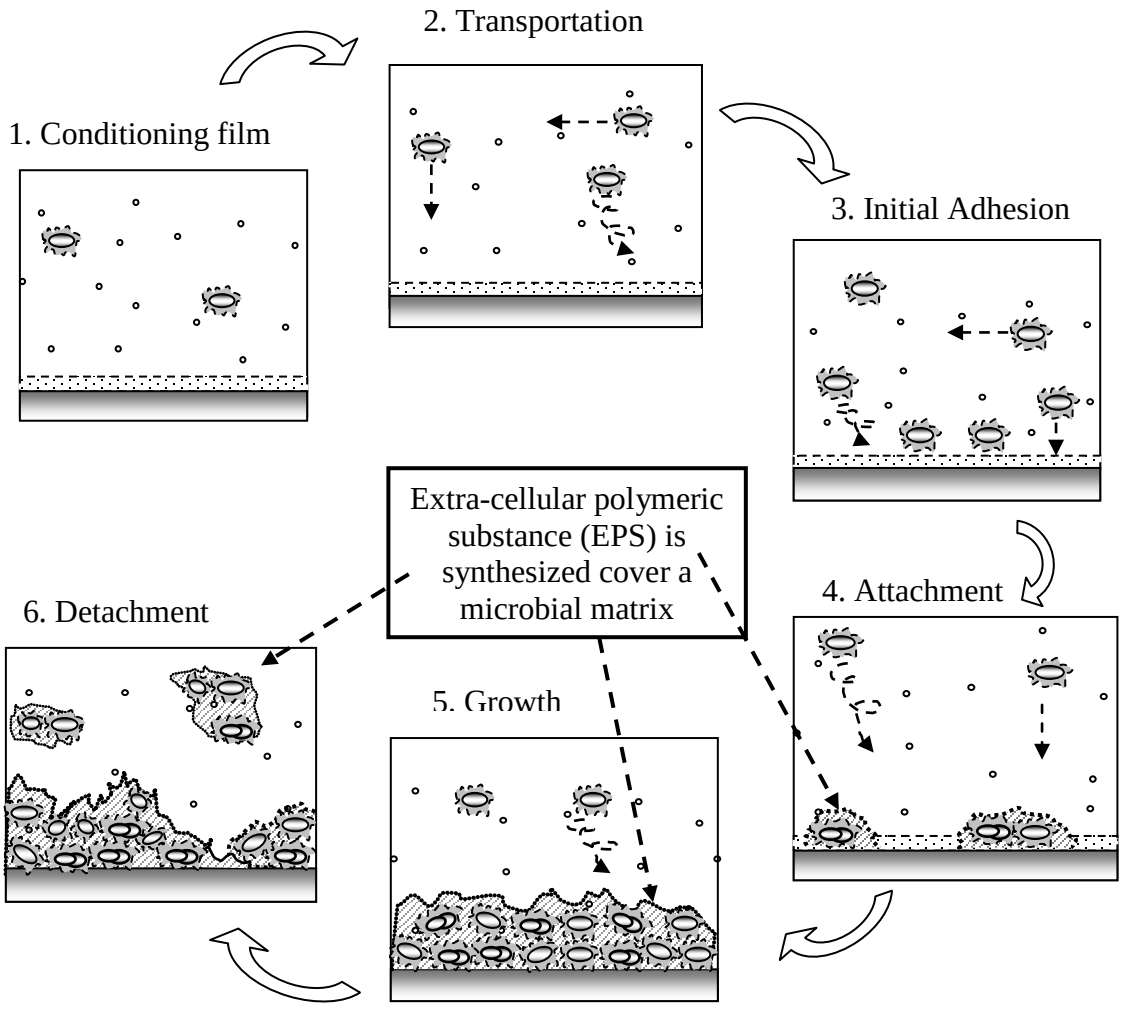

Fig. 2.4 Sequential steps in biofilm formation. (adapted Gottenbos *et al.*, 1999)

(6) Localized detachment of biofilm organisms caused by occasionally high fluid shear or other detachment forces operative starts after initial adhesion, although adhesion of individual microorganism is frequently considered irreversible (whether justified or not), and increase with time as it is related to the number of microorganisms present in the biofilm (Strathmann *et al.* 2002). Detachment of parts of a biofilm can occur by cohesive failure inside the bulk of the biofilm involving interfacial rupture. Furthermore, as the number of biofilm organisms increases, growth rates will decrease due to nutrient and oxygen limitations and accumulation of

organic acids, eventually leading to a stationary biofilm thickness, where adhesion and growth counterbalance detachment (Gottenbos *et al.* 1999).

Therefore the biofouling mechanism described above indicates that the thickness of biofouling changes with time. The attachment and accumulation of biofouling introduce to the maximum biofouling thickness which later sloughs off due to the shortage of substrate and oxygen for the layer cells next to the membrane. However, in crossflow membrane filtration, the density of the biofilm thickness increases with time until reaching the steady state owing to the effect of continuous shear migration force.

2.4.2 Stages of MBR fouling

For a better understanding of MBR fouling, leading to enhancement of membrane performance in this challenging application, the MBR fouling profile is provided as shown in Fig. 2.5.

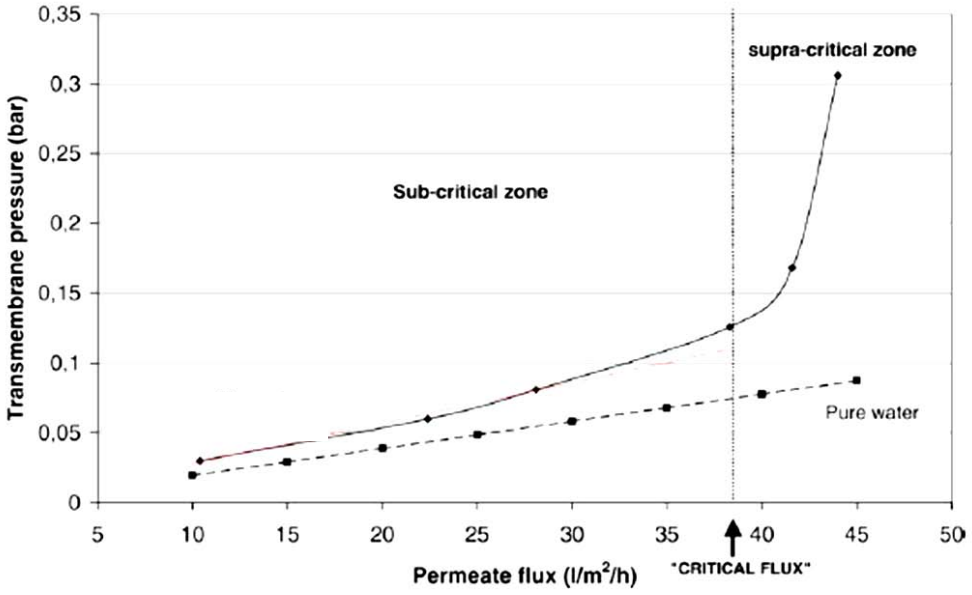

Fig. 2.5 Experimental determination of critical flux (Ognier *et al.* 2004)

Also, Fig. 2.6 depicts a three stage history for membrane fouling in MBRs (Zhang *et al.* 2006) with:

(1) Stage 1: an initial short term rise in trans-membrane pressure (TMP) due to 'conditioning'

(2) Stage 2: long-term rise in TMP, either linear or weakly exponential

(3) Stage 3: a sudden rise in TMP with a sharp increase in dTMP/d*t*, also known as the TMP jumps (Cho and Fane 2002).

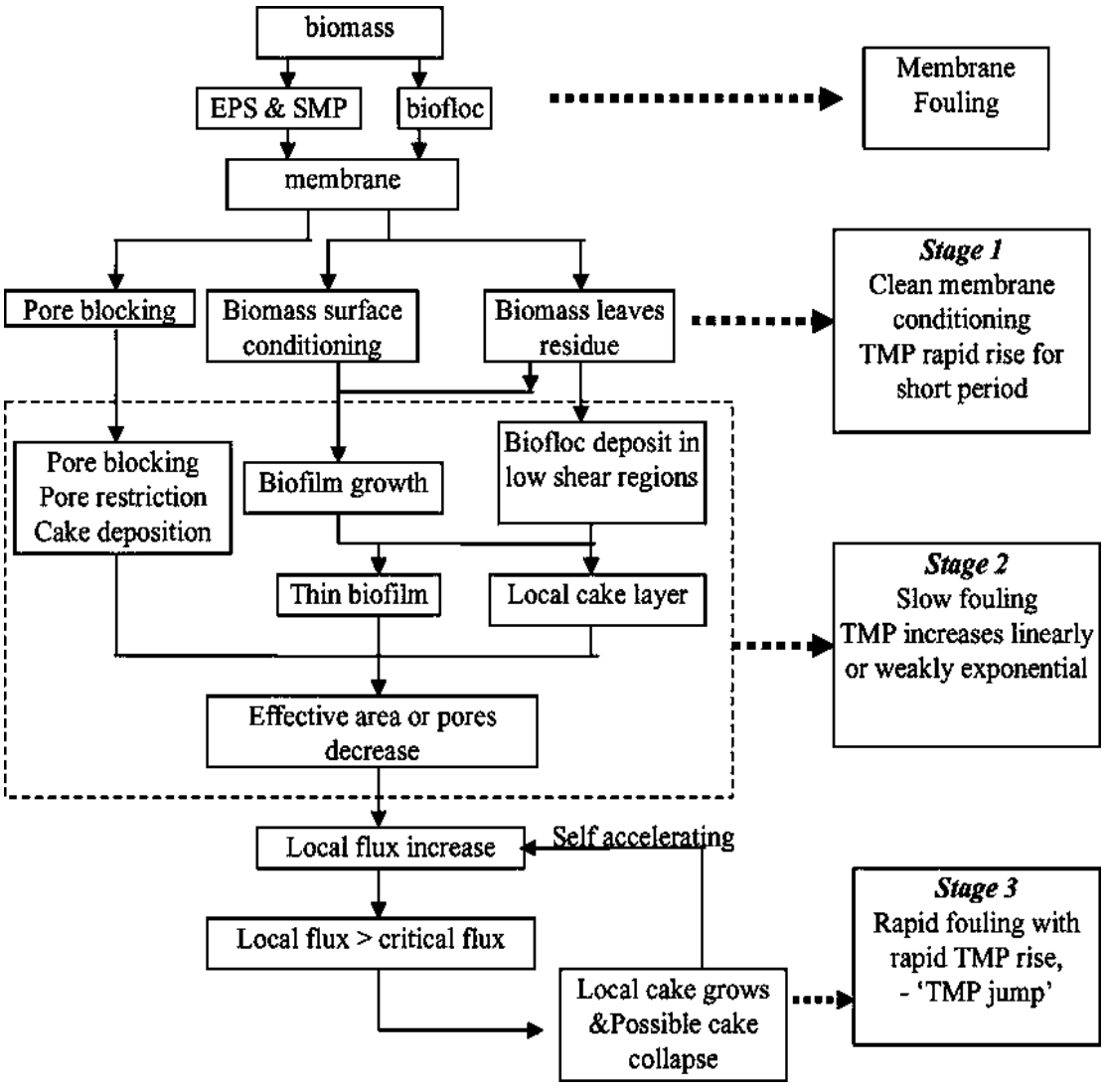

Fig. 2.6 The three stages of MBR fouling (Zhang *et al.* 2006)

The stages 2 and 3 behavior are typified in the literature by the results of previous studies (Cho and Fane 2002; Ognier *et al.* 2002) . When operating at fluxes well below the apparent critical flux of the mixed liquor suspended solids, a slow steady rise in TMP (stage 2) was observed which eventually changed to a rapid rise in TMP (stage 3) (Zhang *et al.* 2006). For sustainable operation the aim would be to limit the extent of stage 1, prolong stage 2 and avoid stage 3 since it could be difficult to restore.

2.4.3 Factors affecting performance in submerged MBR

Zhang *et al.* (2006) described that the degree of fouling in an MBR will be determined by three basic factors: (1) the nature of the feed; (2) the membrane properties; (3) the hydrodynamic environment experienced by the membrane.

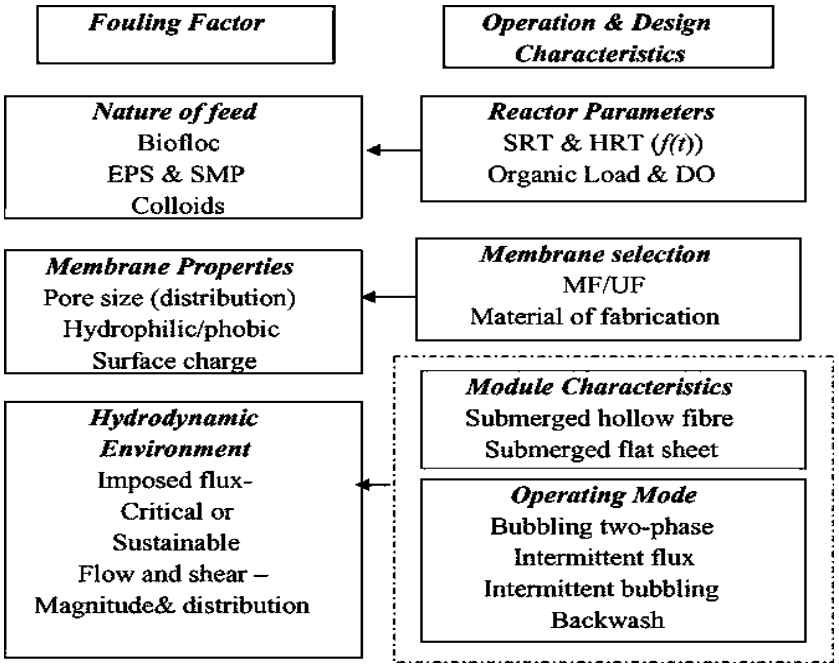

Fig. 2.7 MBR fouling factor roadmap (Zhang *et al.* 2006)

The interactions between these parameters are complex and, not surprisingly, there are some contradictions in the literature that need to be resolved by further analysis (Zhang *et al.* 2006). Fig. 2.7 (at the left-hand side) depicts the 'fouling factors' and illustrates the complex nature of the feed and the features of the hydrodynamic environment. On the right of Fig. 2.7 are the 'operation and design characteristics' of the MBR that are believed to influence the fouling factors.

2.5 MBR FOULING AND SLUDGE COMPONENTS

Membrane fouling and activated sludge components can be outlined in the following section including fouling caused by mixed liquor suspended solids (MLSS), fouling caused by extra-polymeric substance (EPS), and fouling caused by fractions of activated sludge.

2.5.1 Fouling caused by mixed liquor suspended solids (MLSS)

In the development of MBR technology, many studies have focused on the effects of MLSS concentration on membrane fouling. However, the effects of MLSS on membrane fouling are not yet fully understood and controversial reports about the effects of this parameter have been presented. Magara and Itoh (1991) reported that membrane fouling took place more rapidly at higher MLSS concentration similar to the study of Sato and Ishii (1991). Chang *et al.* (2002) and Defrance and Jaffrin (1999) also came to the same conclusion. On the other hand, some authors have claimed that sludge concentration is not a main influencing factor or has little impact on membrane fouling (Ross *et al.* 1990; Hong *et al.* 2002; Le Clech *et al.* 2003).

Besides, Lee *et al.* (2003) suggested that higher MLSS concentration is beneficial to fouling control. No significant effect of MLSS concentration higher than 30,000 mg/L on irreversible fouling was observed by Lubbecke *et al.* (1995). Also, an exponential relationship between MLSS concentration and membrane fouling resistance was reported in the study of Meng *et al.* (2006). Nevertheless, all these experiments were carried out on different scales, different operational conditions and different ranges of MLSS concentration. Cho *et al.* (2005) suggested that influence and interaction of MLSS on membrane fouling should be simultaneously studied together with the changing of operating condition and changing of EPS.

2.5.2 Fouling caused by extra-polymeric substance (EPS)

Extra-cellular polymeric substances (EPS) are products of active secretion, cell surface material shedding, cell lysis and sorption from the environment (Wingender *et al.* 1999) and EPS has been identified as the main foulant in MBR processes (Rosenberger and Kraume 2003; Janga *et al.* 2007). The EPS matrix is very heterogeneous and can be characterized by its relative levels of polysaccharides, proteins, and more rarely lipids and nucleic acids (Frolund *et al.* 1996; Nuengjamnong *et al.* 2005). EPS is produced by most bacteria and participate in the formation of microbial aggregates whether the bacteria grow in suspended culture or in biofilms (Flemming and Wingender 2001).

EPS is mainly responsible for the structural and functional integrity of biofilms, since it forms a protective layer for the cells against harmful external environment such as biocides and sudden changes in pH; absorbing exogenous nutrients and organic molecules; and aggregating bacterial cells in flocs (Fan 2005).

Consequently, EPS plays an important role in the flocculation, settling and dewatering of activated sludge (Liao 2000). Therefore, the EPS content of activated sludge was suggested as one of the probable indexes for the membrane fouling in MBR system.

An equivalent reduction in the cake hydraulic resistance due to a 40% reduction in EPS was reported in the study of Chang and Lee (1998). Nagaoka *et al.* (1996; 1998) found that EPS was accumulated both in the mixed liquor and on the membrane, which was observed as the reason for the increases of the viscosity and the filtration resistance. Rosenberger and Kraume (2002) compared the concentration of suspended EPS in the liquid phase of eight MBRs and found that the higher the suspended EPS concentration, the lower the filtration index. On the contrary, some research showed that the higher EPS caused a lower shear sensitivity and lower dispersion degree, which led to the better filterability and lower filtration resistance (Mikkelsen and Keiding 2002).

EPS can be classified as extracted EPS which are artificially produced from the biological cell flocs and the soluble EPS which are present in the activated sludge supernatant and are not associated with the cell (soluble microbial products or SMP) (Le Clech *et al.* 2006). So far no standard method for EPS extraction exists, which causes difficulty in making a comparison between research groups.

2.5.3 Fouling caused by fractions of activated sludge

Activated sludge generally contains a range of metabolites produced during the biological reaction and the biomass itself in the form of flocs. Organic compounds from the suspension phase are usually divided into three fractions (Levine *et al.* 1991).

- Biomass: bacterial flocs which contain bacteria, attached EPS and some inorganic. Normally, the sizes of bacteria aggregates are bigger than 1 µm.
- The colloidal fraction from 0.01 to 1 µm.
- The soluble fraction: such as biopolymer and soluble EPS.

A number of research have been focused on the contribution effects of suspended solids, colloids and soluble fraction to the fouling of the MBR for activated sludge (Wisniewski and Grasmick 1998; Defrance *et al.* 2000; Bouhabila *et al.* 2001; Lee *et al.* 2003). In general, suspended solids (SS) can be separated from the mixed liquor by settling or centrifugation with the supernatant containing colloids and dissolved solids. Then, the dissolved solids are separated from the supernatant by flocculation followed with settling or centrifugation or by filtration (0.05 µm). The MBR fouling affected by different fractions of activated sludge is shown in table 2.3.

Table 2.3 Fouling contribution of different activated sludge fractions (Ye 2005)

Resource	Membrane	MLSS (g/L)	Solutes	Colloids	Suspended solids	Operational conditions
Wisniewski *et al.* (1998)	0.1 µm tubular di = 6.5 mm	10-15	52%	25%	23%	u = 5 m/s TMP = 100 kPa Back washing
Defrance *et al.* (2000)	0.1 µm tubular di = 6.5 mm	4.5	5%	30%	65%	u = 3 m/s TMP = 100 kPa SRT 60 days
Bouhabila *et al.* (2001)	0.1 µm hollow fibre	20.7	26%	50%	24%	Bubbling SRT 20 days
Lee *et al.* (2003)	0.4 µm hollow fibre	2.8	37%		63%	SRT 20 days
		4.4	28%		72%	SRT 40 days
		5.5	29%		71%	SRT 60 days

2.5.4 Fouling caused by sludge categories

Some studies reported that different types of sludge (such as normal sludge, bulking sludge and de-flocculated sludge) could cause different degree of fouling. Meng and Yang (2008) reported that the bulking sludge could cause severe cake fouling due to the deposition of irregular shaped sludge flocs. Comparatively, the normal sludge had a slight membrane fouling tendency. The bulking sludge had a higher bound extracellular polymeric substances (EPS) concentration, however, the deflocculated sludge had a higher free EPS concentration, and the increase of free EPS concentration would do great harm to membrane bioreactor. Confocal laser scanning microscopy (CLSM) analysis also showed that the bulking sludge and deflocculated sludge could form a dense cake layer as compared with normal sludge.

2.6 CRITICAL FLUX

2.6.1 The concept of critical flux

In membrane processes, permeate flux is an important parameter determining fouling rate (Zeman and Zydney 1996). It is generally considered that higher productivity can be achieved by operating at a higher flux, which may initiate more fouling profoundly. In order to prolong the membrane life and make a compromise between high production rate and low fouling rate, the so-called critical flux is applied. It has been reported that fouling is not observed when the flux was maintained below the some certain flux (or critical flux) (Chang *et al.* 2002).

The concept of critical flux was introduced by Field and co-workers (1995). The postulation of the critical flux was based on the following definition (Field *et al.*

1995): “The critical flux hypothesis for microfiltration is that on the start-up there exists a flux below which a decline of flux with time does not occur, above it fouling is observed. This flux is the critical flux and its value depends on hydrodynamics and probably other variables.”

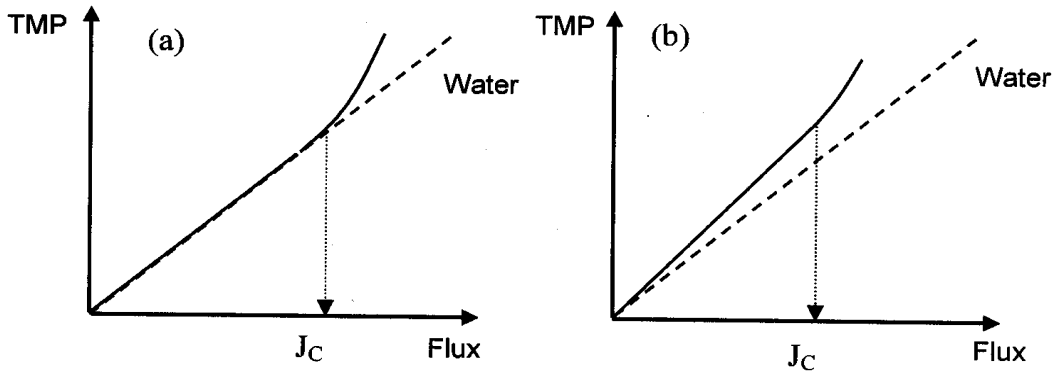

Fig. 2.8 Schematic representations of (a) the strong form critical flux, and (b) the weak form critical flux (Fradin and Field 1999)

There are two forms of critical flux: strong form and weak form. The strong form states that the sub-critical flux and TMP relationship shows a straight line of the same slope as that of pure water for the same operating pressure, while the weak form shows a straight line, the slope of which differs from that of pure water. Any deviation from the straight line for either form indicates above critical flux conditions. Fig. 2.2 shows the strong and weak forms of the critical flux.

2.6.2 Critical flux determination

2.6.2.1 Material balance

Material balance technique was employed by Kwon *et al.* (2000) by measuring the rate of particle deposition at the membrane surface and observing the variation of

particle concentration in the feed entering and leaving the modules. The defined critical flux was the maximum flux at which the feed concentration did not change. Kwon *et al.* (2000) compared the critical flux for latex particles determined by mass balance and by TMP monitoring. They found that the critical fluxes identified by resistance assessment were significantly higher than those based on mass balance. The difference between these two critical fluxes increased with the particle's size. This indicates that the assessment of filtration resistance cannot always determine the flux at which particles start to deposit onto the membrane if the particles can form a loose cake layer.

2.6.2.2 Direct observation through the membrane (DOTM)

Non-intrusive observation was experimented by Fane and teamwork (Li *et al.* 1998). They studied the critical flux of yeast and latex particles in crossflow microfiltration using in situ observation of particle deposition on the membrane surface through a microscope and video camera recording. The critical flux was recognized as the highest flux where the particle deposition on the membrane surface remained unobservable. The particle build-up became significant as the flux exceeded the critical flux. Relying on light transmission through the system, this method requires a transparent membrane and this viewing technique is restricted to particles greater than 0.5 μm due to the magnification of the microscopic lens (Chen, Li *et al.* 2004). This method was used to identify critical flux for filtration of yeast, latex and bacterial particles (Li *et al.* 1998; Li *et al.* 2003).

2.6.2.3 Flux and TMP monitoring

In general, if the filtration is performed at a fixed permeate flux, the TMP increases during filtration. An increase of TMP is due to the increase in filtration resistance. In this case, the critical flux can be defined as the highest flux where the filtration resistance remains constant (also constant TMP). This determination method can be performed with long term filtration or conveniently with shorter filtration duration using the flux stepping technique. The flux stepping technique has been widely used by many MBR research (Wu *et al.* 1999; Madec *et al.* 2000; Cho and Fane 2002; Le Clech *et al.* 2003). In this method, the fixed flux filtration is carried out for a certain time and this procedure is repeated by incrementally increasing the flux until a noticeably steady increase in trans-membrane pressure is observed.

2.6.3 Factors affecting the critical flux

2.6.3.1 Feed properties

(1) Particle size: Several sizes of latex particles ranging from 0.1 to 11.9 μm were tested in a crossflow micro-filtration system (Kwon *et al.* 2000). For small particles from 0.1 to 0.46 μm, the critical flux decreased as the particles size increased due to the greater Brownian back diffusion force of the smaller particle size. The reverse trend occurred in larger particles from 0.46 to 11.9 μm, which might be due to the cake formed by the large particles being too loose to create resistance compared with the membrane resistance. This phenomenon can be explained using the concentration polarization model which shows the sub-micron particles are likely to

cause Brownian diffusivity while shear induced hydrodynamic seem to be dominant for micron sized particles (Kwon *et al.* 2000).

(2) Feed concentration: Fradin and Field (1999) and Kwon *et al.* (2000) reported the decrease of critical flux with the increase of particle concentration due to the higher particle deposition on the membrane at the higher concentration. A similar finding obtained from Aim and co-workers using bentonite concentration is reported. On the other hand, the increase in MLSS concentration to 12 g/l could noticeably reduce the fouling performance (Le-Clech *et al.*, 2003b). In summmary, the effect of MLSS concentration on the critical flux is not very obvious and difficult to compare results from different research due to the sludge complexity.

(3) pH and ionic strength: Kwon and Vigneswaran (1998) observed that ionic strength of particles has a significant effect on the critical flux. In this experiment, the increase in ionic strength from 10^{-5}-10^{-2} M decreased the critical flux value, thereafter the critical flux increased. Also, Li *et al.* (2000) suggested considering surface charge of the particles as one of the influencing factors for particle back-transport mechanisms. Chan and Chen (2001) studied the effects of pH on critical flux and presented that the critical flux at pH 4.8 was found lower than at pH 3.0 and pH 9.0.

2.6.3.2 Membrane properties

(1) Membrane pore size: The effect of membrane pore size on the critical flux using 50 kDa and 100 kDa membranes for 5% baker's yeast filtration showed that the larger membrane pore size tended to have lower critical flux due to the internal fouling of cell debris and small components (Wu *et al.* 1999). Chen, (1998) reported that the critical flux of 0.4% BSA solution was increased with tracked-etched

membrane pore size (0.1, 0.2 and 0.4 μm). On the other hand, Kwon and co-workers (2000) found that the critical flux was insensitive to the membrane pore sizes (0.1, 0.2, 0.45 and 0.65 μm). This phenomenon can be explained in that the total drag force for different membrane pore sizes was identical at the same flux and causing similar deposit latex particles.

(2) Zeta potential: Huisman *et al.* (1999) found that neither the zeta potential of the silica particles (0.53 μm) nor the membrane had an impact on the critical flux similar to the investigation of Persson *et al.* (2001). In earlier works reported that the specific resistance is strongly dependent on zeta potential of colloids. Lee *et al.* (2002) found that the zeta potentials changed significantly after fouling by humate reducing cationic functionality and adsorption of anions resulting in reduced zeta potentials. Combe *et al.* (1999) reported that the modification of membrane surfaces by oxidation increased the fouling and they suggested mitigating fouling by decreasing of interaction between foulants and membrane zeta-potential.

(3) Hydrophilicity/hydrophobicity: Madaeni *et al.* (1999) observed the effect of hydrophilic and hydrophobic membranes on the critical flux and found that a larger critical flux appeared for hydrophilic membrane. Chan *et al.* (2004) reported that protein deposition above and below the apparent critical flux using a hydrophobic membrane while the coverage was only found above critical flux when a hydrophilic membrane was used.

2.6.3.3 Hydrodynamics

Some hydrodynamic factors such as crossflow velocity and air sparging have been accounted to affect the critical flux. Most research showed the increase of

critical flux with increase of crossflow velocity and air sparging (Li *et al.* 1998; Madec *et al.* 2000) due to shear-induced diffusion and inertial lift. In addition, the effect of the constant pressure operation and constant flux operation on the critical flux was compared and presented by Defrance and Jaffrin (1999). The results showed that the constant flux operation created less hydraulic resistance than constant pressure operation due to different fouling histories and fouling initiation. Madec *et al.* (2000) also described a linear relationship between air flow rate and critical flux in the submerged hollow fibre membrane system.

2.7 MEASURES AGAINST FOULING IN SUBMERGED MBR

There are several strategies to control fouling in a submerged MBR system. Most of the measures involved turbulence induction which manipulates the particle back-transport from the membrane surface. Fluid movement and/or membrane movement are performed to remove and reduce the hydraulic resistance from cake and accumulated solutes. Providing unstable fluid flow in the MBR system is one of the simplest methods to control the thinner and less concentration polarization.

2.7.1 Air scouring outside the membrane module

A number of researchers have found that the air scouring method could be achieved to improve MBR performance. Ueda *et al.* (1997) discovered the effect of aeration on cake removal and showed that the further increase of aeration is unable to enhance the filtration effectiveness. Bouhabila *et al.* (1998) described the decline of resistance ratio with the air flow rate increase until the optimum aeration at about 600 L/H. Likewise, Chang *et al.* (2002) confirmed the significant impact of aeration on

fouling improvement. Wicaksana *et al.* (2006) also suggested increase of the aeration intensity to limit the membrane fouling.

2.7.2 Air sparging inside the membrane module

A new idea of using air injection inside a membrane module was introduced to be applied in a tubular and hollow fibre membrane. Mercier *et al.* (1997) found the enhancement of flux by factor of 3 after using gas-liquid two phase flow in the tubular ultra-filtration membrane. Similarly, Cui and Wright (1994) observed an increased flux about 90% for bovine serum albumin (BSA) and about 60% for dextran due to the injection of air into the feed stream. Cabassud *et al.* (1997) found the same benefit of bubbling injection inside hollow fibre membrane for bentonite filtration despite the difference hydrodynamics between tubular and hollow fibre membrane. It showed enhancement of flux (about 60%) even at low gas velocity (0.1 m/s).

2.7.3 Aeration mode

Based on the energy cost minimization, a variation of the aeration modes is interesting. Several studies have found that implementation of intermittent aeration and fluctuation of the aeration intensity could offer better filtration performance than that with continuous aeration. Li *et al.* (1997) found that a higher permeate flux can be obtained by increasing the bubble frequency and the bubble size was controlled by air flow rate variation. Guibert *et al.* (2002) evaluated fouling propensity using interchangeable air injection between different locations and found that this could generate adequate liquid turbulence to minimize the fouling formation. The results

displayed a lower fouling rate at the intermittent aeration mode compared to the continuous mode.

2.7.4 Sub-critical flux filtration

The sub-critical flux operation may be a desirable operational target for a clean MBR plant due to low energy and low cleaning cost requirement. Because of that, many works are focused upon developing its enhancement to avoid severe fouling. By correctly selecting the initial flux or TMP, the rate of membrane fouling can be greatly reduced. Psoch and Schiewer (2005) described that it was impossible to maintain the initial flux which is above the critical flux. However, the critical value of this flux (or TMP) is very much system specific (Field *et al.* 1995; Gander *et al.* 2000).

2.7.5 Intermittent filtration

Yamamoto *et al.* (1999) has conducted experiments to determine the optimum suction mode and found that the intermittent suction mode was better for long term operation of the membrane system compared to continuous suction mode. Ahn and Song (2000) studied the impact of membrane suction modes and confirmed their optimal operational setting using intermittent filtration of 10 minute on and 2 minute off permeate pumping. In addition, Hong *et al.* (2002) studied the effect of operational mode on membrane fouling and the results clearly showed that membrane performance was significantly improved with intermittent filtration. This finding was explained by the enhanced foulant back transport under filtration relaxation.

2.7.6 Backwashing

Backwashing or back flushing is a cyclic reversal of the gas or liquid (or some cleaning agents) back into the feed path. This technique has been commonly practiced in industry for many years and is a fairly simple effective way to fight fouling (Psoch 2005). Unlike other methods, the backwashing technique is able to dislodge both foulants inside membrane pores and on membrane surface. However, the back flushing strategy is normally applied for submerged hollow fibre membrane systems, not for the submerged flat sheet membrane process due to different back pressure tolerances.

2.8 SUMMARY

Studies in the literatures have described that the submerged membrane bioreactor (SMBR) has advantages in wastewater treatment over the conventional activated sludge process. This SMBR based system has been widely used which, later, triggers conduction of numerous research. However, the beneficial points of this SMBR are countered by membrane fouling problem. Previous investigators have suggested that some biological parameters (e.g. MLSS, EPS) and operational parameters (e.g. air sparging, critical flux) played key roles on the fouling problem and mitigation. To solve this fouling problem, operating SMBR system under sub-critical flux and enhancement of aeration to scour membrane surface are ones of the most well-liked suggestion written in many studies.

Although there are many studies of SMBR pointed out the importance and usefulness of critical flux, a comparison of the critical flux among various researcheds has never been observed and tested before. Some variables (such as step height, step

length, flux stepping and flux cycling) have been reported in a few research to have influence on critical flux values. Therefore, in this thesis, an update of critical flux study will be carried out using all literacy critical flux methods variables.

The fouling mechanisms for a different group of activated sludge component such as MLSS, EPS protein, colloid and EPS carbohydrate have been broadly studied by analyzing the flux and TMP data and membrane fouling characterization. However, none of research ever examined the effect of these parameters variation on SMBR fouling under different flux stages before (e.g. sub-critical flux, supra-critical flux). Accordingly, the overall pictures of actual fouling mechanisms are still not very clear. For example, how difference of pore fouling mechanisms happen between sub and supra critical flux conditions. Hence, in this thesis the fouling mechanisms of MLSS, EPS protein, colloid and EPS carbohydrate will be investigated in under and beyond critical flux conditions.

Since the filtration and aeration are attributed to the majority of energy consumption cost, numerous studies attempted to minimize these by modifying the aeration and filtration modes. Previous studies showed that intermittent operations of aeration and filtration gave better performance of SMBR with less fouling. However, among these research, none of them ever considered the changing of filtration yield to a variation of aeration. Most studies reported less fouling under intermittent filtration mode which means less yield of filtration as well. Thus, based on the assessment of literatures, this thesis will try to fill up some lack points of SMBR studies based on the effect of aeration and filtration modes. An optimum operating condition of these parameters will also be explored.

CHAPTER 3

DESIGN, CONSTRUCTION AND TREATMENT PERFORMANCE OF A PILOT SCALE SUBMERGED MEMBRANE BIOREACTOR

3.1 INTRODUCTION

For most submerged membrane bioreactor (SMBR) systems, a major obstacle is the rapid decline of the permeate flux as a result of membrane fouling. Membrane fouling is known to be influenced by several physical–chemical and biological properties of sludge: floc size, mixed liquor suspended solids (MLSS) concentration, dispersed bacteria concentration, sludge hydro-phobicity, surface charge, soluble and bound exo-polymeric substances, *etc.* (Rosenberger and Kraume 2002; Ng and Hermanowics 2004; Ng and Hermanowicz 2005). Determination of the relative significance of these parameters in relation to bioreactor and membrane operating conditions (trans-membrane flux, hydrodynamic conditions and chemical cleanings) constitutes a major effort of current SMBR research.

Since SMBR system involve living microorganisms, their properties and their relative contributions on membrane fouling may vary with experimental conditions from one study to another. Moreover, most SMR research have been carried out with bench or small scales, under conditions far from those prevailing at full scales. In many cases, many research have used synthetic sewage which has substantially different fouling characteristics to those of real sewage. On the other hand, it is too

costly to conduct a variety of SMBR studies based on the full process. Hence, pilot scale fed with real sewage is a reasonable option to represent fouling behavior happening in the actual SMR process. In order to reach in a successful SMR process based on high treatment efficiency and low biofouling, the pilot SMR is also needed to be aware since a design, construction and commissioning.

The objectives of this chapter are therefore three fold: (1) to assess the influence of operational parameters on the SMR design using both simulation and simple calculation (2) to give details of construction and commissioning of the pilot scale SMBR consisting of flow analysis, trans-membrane pressure analysis, consideration of program-logic control and sludge seeding; (3) to investigate the treatment performance happening in the pilot scale SMBR after the starting –up period.

3.2 MBR MODELLING BASED DESIGN

3.2.1 MBR configuration and simulation models

Due to high levels of ammonium and phosphate in Townsville municipal wastewater (Fig. 3.1), a pilot scale SMBR unit is designed based on combining a nitrogen and phosphorous biological removal process including anaerobic, anoxic and aerobic retrofitted membrane units. Details of a pilot scale SMBR configuration are shown in Fig. 3.1 and Table 3.1. From Fig. 3.1, the raw wastewater passing through a bar screen (3 mm) is pumped continuously to an anaerobic unit, which can release more phosphorous for the next anoxic and aerobic stages. Aeration is supplied in a membrane unit in order to give oxygen for nutrient degradation of aerobic micro-organisms and create shear scouring to remove fouling on the membrane surface. By

returning the activated sludge to the anaerobic stage, nitrate concentration will be eliminated and phosphorous will again be released more. The internal recycle (QIR) provides for increased organic utilization in the anoxic stage. A size of aerobic membrane unit is also necessarily fixed at 1.35 m^3 owing to the dimensional limitation of membrane filtration operation.

Table 3.1 Characteristics of raw municipal wastewater at the Mt St John treatment plant, October - November 2005 (data from Townsville CitiWater)

Raw wastewater characteristics (mg/L)			Membrane characteristics	
Parameters	Std. deviation	Average	Type (Kubota, LF10)	Flat sheet
pH	0.148	7.34	Material	Polyethylene
SS	70.62	233.37	Pore size	0.4 micron
BOD	109.47	263.44	Membrane panel dimension	0.8 m x 0.5 m
COD	226.75	426.41	Membrane effective area	8 m^2, 10 panels
NH_3 as N	12.51	38.63	Minimum clean water flux	7 L/min
TKN	8.64	50.48	Suggested flux in sludge	150 L/h
Ortho-PO4	1.33	6.18	Space apart between MB	0.8 cm
Total –P	1.88	9.36	Filtration pressure	$\leq$ 20 kPa
BOD_5 / N / P ratio = 28.14 : 5.4 : 1			Aerobic membrane unit	1.35 m^3

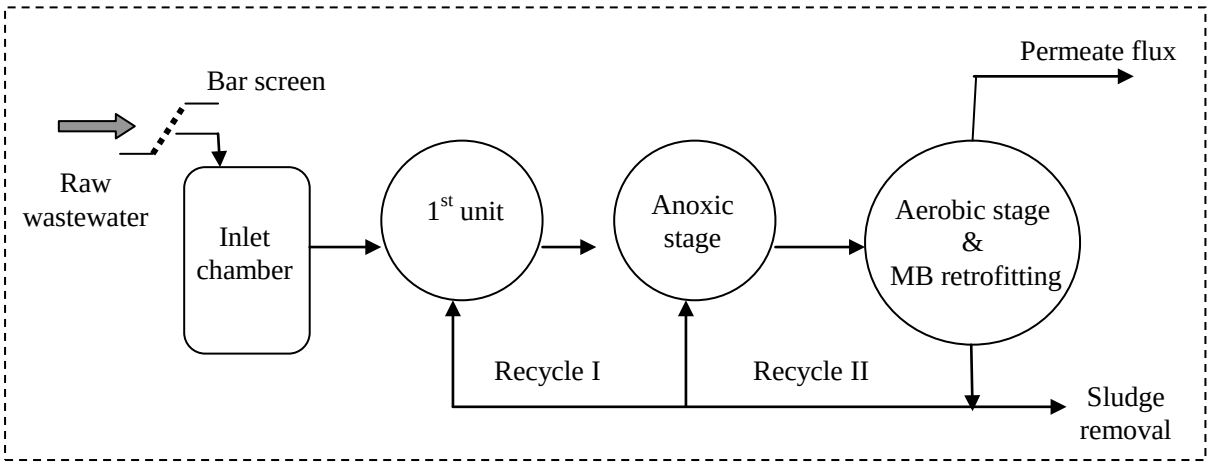

Fig. 3.1 Schematic diagram of submerged MBR pilot plant

research shows that TUDP model is capable to describe full-scale conditions of wastewater treatment, without significant adjustment (Van Veldhuizen *et al.*, 1999; Brdjanovic *et al.*, 2000). The TUDP model used in this study follows the last updated version of TUDP model (Meijer, 2004) by neglecting the effect of substrate competition. The MLSS concentration from TUDP model is linked with the EPS generation model from Nagaoka's work. The accumulation and consolidation of EPS on membrane surface coupling with a shear detachment follow the concept of Nagaoka and co-workers (Nagaoka *et al.*, 1998). A shear stress term using in Nagaoka's model is calculated by a shear Equation referred in the study of Merlo and co-workers (Merlo *et al.*, 2004). Relationship between dissolved oxygen (DO) concentration and aeration supply is also followed the film theory of oxygen transfer model. The AQUASIM 2.0 software is used for simulation of the pilot scale SMBR. More details of all models and Equations are shown in appendix A.1.

3.3 SOME IMPORTANT SMBR DESIGN CONSIDERATIONS

3.3.1 Design considerations based on biological treatment factors

3.3.1.1 Sludge production and nutrient requirements

Sludge production indicates the transformation between BOD (and/or COD) up-taken and the amount of particulate biomass increase in the system (Tchobanoglous *et al.* 2003). Sludge production can be calculated by the following:

Sludge production: $P_x = Y_{obs}\,(Q_{in})(S_o - S)$ **3.1**

To determine the nutrient requirement as shown in Equations 3.2 – 3.5 below (Benefield and Randall 1980), biomass production and loading of nitrogen and phosphorous are needed .

$$\textit{Nitrogen (N) requirement} = 0.122 \times P_x \quad \textbf{3.2}$$

$$\textit{Nitrogen - loading} = Q_{in} \times \textit{influent TKN} \quad \textbf{3.3}$$

$$\textit{Phosphorous (P) requirement} = 0.023 \times P_x \quad \textbf{3.4}$$

$$\textit{Phosphorous - loading} = 8.34 \times Q_{in} \times \textit{influent P} \quad \textbf{3.5}$$

If the loading is higher than the requirement, the loading consideration is satisfied. Otherwise, more nutrients should to be supplied. From calculation details shown in appendix A, there is sufficient nutrient in the Townville municipal wastewater supplied to the SMBR pilot plant.

3.3.1.2 Oxygen requirement

Aeration introduces air into liquid phase, which not only supplies required oxygen, but also provides mixing and circulation to the system so that the micro-organisms can contact organic materials. Without sufficient dissolved oxygen, aerobic bacteria cannot survive and the aerobic treatment stage cannot occur.

Oxygen requirement for carbonaceous organic matter

Oxygen required to oxidize a unit of biomass can be written as (Benefield and Randall 1980):

$$C_5H_7NO_2 + 5\,O_2 \rightarrow 5\,CO_2 + 2\,H_2O + NH_3$$

113 : 1 cell (5x32)

= 1.42 where 5 x32/113 = 1.42 mass units O_2/mass unit biomass oxidized

Oxygen requirement for nitrification (Tchobanoglous *et al.* 2003):

Step I: $2\,NH_4^+ + 3O_2 \xrightarrow{Nitrosomonas} 2\,NO_2^- + 2\,H_2O + 4H^+$

where O_2 required = 3.43 g/g-N oxidized

alkalinity = 7.14 g $CaCO_3$/g N-oxidized

Step II: $2\,NO_2^- + O_2 \xrightarrow{Nitrobacter} 2\,NO_3^-$

where O_2 required = 1.14 g/ g N-oxidized

Thus, O_2 requirement for step I and II is (3.43+1.14) = 4.57 g O_2/g N-oxidized

Total oxygen requirement for both carbonaceous and nitrogen removal can be calculated using Equation 3.6 below:

$$\therefore Total\ O_2\ requirement\ (kg/d) = \frac{Q_{in}\,(S_o - S)}{f} - 1.42\,(P_x) + 4.57\,Q_{in}\,(N_o - N) \quad \textbf{3.6}$$

Based on Equation 3.6 and more calculation details shown in appendix A.2, total oxygen requirement is 1.66 kg/d.

3.3.1.3 Air flow rate requirement

Aeration can be estimated using Equation below (Tchobanoglous *et al.* 2003):

$$Air\ flow\ rate\ (m^3/min) = \frac{(SOTR\ kg/h)}{[(E)(60min/h)(kg\ O_2/m^3\ air)]} \quad \textbf{3.7}$$

Based on Equation 3.7 and calculation shown in appendix A.2, necessary air flow rate is 22.56 l/min. Therefore, the blower used in the pilot SMBR has to cover at

least 22.56 l/min of aeration due to limitation of oxygen requirement for aerobic microbial growth.

3.3.2 Design considerations based on hydrodynamics

Design considerations based on hydrodynamics are shown in the following sections including fluid flow, head loss and trans-membrane pressure analysis.

3.3.2.1 Fluid flow and head loss

Minimum fluid flow velocity and pipe selection should be carefully designed to prevent solid sedimentation in the system. From Fig. 3.2, head loss in each flow line can be calculated using the modified Bernoulli Equation (3.8), shown below. A summary of head loss calculation is presented in appendix A.2.

Energy Equation for fluid flow: $$Z_1 + \frac{P_1}{\rho g} + \frac{V_1^2}{2g} = Z_2 + \frac{P_2}{\rho g} + \frac{V_2^2}{2g} + h_L \qquad \textbf{3.8}$$

From calculation data shown in appendix A.2, a two inch diameter pipe was chosen for the overflow lines to avoid flow limitation and prevent the liquid level increasing up in the anaerobic and anoxic unit. A half inch and one inch diameter pipe were selected for the returning flow from the aerobic-membrane unit to the anaerobic unit and from the aerobic-membrane unit to the anoxic unit, respectively, in order to prevent sedimentation of a low flow rate.

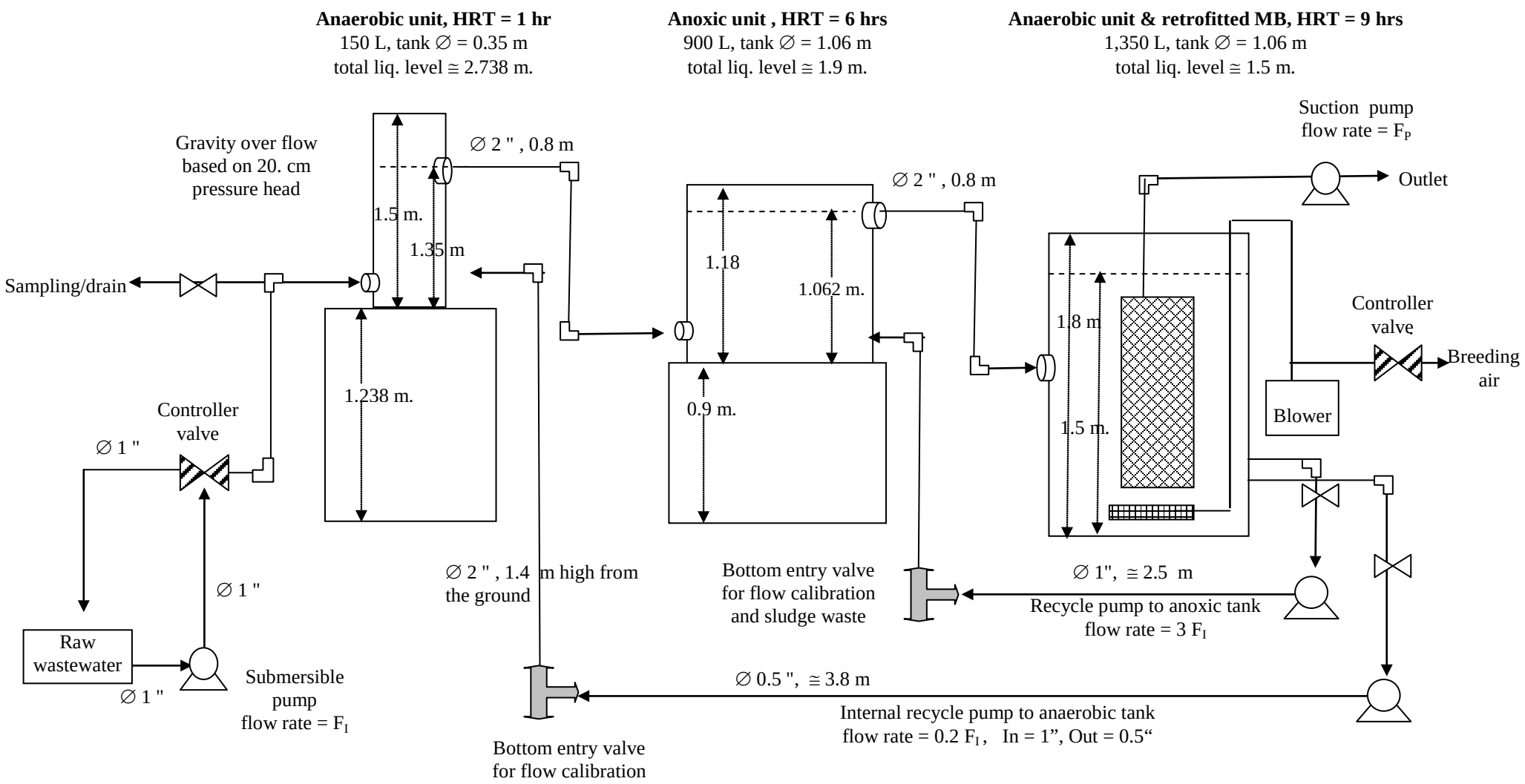

Fig. 3.2 Schematic diagram of fluid flow in the pilot scale MBR

3.3.2.2 Trans-membrane pressure (TMP) analysis

Trans-membrane pressure (TMP) is a very important parameter to indicate how the membrane and fouling perform. Therefore, evaluation of TMP in a membrane process needs to be well planned and detected. In this study, the aerobic-membrane unit is constructed with two level scaffolding due to a convenience of lifting up the membranes for cleaning and sampling purposes. In Fig. 3.3 below, liquid at position P_2 is pumped through the membrane layer (P_3) and flows upward passing a vacuum gage (position P_4) to become permeate. TMP based on pressure drop across membrane in Fig. 3.4 can be evaluated as Equations below.

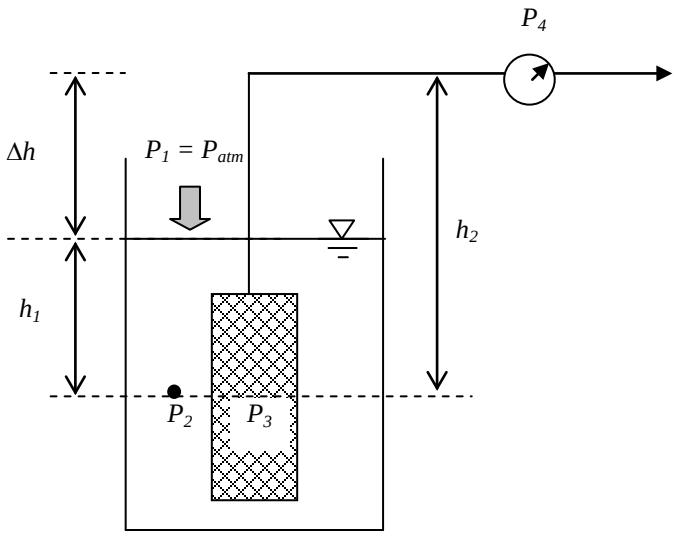

Fig. 3.3 Schematic diagram for TMP evaluation

From Fig. 3.3, TMP = pressure drop across membrane

$$TMP = P_2 - P_3 \qquad \textbf{3.9}$$

where $P_2 = P_1 + \rho g h_1$

On the other hand, energy balances of fluid flow from position P_3 to P_4 is

$$\frac{P_3}{\rho g} - h_2 + \frac{V_3^2}{2g} = \frac{P_4}{\rho g} - \frac{V_4^2}{2g} - h_L \text{ ; at position 3, } V_3 = 0$$

$$P_3 = \left(\frac{P_4}{\rho g} + \frac{V_4^2}{2g} + h_2 - h_L \right) \times \rho g$$

$$P_3 = P_4 + \left(\rho \frac{V_4^2}{2} \right) + (h_2 \rho g) - \left(f \frac{L}{D} \rho \frac{V_4^2}{2} \right)$$

$$P_3 = P_4 + \rho \frac{V_4^2}{2} \left(1 - f \frac{L}{D} \right) + (h_2 \rho g)$$

From Equation 3.9, $TMP = (P_1 + \rho g h_1) - P_3$

$$TMP = (P_1 + \rho g h_1) - \left[P_4 + \rho \frac{V_4^2}{2} \left(1 - f \frac{L}{D} \right) + (h_2 \rho g) \right]$$

Thus, $$TMP = P_1 - P_4 - \rho g (h_1 - h_2) - \rho \frac{V_4^2}{2} \left(1 - f \frac{L}{D} \right) \quad \textbf{3.10}$$

Atmospheric pressure, vacuum pressure and liquid level (position 1 and 4) are continuously measured and recorded via pressure transmitters. The TMP value based on the Equations above will be automatically calculated, displayed and recorded through the program logic control (PLC) device.

3.3.3 Design consideration based on program logic control

3.3.3.1 Liquid level control

The pilot-scale MBR is controlled by a program logic control (PLC) device which can be programmed to perform complex functions based on an integrated manipulation. PLC can be calibrated between reading pressure (from pressure transmitter: PT) and the liquid level. A minimum liquid level is fixed at about 1.5 m

(30 cm above membrane cartridge) by setting up of a floating switch to stop permeate pump if the level go below the minimum. A maximum liquid level in the aerobic-membrane unit (1.85 m) can also be specified and controlled through the PLC in order to stop the inlet pump if the level goes beyond this point. However, the minimum and maximum liquid levels should normally not be reached because the PLC will control the liquid level to be stable at the set point between these two values.

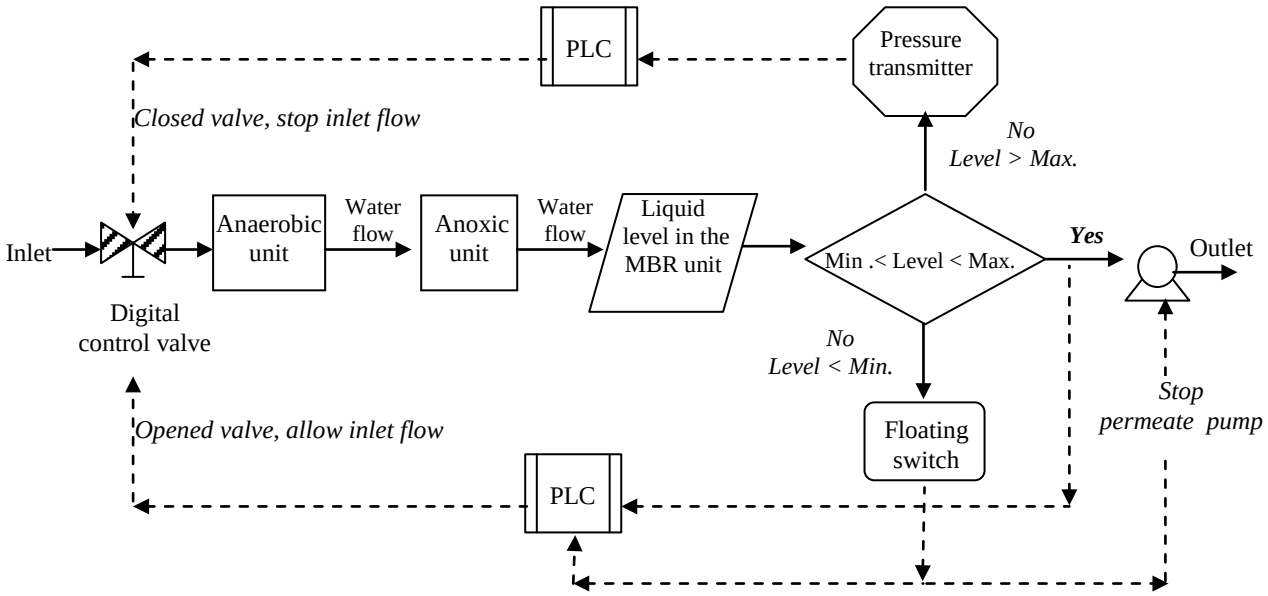

Fig. 3.4 Schematic diagram for level control in the MBR system

For the whole system level control (see Fig. 3.4), when the liquid level in the aerobic-membrane tank higher than the set point, the PLC will send signal to close the inlet valve temporarily and allow only the permeate pump releases the liquid from the system. In contrast, when the level lower than the set point, the PLC will send signal to stop the permeate pump for the short term and in the mean while it will send signal to open the inlet valve allow the liquid level rise up to the set point. Using the control logic described above, liquid level in all units of the SMBR system including

anaerobic, anoxic and aerobic-membrane unit can be controlled at the desired level due to the system mass balance.

3.3.3.2 Aeration and air scouring control

For aeration control (Fig. 3.5), an air rota meter was used to fine tune the air flow rate coming to the SMBR tank. Instead of using only one large capacity blower, two medium size blowers were chosen for safety reason to prevent a severe fouling if one blower was broken. The air beyond requirement will be released through the digital breaching valve which is normally under opening stage. When the air scouring mode is scheduled, the digital valve will be closed and pushing more air supply to clean the membranes in the aerobic-membrane unit. On the other hand, if no air pressure can be detected due to trouble of the blowers, the PLC will realize this crisis through the PT reading value and will also send signal to stop the filtration process. With this aeration design and control, membranes in the aerobic unit are barely serious fouled.

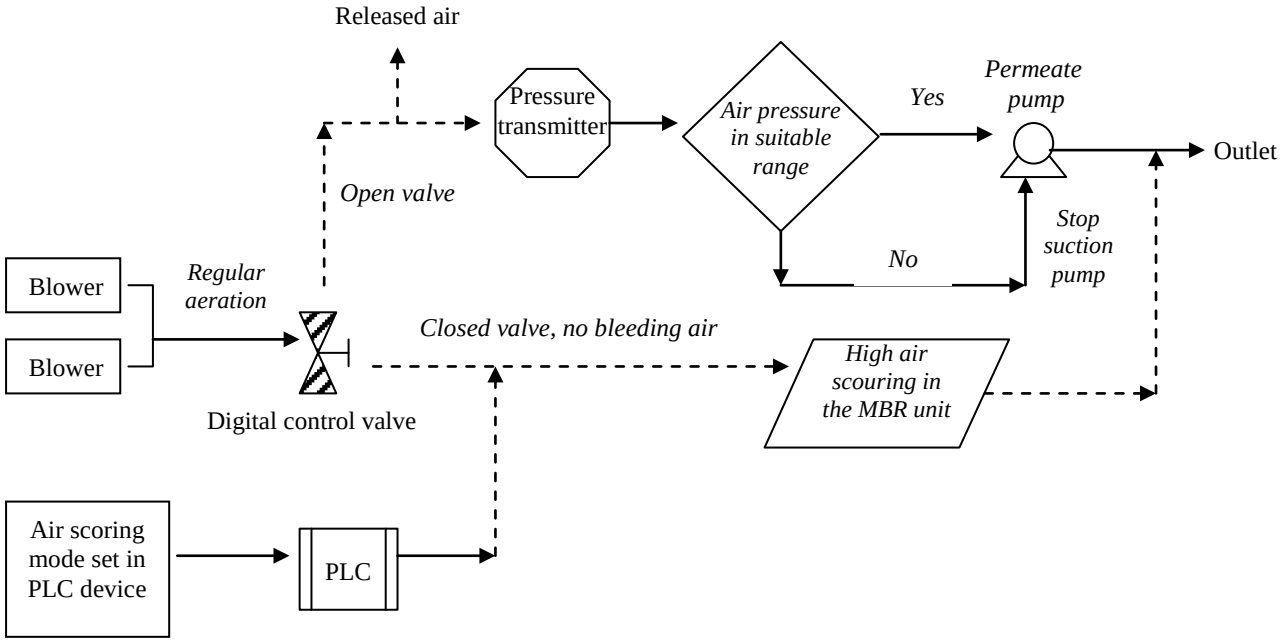

Fig. 3.5 Schematic diagram for air scouring in the membrane unit

TMP value is always automatically checked and the PLC will stop the permeate pump and the inlet valve if the TMP reaches 20 kPa which is the tolerant limitation of the membrane. Emergency override mode is also programmed and set on the control panel to stop the system immediately in emergency case. Data from electronic sources such as TMP, permeate flow, air pressure etc can be logged directly to a PLC memory card.

3.4 CONSTRUCTION AND COMMISSIONING

3.4.1 Construction of the SMBR system

3.4.1.1 Anaerobic unit

A 150 liter closed anaerobic tank diameter 0.35 m tall 1.6 m made of fibre plastic is used to store the anaerobic sludge (Fig. 3.6). Two inlet channels, 1 and ½ inch diameter at the bottom of the tank, are for receiving influent and returning flow from inlet source and aerobic unit, respectively. The overflow outlet is at a top portion of the tank with 2 inch diameter. To prevent sedimentation, a centrifugal pump for recirculation is provided.

3.4.1.2 Anoxic unit

A plastic tank height 1.3 m, diameter 1.06 m, volume 900 liters, is used to contain anoxic sludge with two inlet streams coming through 1 inch diameter pipes from the anaerobic and aerobic-meane unit at the bottom and middle channels of the tank, respectively (Fig. 3.6). Anoxic outlet will overflow gravitationally to the next aerobic-membrane unit through the top 2 inch diameter channel. A recirculation pump to prevent sedimentation is also externally set up.

3.4.1.3 ***Aerobic unit***

An aerobic-membrane unit (Fig. 3.6) was made of fiber plastic tank diameter 1.06 m height 2.0 m filled with activated sludge volume around 1,400 liters. Ten flat-sheet Kubota membranes, pore size 0.4 micron, placed in the filtration case were submerged directly in the centre of the aerobic tank. A circulation pump is not necessary due to aeration supply in this unit.

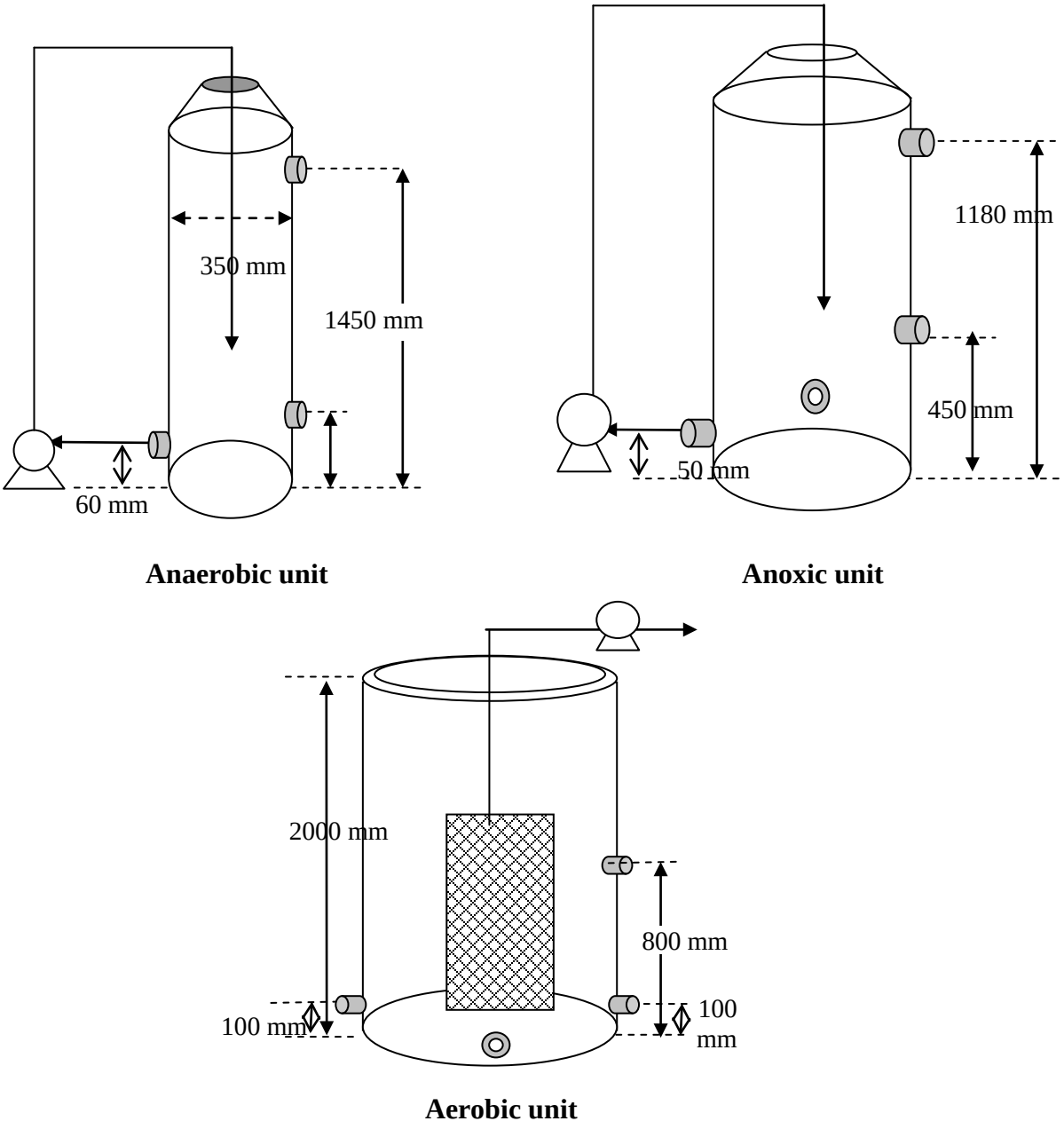

Fig. 3.6 Schematic diagram of each unit construction in the MBR system

3.4.1.4 Setting of the membrane rig in the aerobic unit

Position of the submerged membrane in the aerobic tank should also be aware about mixing zone and sedimentation. Spaces between membrane case and tank wall are suggested at 300 mm (Kubota-Corporation 2004) and more calculation details of the membrane rig setting in the aerobic unit are shown below. Details of the membrane rig set in the aerobic unit from front view and top view are shown in Fig. 3.7.

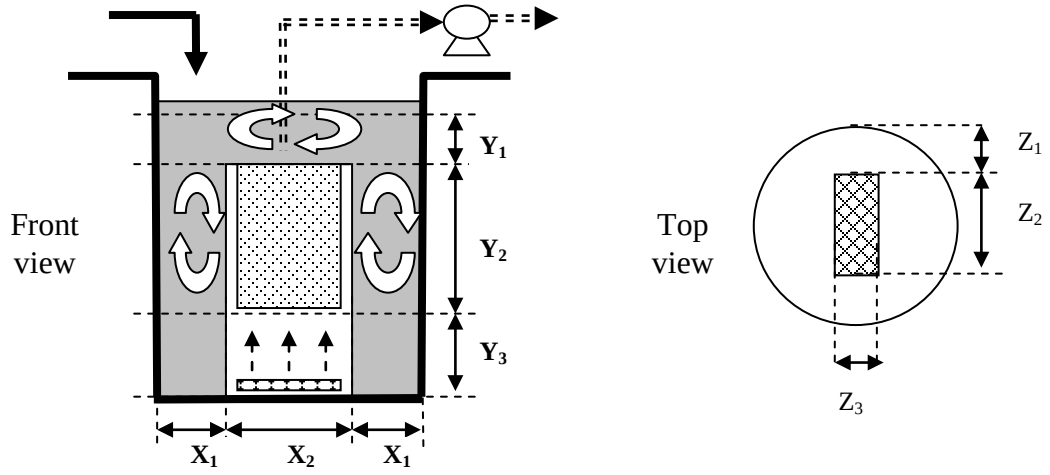

Fig. 3.7 Front view and top view of the membrane case in the aerobic unit

Height = $(Y_1+Y_2+Y_3)$ = (30+80+50) = 1.6 m.

Tank cross-section area: = $\pi [(X_2+2X_1)/2]^2 = \pi (1.06/2)^2 \approx 0.883\ m^2$

Mixing area = Tank area – membrane case area

= $0.883 - (Z_2 \times Z_3) = 0.883-(0.2\times0.5) = 0.748\ m^2$

Mixing volume around membrane cartridge = $0.748 \times 1.6 \approx 1.197\ m^3$

3.4.2 Commissioning of the pilot scale SMBR

Fig. 3.8 – Fig. 3.12 shows the experimental set up of the pilot plant MBR system. At first, the SMBR system was designed, constructed (with re-assembled materials) and preliminary tested in School of Engineering, James Cook University. Then, the whole SMBR system was moved to be re-established at Mt. St. John purification plant (Townsville city, north Queensland, Australia), which can supply a large volume of raw municipal wastewater.

Fig. 3.8 Pilot scale SMBR

Before commissioning with real sludge, membrane permeability and clean membrane resistance were determined using clean tap water. Later, municipal wastewater at Mt St John treatment plant was pumped through the anaerobic unit at a flow rate 150 L/h and passing through anoxic unit and aerobic-membrane unit,

respectively. MLSS concentration in the anaerobic, anoxic and aerobic-membrane units is initially seeded at around 3,600 mg/L. The solid retention time (SRT) can be arranged manually by daily volumetric discharged sludge. However, there was no sludge waste from the system in the beginning due to low sludge concentration. The coarse bubble aeration was supplied to the membrane tank in order to prevent membrane clogging as well as to provide oxygen for microbial growth.

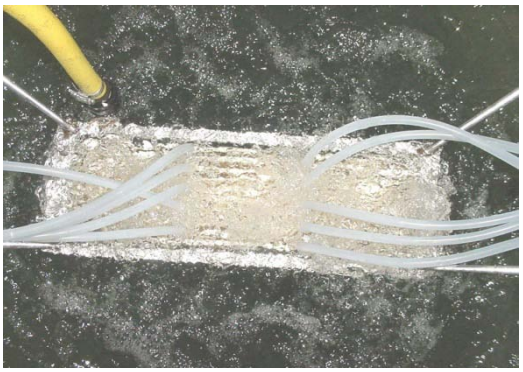

Fig. 3.9 Membrane unit in clean water

Fig. 3.10 PLC monitor of the system

Fig. 3.11 New membrane sheet

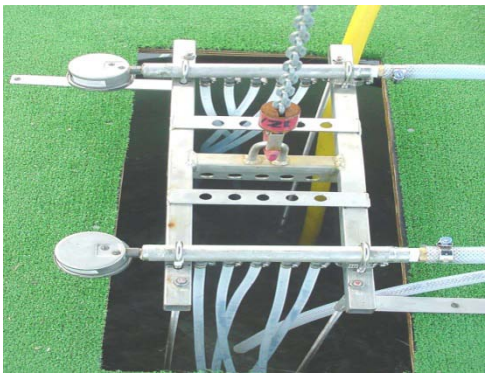

Figg. 3.12 Lifting up system of membranes

3.5 SMBR MODELING BASED DESIGN AND PERFORMANCE

3.5.1 Simulation results

3.5.1.1 Effect of anaerobic HRT and anoxic HRT

A size of anaerobic unit is determined in this study by simulation the efficiency of phosphate-phosphorous removal happening in this sequential treatment based on the steady state liquid flow (Qin = Qout) at fixed membrane flux 0.15 m^3/h. From Fig. 3.13, when the same sizes of anoxic (0.2 m^3) and aerobic membrane units (1.35 m^3) are applied in the simulation, the anaerobic unit shows different trends of phosphate removal at different HRT and SRT. The anaerobic unit does not present the effective removal of phosphate at the SRT 5 days as well as SRT 10 days removing phosphate less than 70 %. For SRT above 30 days, the efficiency of phosphate removal is similar and more than 90% for HRT 3 and 4 hrs, whereas the phosphate removal efficiency at HRT 1 and 2 hrs are about 70-80 %. Thus, HRT 1 hrs of anaerobic unit is selected as the satisfied HRT value for biological phosphate removal of this pilot SMBR. Few hours of anaerobic HRT which was sufficient for phosphate removal was informed in a study of Kargi and Uygur (Kargi and Uygur, 2002).

From Fig. 3.14, when the size of anaerobic and aerobic are fixed at 0.15 m^3 and 1.35 m^3, the removal efficiency of COD, NH_4-N and PO_4-P reach 70% and above for every anoxic HRT. MLSS concentration gradually declines as the expansion of HRT in anoxic stage. From EPS generation model (Nagaoka *et al.* 1998), the higher MLSS caused more EPS concentration that leads to the higher membrane fouling rate.

Therefore, the anoxic HRT 6 hrs is chosen as the operated HRT of the SMBR because of the lower number of MLSS increase.

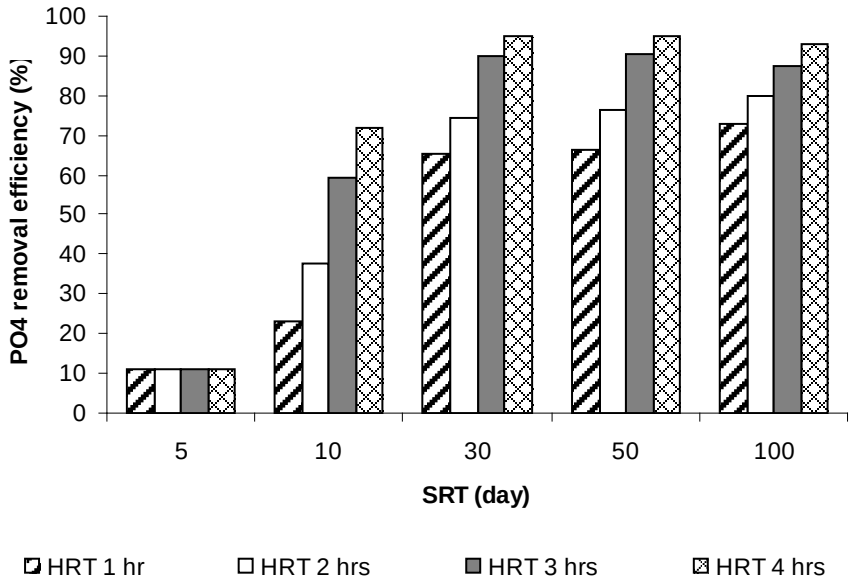

Fig. 3.13 Effect of anaerobic HRT on nutrient removal efficiency

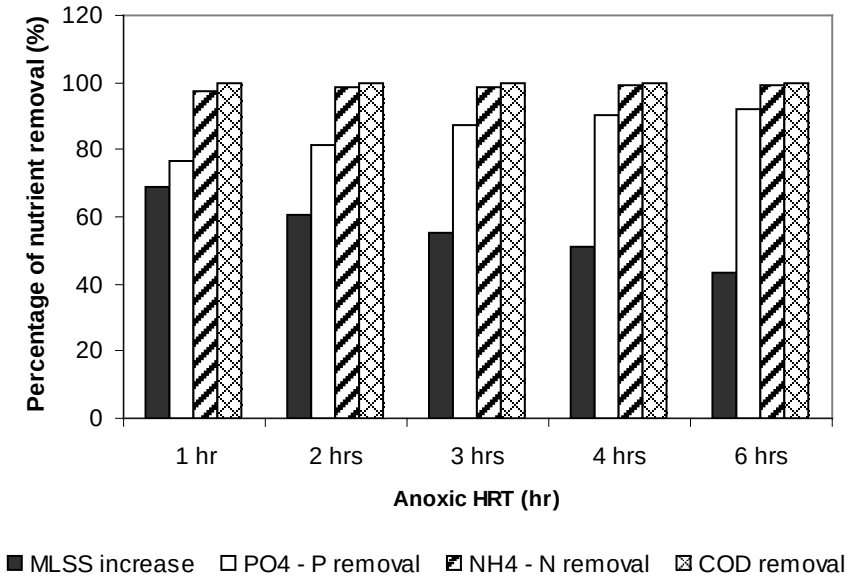

Fig. 3.14 Effect of anoxic HRT on nutrient removal efficiency

3.5.1.2 Effect of activated sludge ratio and internal recycle ratio

As shown in Fig. 3.15, some of the activated sludge waste is returned back to the anaerobic stage called return activated sludge while part of the outlet from aerobic unit is also went back to the anoxic stage called internal recycle. Tchobanoglous and Burton (2003) suggested typical design values of QRS 20%-50% influent and QIR 100%-300% influent for a combined nutrient removal system.

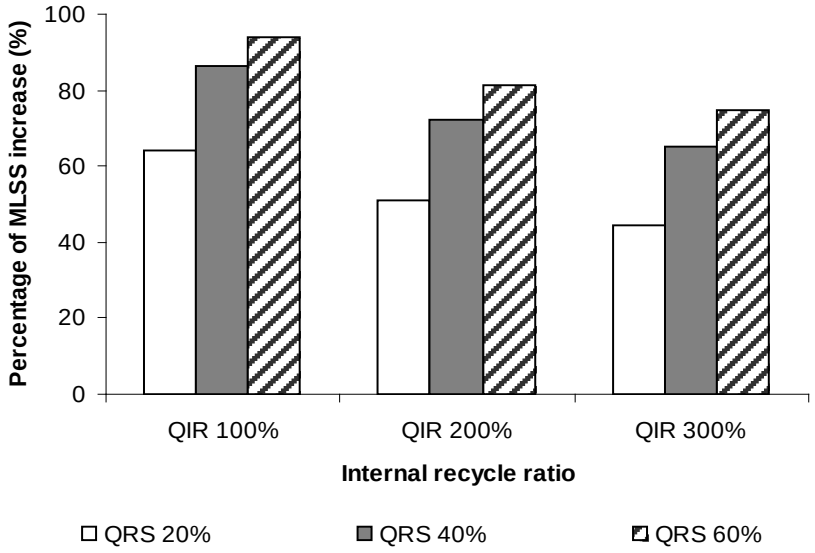

Fig. 3.15 Effect of return activated sludge and internal recycle

Ratio of QRS and QIR based on the inlet flow are simulated to see the effect of these two parameters on the treatment characteristics of the SMBR. Only the trends of MLSS concentration at different QRS and QIR are plot in Fig. 3.15 because the variation of QRS and QIR does not represent the significant differences of COD, NH_4-N and PO_4-P removal when the reactor volume of this sequential treatment are fixed. The suitable operational value of QIR and QRS can be justified at 300% and

20% respectively due to the reason of lower MLSS and membrane fouling as previous mentioned.

3.5.1.3 Optimum SRT

The percentages of relative membrane fouling are shown in Fig. 3.16. The higher SRT provides more time for microbial activities including cells and EPS synthesis which is the important substance to foul on membrane. Clearly, the membrane fouling trends caused by SRT are similar among SRT 30, 50 and 100 days, while the less membrane fouling happens at SRT 5 and 10 days. When the SRT is less than 10 days, the MLSS concentration reduce from the initial concentration down to some very low values because of higher wash-out rate than the growth rate of microbial. Therefore, the SRT 30 days is considered as the optimum SRT in this study because of no wash-out phenomena and less fouling trend. Similar results of fouling, MLSS increase and SRT were reported by Lee *et al.* 2002.

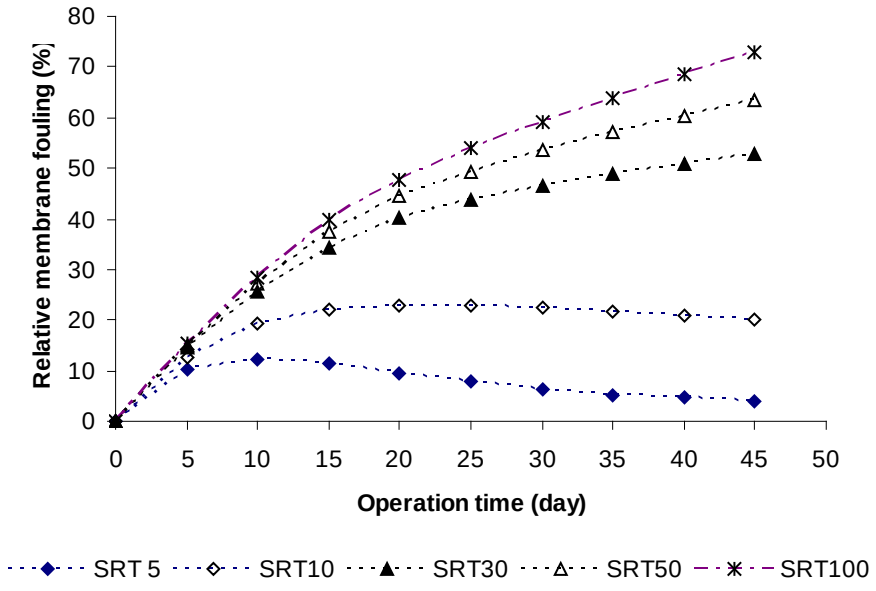

Fig. 3.16 Effect of return activated sludge and internal recycle

3.5.1.4 Summary of simulation results

Some design parameters of the pilot scale SMBR were evaluated by AQUASIM 2.0 process simulation program and can be summarized as follows:

- HRT 1 hour and 6 hours are recommended for operation of anaerobic and anoxic stages due to the high treatment efficiency and less sludge production.

- Return activated sludge 20% and internal recycle 300% influent are capable to maintain the high efficiency of nutrient removal at the less MLSS concentration.

- SRT 30 days is considered as the optimum SRT value which give the excellent treatment performance, less sludge production and slow fouling rate.

Samples were collected from the SMBR system once a week at the following 5 different positions: inlet and exit point of the system, within anaerobic, anoxic and aerobic-membrane unit. Determination of mixed liquor suspended solid (MLSS) concentrations were followed the standard methods for the examination of water and wastewater (APHA 2005). Dissolved oxygen (DO) and pH were measured using DO electrode (model ED1 (Aqua-D) version 1) and a pH meter (model IJ44 (Aqua-pH)) respectively, both from TPS company, Australia. Determination of Chemical oxygen demand (COD), ammonia, nitrate and phosphate were determined by Hach analyzer (Hach company, USA). The results of the SMBR treatment performance are shown in the following sections.

3.5.2 Sludge physical properties

Sludge physical properties of the SMBR system are detected including pH, oxidation-reduction potential (ORP), temperature, total dissolved solid (TDS). From Fig. 3.17, the inlet wastewater showed slightly higher average pH values than the other units due to a high ammonia loading in this incoming stream. However, it can be concluded that the average pH in all units of the SMBR system are fluctuating in the neutral range (6.4-7.6). On the other hand, a negative ORP value occurred at a very high TDS concentration in the inlet sample (Fig. 3.18 and Fig. 3.21). The higher oxidizing agent in water, the higher ORP will be obtained. A high enough ORP (650+ mV) can kill most bacteria, which is suitable for drinking water purification (Holmes-Farley 2002). As shown in Fig. 3.18, ORP profile visualized a reflect image to pH profile.

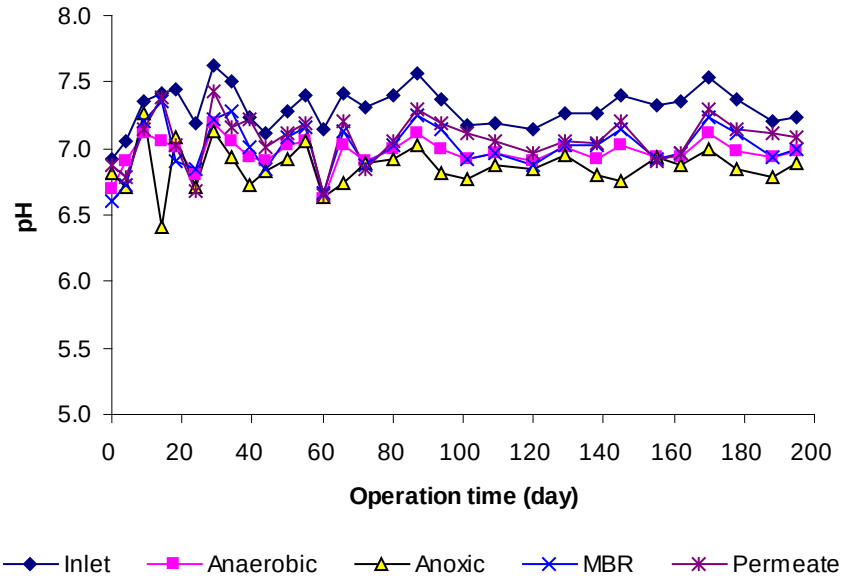

Fig. 3.17 Variation of pH values in the SMBR wastewater treatment

The SMBR system was kept in the climatic conditions with average temperatures between 23 and 31 ^{0}C. From Fig. 3.20, the inlet stream (from underground chamber) has a little lower average temperature than other outdoor units. Compared to the anaerobic and anoxic units, aeration in the aerobic-membrane unit also helps to reduce temperature 1-2 degree in membrane tank and permeate stream. From Fig. 3.21, the highest total dissolved solid (TDS) concentrations from the inlet stream sharply decreased in the anaerobic, anoxic and permeate, respectively. A slight increase of TDS occurred in the SMBR unit probably due to soluble microbial products produced in the aerobic system and also some dead cells decayed to become a readily biodegradable substance.

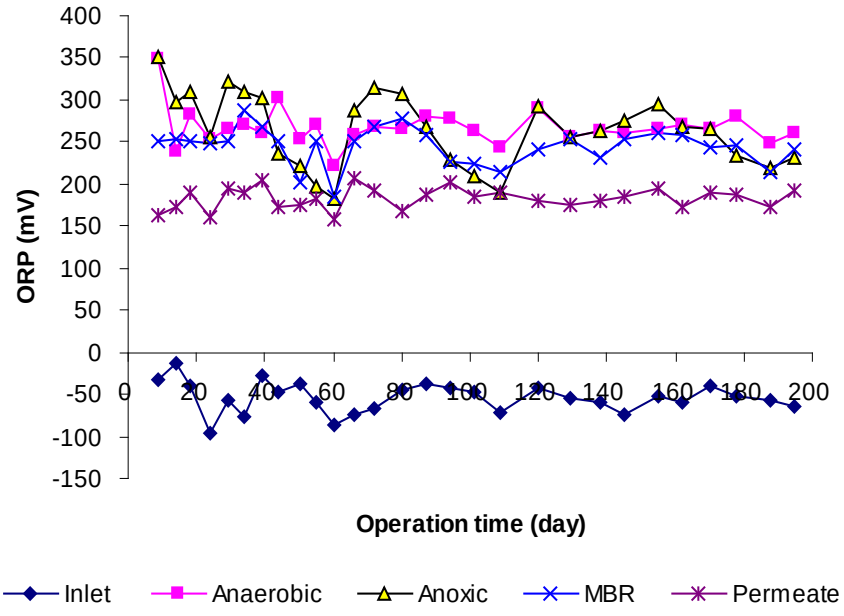

Fig. 3.18 Variation of ORP values in the SMBR wastewater treatment

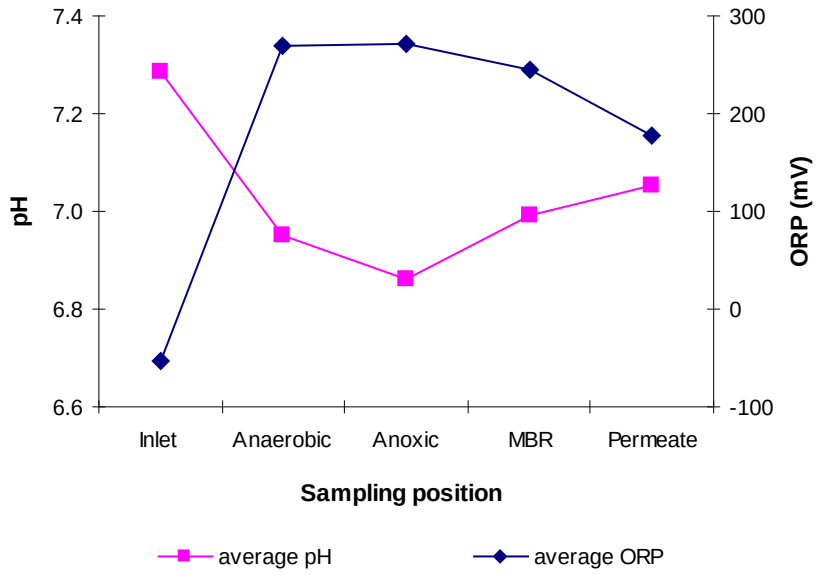

Fig. 3.19 Relationship between average pH and ORP in the SMBR system

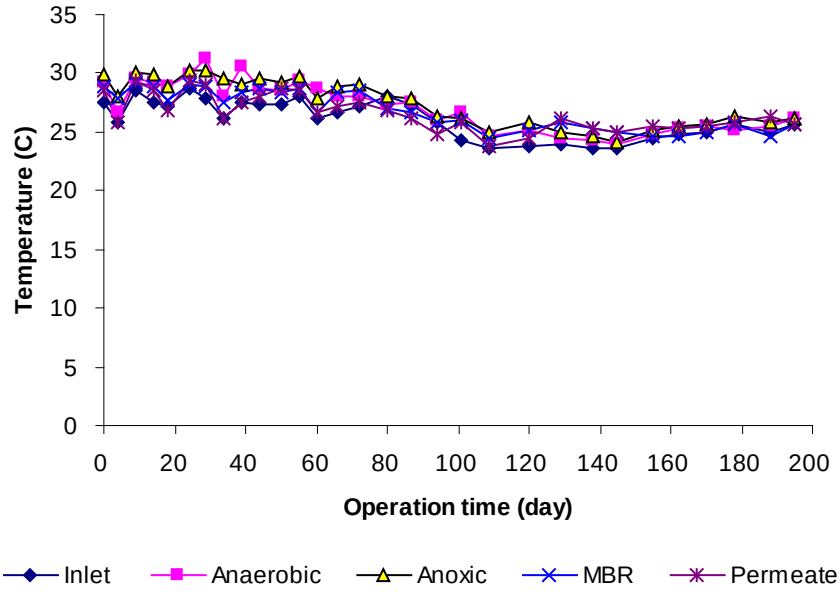

Fig. 3.20 Variation of temperature values in the SMBR wastewater treatment

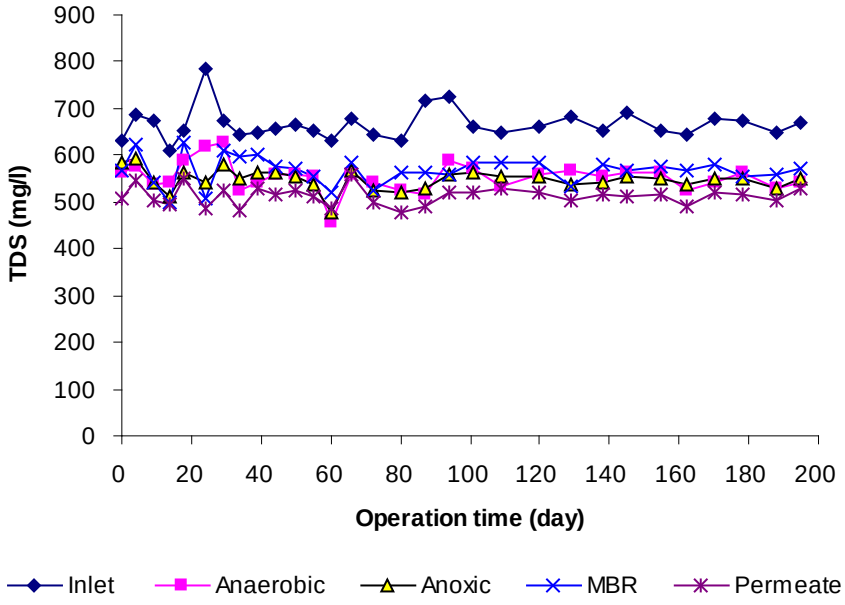

Fig. 3.21 Variation of TDS values in the SMBR wastewater treatment

3.5.3 DO and MLSS concentration

Fig. 3.22 and Fig. 3.23 showed the DO and MLSS concentrations of the SMBR system. From Fig. 3.22, the MLSS increased gradually from 3600 mg/L to 8,600 mg/L in the SMBR system. Coarse bubble aeration was provided in the aerobic unit, therefore, DO concentration (Fig. 3.22) in the membrane tank and permeate are higher than other units. As seen, the DO concentration in all units of the SMBR system is always greater than 1.5 mg/L which means the real anaerobic stage can not be happen properly as expected. A broken recirculation pump of the anoxic unit happened on the day 14th caused a sudden increase MLSS and particle sedimentation in anoxic unit following with a decrease MLSS concentration in the SMBR and anaerobic section (Fig. 3.23). Accordingly, on the day 14th, DO concentration (Fig. 3.22) is lower in the anoxic unit because of the greater oxygen consumption. Later, the broken pump was fixed and the regular trends of MLSS and DO continued.

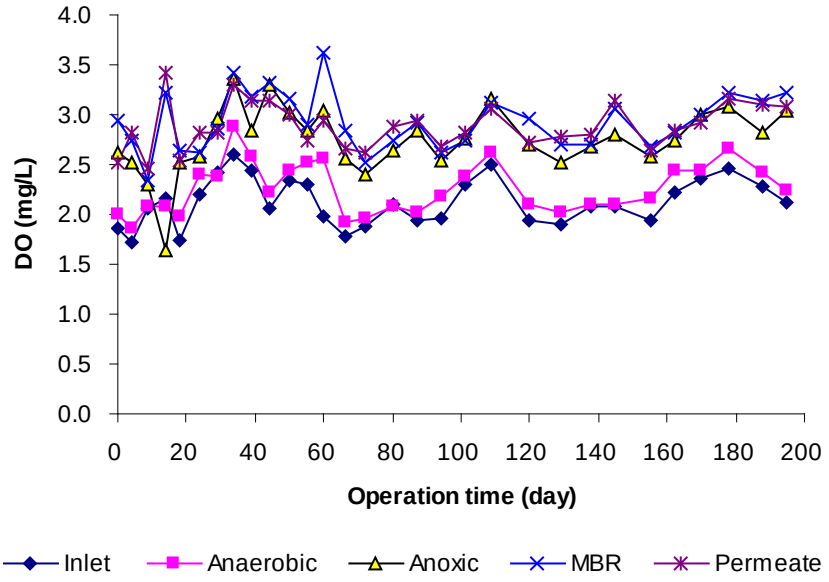

Fig. 3.22 Variation of DO values in the SMBR wastewater treatment

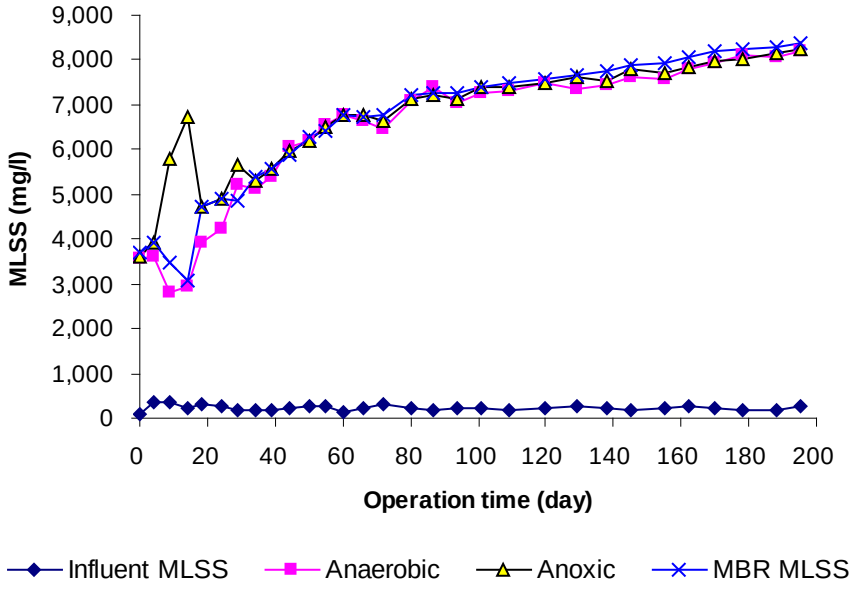

Fig. 3.23 Variation of MLSS values in the SMBR wastewater treatment

3.5.4 Nutrient removal in the SMBR system

From Fig. 3.24, the SMBR system displayed an excellent and stable removal of ammonia with nearly 100% removal efficiency since the 4th day by degrading all ammonia that presented in the raw wastewater. In theoretically, only the anoxic stage is sufficient to convert most the ammonia (NH_3) to nitrate (NO_3^-) through nitrification process.

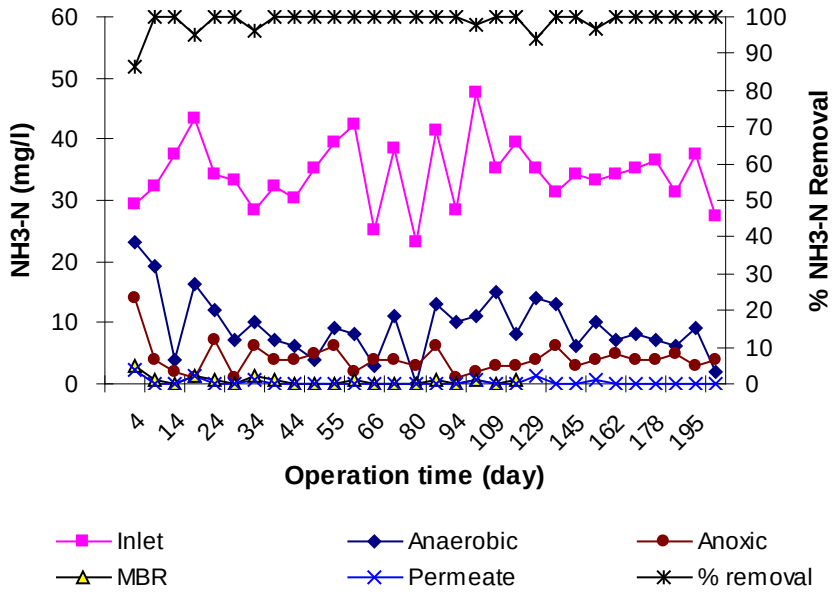

Fig. 3.24 NH_3-N removal in the SMBR wastewater treatment

From Fig 3.25, there was no nitrate concentration presented in the inlet stream of anaerobic unit. However, nitrate was highly produced in the anoxic and aerobic unit. With high DO concentration shown in Fig. 3.22, it can be implied that de-nitrification has not been initiated in the SMBR system yet. Thus, only nitrification process took place in the SMBR system conversing ammonium (NH_4^+) to nitrite (NO_2^-) and finally to nitrate (NO_3^-) by *Nitrosomonas* and *Nitrobactors*

bacteria, respectively (Beranek 2001). To remove nitrate, de-nitrification condition with deficiency of dissolved oxygen are needed for bacteria to consume nitrate as a terminal electron acceptor and convert it to nitrogen gas (Beranek 2001).

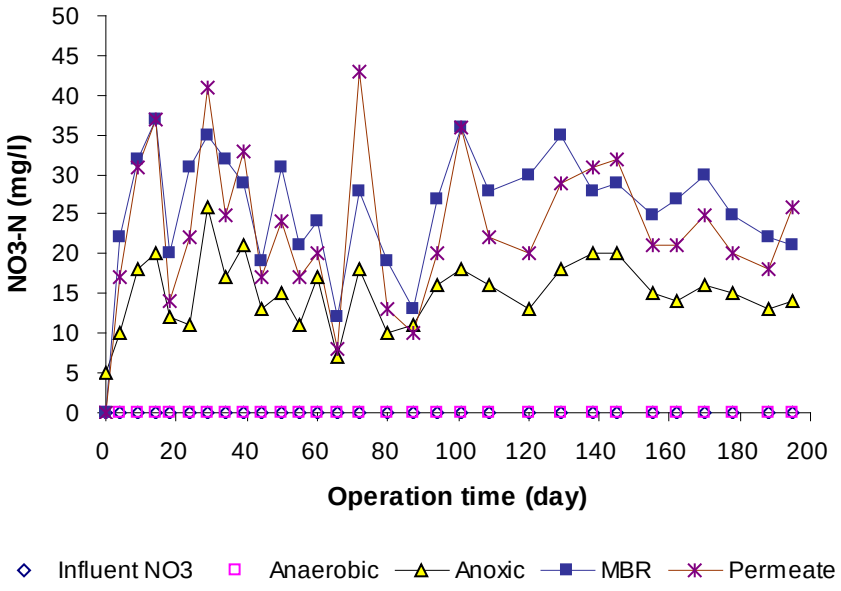

Fig. 3.25 NO_3^--N removal in the SMBR wastewater treatment

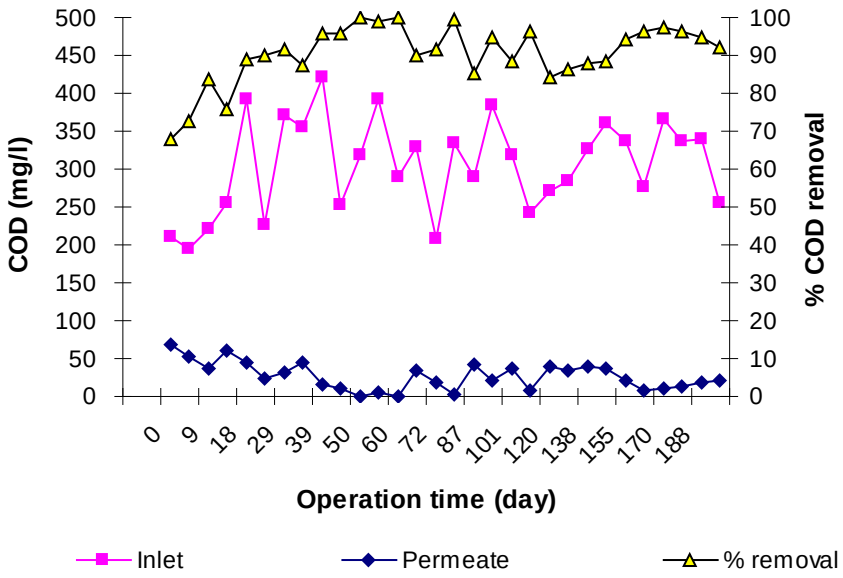

Fig. 3.26 COD removal in the SMBR wastewater treatment

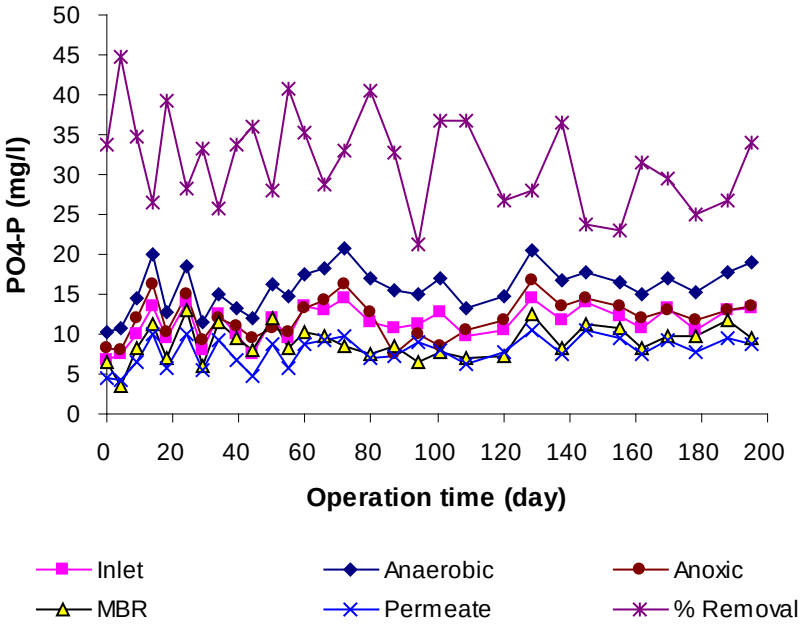

Fig. 3.27 PO_4-P removal in the SMBR wastewater treatment

Average COD removal of this SMBR system (Fig. 3.26) was about 90% and varied from 68 to 100%. In the anaerobic unit, phosphate-phosphorous concentration was increased around 1.4 times (Fig. 3.27) because of phosphorous accumulating organisms and slowly decreased consequently later in the anoxic, and aerobic-membrane unit, respectively. The total removal percentage from the influent was about 32% for phosphorous which could not be considered as good removal efficiency yet. Saito *et al.* (2004) reported that the presence of nitrite inhibits both aerobic and anoxic (denitrifying) phosphate uptake. In the same way, Beril and Ugurlu (2004) suggested that nitrate can affect phosphate release and lead to a reduction in the efficiency of biological phosphorus removal process. Further, when the ratio of the hydraulic retention times in the aerobic and anaerobic phases was around 0.6, phosphorous removal efficiency was higher than 90% (Sommariva *et al.* 1997).

3.6 CONCLUSIONS

A three stage SMBR pilot scale (total volume around 2.4 m^3) was designed and set up at Mt St John wastewater treatment plant (Townsville, Queensland). Some operating parameters are designed and evaluated by AQUASIM 2.0 process simulation and the results can be summarized as:

- Due to the excellent treatment performance, less sludge production and slow fouling rate, HRT 1 and 6 hours are recommended for operation of anaerobic and anoxic stages and SRT 30 days is considered as the optimum SRT.

- Return activated sludge 20% and internal recycle 300% influent are capable to maintain the high efficiency of nutrient removal at the less MLSS concentration.

A design based on biological treatment factors, fluid hydrodynamic factors and control logic factors were also considered and demonstrated. A construction and commissioning were accomplished and described. To investigate performance of the system, nutrient removal of this pilot scale SMBR were also detected and the following conclusions can be drawn:

- The SMBR sludge physical properties namely: pH, temperature, TDS, DO and MLSS were quite stable in the range of 6.4-7.6, 24-31 ^{0}C, 480-780 mg/L and 1.5-3.6 mg/L and 3,600-8,300 mg/L, respectively. The ORP profile was during -100 to 350 mV and visualized a eflect image to the pH profile.

- Although nitrate and phosphate removal has not been well achieved because of a high DO concentration interrupting the anaerobic and anoxic stages, the pilot-scale SMBR still presented a very good treatment efficacy of ammonia and COD.

CHAPTER 4

INFLUENCING PARAMETERS OF CRITICAL FLUX ASSESSMENT

4.1 INTRODUCTION

For submerged membrane technology, fouling is considered as the most severe hindrance to the system operation. There is a suggested border to handle this fouling problem called critical flux. Critical flux was initially defined in two ways: one is that the flux through the membrane has no increase in trans-membrane pressure (TMP) with time (Field *et al.* 1995) and another is the flux below which there is no deposition of colloids on the membrane (Howell 1995). In general, these will not give the same flux value. Above the critical flux, irreversible fouling of suspended solids forms a stagnant, consolidated and aggregated layer on the membrane surface, which can make flux decline rapidly. On the other hand, below the critical flux condition, called sub-critical flux, it has been reported that fouling is not observed (Chang *et al.* 2002). Consequently, the concept of critical flux is a key parameter for characterizing fouling.

Determinations of the critical flux have been proposed in three categories based on different considerations and analysis techniques. Based on direct observation, critical flux is the flux at which particles start depositing on the membrane surface, which has been observed by optical microscope (Li *et al.* 1998). This non-intrusive technique is normally applied for small size of glass flow cell membrane. Based on particle mass balance, critical flux can be observed by

measuring particle concentration at the inlet and outlet of the filtration unit and the maximum flux without particle deposition on the membrane surface can be considered as the critical flux (Kwon and Vigneswaran 1998). Based on filtration profile, the critical flux can also be defined as the point where the flux and TMP relationship becomes non-linear (Le Clech *et al.* 2003). Among these critical flux determination techniques, only the filtration profile is practical for pilot and full scale submerged membrane bioreactors (SMBR).

Moreover, critical flux can be considered in two forms: the strong form and the weak form. The strong form states that the sub-critical flux and TMP relationship shows a linear relationship with the same slope as that of pure water filtration. The weak form is also linear, but the slope is different from that of pure water (Fradin and Field 1999; Ye 2005). Until now, there is no standard methodology or precisely agreed-upon protocol to define the exact value of the weak form of critical flux.

Some studies suggested that it is possible to identify the weak form critical flux for SMBR systems at about two-third of the maximum flux at various operational conditions (Bacchin 2004). Many have defined the weak form critical flux as the point at which TMP and flux profile become non-linear (Metsämuuronen *et al.* 2002). Espinasse *et al.* (2002) showed an assessment of weak form critical flux based on a concept of fouling reversibility. In addition, a consideration of 90% permeability was reported for weak form critical flux determination (Le Clech *et al.* 2003). A hysteresis filtration profile has also been adopted as an *in situ* technique in submerged SMBR systems (Howell *et al.* 2004).

Recently, the concept of sustainable flux has been used to control membrane fouling problems. The sustainable flux is a more relaxed concept than the critical flux and considers membrane system operated at a low, rather than zero, fouling rates. The sustainable flux is the significant changing point of the fouling rate and relates to the operation and sustainability of a membrane process, but they are not critical fluxes as defined above (Bacchin *et al.* 2006).

In general, a short term critical flux determinations can be made with flux-stepping method. The main variables involved in this method are step height and step length. Le Clech *et al.* (2003) were the first one focused on the effect of these variables on the critical flux evaluation. They have shown that the step length between 5 to 60 minutes did not significantly affect the critical flux value, but the increasing of step height from 3 to 9 $L/m^2.h$ increased membrane fouling.

Fane (2002) described three factors affecting critical flux and membrane fouling, which include membrane materials and configurations, operating parameters and sludge characteristics. The effects of mixed liquor suspended solids (MLSS) concentration on critical flux have been subjected to numerous studies because membrane fouling is often considered to be caused by the particle cake formation on the membrane surfaces. Madaeni *et al.* (1999) observed that critical flux was inversely related to MLSS concentration range 0 to 10 g/L. On the other hand, Le Clech *et al.* (2003) indicated that significant increase in critical flux happened only when the MLSS concentration was 12 g/L but with no difference of critical flux for MLSS range 4-8 g/L. Although the same type of membrane and similar hydrodynamic conditions were used in the experiments, significantly different critical flux values were reported by Madaeni *et al.* (1999) and Cho and Fane (2002): 62

$L/m^2.h$ for 4 g/L MLSS and 22 $L/m^2.h$ at 2.5 g/L, respectively. This observation demonstrates the importance of carrying out tests under the same biological conditions for assessing hydrodynamic parameters and impacts. The actual method of changing MLSS concentration can impact biomass characteristics, since it can be changed both with and without acclimatization (Cicek *et al.* 1998).

Membrane operation with little to no fouling and low energy consumption is a desirable target for any membrane plant. Hence, the relationship between aeration and critical flux should be studied and optimized as they are the main parameters determining economic viability. Bouhabila *et al.* (2001) reported that increasing the air intensity from 1.2 to 3.6 $m^3/m^2.h$ decreases the total filtration resistance, thus increasing the filtrate flux by a ratio of 3 in a pilot submerged MBR. Chang *et al.* (2002) applied two coarse bubble aerations in a submerged tubular MBR and reported that the flux was increased by 43%. Ueda *et al.* (1997) also described aeration as a significant factor governing the filtration conditions and cake removal.

In most of the previous critical flux analysis, filtration was carried out with lab scale and sometimes fed with synthetic sewage which, in fact, has substantially different fouling propensities compared to those of pilot or full scale operating with real sewage. The aims of this chapter are therefore threefold: (1) to determine critical flux using a pilot scale SMBR fed with real sewage; (2) to compare the critical flux values obtained from various determination methods; (3) to understand the impacts of assessment variables on the critical flux including step length, step height of filtration, MLSS concentration and aeration.

4.2 EXPERIMENTAL MATERIALS AND METHOD

4.2.1 Experimental facility

A pilot scale SMBR used in this study was installed at Mt St John – Townsville Fig. 4.1) consisted of a 150 liter first treatment unit, a 900 liter anoxic treatment unit and a 1,400 liter aerobic unit fitted with a Kubota submerged flat-sheet membranes model LF10. The membrane unit comprises of ten flat sheets (chlorinated polyethylene) with nominal pore size 0.4 µm, total effective area 10 m^2. Permeate was removed using a helical rotor pump passing through permeate line and flow transmitter. Pressure transducers (PT) were located at the base of the membrane reactor and on the permeate line. The aeration process was conducted using two blowers and controlled using air rota-meter and digital control valve. Operation of the influent pump was controlled by floating switch and water level in the aerobic tank.

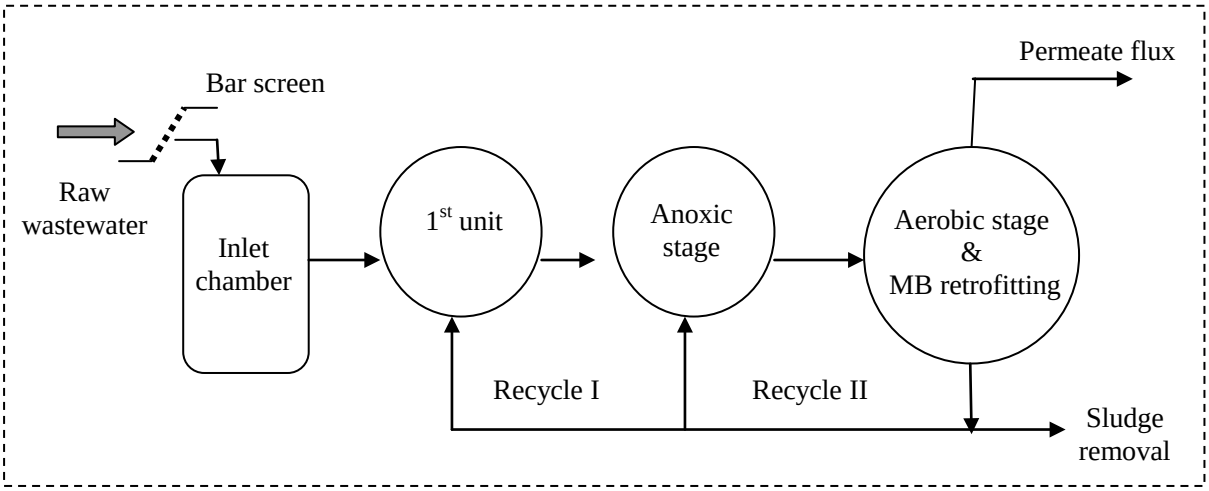

Fig. 4.1 Schematic diagram of SMBR pilot plant

A programmable logic controller (PLC) device collected the data of the PT and all the control variables of the system were realized through it. The SMBR system was originally seeded with sludge from a full scale SMBR plant existing in Townsville. Real municipal wastewater was then used as a feed to the system, flowing to the first unit and overflowing to the second and last units in series. Sludge from the aerobic compartment was recycled to the first and the second units with recycle ratio (Q_{rec}/Q_{in}) of 0.2 and 3, respectively. The characteristics of wastewater used in the experiment were shown in table 4.1.

Table 4.1 Characteristics of wastewater used in the experiment

Parameter	Inlet	1st unit	Anoxic	SMBR	Permeate
pH	7.17 ± 0.1	7.00 ± 0.1	6.93 ± 0.1	7.08 ± 0.1	7.11 ± 0.1
Temp (^{o}C)	27.3 ± 0.7	28.2 ± 0.7	28.6 ± 0.7	27.6 ± 0.9	27.2 ± 0.8
DO (mg/L)	2.00 ± 0.17	2.18 ± 0.26	2.64 ± 0.20	2.93 ± 0.34	2.81 ± 0.13
Conduct. (µS)	1282 ± 59	1075 ± 55	1094 ± 70	1118 ± 35	1023 ± 66
ORP (mV)	-61.5 ± 16.4	260.5 ± 18.9	258.8 ± 51.8	248.3 ± 30.3	182.2 ± 16.1
MLSS (mg/L)	219 ± 76	5963 ± 312	6836 ± 280	6839 ± 298	N/A
NH_4-N (mg/L)	33.2 ± 7.8	7.6 ± 4.6	3.4 ± 1.6	0.3 ± 0.5	0.0 ± 0.0
NO_3-N (mg/L)	0.0 ± 0.0	0.0 ± 0.0	37.2 ± 11.4	19.5 ± 5.7	18.5 ± 11.7
PO_4-P (mg/L)	12.2 ± 1.7	17.3 ± 1.9	12.4 ± 2.8	8.9 ± 0.9	7.9 ± 1.4
COD (mg/L)	307 ± 56	N/A	N/A	N/A	17 ± 16

Note: ± term is represent standard deviation

4.2.2 Experimental design

The influences of step height (or the size of flux increasing in each step), step length (or the duration of filtration in each step) and determination methods of critical flux were investigated as shown in table 4.2. The TMP and permeate data of the experiments were logged every minute on the PLC device. For testing the influence of aeration and sludge concentration, four aerations (60, 90, 120 and 150 l/min) and three MLSS concentrations (4.2, 6.3 and 8.5 g/L) were carried out in a total of 12 runs. After finishing each test, the membrane surface was cleaned with soft sponge to ensure removal of sludge particles from the membrane surface and a chemical cleaning of 0.5% sodium hypochlorite was proceeded in place to remove irreversible fouling from membrane pore blocking. Then the next test was continued.

Table 4.2 The operational conditions for testing the effect of step height, step length

Step length (min)	Step height ($L/m^2.h$)	Filtration method	Critical flux determination method
15	2 4 8	Flux stepping/ Flux cycling	- based on 2/3 flux limitation - based on flux linearity - based on 90% permeability - based on hysteresis curve - based on flux reversibility[1]
30	2 4 8	Flux stepping/ Flux cycling	

Note: MLSS 4.2 g/L and aeration 60 L/min, Only flux cycling is applied for flux reversibility which is based on Espinasse *et al.* (2002).

4.2.3 Flux stepping and flux cycling methods for critical flux test

In this study, critical flux was assessed using short-term tests using flux stepping and flux cycling methods. The flux stepping method (Fig. 4.2) has been

widely used for critical flux assessment (Madec *et al.* 2000; Cho and Fane 2002; Le Clech *et al.* 2003). In this method, the filtration is carried out at a fixed flux for a certain time. This procedure is repeated by incrementally increasing the flux until a noticeable increase in trans-membrane pressure (TMP) is observed (Wicaksana 2006). The hysteresis curve can also be done by stepping the filtration downward.

TMP and flux data obtained from the short term experiments can be used to produce derived parameters (Le Clech *et al.* 2003) as follows:

Permeability of the system: $$K = \frac{J}{P_{ave}} \quad \textbf{4.1}$$

Filtration resistance-series model : $$J = \frac{\Delta P}{\mu R_i} = \frac{\Delta P}{\mu (R_m + R_f)} \quad \textbf{4.2}$$

All parameters used in equation 4.1 and 4.2 are addressed in appendix E.

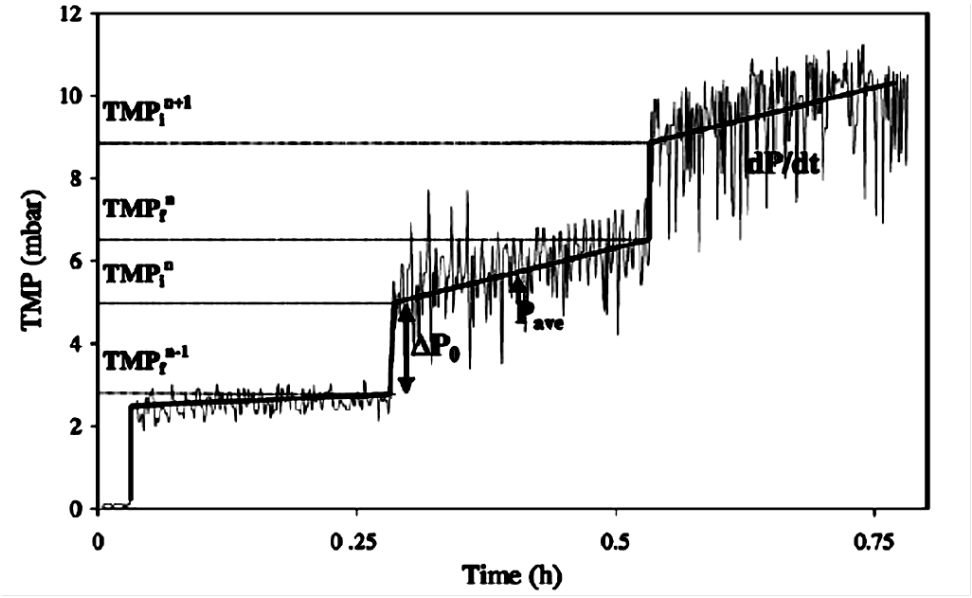

Fig. 4.2 Flux stepping filtration (Le-Cleach *et al.* 2003a)

On the other hand, the flux cycling procedure proposed by Espinasse *et al.* (2002) is to alternate positive and negative pressure changes, as shown schematically

in Fig. 4.3. Anytime the pressure is set to any new value, the flux is monitored and the system waits until the flux stabilizes over time. A new pressure value can then be set. By comparing the steady-state flux obtained at steps 1 and 4 (in Fig. 4.2), one can deduce if a flux limitation observed in step 3 is due to an irreversible fouling or to reversible phenomena. For example, if the flux in step 4 is on point *b*, fouling is 100% irreversible, and, if the flux is on point *a*, fouling is totally reversible; therefore, a fraction of reversibility can be ascribed according to the flux value at step 4 (included on segment *a*-*b*) (Espinasse *et al.* 2002).

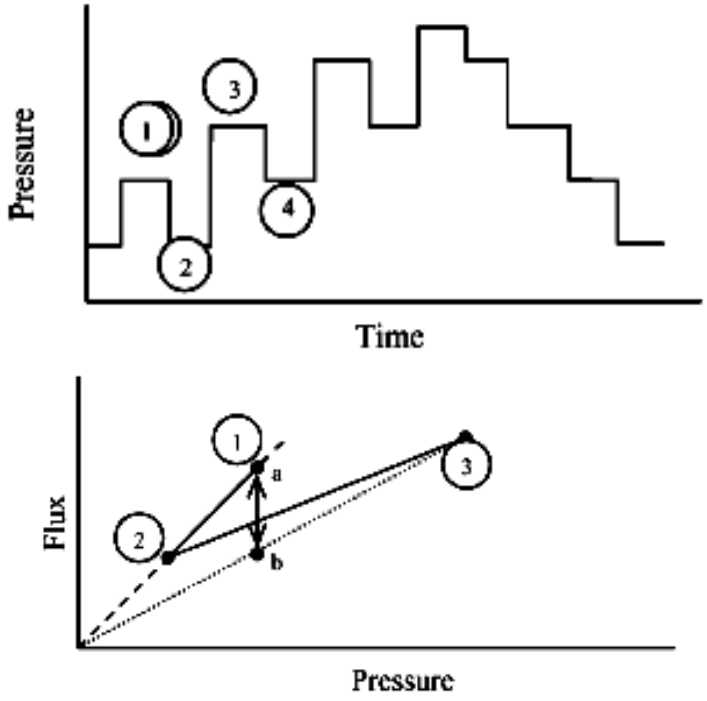

Fig. 4.3 Critical flux determination by flux cycling method (Esspiness *et al.*, 2002)

Such a procedure makes possible the differentiation between reversible fouling and a deposit all along a range of pressure and flux. This procedure is developed for searching critical flux as a decrease in pressure after each increasing pressure step allows determining fouling irreversibility (Howell 1995; Chen *et al.* 1997; Gesan *et*

al. 1999). In this study, the flux cycling filtration was operated followed Bacchin *et al.* (2006) by increasing flux two steps and then decreasing one step and TMP was measured at each operating step.

4.3 RESULTS AND DISCUSSION

Results and discussion of the experiments are described in the following sections including clean water flux test, strong and weak form critical flux, sustainable flux and influencing parameters for critical flux enhancement.

4.3.1 Clean water flux tests

Clean water flux tests at different aeration rates were conducted as a reference for new membrane performance, before replacing clean tap water with activated sludge in the aerobic membrane unit.

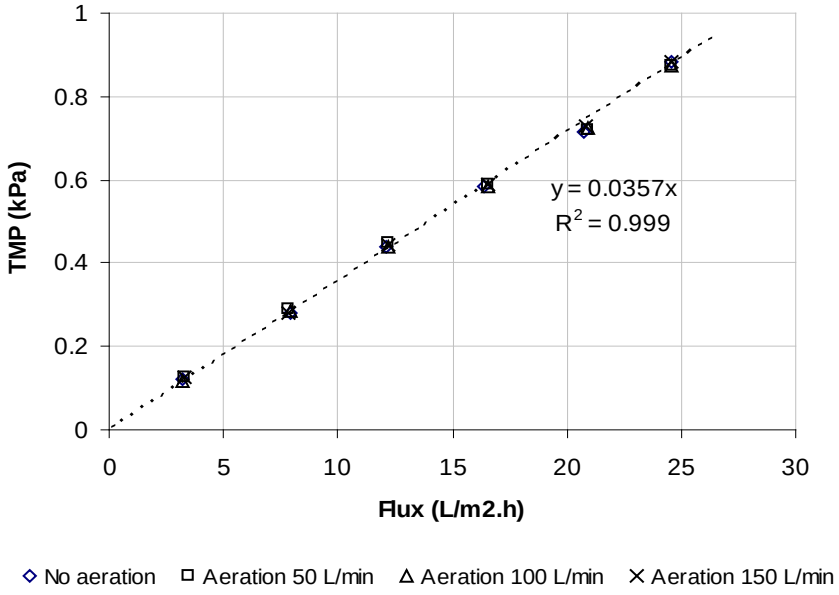

Fig. 4.4 Clean water flux test at different aeration intensities

As shown in Fig. 4.4, aeration showed no significant influence on the water filtration rates. A linear relationship between the permeate flux increase and the TMP increase was observed. The new membrane resistance is 1.285 x 10^{11} (1/m) estimated using Darcy's Law in Equation 4.2 by neglecting the fouling resistance term due to clean water filtration.

4.3.2 Strong form critical flux

The strong form critical flux which has a linear relationship between flux and TMP with the same slope as that of pure water can be evaluated based on the deviation between the clean water and the sludge filtration profiles.

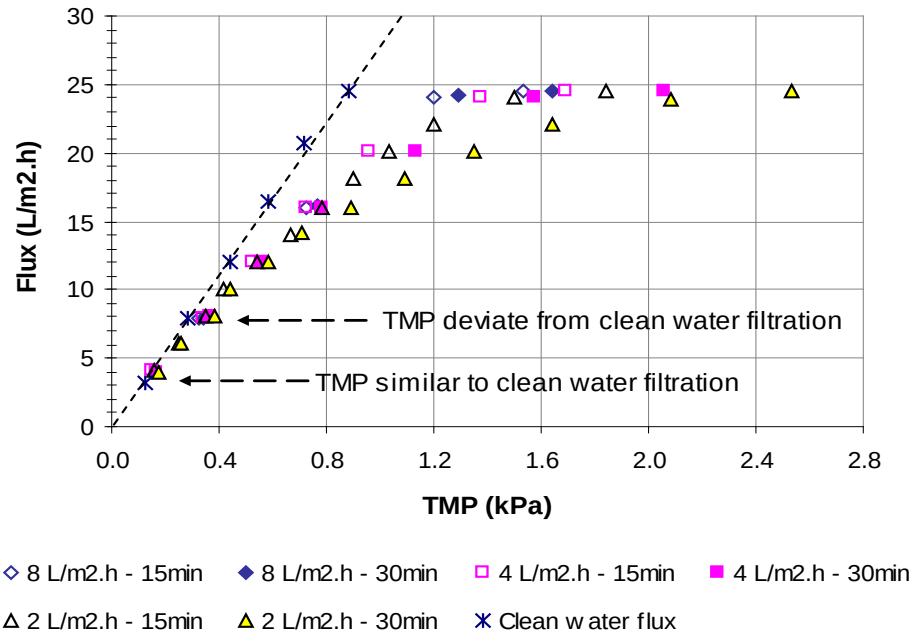

Fig. 4.5 Strong form critical flux at different step lengths and different step heights

The straight line in Fig. 4.5 represents pure water TMP as a function of flux measured before the sludge filtration. As shown in Fig. 4.5, the TMP followed fairly

closely the pure water TMP in the beginning and gradually increased until flux exceeded a particular value then TMP increased much more rapidly. From Fig 4.5, the strong form critical fluxes for all tests are around 5-6 L/m^{2}h. There was no substantial difference of strong form critical fluxes obtained using various step heights and step lengths. However, the strong form critical fluxes are normally not recommended for membrane operations due to very low permeate yields.

4.3.3 Weak form critical flux

4.3.3.1 Determination of critical flux through limiting flux

The limiting flux is classically defined as the maximum steady state flux obtained when increasing the TMP (Bacchin *et al.* 2006). The limiting flux is reached when the membrane surface operates above the critical flux and corresponds to a flux for which the fouling saturates the filtration capacity of the membrane (*i.e.* when a further increase in flux at any point on the membrane surface leads to another layer deposit fully compensating the increased pressure drop) (Defrance and Jaffrin 1999). The limiting flux and weak form critical flux can be theoretically related by considering a simple model for critical deposit of colloidal system.

The difference between the values of critical flux and limiting flux can thus be physically related to the existence of a critical flux distribution of different properties along the membrane surface as explained by Bacchin (2004). By taking into account the distribution of mass transfer coefficient along the membrane induced by the boundary layer development, Bacchin (2004) estimated critical flux has a value of

two-thirds the limiting flux. This means a filtration should never be exceeded by two-third of the limiting flux to avoid any deposit on the membrane.

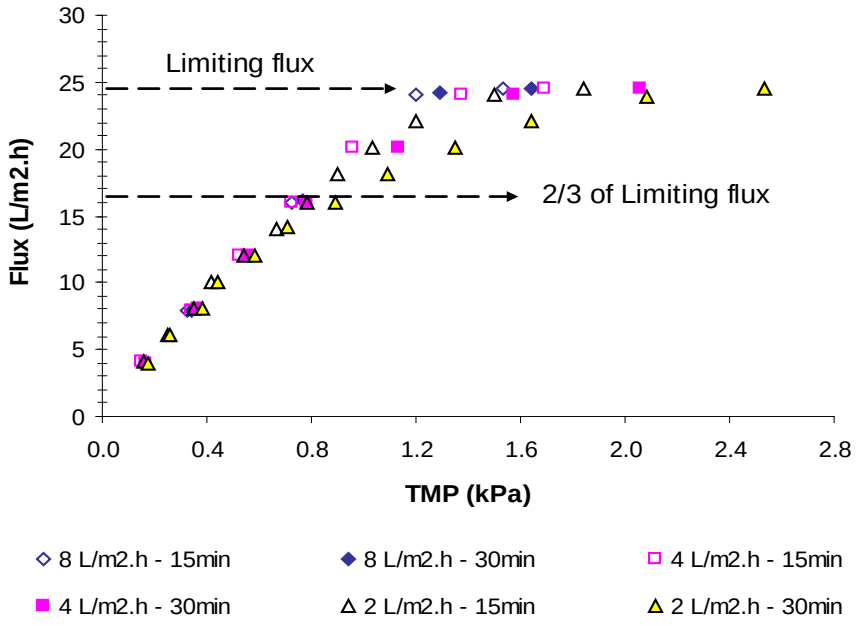

Fig. 4.6 Critical flux evaluated based on two-third limiting flux at different step lengths and step heights

Fig. 4.6 indicates a limiting flux around 24 L/m^{2}h for all filtrations. A critical flux of approximately 16 L/m^{2}h based on two-third limiting flux is drawn for all filtrations. Clearly, the critical flux determined based on its relationship with the limiting flux is constant and independent from a variation of step heights and step lengths. In addition, the same limiting flux obtained using fixed TMP and fixed flux operating modes were reported, although they corresponded to different cake formation processes (Defrance and Jaffrin 1999). Psoch and Schiewer (2005) estimated their critical flux for sludge filtration (approximately 13 L/m^{2}h) based on two-third of their limiting flux and the new flux below the critical point (11.5 L/m^{2}h) was chosen as an optimal condition. However, no sub-

critical conditions were observed, since fouling occurred. This implies that the flux exceeded the critical flux (defined as the flux below which no fouling occurs).

4.3.3.2 Determination of critical flux through flux linearity

Determining a weak form critical flux by inspecting the point for which there is a departure from linearity is shown in Fig. 4.7. As seen in Fig. 4.7, there are two zones of the filtrations that are of note: the dependant and independent pressure zones. However, there is no sharp transition between these regimes. From Fig. 4.7, the linearity between the flux and the TMP remain until the flux reaches 12 L/m^{2}h of the filtration at 30 min step length and 4 L/m^{2}h step height. Above the flux 12 L/m^{2}h, the TMP increases markedly. Accordingly, the critical flux based on flux linearity in Fig. 4.7 can be estimated at the last observed linear flux and the flux beyond (12 + 16)/2 = 14 L/m^{2}h.

Fig. 4.8 presents the critical flux values based on flux linearity at different runs with different filtration variables (more details of experimental data are shown in appendix B). From Fig. 4.8, the step heights (2, 4 and 8 L/m^{2}h) have more influence on the variation of the critical flux than the step lengths (15 and 30 minutes) and an inverse relationship between step height and critical flux is clearly observed. Only at the step height 2 L/m^{2}h, the different step lengths give a significant difference on the critical flux values.

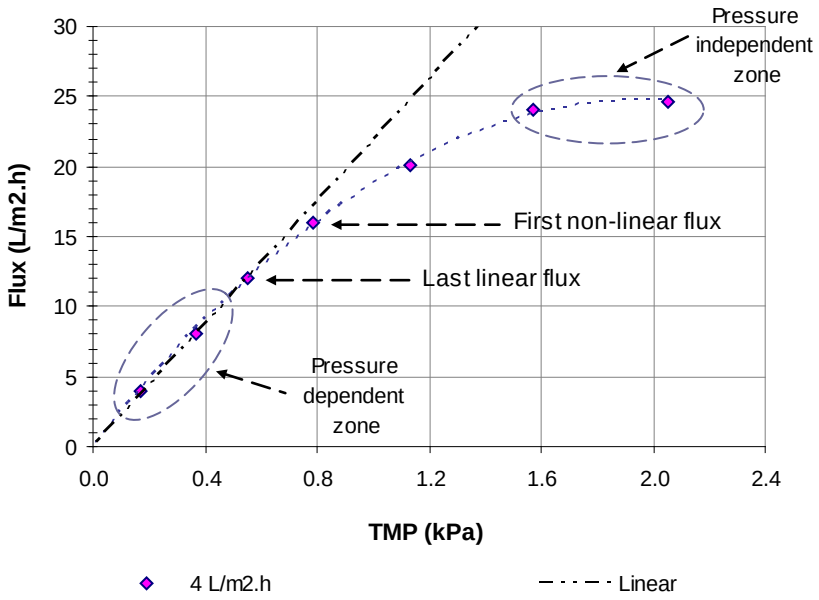

Fig. 4.7 Flux and TMP profile at step height 4 L/m^{2}h and 30 min step length

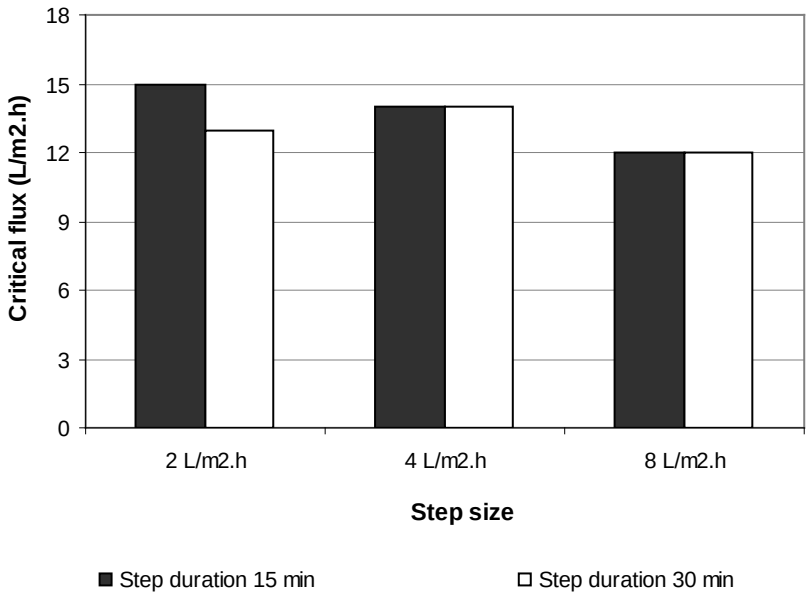

Fig. 4.8 Comparison of critical flux evaluated based on flux linearity at different step heights and step lengths

In fact, the accuracy for the evaluation of critical flux based on flux linearity is directly related to the step increment chosen for the experiment due to the critical flux averaging between the final linear flux and the non-linear flux beyond. Thus, the larger the flux step applied, the more error the critical flux averaging can be occurred. Defrance and Jaffrin (1999) suggested an optimal operation lying at the upper boundary of the sub-critical region, at a permeate flux just below the critical flux. Therefore, the critical flux averaged from different flux step values can affect the selection of sub-critical flux condition. In this case, a small step height is suggested to perform for critical flux assessment due to lower error of flux averaging.

4.3.3.3 Determination of critical flux through 90% permeability

According to the permeability definition in Equation 4.1, weak form critical flux can be defined at the maximum flux for which K remains linear. Le Clech *et al.* (2003b) assumed it to be the flux at which permeability decreases to below 90% of the permeability recorded for the first filtration step. Therefore, the critical flux can be taken as the mean of the maximum flux at which K is higher than $0.9K_0$ and the subsequent flux-step value, since these two values, respectively, represent the lower and upper boundaries of the critical flux region (Guglielmi *et al.* 2007).

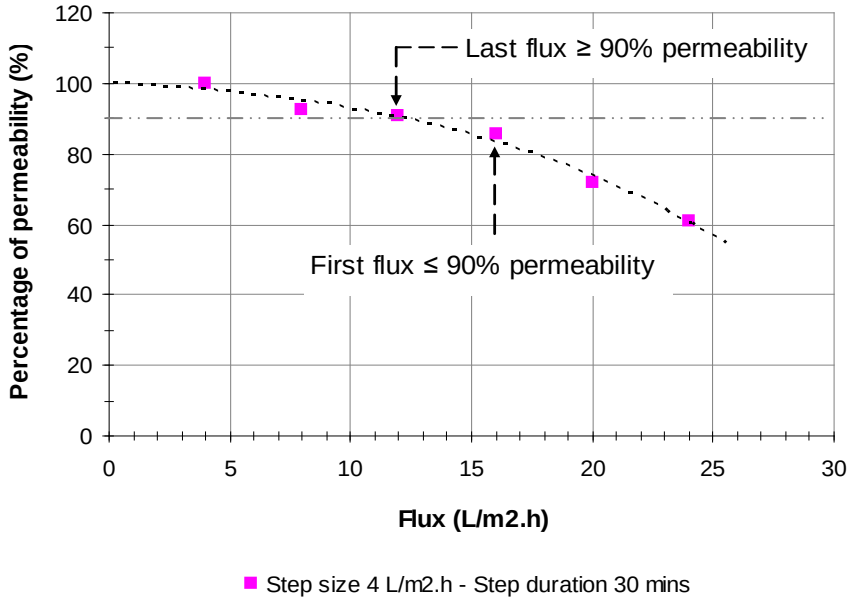

Fig. 4.9 Permeability at step heights 4 L/m^{2}h and 30 min step length

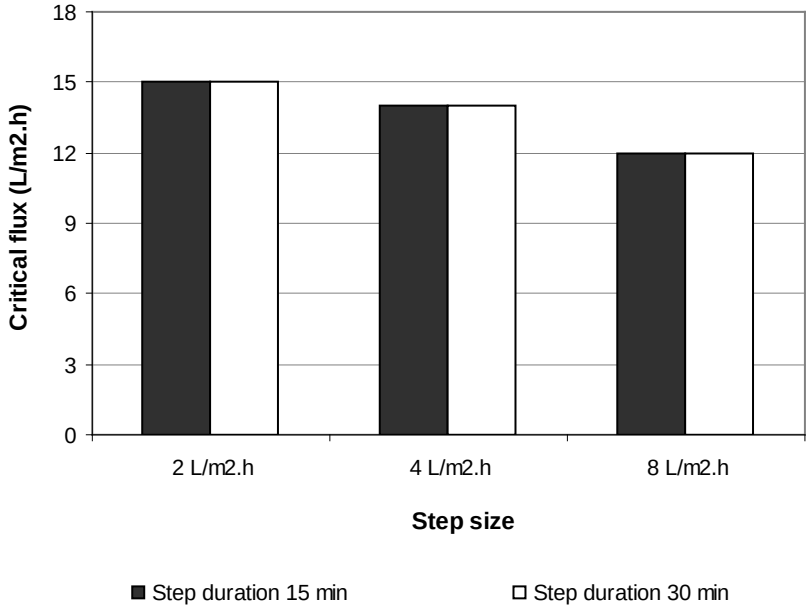

Fig. 4.10 Comparison of critical fluxes evaluated based on 90% permeability at different step heights and step lengths

Fig. 4.9 showed the trend of permeability and imposed fluxes. The critical flux determined based on such method using different variables is illustrated in Fig. 4.10 (more details of experimental data are shown in appendix B). Critical flux based on 90% permeability and flux linearity gives similar critical flux values with slight differences for a step height of 2 L/m^2h and 15-minute step length. Clearly, only the step heights of flux increment have significant impact on the critical flux values while there is no effect of the step length can be found in Fig. 4.10. Also, Fig. 4.10 reveals a negative relationship between the increasing step heights and critical flux decrease.

4.3.3.4 Determination of critical flux through fouling reversibility

Membrane fouling reversibility can be accomplished using both flux-stepping and flux-cycling methods. To assess the reversibility of fouling using flux-stepping, steps of filtration have been carried out upwards and then downwards to the initial flux (see Fig. 4.11). Hysteresis of TMP was observed when the flux was reduced, as it had been when the flux was being increased. This hysteresis technique was useful to identify critical flux based on reversible fouling *in situ* the submerged MBR processes (Howell *et al.* 2004). The reversibility of fouling can also be evaluated using the flux cycling method (Espinasse *et al.* 2002; Bacchin *et al.* 2006) (see Fig. 4.12). Differences in TMP measured at the same flux represent the points of when irreversible fouling occurs in the system. Compared with Fig 4.11, the flux cycling technique (in Fig 4.12) gives slightly greater TMP recovery than the hysteresis of flux stepping. However, flux cycling technique can reduce the disadvantage of accumulative TMP in the low flux stage because it allows immediate flux recovery.

The decline in flux (in Fig. 4.12) decreased the convection towards the membrane, which makes it possible for solute to back-diffuse away from the membrane surface.

In this study, experiments operated using the hysteresis of flux stepping and flux cycling methods were also carried out at various step heights (2, 4 and 8 L/m^{2}h) and step lengths (15 and 30 min). Results are presented in Fig. 4.13 and Fig. 4.14 in terms of imposed flux versus TMP. Details of these experiments are shown in appendix B. A critical flux determination is taken between two experimental points: here *a* and *b* (the reversible and irreversible filtration points, respectively), and an average flux is taken of these two fluxes (J_a and J_b). If irreversible flux occurred in the system, it means a balance between convective transport and back transport at such a flux condition cannot be maintained, thus exceeding a critical flux condition.

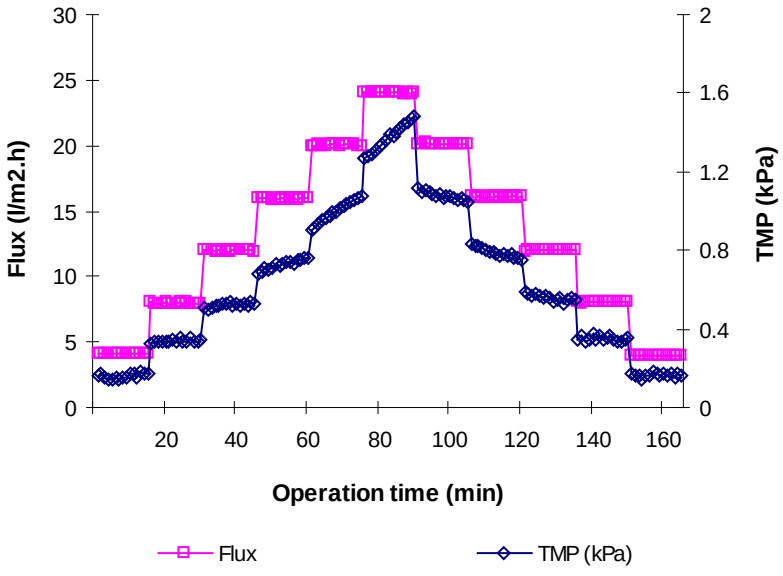

Fig. 4.11 Stepping filtration at step height 4 L/m^{2}h and 15 min step length

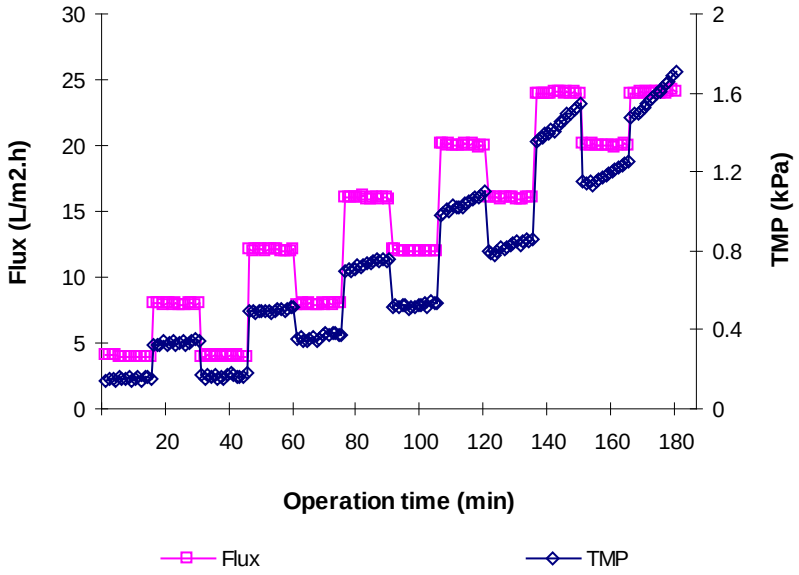

Fig. 4.12 Cyclic filtration at step height 4 L/m^{2}h and 15 min step length

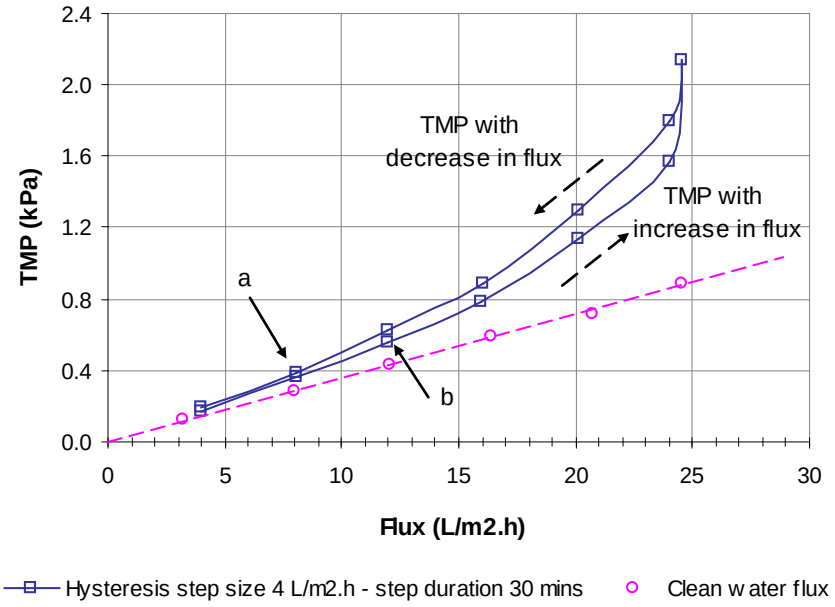

Fig. 4.13 Flux reversibility of stepping filtration at step height 4 L/m^{2}h and 15 min step length, where a = the last reversible flux and b = the first irreversible flux

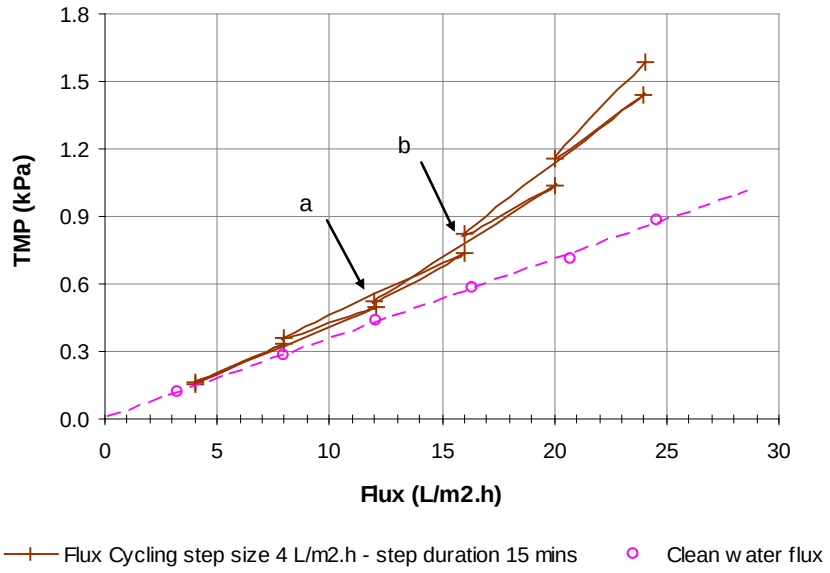

Fig. 4.14 Flux reversibility of cyclic filtration at step height 4 L/m^{2}h and 15 min step length, where a = the last reversible flux and b = the first irreversible flux.

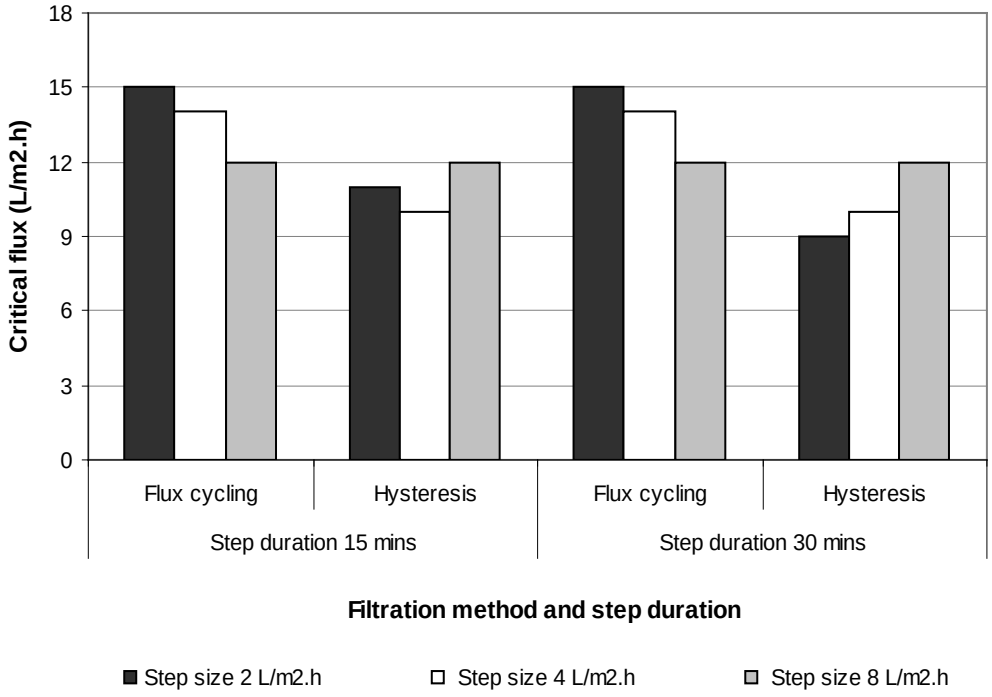

Fig. 4.15 Comparison of critical fluxes evaluated based on fouling reversibility of stepping filtration and cycling filtration

In fact, not all membrane experiments display reversibility in the fouling hysteresis using this flux stepping technique. Many studies have reported that there were significant differences between the first and next cycles of filtration and the hysteresis affects the way in which subsequent fouling can occur (Ognier *et al.* 2001; Howell *et al.* 2004). With similar step height and step length, changing filtration methods (flux stepping/flux cycling) has a significant impact on the reversible flux as illustrated in Fig. 4.13 and Fig. 4.14 as examples

Fig. 4.15 summarized all critical fluxes obtained based on flux reversibility using different filtration variables. It can be seen that the critical fluxes achieved from the flux cycling technique were considerably greater than critical fluxes obtained from the hysteresis of flux stepping technique. With the same filtration method, there is almost no significant effect of step lengths (15 and 30 min) on the critical fluxes obtained for all tests performed using different step heights. For all tests using the flux cycling method, the inverse relationship between the step heights and critical flux values is obviously found. This is because the additional fouling from the previous filtration of the small step height can be easily recovered when the next instantly reduced flux cycling is performed and results in the greater reversible flux and higher critical flux compared to the bigger step height.

On the other hand, a relative increase in critical flux because of the step height increase was discovered in the hysteresis of the stepping filtration. This is probably because the smaller flux increment in the repeated filtration retains more filtration time and more number of steps than the bigger step height. Consequently, it produces more liquid filtered and more fouling which is more difficult to fully re-disperse those fouling even when the flux was descending. This indicates the formation of residual

fouling resulting in the low or sometimes no reversible flux from this hysteresis of stepping filtration technique, which leads to a requirement of the membrane cleaning.

4.3.4 Sustainable flux

The original definition of the critical flux stated that operation was sub-critical if little or no fouling occurs (Bacchin *et al.* 2006). If the imposed flux is operated in SMBR system, the rate of membrane fouling can be described as an increase of TMP over the operating period. This means the rate of fouling is strongly dependent on the flux. It is simply not feasible to operate SMBR at a zero fouling condition. A new term called sustainable flux was introduced based on significant differences between low and high fouling rate zones (Bacchin *et al.* 2006). Thus, operation at sustainable flux is capable of controlling membrane fouling with more relaxing of the criteria compared to the critical flux because it considers a low, rather than zero, rate of fouling operation. Fig. 4.16 shows an example of flux and fouling rate $(dTMP/dt)$ profile at step height 2 L/m^{2}h and 30 min step length. In Fig. 4.16, an exponential relationship between flux and fouling rate was observed in the SMBR process, which agreed with the study of Guglielmi *et al.* (2007). Here, the sustainable flux was indicated at the transient range of the fouling rate. All sustainable fluxes obtained from all filtrations were shown in Fig. 4.17 (more experimental data are shown in appendix B). The data suggest that an increase in step height decreases sustainable flux and no influence of step length on sustainable flux can be realized

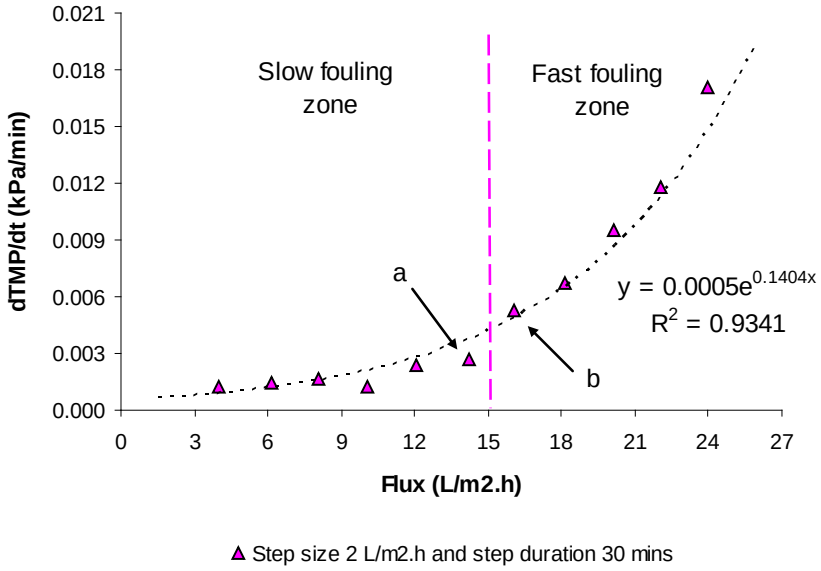

Fig. 4.16 Fouling rate profile at step height 2 L/m^{2}h and 30 min step length, where a = the last-slow fouling flux and b = the first-fast fouling flux

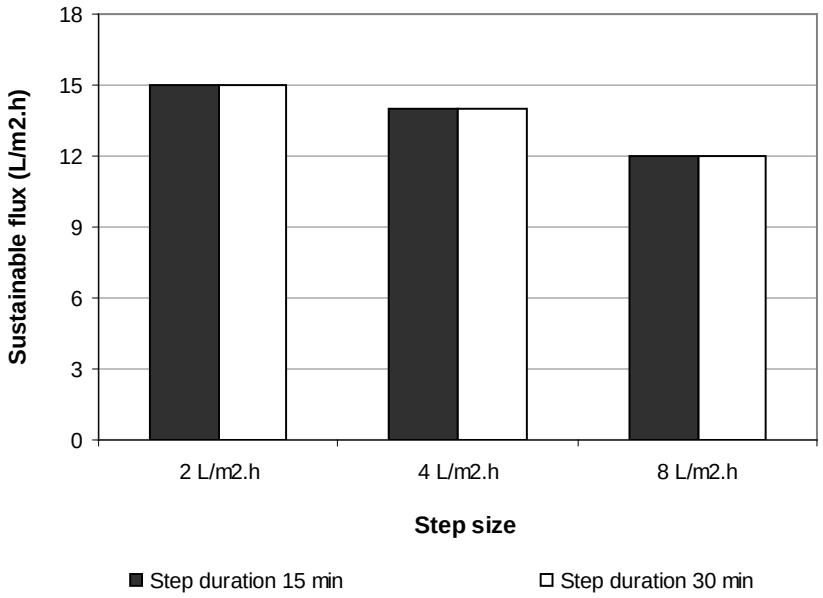

Fig. 4.17 Sustainable fluxes at different step heights and step lengths

4.3.5 Comparison of critical flux based on different determination methods and sustainable flux

The sustainable fluxes and critical fluxes evaluated by different methods mentioned in section 4.3.3 and 4.3.4 were compared and plotted in Fig 4.18. Obviously, the critical fluxes and sustainable fluxes were affected by the filtration variables, namely step height and step length. The decline of critical flux as the step height increases has been noticed in most critical flux determination methods namely; flux linearity, 90% permeability, and reversibility of flux cycling, which is similar to the observation based on flux linearity in Wu *et al.* (2008). Of course, it would be better to use small step heights to determine critical flux value in order to prevent large errors from flux averaging. Unlike other methods, hysteresis of flux stepping filtration shows a positive relationship between the step height and critical flux values. On the other hand, the step length has no obvious effect on the critical flux assessed from all determination methods, which is similar to the discovery of Le Clech *et al.* (2003) but conflicted with the observation of Wu *et al.* (2008) which reported that the increase of step length would lower the critical flux. Noticeably, only the critical fluxes based on the two-third limiting flux method are constant and independent from the influence of step height and step length. A similar pattern between the sustainable flux and most critical flux affected by step height and step length was also observed.

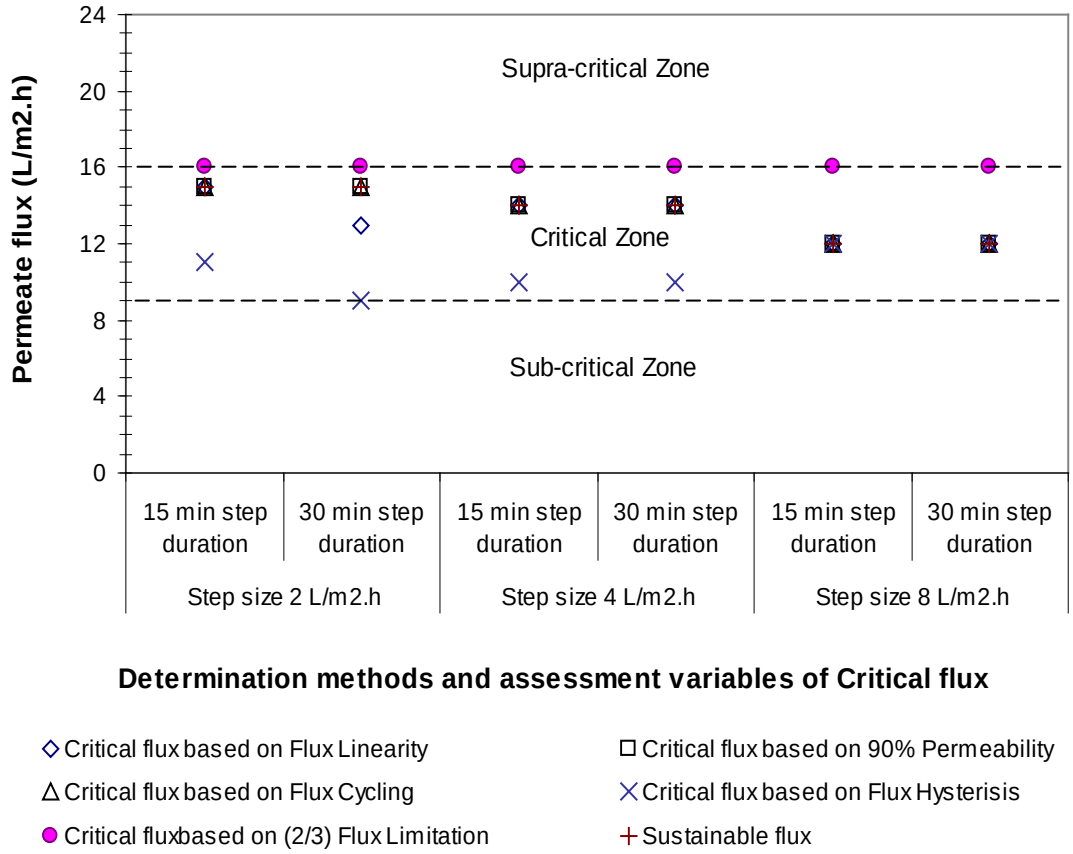

Fig. 4.18 Comparison of sustainable flux and critical fluxes obtained from different determination methods and different filtration variables

In fact, fouling was reported to develop in the transient behavior (Hong *et al.* 1997). Therefore, it is reasonable that various determination methods of critical flux can give slightly variations of the critical flux values. From Fig. 4.18, the highest and lowest critical flux values are obtained from the two-third limiting flux and the hysteresis of stepping filtration, respectively. It is suggested that the two-third limiting flux and the flux hysteresis are likely to indicate upper and lower border of the critical zone, respectively. Operating beyond this point is likely deleterious to SMBR operation. Short term experiment is only sufficient to indicate critical flux but

not relevant to the stability of this critical flux over longer periods of time (Bacchin *et al.* 2006). Therefore, the recommended flux for membrane operation is dependent upon the application period which some fouling rate can be tolerated when operating in the short term, but unacceptable for long term filtration.

4.3.6 Influencing parameters for critical flux enhancement

According to literature, critical flux can be affected by certain controllable parameters, including aeration rate and sludge concentration. Fig. 4.19 presents experimental results showing the variations of critical fluxes at different aeration intensities and different MLSS concentration. In Fig. 4.19, a 2 L/m^2h step height and 15 minute step length with the 90% permeability was used for the critical flux determination, due to its simplicity. In Fig. 4.19, MLSS concentration strongly affects the critical flux. An increase in MLSS concentration will increase the convective flow of solids towards the membrane surface resulting in the lessening of critical flux. On the other hand, greater aeration intensity can generate higher cross-flow velocity with more turbulence, which induces a greater shear against the membrane surface. Therefore, an increase in the sparged gas flow rate will increase the back transport of solids from the membrane surface, thus increasing the critical flux. For SMBR operating under high sludge concentration, large aeration intensity would be required in order to maintain a certain value of critical flux. In practical applications, even the improved aeration intensity can enhance the critical flux; however, it will increase the energy cost of the system. Therefore, further studies concerning the optimal aeration intensity and optimal sludge concentration are recommended.

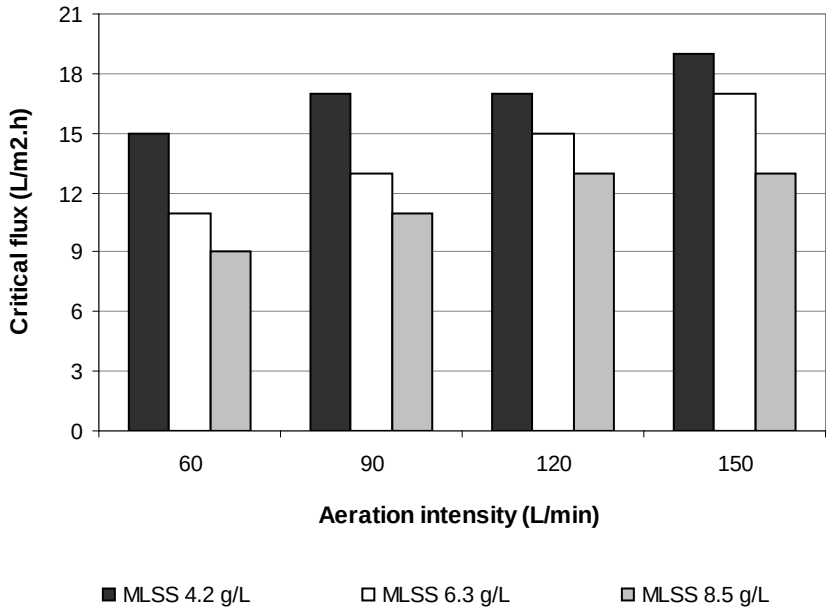

Fig. 4.19 Critical flux at different aeration and MLSS concentration

In other studies, it was also reported that an increase in aeration restrained fouling and increased critical flux (Madaeni 1997; Bouhabila *et al.* 1998; Le Clech *et al.* 2003; Wu *et al.* 2008); however the reports on the effects of sludge concentration on critical flux among research are different because of the complexity and variability of the biomass components. The increase in MLSS concentration alone was reported to have a mostly negative effect on the flux obtained in a side-stream MBR (Fane and Fell 1981), while some other studies have discovered no effect of MLSS on fouling up to a threshold concentration (Yamamoto *et al.* 1999; Le Clech *et al.* 2003). Silva and his co-workers (Silva *et al.* 2000) also observed that in membrane tanks with high shear rates, particle transport is dominated by hydrodynamic-induced shear, which is proportional to the square of the particle size. Consequently, the larger particles deposited on the membrane surfaces would become much easier to be sheared away from the membrane surface than would small particles.

Over a similar type of membrane and similar range of hydraulic condition, critical flux values differed significantly, i.e., 62 L/m^{2}h for an MLSS 4 g/L reported by Madaeni *et al.* (1999) compared with a value of 22 L/m^{2}h at MLSS 2.5 g/L reported by Cho and Fan (1999). Such disparities could imply that it is very essential to perform tests under the same sludge conditions for classifying the impacts of hydraulic parameters on critical flux. In this study, the same sludge characteristics were maintained to the determination of critical flux values, and the results were expected to provide a sensible understanding of the influence of MLSS concentration and aeration.

4.4 CONCLUSIONS

This study has examined the effect of assessment parameters on critical flux including step heights, step lengths and various determination methods in a submerged flat sheet membrane bioreactor. The results indicated that the decline of critical flux as the step height increased has been noticed in most critical flux determination methods, including: flux linearity, 90% permeability, and flux cycling, while there is an independent and positive relationship between critical flux and step height presenting in the two-third limiting flux and hysteresis of stepping filtration, respectively. In order to prevent a large error from flux averaging, smaller step heights are recommended for critical flux determinations. On the other hand, the step length has almost no effect on critical flux, regardless of the determination methods employed. A similar pattern between sustainable fluxes and most of the critical flux affected by step height and step length were observed. The effects of aeration and MLSS on the critical flux enhancement were also investigated. Experiments on

different aeration intensities have shown that an increase of air sparging leads to increased critical flux, while high biomass concentration influenced the greater fouling phenomena, resulting in lower critical flux.

CHAPTER 5

MEMBRANE FOULING BEHAVIOR UNDER DIFFERENT SLUDGE COMPOSITIONS AND DIFFERENT FLUX STAGES

5.1 INTRODUCTION

Among biological wastewater treatment, the activated sludge process is used worldwide to remove nutrient organic matter in municipal and industrial wastewater treatment and reclamation processes. One disadvantage of the activated sludge process is the difficulty of separating suspended matter from the effluent by settling (Benefield and Randall 1980) which limits the biomass concentration to about 5 g/L (Bailey *et al.* 1994) and requires large-size tanks (Defrance *et al.* 2000). Over the last decades, a modification of the conventional activated sludge process using submerged membranes technology called submerged membrane bioreactor (SMBR) has been used to separate of the effluent, replacing sedimentation, which reduces the plant size due to the absence of settling tanks. It has been shown that all microorganisms from wastewater were retained and treated effectively by this SMBR system. Although their several advantages are well recognized, the SMBR process also has as its principal limitation on membrane fouling, which causes permeate flux decline and necessitates frequent cleaning and/or replacement of membranes.

In the SMBR process, direct contact between membrane and mix liquor sludge is inevitable and causes membrane fouling attributed to deposition and interaction

between sludge and membrane surfaces. Previous studies reported that the higher microbial sludge concentration caused more fouling in SMBR (Magara and Itoh 1991; Manem and Sanderson 1996), while others suggested that less fouling at the higher sludge occurred under their certain conditions (Defrance and Jaffrin 1999; Lee *et al.* 2001). It was implied that membrane fouling is related to not only sludge quantity but also sludge characteristics.

Activated sludge can be classified into two fractions: microbial flocs and the liquid phase, containing colloids, soluble matters and extra-cellular polymeric substances (EPS). Recent studies have quantified the fouling caused by these sludge fractions. For example, Bouhabila *et al.* (2001) and Rosenberger (2002) found that the composition of the liquid phase affected predominantly on the filterability of the activated sludge in microfiltration. Wisniewski and Grasmick (1998) concluded that the liquid fraction accounted for 76 % of the fouling resistance with the colloidal fraction for 24% and the dissolve one for 52%. Similarly, Bouhabila *et al.* (2001) reported that the supernatant consisting of solutes and colloids contributed 76% to the membrane fouling resistance. In contrast, Defrance *et al.* (2000) and Lee *et al.* (2001) reported that the relative contribution of supernatant to overall membrane fouling was up to 37% , which were much lower than that of the microbial flocs (63%).

In spite of the differences of these results, the extra-cellular polymeric substance (EPS) of activated sludge is a well known factor affecting membrane fouling (Chang and Lee 1998; Nagaoka *et al.* 1998; Rosenberger and Kraume 2003; Hernandez Rojas *et al.* 2005). EPS comes from the natural secretions of bacteria, cell lysis and hydrolysis products, and is mainly composed of proteins and carbohydrates. Lee *et al.* (2003) found that the protein to carbohydrate ratio in EPS appeared more

important than the total quantity of EPS with respect to sludge fouling, while there was no relationship between EPS composition and properties on the supernatant fouling. On the other hand, Hernandez Rojas *et al.* (2005) reported that bound EPS (or EPS in the microbial flocs) have no effect on the fouling resistance variations and only soluble EPS in liquid fraction is responsible for membrane fouling.

As indicated above, the information of sludge and supernatant fouling is uncertain and, as such, should be further investigated. In addition, no research to date indicates role of different sludge components at different filtration rates (sub-critical flux and supra-critical flux) on membrane fouling behavior. Accordingly, these parameters should also be tested for better understanding of how fouling mechanisms varied with different concentrations of each sludge fraction and stage of operation. Therefore, the aims of this chapter are to demonstrate the effects of sludge composition (microbial flocs and supernatant) at different filtration stages (sub-critical fluxes and supra-critical fluxes) on membrane fouling. A variation of these operational parameters was performed using factorial design with high and low level yielding a base of eight experimental runs. The membrane fouling mechanisms including pore blocking and cake fouling were determined. Membrane fouling morphologies were also observed using a scanning electron microscope.

5.2 EXPERIMENTAL MATERIALS AND METHOD

5.2.1 Experimental facility

A pilot scale SMBR used in this study was the same SMBR system described previously in chapter 4. The characteristics of wastewater used in the experiment were shown in table 5.1.

Table 5.1 Characteristics of wastewater used in the experiment (day 90 to day 150)

Parameter	Inlet	Anaerobic	Anoxic	SMBR	Permeate
pH	7.34 ± 0.11	6.98 ± 0.06	6.89 ± 0.06	7.03 ± 0.11	7.09 ± 0.12
Temp (oC)	25.2 ± 0.5	25.3 ± 0.4	25.2 ± 0.4	25.2 ± 0.4	25.1 ± 0.3
DO (mg/L)	2.24 ± 0.17	2.40 ± 0.16	2.80 ± 0.18	3.02 ± 0.21	2.96 ± 0.18
Conduct. (*u*S)	1310 ± 34	1099 ± 30	1099 ± 31	1139 ± 22	1036 ± 28
ORP (mV)	-54.3 ± 7.3	265.0 ± 9.7	252.2 ± 26.1	244.0 ± 14.9	185.2 ± 9.3
MLSS (mg/L)	226 ± 39	6996 ± 169	7971 ± 185	8189 ± 157	N/A
NH4-N (mg/L)	35.5 ± 3.4	6.6 ± 2.2	4.2 ± 0.7	0.3 ± 0.5	0.0 ± 0.0
NO3-N (mg/L)	0.0 ± 0.0	0.0 ± 0.0	43.7 ± 3.2	25.0 ± 3.0	21.8 ± 2.8
PO4-P (mg/L)	12.1 ± 1.1	16.7 ± 1.4	12.8 ± 0.7	10.0 ± 1.1	8.7 ± 0.8
COD (mg/L)	340 ± 39	N/A	N/A	N/A	15 ± 5

Note: ± term is represent standard deviation

5.2.2 Experimental design

The influence of microbial flocs, supernatant EPS and filtration modes on membrane fouling mechanisms was investigated at high and low level, yielding a 2^3 factorial design as shown in table 5.2. High and low values for MLSS, supernatant EPS and filtration mode (sub-critical flux and supra-critical flux) were adopted as the base of eight experimental runs. The systems were operated for 100 and 200 minutes for supra-critical and sub-critical flux operation, respectively. In this case, the critical flux was indicated at 17 L/m^2h. Sub-critical flux and supra-critical flux were operated at 80% and 120% of critical flux, respectively. The critical flux evaluation using short-term flux stepping technique was performed primarily in order to know the

stage of filtration (see more details in appendix C.1). The trans-membrane pressure (TMP) and permeate of the experiments were logged every minute on the PLC device. After finishing each test, the membrane surface was cleaned with soft sponge, which was adopted to ensure removal of sludge particles from the membrane surface and a chemical cleaning of 0.5% sodium hypochlorite was proceeded in place to remove irreversible fouling from membrane pore blocking. Then the next test was continued.

Table 5.2 Assignment of operational parameters in the 2^3 factorial designs

Run	MLSS (mg/L)	Supernatant EPS (mg/L)	Filtration mode	Operation time (min)
1	4,000	High (106.4)	Sub-critical flux	200
2		High (106.4)	Supra-critical flux	100
3		Low (30.36)	Sub-critical flux	200
4		Low (30.36)	Supra-critical flux	100
5	8,000	High (172.56)	Sub-critical flux	200
6		High (172.56)	Supra-critical flux	100
7		Low (71.44)	Sub-critical flux	200
8		Low (71.44)	Supra-critical flux	100

Note: the critical flux (Jcrit) = 17 L/m^{2}h, Sub-critical flux (80% Jcrit) = 13.6 L/m^{2}h, supra-critical flux (120% Jcrit) = 20.4 L/m^{2}h (see more detail in appendix C.1)

5.2.3 Laboratory analysis

5.2.3.1 Measurement of mixed liquor suspended solid (MLSS)

Determination of MLSS concentrations followed the standard methods for the examination of water and wastewater (APHA 2005).

5.2.3.2 Measurement of colloids

Total organic carbon (TOC) was analyzed by a TOC analyzer (TOC-VCSH, Shimadzu, Japan). The difference between the filtrate passing through a 1.5 μm filtration paper and permeate directly collected from the pilot SMBR module is referred to as colloidal TOC in order to represent the concentration of colloidal particles (Fan *et al.* 2006).

5.2.3.3 Extraction of EPS

Soluble EPS was measured from supernatant after centrifugation of the samples at 2000g for 30 min and was calculated by summing the contents of carbohydrate and protein substances (Fan *et al.* 2006). Modified Hartree-Lowry and Anthrone assays were applied for assessment of protein and carbohydrate respectively (Dische 1962; Hartree 1972). For bound EPS, the settled pellets were suspended in a buffer (2mM $Na_3PO_4.12H_2O$, 4mM NaH_2PO_4. $2H_2O$, 9m MNaCl, 2mM KCl) and extraction of bound EPS was then performed by mixing this sample with a cation exchange resin (DOWEX 50X) at 4 ^{0}C for 45 min at 500 rpm (Frolund *et al.* 1996; Masse *et al.* 2006). Then the sample (resin+sludge) was settled for 5 minutes and the recovered liquid phase was centrifuged at 20,000g for 15 minutes to separate the EPS from the biomass. Afterwards, carbohydrate and protein analyses were made.

5.2.3.4 Carbohydrate assay

Carbohydrate concentration was measured with the colorimetric method (Dische 1962). 1 ml of sample was mixed with 2 ml of Anthrone reagent (0.2% anthrone in concentrate sulfuric acid) and heated in a boiling water bath for 20 minutes. The mixture was then left until cool at room temperature. The contents of

each tube were transferred to cuvettes and analyzed using the spectrophotometer against the blank at a wavelength of 625 nm. The carbohydrate concentration was determined from a calibration curve shown in appendix C.2.

5.2.3.5 Protein assay

Protein concentration was measured using the modified Hartree-Lowry method (Hartree 1972). Three solutions, solution A, solution B, and solution C were prepared prior to the analysis. Solution A consists of 2 g sodium potassium tartrate x 4 H_20, 100 g sodium carbonate, 500 ml 1N NaOH, adjusted volume to one liter (that is, 7mM Na-K tartrate, 0.81M sodium carbonate, 0.5N NaOH final concentration). Solution B consists of 2 g sodium potassium tartrate x 4 H_20, 1 g copper sulfate ($CuSO_4$ x $5H_20$), 90 ml H20, 10 ml 1N NaOH (final concentrations 70 mM Na-K tartrate, 40 mM copper sulfate). Solution C consists of 1 volume of Folin-Ciocalteau reagent diluted with 2 volumes of water; prepared immediately daily, just before use. When analyzing the samples, a volume of 1.0 ml of sample and 0.9 ml of solution A was mixed and incubate the tubes 10 min in a 50 ^{0}C bath, then cooled to ambient temperature. Solution B (0.1 ml) was added and after mixing, the tubes were allowed to stand for 10 minutes at room temperature. Solution C was then added in 3 ml portion rapidly mixed and incubated for 10 minutes in the 50 ^{0}C bath. The tube was cool to room temperature before reading absorbance at 650 nm. The protein concentration was determined from a calibration curve based on bovine serum albumin (BSA) as a standard solution (see more detail in appendix C.2).

5.2.4 Membrane fouling analysis

The degree of membrane fouling was quantitatively calculated, using the resistance in series model (Mulder 1996; Chang and Lee 1998):

$$R_t = \frac{\Delta P}{\mu J} = R_m + R_c + R_p \quad \textbf{5. 1}$$

All parameters in equation 5.1 were addressed in appendix E.

The filtration resistance (R) was measured step by step as follows in Fig. 5.1. The intrinsic membrane resistance (R_m), the cake resistance caused by cake layer formed on the membrane surface (R_c) and the fouling resistance caused by pore plugging and irreversible adsorption of foulants onto the membrane pore wall (R_p) can be calculated using the following Equations (Bae and Tak 2005):

$$R_m = \frac{\Delta P_w}{\mu J_w} \quad \textbf{5. 2}$$

$$R_p = \frac{\Delta P_{w,\,final}}{\mu J_{w,\,final}} - R_m \quad \textbf{5. 3}$$

$$R_c = \frac{\Delta P_{sludge}}{\mu J_{sludge}} - R_m - R_p \quad \textbf{5. 4}$$

All parameters in equation 5.2-5.4 were addressed in appendix E.

The activated sludge consists of supernatant and suspended solids. The filtration resistance of the activated sludge could be considered to be equal to the summed resistance product of the suspended solids and the supernatants. In this study, severe membrane fouling due to cake deposition on the membrane surface was assumed to be caused by the suspended solids, which were readily removable and

often classified as reversible fouling (Chang and Lee 1998). On the other hand, colloids and dissolved material from the supernatant was assumed to cause pore blocking that could only be removed by chemical cleaning and so called irreversible fouling.

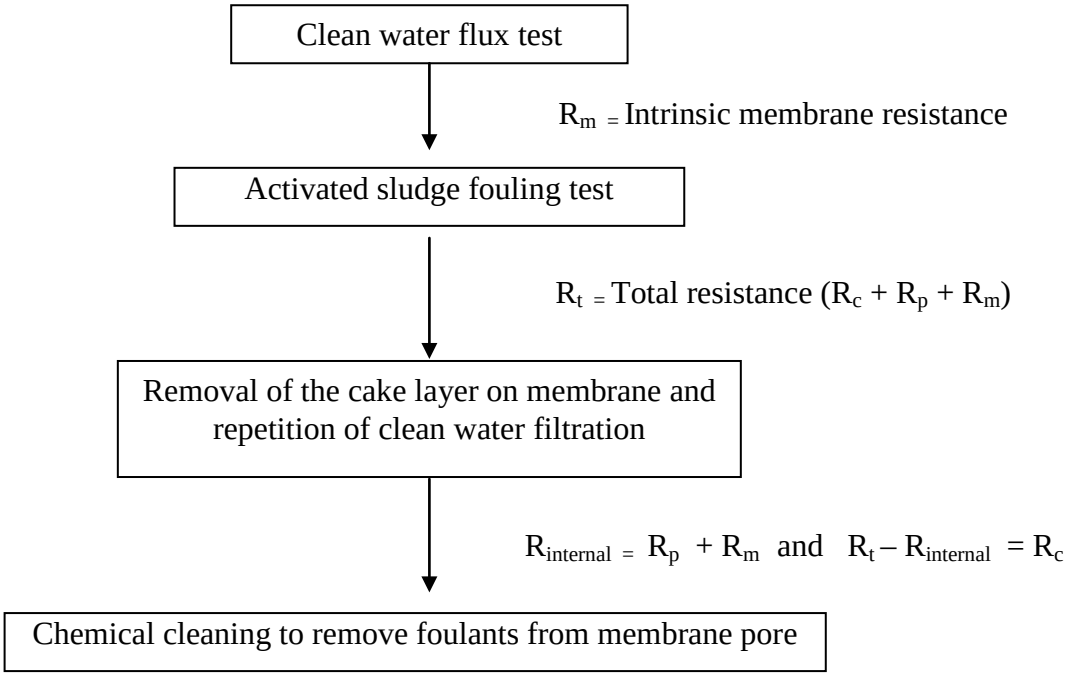

Fig. 5.1 Steps to measure each filtration resistance

5.2.5 Observation of membrane fouling morphology

The cake surface and cross-sectional structure were observed using a scanning electron microscope (SEM) (JEOL JSM-5600LV, Tokyo, Japan). After each experimental run, a membrane samplewas cut from the membrane cartridge for analysis. The samples were fixed with 3.0% glutaraldehyde in 0.1M phosphate buffer at pH 7.2. The samples were dehydrated with ethanol, gold-coated by a sputtering and observed in the SEM (Meng *et al.* 2005).

5.3 RESULTS AND DISCUSSION

5.3.1 Fouling contribution

The analysis of membrane fouling resistances is presented in table 5.3 (see more experimental detail in appendix C.3). It was observed that filtration resistance was much higher in the supra-critical flux region of operation compared with the sub-critical flux operating range due to the accumulation of a cake layer. Beyond critical flux operation, high suction force resulted in more particle accumulation which will affect on increasing of cake thickness and compactness (Meng *et al.* 2005). Accordingly, cake formation accounted for a large portion of total resistance (50-65%) for all sludge compositions while the fouling resistance caused by adsorption or pore plugging under supra-critical flux was marginal (5-7%).

Table 5.3 Fouling contribution at different sludge compositions and filtration modes

MLSS (mg/L)	Total soluble EPS (mg/L)	Filtration mode	R_{cake} (1/m)	% R_{cake}	R_{pore} (1/m)	% R_{pore}	R_m (1/m)	% R_m	R_{total} (1/m)
8,058	High (172.56)	$J < J_c$	-	-	3.17E+10	18.59	1.43E+11	81.41	1.76E+11
8,058	High (172.56)	$J > J_c$	3.17E+11	65.25	2.68E+10	5.52	1.42E+11	29.23	4.86E+11
8,016	Low (71.44)	$J < J_c$	-	-	2.31E+10	14.84	1.38E+11	85.16	1.62E+11
8,016	Low (71.44)	$J > J_c$	2.43E+11	59.93	2.25E+10	5.55	1.40E+11	34.53	4.06E+11
4,118	High (106.4)	$J < J_c$	-	-	2.67E+10	16.94	1.35E+11	83.06	1.63E+11
4,118	High (106.4)	$J > J_c$	2.05E+11	55.41	2.50E+10	6.76	1.40E+11	37.84	3.70E+11
4,076	Low (30.36)	$J < J_c$	-	-	1.79E+10	12.01	1.36E+11	87.99	1.55E+11
4,076	Low (30.36)	$J > J_c$	1.57E+11	50.65	1.60E+10	5.16	1.37E+11	44.19	3.10E+11

Hint: $J < J_c$ = sub-critical flux (80% J_{crit}), $J > J_c$ = supra-critical flux (120% J_{crit})

Under sub-critical flux operation (see table 5.3), the total hydraulic resistance for all sludge fractions was about 1.5 - 1.8E+11 m^{-1} much lower than that of supra-critical flux filtration (3.1 - 4.9 E+11 m^{-1}). These results indicated that the reduction of total resistance of the sub-critical flux system mainly came from the absent in the cake resistance. Consequently, operating at sub-critical flux is a key factor to minimize membrane fouling. In comparison, pore fouling resistance has more responsible (12-18%) in the sub-critical flux filtration than in the supra-critical flux operation (5–7%).

5.3.2 Effect of colloids on membrane fouling mechanisms

Among other characteristics of sludge samples, colloid matter in activated sludge was reported that it almost exclusively correlated as a key factor of membrane fouling (Fan *et al.* 2006).

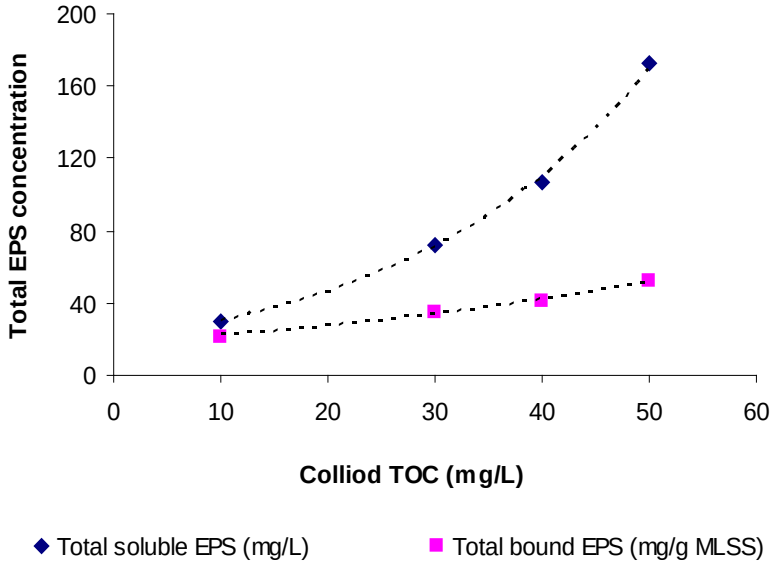

Fig. 5.2 EPS and colloidal concentration

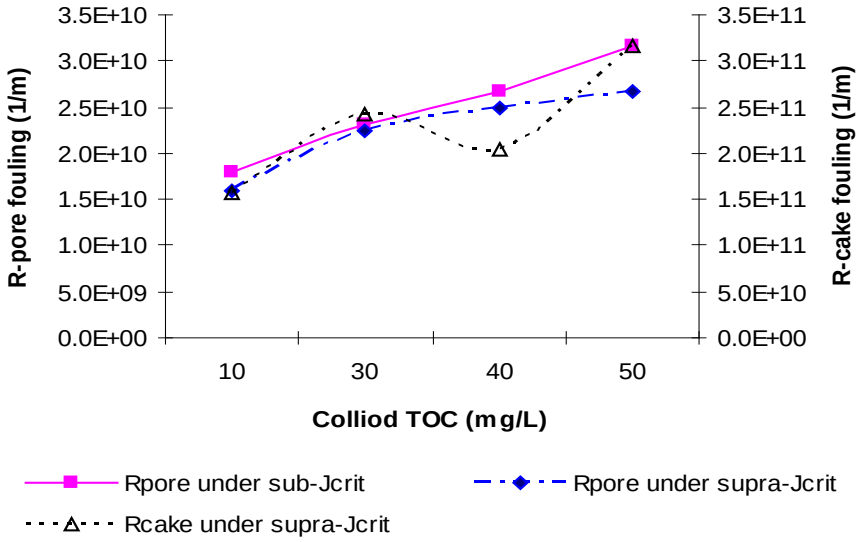

Fig. 5.3 Colloidal concentration and different fouling resistance

In wastewater treatment, colloidal particles have been defined as a portion of particles ranging from 0.01 to 1.0 μm (Tchobanoglous *et al.* 2003), which are comparable to the nominal pore sizes of membrane filters. The colloidal particles consist of both fine inorganic precipitates and many organic constituents such as EPS and other cell debris (Defrance *et al.* 2000).

From Fig. 5.2, a good consistency could be seen between the colloid concentration and the soluble EPS, while little correlation existed between the colloid quantity and the bound EPS. This is agreed with Fan study (Fan *et al.* 2006) which reported that the characteristics of colloidal particles might be mainly determined by the microbial by-products such as soluble EPS in MBR wastewater treatment systems. Positive variations in the concentration of the colloids were further concurrent with the increase of the pore fouling resistance than the cake fouling resistance (Fig. 5.3). In Fig. 5.3, there is no predictable trend between a variation of colloidal concentration

and cake fouling resistance. A fluctuation between colloid TOC and cake fouling resistance during 30 mg/l TOC (low MLSS with high soluble EPS) and 40 mg/l TOC (high MLSS with low soluble EPS) showed that colloid concentration is not depend on only MLSS but also EPS concentration.

5.3.3 Effect of EPS contents on membrane fouling mechanisms

5.3.3.1 EPS contents and membrane pore fouling

Extractable EPS was suggested to be used as a probable index for membrane fouling (Chang and Lee 1998). Laspidou and Rittman (2002) and Hsieh *et al.* (1994) reported that EPS in activated sludge could be divided into two categories: bound EPS on floc biomass (sheaths, capsular polymers, condensed gel, loosely bound polymers, and attached organic material) and soluble EPS (soluble macromolecules, colloids and slimes). It has been widely known that the EPS components are included carbohydrate, protein, humic substance, uronic acids and DNA. Among these EPS components, carbohydrate and protein are acceptable as the main constituents of the total measurable EPS (Ji and Zhou 2006). Therefore, only carbohydrate and protein of the soluble and bound EPS were subsequently measured throughout the study.

Further analysis was made to reveal whether there is any relationship between the membrane pore fouling resistance and the different groups of soluble and bound EPS. As shown in Fig. 5.4 and Fig. 5.5, the higher the soluble and bound EPS concentration were, the higher the pore fouling resistance. In this study, soluble carbohydrate would have greater impacts on membrane pore fouling than would soluble protein. Likewise, bound EPS carbohydrate exhibited a higher influence on the membrane pore fouling than bound EPS protein even the quantity of bound EPS

protein is much higher. Li *et al.* (2007) reported a positive correlation between bound EPS and membrane fouling rate i.e. the membrane-fouling rate decreased as the bound EPS decreased.

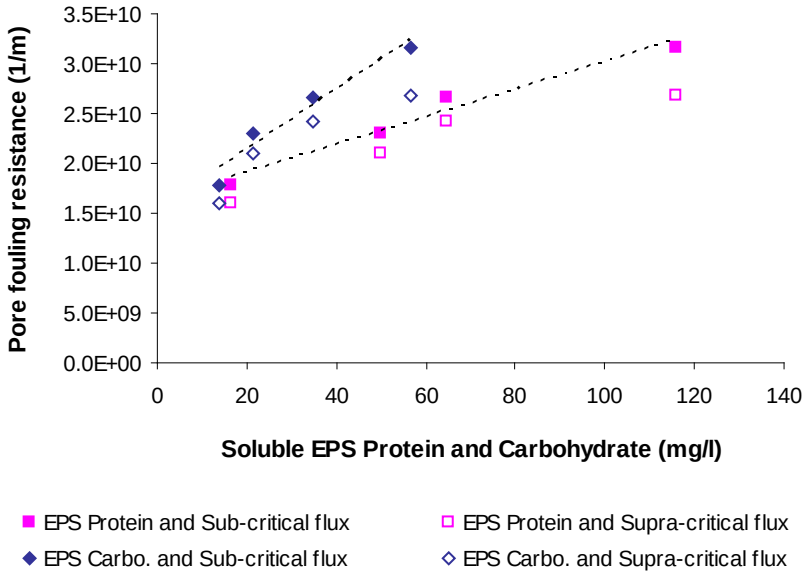

Fig. 5.4 Soluble EPS contents and membrane pore fouling

In some studies, membrane fouling was found to be more heavily affected by the EPS of the activated sludge than the dissolved organic matter (Pierre *et al.* 2006) and soluble organics alone could not predict membrane fouling in MBR (Lee *et al.* 2001). On the other hand, some research (Geng and Hall, 2007) found no correlation between bound EPS content and membrane fouling, but soluble EPS matter.

Noticeably, results from Fig. 5.4 and Fig. 5.5 showed that the effects of all bound and soluble EPS contents on the membrane pore fouling were slightly more distinguished under sub-critical flux operation than the supra-critical flux mode. This can be implied that the cake form on the membrane surface during the supra-critical flux filtration may be able to act as a pre-filter preventing the passage of colloidal

particles through the membrane pore, while this phenomenon was not occurred under sub-critical flux causing more membrane pore fouling. An acting as a secondary membrane of cake layer (preventing further pore blocking in SMBR) was also stated in research of Metzger and co-worker (Metzger *et al.* 2007).

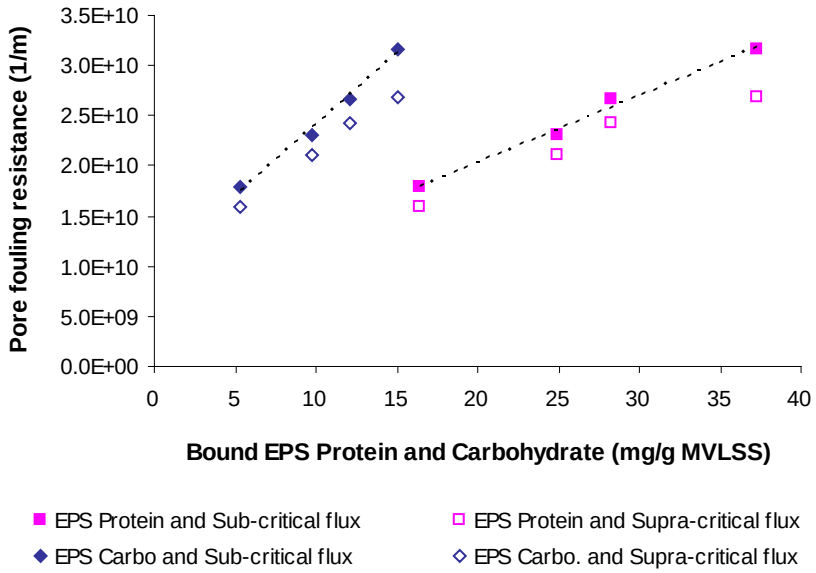

Fig. 5.5 Bound EPS contents and membrane pore fouling

The membrane pore fouling was also increased with the increase of soluble protein to carbohydrate ratios (Fig. 5.6). Metzger *et al.* (2007) observed that protein seems to have higher potential for deposition/adsorption directly on the membrane surface and appear to be more strongly attached to the membrane than carbohydrates during filtration. It is expected that proteins attach more tightly to membranes due to their heterogeneous properties (Chu and Li 2005) and can only be partly removed by backwashing or through chemical cleaning. In contrast, the increase of bound EPS protein to carbohydrate ratios decreased in the pore fouling resistance (see Fig. 5.5). Masse *et al.* (2006) found that the decrease of bound protein to polysaccharide ratio

resulted in the decrease of floc size. Thus, it can be assumed that the increase of bound EPS protein to carbohydrate ratios may affect to the bigger forming of floc sizes causing less chance of membrane pore fouling.

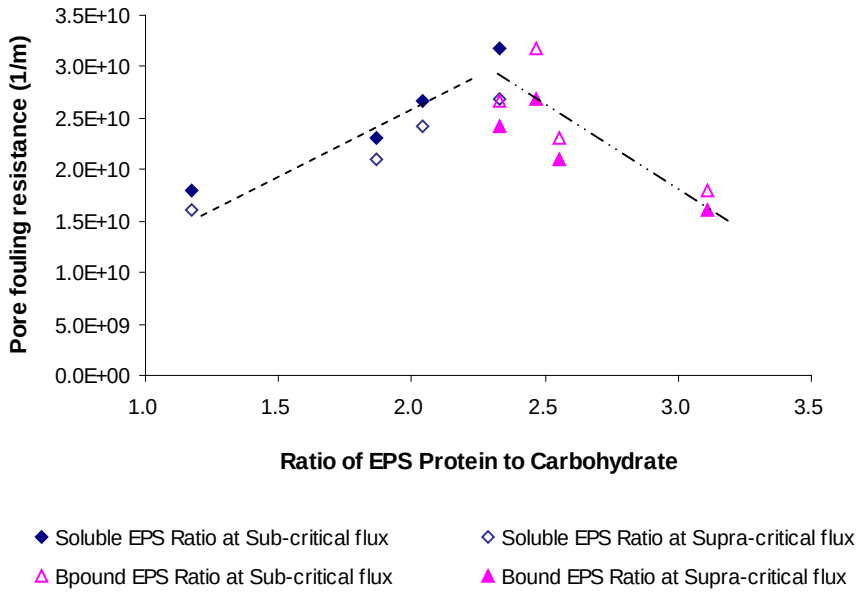

Fig. 5.6 Ratio of EPS protein to carbohydrate and membrane pore fouling

5.3.3.2 EPS contents and membrane cake fouling

It is well accepted that EPS provide a highly hydrated gel matrix in which microorganisms are embedded. The functions of the EPS matrix are multiple including the formation of a protective region around the bacteria, retention of water, adhesion to surfaces, as well as aggregation of bacterial cells in flocs and biofilms (Laspidou and Rittmann 2002). Therefore, a number of research reported that EPS may be responsible for forming a significant barrier to the permeate flow in SMBRs (Nagaoka *et al.* 1996; Chang *et al.* 2001; Orantes *et al.* 2006; Lim *et al.* 2007).

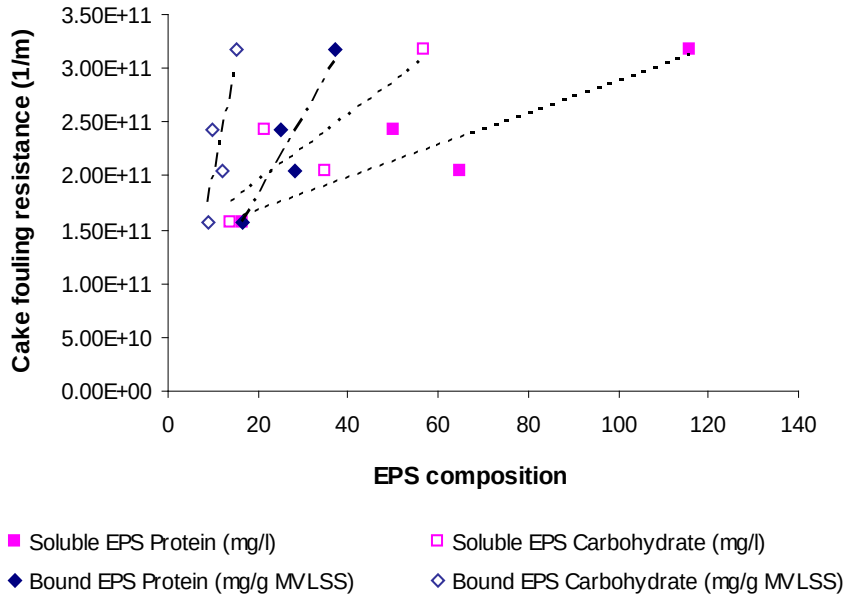

Fig. 5.7 Contents of soluble and bound EPS and cake fouling resistance

From Fig. 5.7, it can be seen that soluble and bound EPS in both protein and carbohydrate forms had a direct significant effect on cake fouling resistance. Nagaoka *et al.* (1998) proposed model described that the membrane fouling cake layer was mainly caused by EPS accumulated on membrane surface. Ahmed *et al.* (2006) studied the membrane fouling in a sequential anoxic/anaerobic reactor and observed a diminution of the specific cake resistance as the bound EPS decreased. It was also reported that the EPS affected membrane performance by filling the void spaces between the cell particles in the cake layer resulting in a dramatic reduction of permeate flux (Lee *et al.* 2007). It might be concluded that the cake layer permeability on membrane surface was strongly affected by the EPS density. In addition, the ratios of EPS protein to EPS carbohydrate (Fig. 5.8) have a positive relationship on membrane cake fouling similar to that of soluble and bound EPS concentration. Lee *et al.* (2003) found that the protein to carbohydrate ratio in EPS

appeared more significant than the quantities of EPS components in controlling SMBR fouling. Metzger *et al.* (2007) found that proteins are preferentially attached to the membrane, whereas carbohydrates are enriched in the intermediate cake layer.

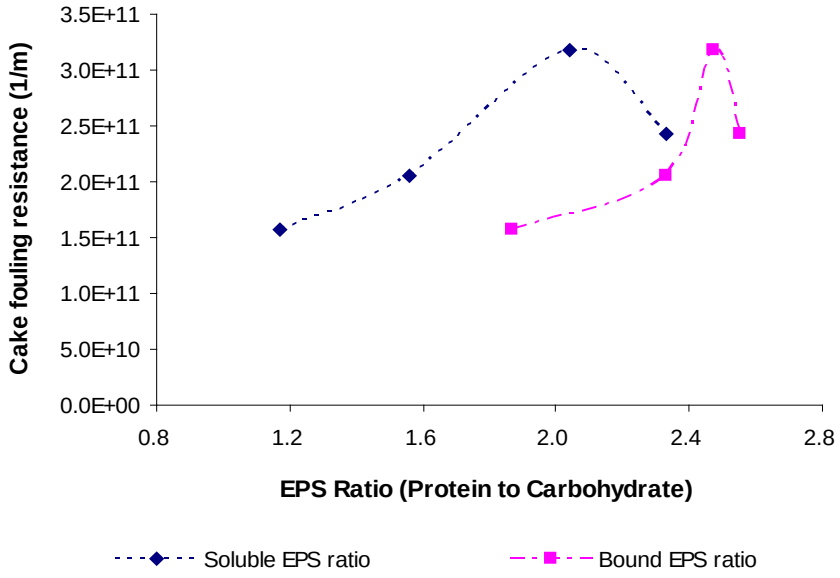

Fig. 5.8 Ratio of EPS protein to carbohydrate and membrane cake fouling

5.3.4 Effect of sludge concentration on membrane fouling mechanisms

The impact of MLSS on SMBR fouling were examined and shown in Fig. 5.9–Fig. 5.11. From Fig. 5.9, total fouling resistance did not vary with the increase of MLSS (4-8 g/L) and EPS concentration (30-170 mg/L) under sub-critical flux operation. This finding may suggested that the impact of shear created by air bubbles under sub-critical flux mode was adequate to maintain a very low membrane fouling behaviors reducing the effect of MLSS and EPS. Severe effect of MLSS and EPS increase in total fouling propensity was clearly showed only under the supra-critical zone.

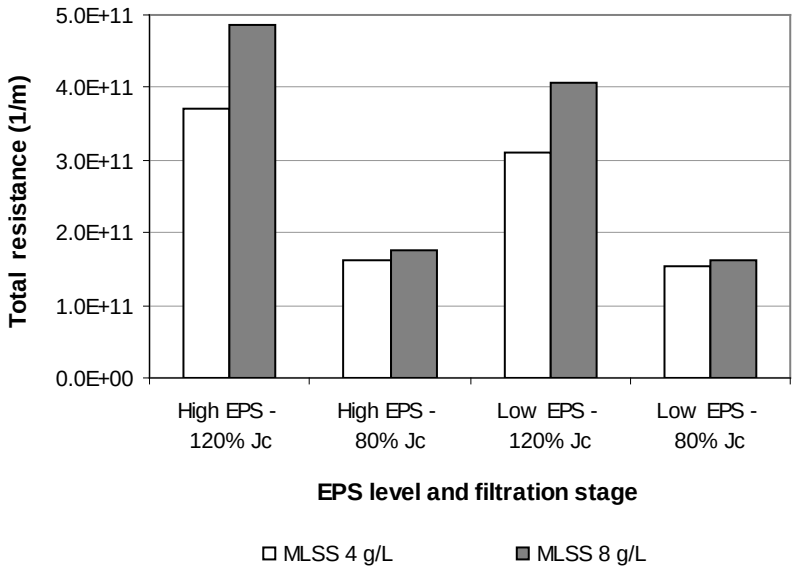

Fig. 5.9 MLSS and total fouling resistance

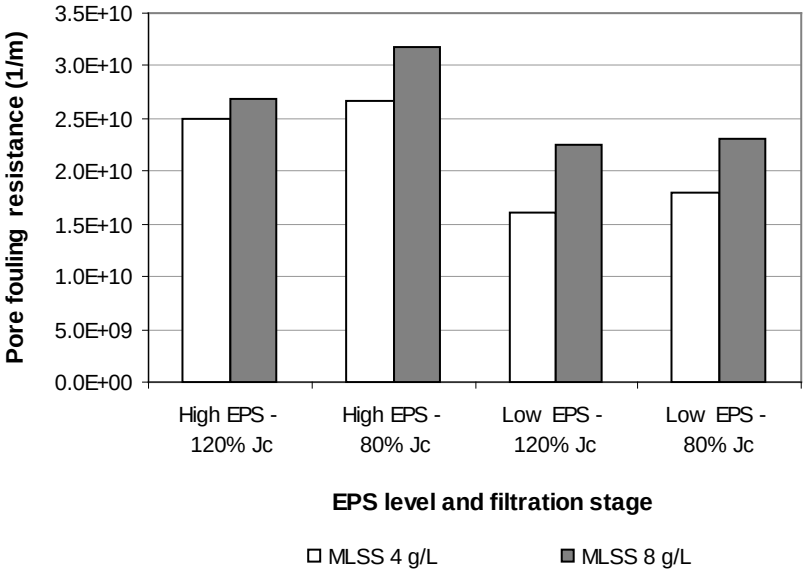

Fig. 5.10 MLSS and pore fouling resistance

The importance of biomass concentration on membrane fouling has been recognized by several research groups. The general consensus among the existing studies was that membrane fouling increased with increasing MLSS concentration, depending on the nature of the biological process (e.g. aerobic and anaerobic) (Brindle and Stephenson 1996). However, some studies reported that fouling was independent of MLSS concentration until a very high value was reached. For example, the investigation done by Ross *et al.* (1990) reported a sharp increase in fouling trend after a stable performance of up to 40,000 mg/L of MLSS concentrations. Yamamoto *et al.* (1999) also found the critical MLSS concentration to be about 30,000-40,000 mg/L, but it varied with operating conditions. No impact of MLSS concentration observed in some study may be due to the low MLSS concentration. For instance, various aerobic SMBR studies reported by Manem and Sanderson (1996) also showed that little fouling was observed for sludge concentrations between 5 -12 g/L.

The effect of activated sludge on membrane pore fouling was also investigated and shown in Fig. 5.10. Results in Fig. 5.10 illustrates that the pore fouling resistances were higher under sub-critical flux than supra-critical flux operation. Besides, in Fig. 5.11, the higher pore fouling resistances happened with the higher MLSS levels were also observed but it was still less than the effect of EPS. The positive correlation between pore fouling resistance and MLSS found in this study concurs with the findings of several previous studies (Sato and Ishii 1991; Yamamoto and Win 1991; Nagaoka *et al.* 1996; Shimizu *et al.* 1996; Fang and Shi 2005). On the other hand, some other studies showed that membrane pore fouling was independent

of MLSS (Defrance *et al.* 2000; Hong *et al.* 2002; Rosenberger and Kraume 2002; Fang and Shi 2005). The discrepancy is likely due to the difference in the membrane and sludge characteristics.

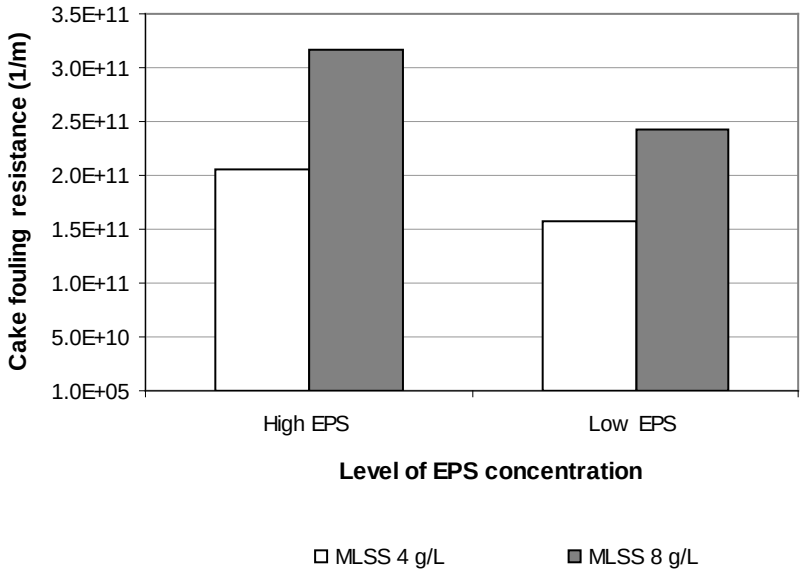

Fig. 5.11 MLSS and cake fouling resistance

Fig. 5.11 showed the cake fouling resistance with different MLSS concentrations. Obviously, cake fouling resistance increased along with the increase of MLSS concentration. The relationship between the cake resistance (R_c) and the sludge concentration can be expressed by the following Equation (Shimizu *et al.* 1993; Rushton *et al.* 2000):

$$R_c = \frac{\alpha V C_b}{A_m} = \alpha w \qquad \textbf{5. 5}$$

All parameters in equation 5.5 were addressed in appendix E.

Thus, the higher the MLSS was (or the higher C_b), the greater the cake fouling resistance can be expected. Likewise, the increase in EPS also had a negative effect

on membrane filterability because the EPS components could induce a very dense cake structure which has a very low permeability, resulting in reduced filtration efficiency.

5.3.5 Fouling Morphology

Scanning electron microscope (SEM) images of the membrane surfaces under sub-critical flux were showed in Fig. 5.12 – Fig. 5.15 and it could be observed that these surfaces were visibly porous and almost free of particles. Obviously, there is no difference of fouling characterization on SEM pictures monitoring under sub-critical flux conditions regardless effect of MLSS (4 and 8 g/l) and EPS concentration (30 – 172 mg/l). Note that, the experiments run in this study were based on a short term tests which might not be covered in the long term operation. Under sub-critical flux operation, the fouling resistances in this fouling stage are closely to the membrane resistance with less than 20% increase.

The presence of cake layer on membrane surface was showed in supra-critical flux operation (Fig. 5.16 – Fig. 5.19). SEM images of the filters from the supra-critical flux experiments showed progressive coverage of the surface by sludge cake, reaching complete coverage (i.e., no visible pores). The result suggested that all the permeation passed through the cake layer became significant after almost all the pores were covered. The SEM pictures monitoring under supra-critical flux conditions show similar full fouling coverage on membrane surface regardless effect of MLSS (4 and 8 g/l) and EPS concentration (30 – 172 mg/l). Thus, all the cake fouling membranes were again watched in the side view in order to specify the difference in the depth observation.

The increase in the fouling rate coincided roughly with the sludge concentration which resulted in different cake thickness. Presumably, the greater the sludge concentration, the thicker the cake layer were (Fig. 5.20 – Fig. 5.23). The later increasing fouling rate could also be due to compression of the cake layer by the over-increasing TMP and the cake layer was seemed to be dense and non-porous. Meng *et al.* (2005) reported the cake porosity and cake permeability were decreased as TMP increased and the increase of cake layer thickness was also consistent with the decline tendency of porosity.

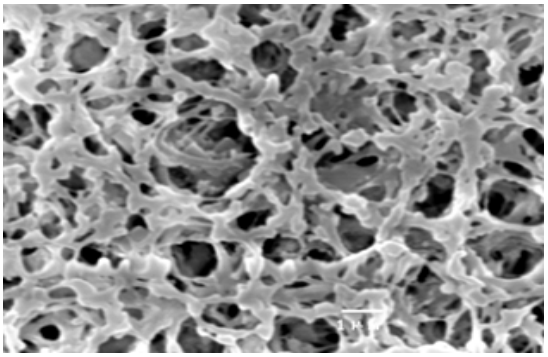

Fig. 5.12 Pore fouling under sub-critical flux operation of sludge 4 g/L and low soluble EPS

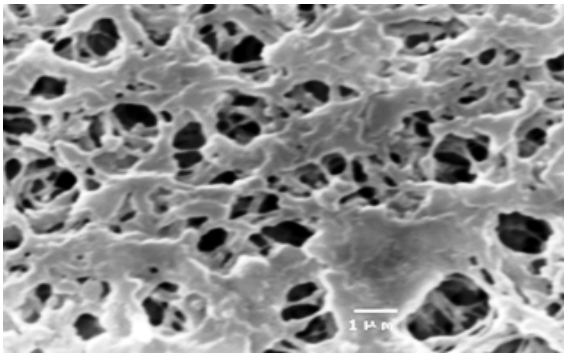

Fig. 5.13 Pore fouling under sub-critical flux operation of sludge 4 g/L and high soluble EPS

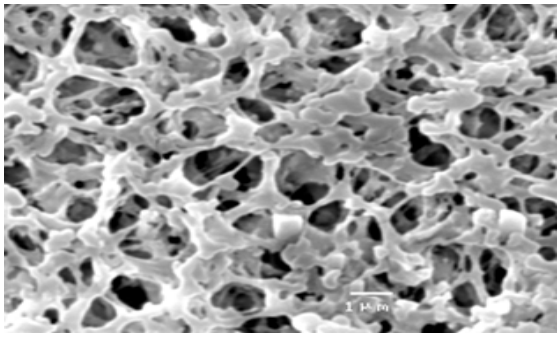

Fig. 5.14 Pore fouling under sub-critical flux operation of sludge 8 g/L and low soluble EPS

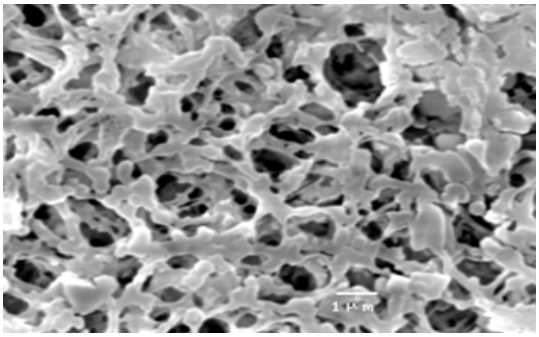

Fig. 5.15 Pore fouling under sub-critical flux operation of sludge 8 g/L and high soluble EPS

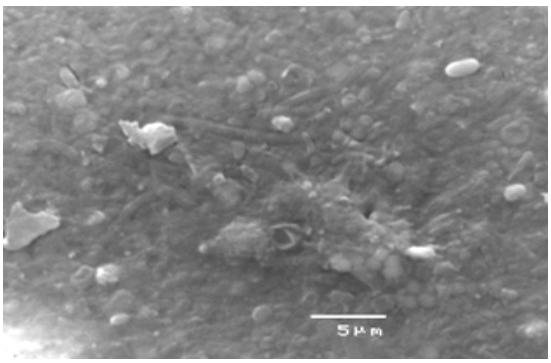

Fig. 5.16 Cake fouling under supra-critical flux operation of sludge 4 g/L and low soluble EPS

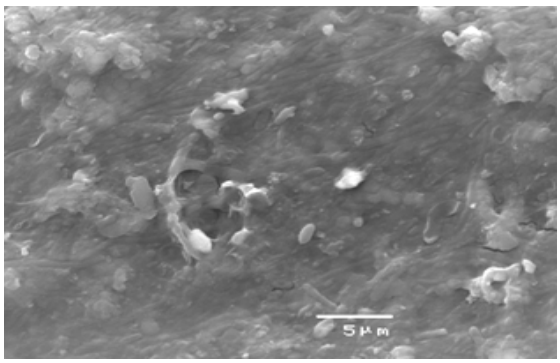

Fig. 5.17 Cake fouling under supra-critical flux operation of sludge 4 g/L and high soluble EPS

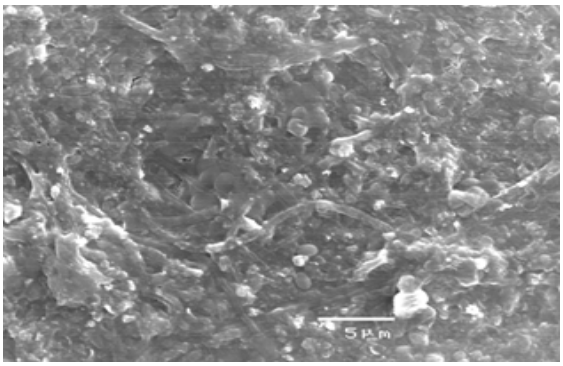

Fig. 5.18 Cake fouling under supra-critical flux operation of sludge 8 g/L and low soluble EPS

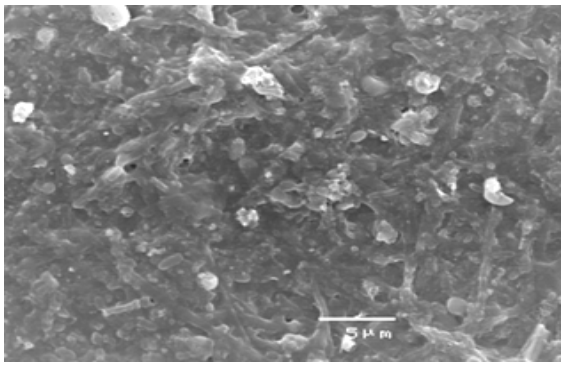

Fig. 5.19 Cake fouling under supra-critical flux operation of sludge 8 g/L and high soluble EPS

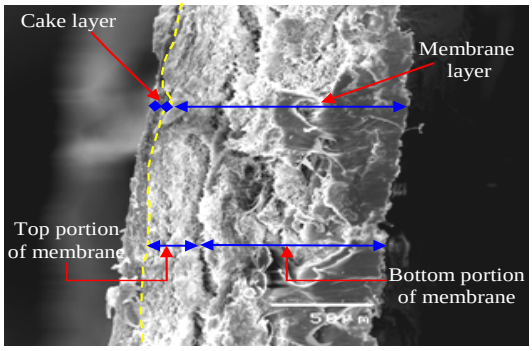

Fig. 5.20 Cross-section view of cake fouled membrane under sub-critical flux operation of sludge 4 g/L and low soluble EPS

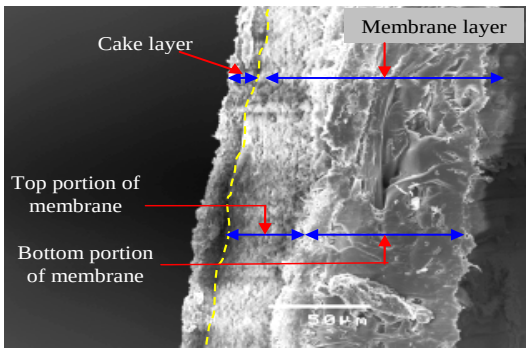

Fig. 5.21 Cross-section view of cake fouled membrane under sub-critical flux operation of sludge 4 g/L and high soluble EPS

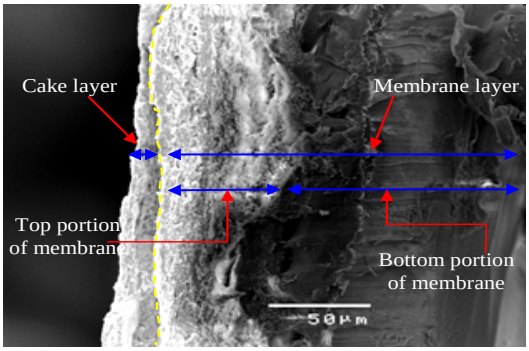

Fig. 5.22 Cross-section view of cake fouled membrane under supra-critical flux operation of sludge 8 g/L and low soluble EPS

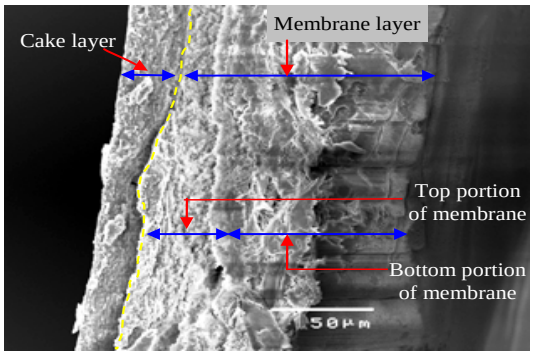

Fig. 5.23 Cross-section view of cake fouled membrane under supra-critical flux operation of sludge 8 g/L and high soluble EPS

5.4 CONCLUSION

In the present study, the influence of sludge compositions and flux stages of filtration on membrane fouling mechanisms was investigated. The critical flux determination at different MLSS concentrations (in this case 4,000 and 8,000 mg/L) was firstly performed as a preliminary consideration. Next, eight factorial designed experiments based on two different levels (low and high) of each factor including MLSS concentration, EPS concentration and flux stage filtration (supra-critical flux and sub-critical flux) were adopted. The resistance series model with different steps of fouling removal was applied to estimate cake fouling resistance and pore fouling resistance in each experiment. The experimental results showed that cake resistance accounted for a large portion of fouling contribution (50-65%) under supra-critical flux operation while pore fouling contributions are marginal for both under sub-critical flux (5-7%) and supra-critical flux (12-19%) operations. EPS and colloids appeared to have dominant fouling potential on membrane pore plugging regardless of MLSS concentration. EPS carbohydrate in soluble and bound forms has greater

impact on both pore fouling and cake fouling than would EPS protein. Under supra-critical flux operation, sludge concentration has a major influence on total fouling resistance due to cake formation whose thickness increase with sludge concentration increase.

CHAPTER 6

OPERATIONAL STRATEGIES AND OPTIMISATION FOR SUBMERGED MEMBRANE BIOREACTOR

6.1 INTRODUCTION

Compared with conventional activated sludge processes (CASP), submerged membrane bioreactors (SMBR) have many advantages, including reduced land requirements (by replacement of clarifier unit), capability to deal with high sludge concentrations, and constant and effective disinfection of treated water. Capital cost of MBR, CASP and wetland treatment plants were compared and reported that there is no significant difference among these treatment plant capital costs (Lesjean and Luck 2006). Lesjean and Luck (2006) explain that the capital costs of newly-built membrane plants are similar to CAS plants because the cost of the membrane units is offset by reduced footprints and land costs.

The operational costs of the SMBR are composed of chemicals for membrane cleaning, maintenance, sludge disposal, power consumption and membrane replacement (Churchouse and Wildgoose 1999). The energy consumption is considered the highest cost among these operational expenses (see Fig. 6.1) (Churchouse and Wildgoose 1999). The process energy required to run the submerged membranes both of fibre-bundles and flat-plate cartridges are dominated by the energy required to generate the two-phase flow (air-liquid) inducing surface shear stress to reduce the serious problem of membrane fouling (Fane 2005). SMBR fouling are results from internal fouling (e.g. pore plugging, pore narrowing) and

external fouling (cake formation of particles or microbial cells). Fouling phenomena on the membrane surface and within the membrane pores reduces long term flux stability, necessitating membrane cleaning, which then adds to the overall cost, as does membrane replacement in cases where cleaning fails to produce adequate flux recovery (Gander, Jefferson *et al.* 2000). Chemical treatment and backwashing techniques are normally used to remove internal fouling, while the external fouling can be minimized by hydrodynamic conditions including reduction of advective flux, promotion of turbulence shear, etc.

Fig. 6.1 shows SMBR plant running costs have decreased during 1992-2004. Sizes of the total area are in proportion to the overall revenue cost, while the partitioned areas inside the circle illustrate how the focus of attention has shifted from membrane replacement towards power and sludge disposal (Churchouse and Wildgoose 1999).

Several studies showed that a combined use of air induced crossflow and backwash is particularly favorable towards fouling suppression (Schoeberl *et al.*

2005) and proposed optimum conditions vary widely (Cote *et al.* 1997; Bouhabila *et al.* 2001). However, backwashing technique is normally applied for hollow fibre and tubular membrane configurations, but is not suitable for the flat sheet membrane due to strength limitations. This makes aeration strategies even more critical in fouling control in flat sheet membrane systems. Aeration in MBR is also a means of oxygen supply and biomass circulation, so that the microorganisms can contact and interact with the dissolved and suspended organic substances.

Lee *et al.* (1993) used an air-slugs entrapped technique to improve permeate flux up to 30% and 100% in a flat sheet-crossflow filtration with membrane pore size 0.2 um and 300 kDa, respectively. In the flat-sheet membrane filtration system, the effect of air injection on reducing protein transmission and increasing permeate flux by 7-50 % due to concentration polarization decrease was examined by Li *et al.* (1998) and a 10% flux increase in the filtration of mixture bovine serum albumin (BSA) and lysozyme was reported by Ghosh and Cui (1998). The effects of gas bubbling on yeast microfiltration flux in flat-sheet membrane system were also studied by Mercier-Bonin *et al.* (2000). They reported the increased flux of up to four times due to gas bubbling influence and more flux improvement was found in the horizontal modules of a cross-flow filtration rig. Ducom *et al.* (2002) studied wall shear stress and flux behavior of bubbling flow in a vertical filtration cell using one side transparent plate which embedded nine electrodes. The gas sparging in this device significantly increased permeate flux for a suspended clay system with less flux improvement for stabilized-emulsion filtration.

An attempt to reduce fouling in SMBR by varying the aeration rates was reported by Howell *et al.* (2004). An intermittent on/off aeration supply was also

studied and showed the increase of fast fouling as soon as air sparging ceases (Psoch 2005; Lim *et al.* 2007). However, the most common technique of aeration applied in SMBR systems is continuous air scouring with a consistent air velocity. No research has been studied before on a combined effect of regular aeration and air scouring frequency on SMBR fouling behavior. Thus, these unstable aeration techniques and SMBR fouling performance is worthy of detailed investigation.

The influence of filtration strategies was also considered as one of the most significant factors affecting fouling rate. For example, Schoeberl *et al.* (2005) studied the combined impact of filtration time, back-flush time and aeration intensity on the tubular MBR fouling fed with dye-house wastewater and the results showed the largest effect of filtration time on membrane fouling control. Moreover, an intermittent filtration mode proved to be an effective technique to reduce membrane fouling rates and allowed stable, long-term operation (Hong *et al.* 2002; Howell *et al.* 2004). However, most of the intermittent permeation experiments did not control the average equivalent flux yield which made the total flux yield of the intermittent mode lower than the continuous permeation and this might have an effect on the less fouling trends. To avoid underestimation, the effect of the intermittent flux with identical total flux yields compared to the continuous filtration mode on the SMBR fouling behavior needs to be observed.

The orthogonal design of experiments is a convenient and effective way to investigate influences of several factors simultaneously (Taguchi 1987) and is applied in a number of membrane studies (Gui *et al.* 2002; Idris *et al.* 2002). There are several methods used to discover optimum conditions of various systems. Simplex optimization is a common method to achieve the best parameter values, based upon

the primary database, which, unfortunately, might encounter only local optimal solutions (Sun *et al.* 1998). Additionally, traditional orthogonal experimental designs are sometimes unsuccessful in obtaining the complete optimal solution (Wu *et al.* 1990). Wu *et al.* (1990) have suggested a new orthogonal experimental design technique, named the Sequential Elimination of Level (SEL). The idea of SEL is opposite to that of the general optimum algorithm: instead of focusing on factor levels that improve the response, SEL focuses on those levels that worsen the response. Based on this idea, the worst level of each factor in each sequence of the experiment will be eliminated and new starting points will be used to iteratively satisfy the solution. The elimination process depends on the aim of optimization corresponding to the minimum, maximum and middle value. Compared with other methods, SEL has many advantages (Wu *et al.* 1990). First, it showed satisfactory characteristics in finding the optimal solution while serious model interactions existed in the system. Second, it can save on the number of experiments over the traditional multi-factorial experimental design. Finally, the analysis algorithm for the experimental data is very simple.

In this chapter, the effects of operational parameters including filtration modes, regular aeration intensity and air scouring frequency on fouling control in a pilot scale SMBR fed with real municipal wastewater were evaluated. A variation of these operational strategies was performed using orthogonal experimental design and the optimum level for each factor is then determined by the SEL technique. The significance and contribution of each factor was statistically analyzed. The confirmation experiment at the optimum condition was also included.

6.2 EXPERIMENTAL MATERIALS AND METHODS

6.2.1 Experimental facility

A pilot scale SMBR used in this study was the same SMBR system described previously in chapter 4. The characteristics of wastewater used in the experiment were shown in table 6.1. Similar diffuser was applied for scouring and aeration with different air flow rate (detail in table 6.2).

Table 6.1 Characteristics of wastewater used in the experiment (day 151 to day 200)

Parameter	Inlet	1st Unit	Anoxic	SMBR	Permeate
pH	7.26 ± 0.1	6.96 ± 0.1	6.95 ± 0.1	7.01 ± 0.1	7.09 ± 0.1
Temp (oC)	24.1 ± 0.8	24.7 ± 1.0	24.9 ± 0.9	24.7 ± 0.8	24.5 ± 0.6
DO (mg/L)	2.11 ± 0.20	2.42 ± 0.20	2.66 ± 0.19	2.85 ± 0.18	2.86 ± 0.16
Conduct. (uS)	1274 ± 69	1126 ± 32	1128 ± 42	1141 ± 28	1059 ± 31
ORP (mV)	-56.3 ± 12.0	264.3 ± 13.5	245.0 ± 34.7	235.1 ± 13.8	185.4 ± 8.5
MLSS (mg/L)	218 ± 31	6361 ± 182	7469 ± 212	7559 ± 238	N/A
NH4-N (mg/L)	36.6 ± 5.0	11.1 ± 3.1	3.6 ± 1.2	0.9 ± 0.6	0.6 ± 0.7
NO3-N (mg/L)	0.0 ± 0.0	0.0 ± 0.0	51.9 ± 6.5	33.3 ± 4.5	27.1 ± 6.0
PO4-P (mg/L)	12.1 ± 1.6	16.4 ± 2.2	12.2 ± 2.6	8.6 ± 2.1	8.5 ± 1.5
COD (mg/L)	326 ± 46	N/A	N/A	N/A	31 ± 11

6.2.2 Experimental design using orthogonal array

For study of several parameters at varying levels, a typical full-factorial experiment may consist of a large number of experiments, take time and be costly, and may possibly be too challenging to specify an optimal parameter. In this case,

one of fractional factorial design named Taguchi orthogonal design, was introduced. Taguchi orthogonal arrays are quick robust forms of partial factorial designs, which provide arrays of economic run size to accommodate a massive number of factors without similarity of any two experiments (or even mirror images) (Wu *et al.* 1990). In this study, experiments were carried out using three statistical techniques including the Taguchi method, analysis of variance (ANOVA) and the SEL technique to design experiments, in order to identify the significance of each factor and evaluate the optimum conditions of membrane operational parameters.

Three values of filtration modes, scouring frequencies and aeration rates were considered in the experiments undertaken. SMBR performance was then analyzed in terms of fouling propensity, based on the equivalent flux yield and equivalent aeration volume. The flux productivity was identical for each filtration mode applied in the experiments and was equivalent to average permeate of 100 L/h (see table 6.3). While permeate was kept constant at 100 L/h during the continuous mode experiment, the intermittent mode featured operational permeate of 110 and 120 L/h in ten minute intervals, followed by 1 and 2 minute relaxation period, respectively. The air intensities were set at 90, 100 and 110 L/min, coupled with different scouring frequencies of 6, 12 and 24 times per day. The air scouring rate was fixed at 170 L/min and the required scouring duration in each experiment was described in Table 6.2 based on the equivalent air volumes.

Table 6.2 Regular aeration and air scouring based on equivalent air volume

Regular aeration (l/min)	Scouring frequency (time/d)	Scouring size (l/m)	Scouring duration (min/time)	Scouring time (min/d)	Volume of scouring (l/d)	Air Volume (l/d)	Compensate scouring (min/d)	Total air volume (l/d)
120	0	170	0	0	0	172800	0	172800
120	0	170	0	0	0	172800	0	172800
120	0	170	0	0	0	172800	0	172800
110	24	170	10	240	40800	172800	0	172800
110	12	170	20	240	40800	172800	0	172800
110	6	170	40	240	40800	172800	0	172800
100	24	170	17	408	69360	172560	1.41	172800
100	12	170	34	408	69360	172560	1.41	172800
100	6	170	68	408	69360	172560	1.41	172800
90	24	170	22	528	89760	171840	5.65	172800
90	12	170	45	540	91800	172800	0	172800
90	6	170	90	540	91800	172800	0	172800

Table 6.3 Membrane flux consideration (fixed flux operation)

Filtration mode	Filtration rate	Filtration yield
Continuous filtration	100 l/h	100 l/h
10 min on : 2 min off	120 l/h	100 l/h
10 min on : 1 min off	110 l/h	100.8 l/h

Table 6.4 Level and factor of orthogonal experiments

Factor	Ref. level	Level 1	Level 2	Level 3
Filtration time	Continuous	Continuous	10 min on:1 min off	10 min on:2 min off
Regular aeration	120 L/min	110 L/min	100 L/min	90 L/min
Scouring frequency	0 time/d	6 time/d	12 time/d	24 time/d

Table 6.5 The SMBR operating conditions of the orthogonal design

No.	Regular aeration (L/min)	Scouring frequency (time/d)	Filtration: non- filtration (min:min)		Filtration rate (L/h)	Blank
			filtration time (min)	non- filtration time (min)		
A	120	0	continuous	0	100	1
B	120	0	10	2	120	3
C	120	0	10	1	110	2
1	110	24	continuous	0	100	1
2	110	12	10	2	120	3
3	110	6	10	1	100	2
4	100	24	10	2	120	2
5	100	12	10	1	110	1
6	100	6	continuous	0	100	3
7	90	24	10	1	110	3
8	90	12	continuous	0	100	2
9	90	6	10	2	120	1

An orthogonal experiment with 9 trials was carried out. Reference level experiments were also conducted with different flux modes and no scouring (runs A, B and C). The level values and experimental arrangement of the 9 trials are shown in table 6.5 with a summary of factors and levels. The blank factor is a dummy variable and is used for error estimation. All experiments in the system operated for 24 hours at each trial. TMP and permeate data for all experiments were logged every 5 min using the PLC device.

6.3 RESULTS AND DISCUSSION

6.3.1 Membrane fouling index

During the membrane filtration process, particulate MLSS and soluble organic material is deposited on the membrane surface leading to membrane fouling. This resulted in an increase of the filtration resistance (R_f) and accordingly the elevation of the TMP in the fixed flux filtration process. Therefore, the membrane fouling status at different operational conditions could be indirectly observed by continuously monitoring the TMP and characterized by the average increase rate of TMP over a certain period of operation. Cho and Fane (2002) described the TMP rise under the normal critical flux as a two-stage process. The first stage was a gradual linear increase in TMP, and the second stage was a sudden increase in the TMP. The two-stage process is attributed to fouling by extra-cellular-polymeric substance (EPS) in stage 1, and fouling by biomass in stage 2. Several authors showed that submerged microfiltration membranes exhibit a greater sensitivity to initial fouling for SMBRs used for wastewater treatment (Nagaoka *et al.* 1998; Rosenberger and Kraume 2003; Janga *et al.* 2007).

The changing course of TMP over each experiment can reflect the membrane fouling status at the selected operational parameters and also can relate to the filtration resistance of the system using Darcy's Law (eq 6.1)

$$J = \frac{\Delta P}{\mu (R_m + R_f)} \qquad \textbf{6.1}$$

All parameters in equation 6.1 were addressed in appendix E.

6.3.2 Membrane fouling results

The TMP increased which during 24 hours of filtration was shown in Fig. 6.2 - Fig. 6.13. In Fig. 6.2 - Fig. 6.13, some sudden jumps or sharp increases of TMP values happened during the few hours of operation. This TMP jump has been reported in the literature (Cho and Fane 2002; Ognier *et al.* 2002; Yu *et al.* 2003) as the phenomenon caused by local flux increasing and exceeding the critical flux of the dominant bio-particles in some regions of the membrane. However, the increase of most TMP as a linear progress of filtration resistance was still clearly observed. The increasing rate of membrane fouling in each experiment was therefore assessed as a slope of linear TMP increase over the experimental period ($\Delta TMP/\Delta t$). The average TMP increasing rates at each trial are also represented in the table 6.6. Trial no.1 and no.9 exhibited the lowest and highest fouling within the range of operational parameters investigated in this study.

Since the experiment was designed in an orthogonal array, when one factor is focused, the effect of other factors could be cancelled out. Hence, effects of the different operational parameters can be extracted independently in terms of the mean response. Taking a factor of the aeration at 100 L/min as an example, the mean response of TMP increase rate obtained in the orthogonal test could be carried out based on table 6.7 as follows: (136.37 + 123.26 + 88.85) / 3 = 116.16 Pa/d. Similarly, the mean responses of all factors were calculated and showed in table 6.7. Effects of each factor on membrane fouling rate were plotted as shown in Fig. 6.14.

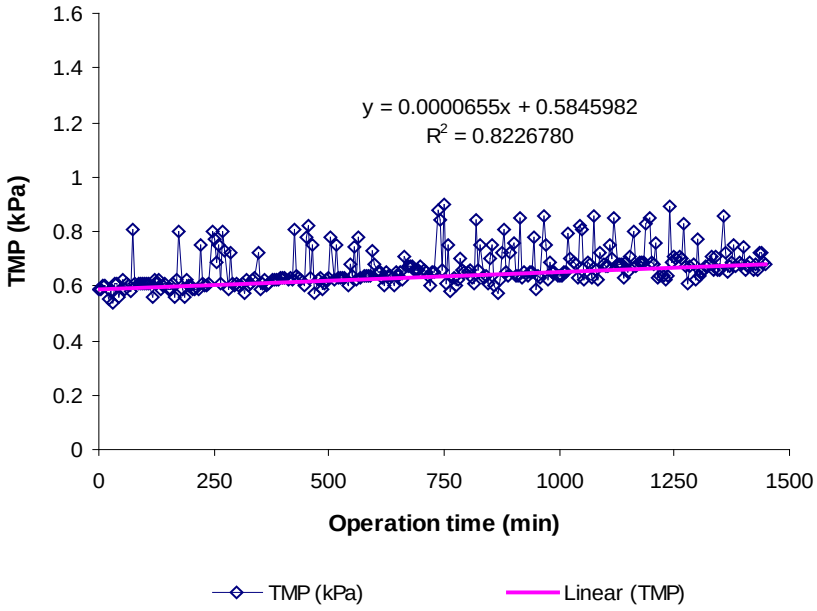

Fig. 6.2 The changing TMP in the experiment A

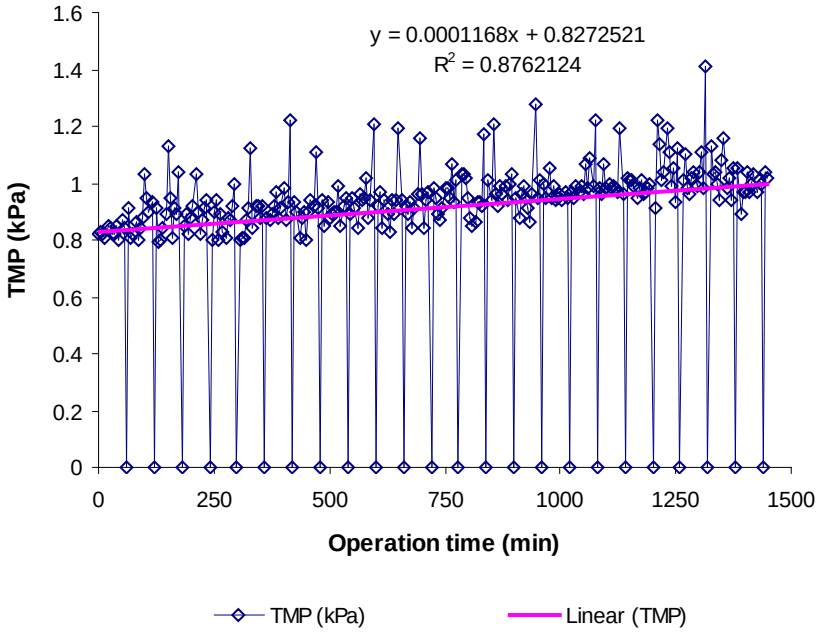

Fig. 6.3 The changing TMP in the experiment B

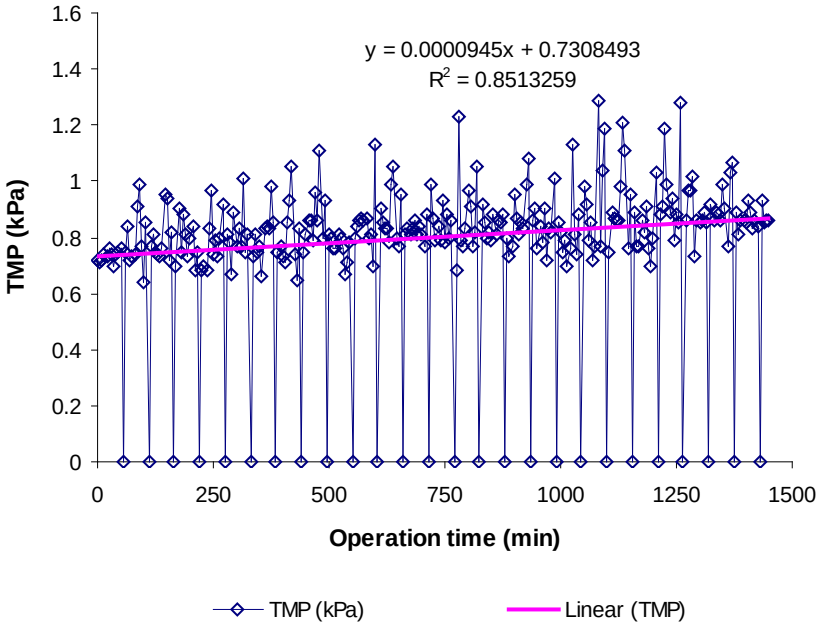

Fig. 6.4 The changing TMP in the experiment C

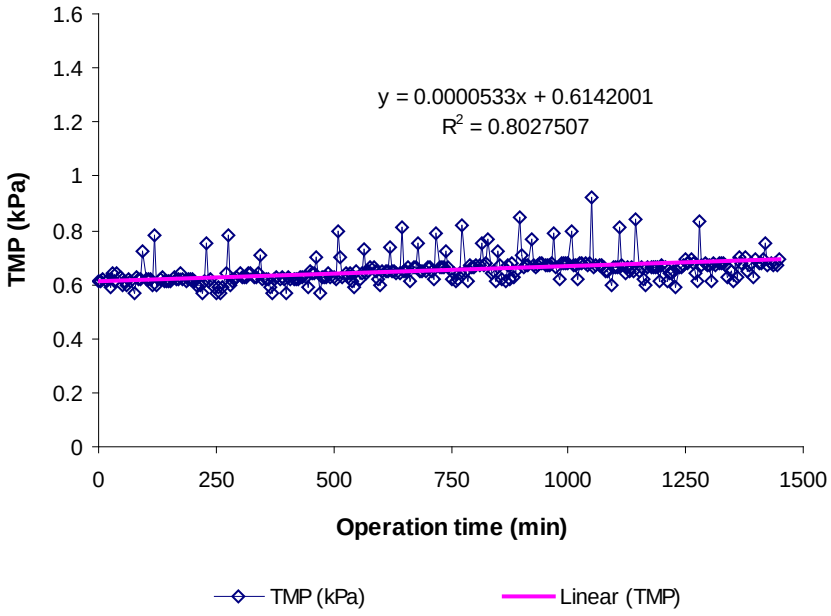

Fig. 6.5 The changing TMP in the experiment no. 1

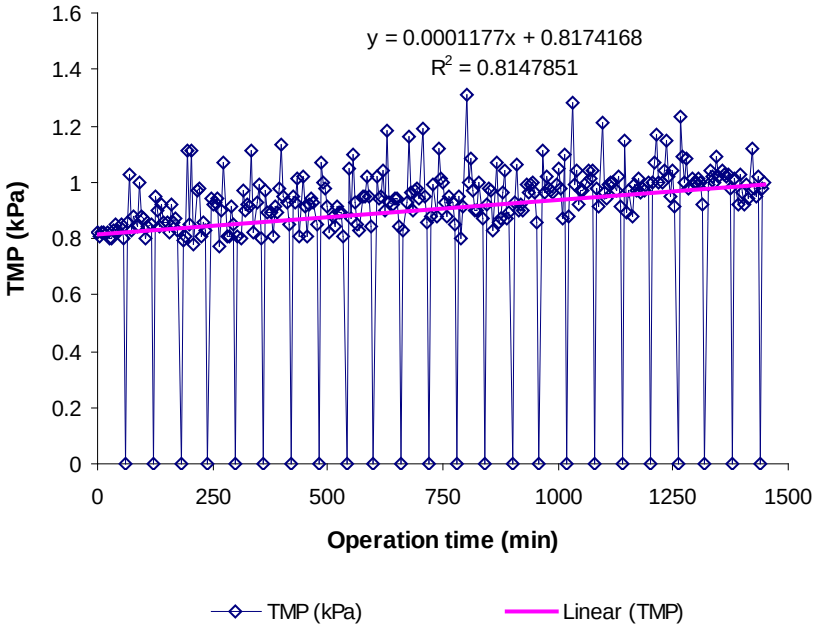

Fig. 6.6 The changing TMP in the experiment no. 2

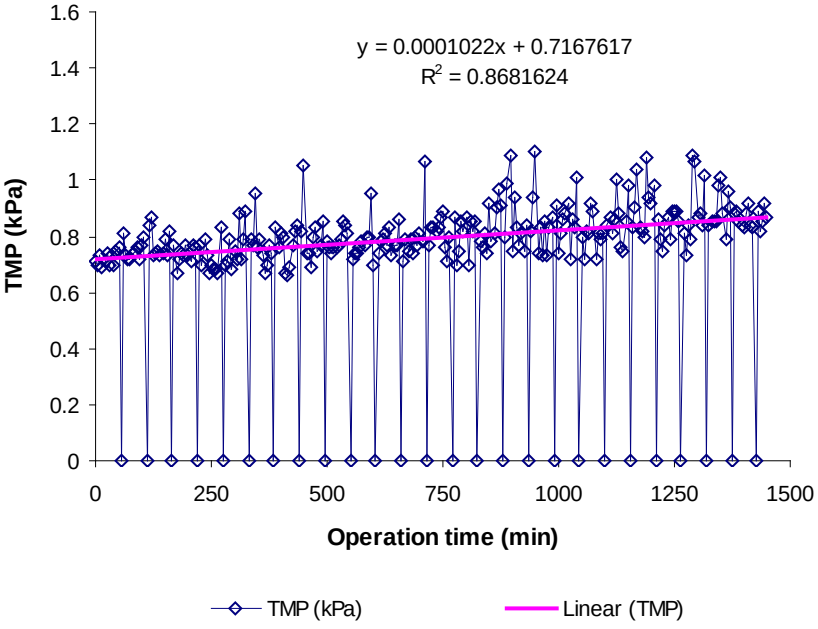

Fig. 6.7 The changing TMP in the experiment no. 3

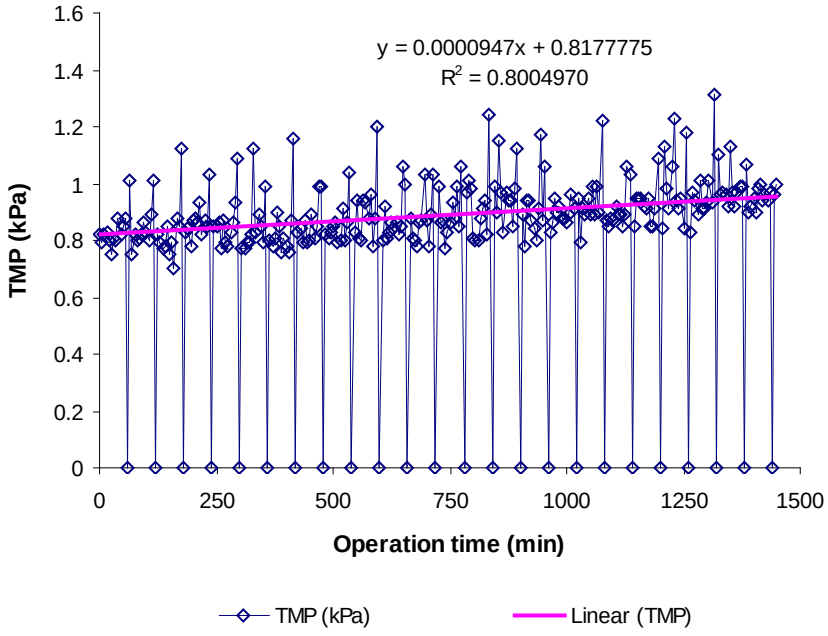

Fig. 6.8 Changing TMP in the experiment no. 4

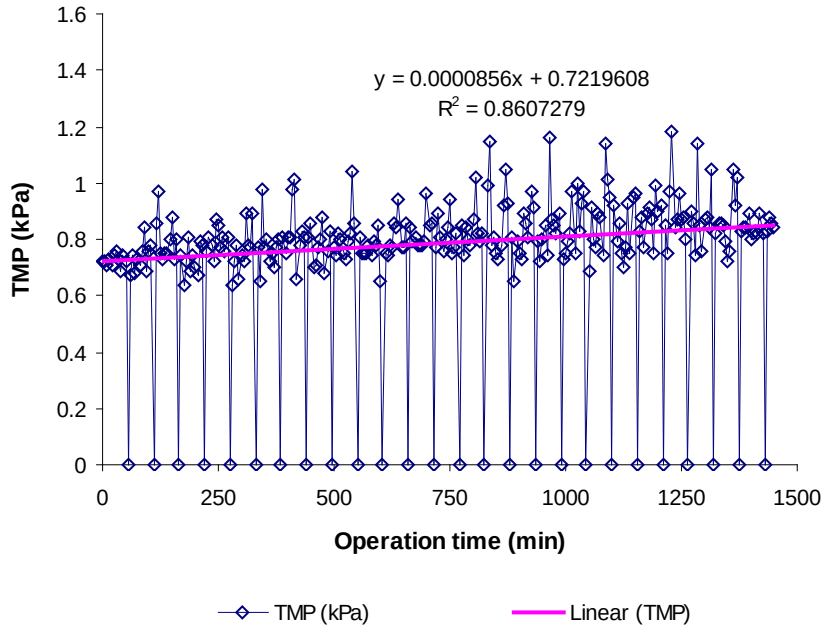

Fig. 6.9 Changing TMP in the experiment no. 5

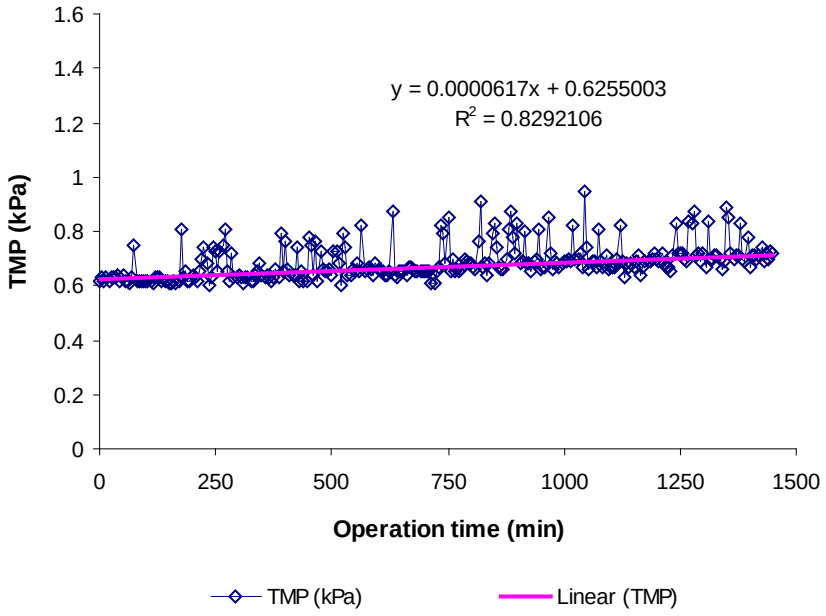

Fig. 6.10 Changing TMP in the experiment no. 6

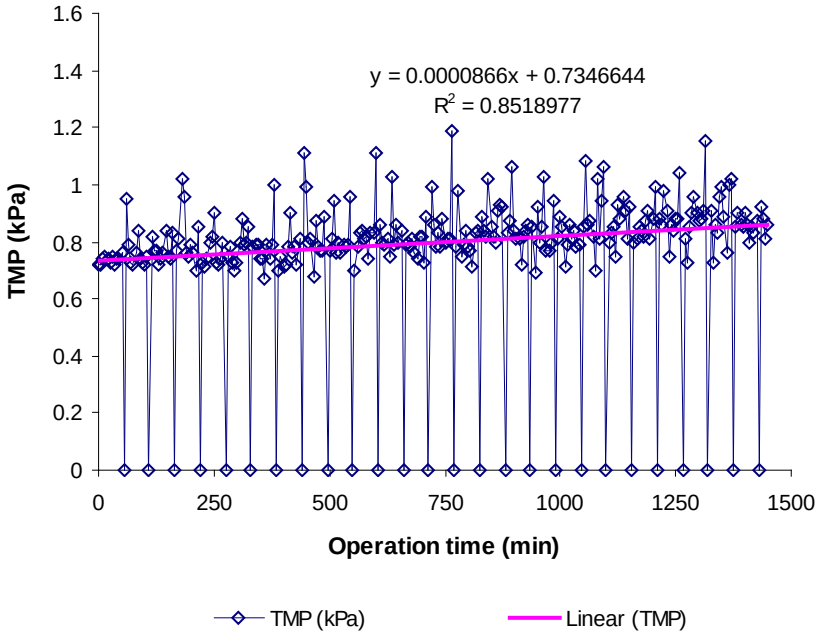

Fig. 6.11 Changing TMP in the experiment no. 7

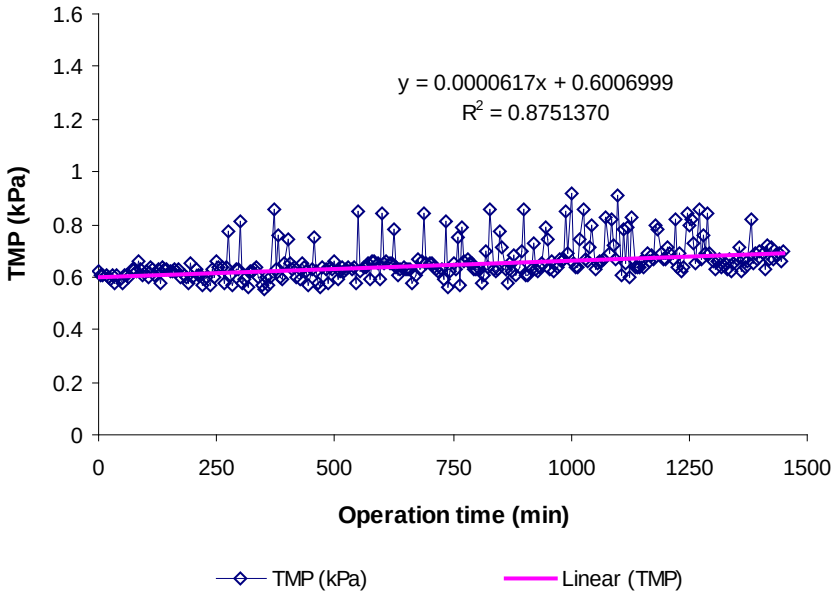

Fig. 6.12 Changing TMP in the experiment no. 8

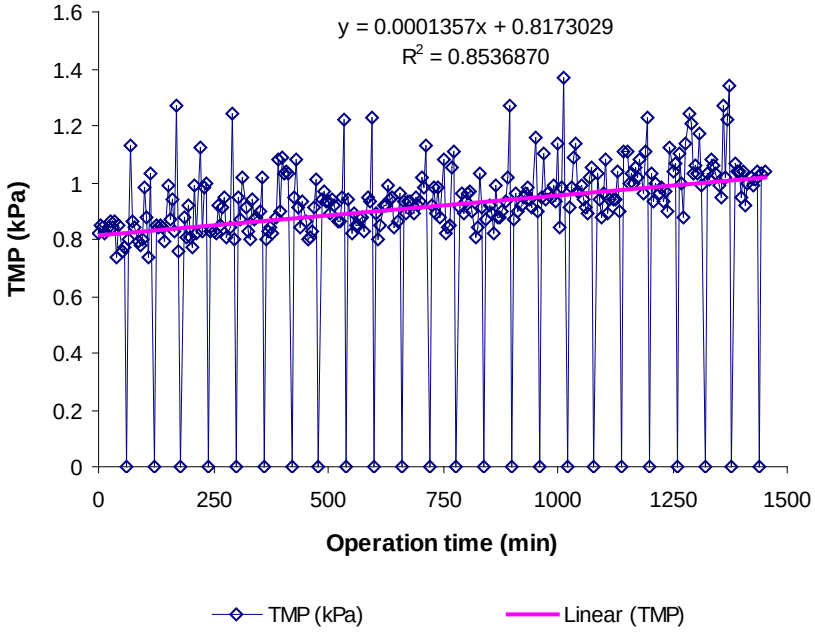

Fig. 6.13 Changing TMP in the experiment no. 9

Table 6.6 Summary the SMBR operating results from Fig. 6.3 – Fig. 6.14

No.	Regular aeration (L/min)	Scouring frequency (time/d)	Filtration time and filtration rate		Blank	$\Delta TMP/\Delta t$ (kPa /min)	$\Delta TMP/\Delta t$ (Pa /d)
			filtration time on : off (min)	filtration rate (L/h)			
A	120	0	continuous	100	1	6.55E-05	94.32
B	120	0	10 :2	120	3	1.17E-04	168.19
C	120	0	10:1	110	2	9.45E-05	136.08
1	110	24	continuous	100	1	5.33E-05	76.75
2	110	12	10 :2	120	3	1.18E-04	169.49
3	110	6	10:1	110	2	1.02E-04	147.17
4	100	24	10:2	120	2	9.47E-05	136.37
5	100	12	10:1	110	1	8.56E-05	123.26
6	100	6	continuous	100	3	6.17E-05	88.85
7	90	24	10:1	110	3	8.66E-05	124.70
8	90	12	continuous	100	2	6.17E-05	88.85
9	90	6	10:2	120	1	1.36E-04	195.41

Table 6.7 Mean fouling response obtained from Taguchi method

Factor	Level	Value	Average fouling rate ($\Delta TMP/\Delta t$)
Regular aeration (L/min)	reference	120	132.86
	1	110	131.14
	2	100	116.16
	3	90	136.32
Scouring frequency (events/d)	reference	0	132.86
	1	6	143.81
	2	12	127.20
	3	24	112.61

Table 6.7 Mean fouling response obtained from Taguchi method (continued)

Factor	Level	Size	Average fouling rate ($\Delta TMP/\Delta t$)
Filtration to non-filtration time (min:min)	1	Continuous	84.82
	2	10 min on :1 off	131.71
	3	10 min on :2 off	167.09

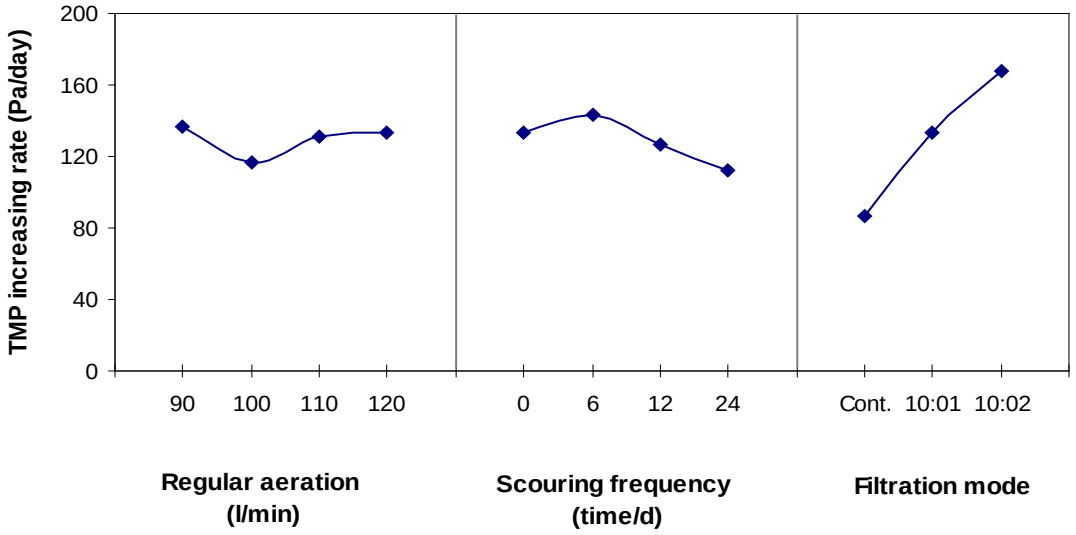

Fig. 6.14 Total comparison of mean fouling responses

From Fig. 6.14, filtration mode was observed to have the largest effect on the rate of membrane fouling. Interestingly, in other studies, when the membrane flux was fixed, an intermittent filtration mode showed a significant improvement in membrane fouling performance, compared against continuous filtration (Hong *et al.* 2002; Howell *et al.* 2004). Most research explained that the intermittent filtration mode would promote foulants back transport under pressure relaxation, diffused away from the membrane surface. At the same time, the removal of foulants by air bubbling was also greatly enhanced under a no-pressure gradient across the

membrane. As a result, foulants accumulation near the membrane surface in the intermittent filtration mode was lessened and the rate of fouling should be reduced significantly. However, most SMBR research based on intermittent filtration have been done without consideration of the equivalent flux yield between the continuous and intermittent filtrations, resulting in the lower flux productivity in the intermittent mode than the continuous mode in those research. In this study, the effect of different filtration modes based on equivalent average flux rates on the SMBR fouling was investigated. The discovered results (Fig. 6.14) were contrasted from the literatures with the greater TMP increase in the intermittent filtration mode, thus increasing fouling over time. Since the first cycle of filtration, the higher flux 10% and 20% during the filtration period of the intermittent filtrations may lead to a greater fouling compared to the lower continuous flux and the pressure-relaxation period in the intermittent filtration modes sometimes may not fully remove the previous fouling occurring in the system.

As for the influence of regular aeration (Fig. 6.14), the mean rate of TMP increase changed slightly with the variation of regular aeration rates from 90 to 120 L/min. This is probably because another part of the aerations were performed in the scouring modes which gave much higher response compared to the regular aerations. In SMBR system, the aeration not only provides oxygen to the biomass, but also maintains the solids in suspension and scours the membrane surface. Both experimental and empirical studies have demonstrated that substantial air shearing stress along the membrane surface could enhance the flux (Li *et al.* 2005). The efficiency of air-induced cross-flow to remove or at least reduce the fouling layer on

the membrane surface has been extensively reported (Ueda *et al.* 1997; Liu *et al.* 2000; Gui *et al.* 2002).

A positive effect of aeration on decrease of the fouling rate could be explained by back transport of deposited foulants from the membrane surface towards the bulk solution induced by shearing stress at the higher air blowing rates. Also, high shear stress promoted from aeration used for minimizing concentration polarization which is the formation of a higher concentration of retained particles or molecules at the membrane surface, compared to that of the bulk suspension, resulting in a concentration gradient and leading to a cake formation fouling on membrane surface. A negative effect of higher regular aeration was presumably described to the change of sludge floc size to the finer size at higher shear stress (Chellam and Wiesner 1998).

As for the influence of scouring frequency (Fig. 6.14), the more the scouring frequency, the less the TMP increase rate, suggesting some removal of deposited foulants. This may be attributed to the fact that when frequent air scouring occurred, it created a sudden turbulent condition in the SMBR system that resulted in severe sweeping away of the vibrant materials, including the concentration polarization layer. It has been reported that the filtration resistance caused by a sludge cake layer formed on the membrane surface depends on the sludge specific resistance and sludge porosity (Chang and Lee 1998). During filtration, sludge porosity decreased and then reached an approximately constant level (Chang and Lee 1998). The thickness of the cake layer is also limited and reaches equilibrium due to constant applied shear forces from the gas sparging process (Chang and Lee 1998). Thus, the unsteady high shear stress from frequent scouring can be interfered a forming stable structure of porous cake layer and routinely removed it.

Table 6.8 ANOVA based on the mean response in run no.1-9 (more detail of ANOVA calculation is given in appendix D)

Factor	Degree of freedom	Sum of squares	Mean square	F Value	Percent of contribution
Aeration	2.00	657.59	328.80	7.43	5.33
Scouring frequency	2.00	1462.51	731.25	16.51	11.85
Filtration mode	2.00	10219.63	5109.82	115.39	82.82
Error (blank)	2.00	88.56	44.28	-	-
Total	8	12428.2	-	-	100

For comparison of the significance in influencing the increased TMP rate of the three variables namely filtration mode, regular aeration mode and scouring frequencies, the analysis of variance (ANOVA) method is used and the results are shown in table 6.8. After the ANOVA is completed, the F statistic can be obtained. The F statistic of any specific control factor is defined as the ratio of the sum of variance square for that control factor and the sum of error variance square obtained and is used for significance testing. The larger the F statistic, the larger the influence of such a control factor will be.

Note that, physically, the value of F statistic represents the ratio of variance explained by control factors to the unexplained variance by errors in the experiment. Table 6.8 presents sum of squares (SS), mean square (variance), factor variance to error variance ratio (F) and contribution percentage of each factor on response (P). As seen, three variables are influential in the TMP increase rate but in the order of filtration mode > scouring frequency > regular aeration. The most significant effect of filtration mode compared to other operating parameters (i.e. aeration, back

flushing) was also reported in some studies (Schoeberl *et al.* 2005). Similarly, Gui *et al.* (2002) investigated effects of operational parameters including aeration intensity, membrane flux, suction time and non-suction time on fouling in a SMBR and obviously found that permeate flux influencing on the TMP increase the most and the aeration intensity became significant only at the high MLSS.

6.3.3 Optimum operating condition of the SMBR system

Based on the results shown in Table 6.9, the so called Sequential Elimination of Level (SEL) technique was applied to optimize the SMBR's operation. At this stage, the level corresponding to the largest fouling rate for each factor in the previous section was eliminated i.e. the level 3, 3, and 1 were eliminated for the filtration mode factor, regular aeration and scouring frequency. Two levels remained for each factor at this time. A new orthogonal design was selected for the remaining 2 levels of 3 factors as shown in table 6.10. In fact, it was carried out only six new experiments because experiment no. 1 and 8 in table 6.10 are the same as no. 1 and 6 in table 6.5.

The results of the TMP increasing rate for the second round experiments are shown in table 6.10 and Fig. 6.15 - Fig. 6.21. Similar to the previous section, more frequent scouring and low flux continuous modes causes reduced membrane fouling rates (table 6.11). Here again, the filtration mode and scouring frequency are important influences upon the increase of membrane fouling rates. The aeration (100 to 110 L/min) has less significant contribution on the membrane fouling, compared with the previous experiments. With the SEL technique, the factor level corresponding to the highest fouling trend was again eliminated. Therefore, the best level of factors corresponding to the optimum (or lowest fouling) membrane operating

condition was 110 L/min aeration with continuous filtration mode and 24 times per day scouring frequency.

Table 6.9 Mean fouling response and level elimination

Factor	Level	Average $\Delta TMP/\Delta t$	Level elimination
Regular aeration (L/min)	120	132.86	reference level (not consider for elimination)
	110	131.14	-
	100	116.16	-
	90	136.32	highest fouling rate (level eliminated)
Scouring frequency (time/d)	0	132.86	reference level (not consider for elimination)
	6	143.81	highest fouling rate (level eliminated)
	12	127.20	-
	24	112.61	-
Filtration to non-filtration time (min:min)	Continuous	87.19	-
	10 min on :1 off	132.80	-
	10 min on :2 off	167.37	highest fouling rate (level eliminated)

Table 6.10 The SMBR operating results in the 2nd round experiments

No.	Regular aeration (L/min)	Scouring frequency (time/d)	Filtration time and filtration rate		$\Delta TMP/\Delta t$ (kPa /min)	$\Delta TMP/\Delta t$ (Pa /d)
			filtration time on (min):off (min)	filtration rate ($L/m^2.h$)		
1	110	24	continuous	10	5.33E-05	76.75
2	110	24	10 :1	11	7.07E-05	101.81
3	110	12	continuous	10	5.55E-05	79.92
4	110	12	10 :1	11	8.01E-05	115.34
5	100	24	continuous	10	5.42E-05	78.19
6	100	24	10 :1	11	0.000075	108.00
7	100	12	continuous	10	5.96E-05	85.82
8	100	12	10 :1	11	8.56E-05	123.26

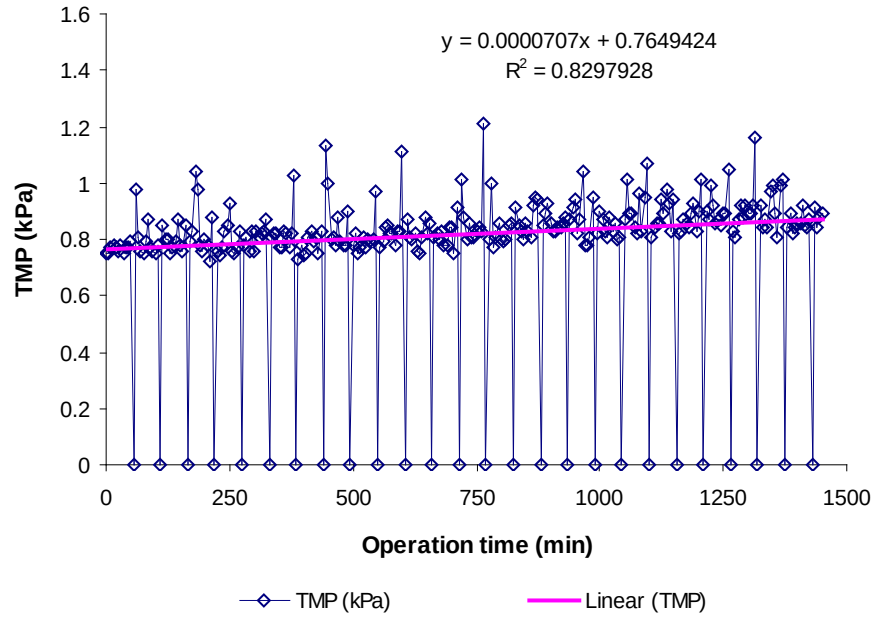

Fig. 6.15 Changing TMP in the experiment no. 2

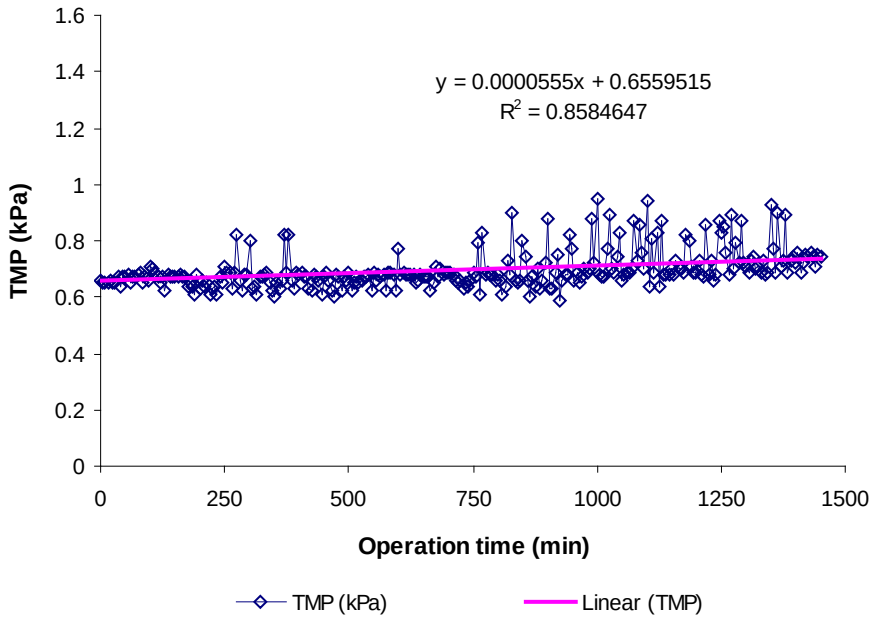

Fig. 6.16 Changing TMP over experiment no. 3

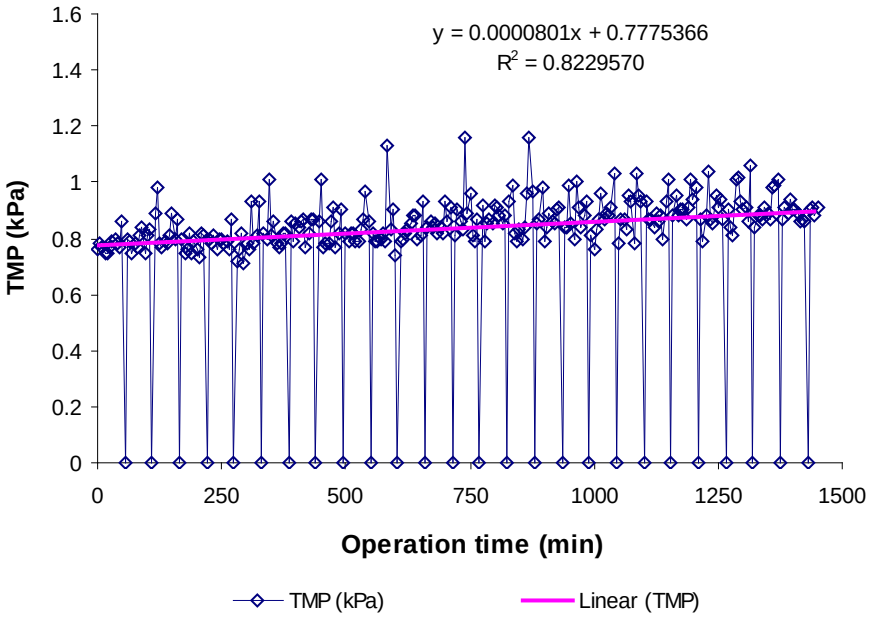

Fig. 6.17 Changing TMP over experiment no. 4

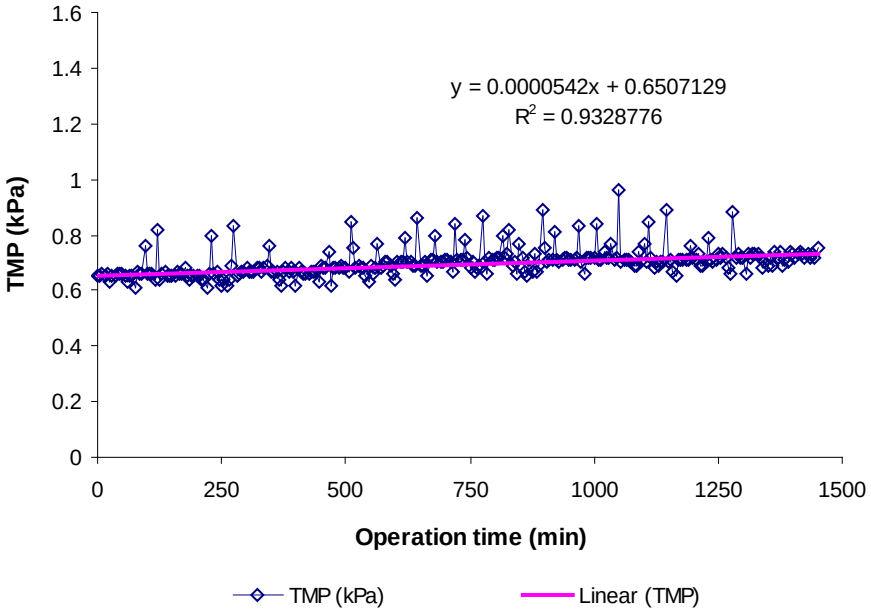

Fig. 6.18 Changing TMP over experiment no. 5

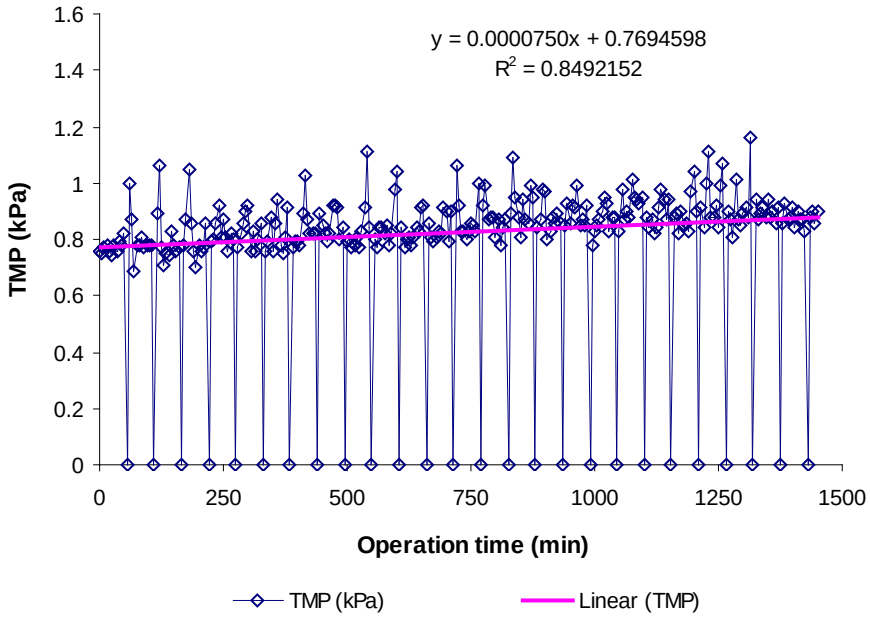

Fig. 6.19 Changing TMP over experiment no. 6

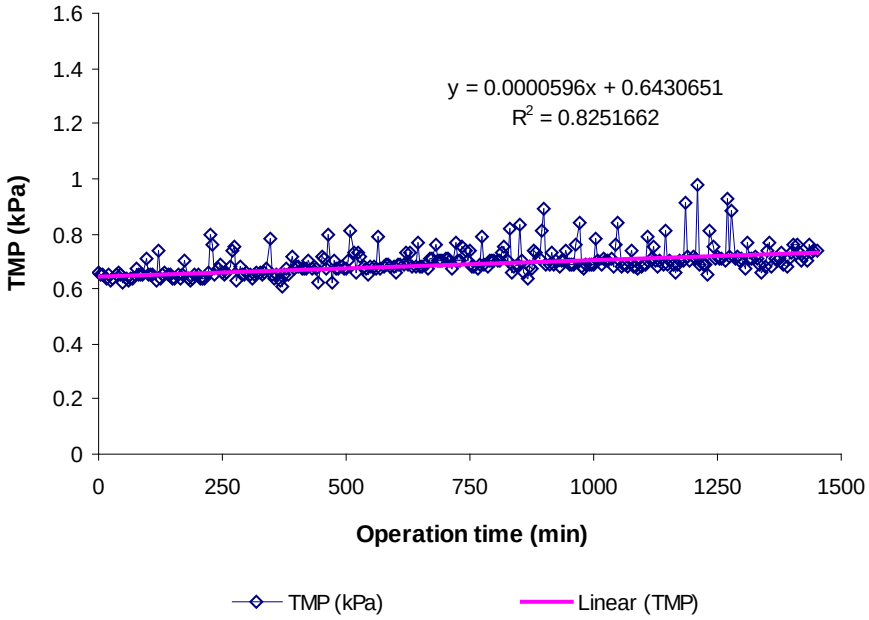

Fig. 6.20 Changing TMP over experiment no. 7

Table 6.11 Mean fouling response and level elimination

Factor	Level	Average $\Delta TMP/\Delta t$	Level elimination
Regular aeration (L/min)	100	98.82	Higher fouling rate (level eliminated)
	110	93.46	-
Scouring frequency (time/d)	12	101.09	Higher fouling rate (level eliminated)
	24	91.19	-
Filtration to non-filtration time (min:min)	Cont.	80.17	-
	10:1	112.10	Higher fouling rate (level eliminated)

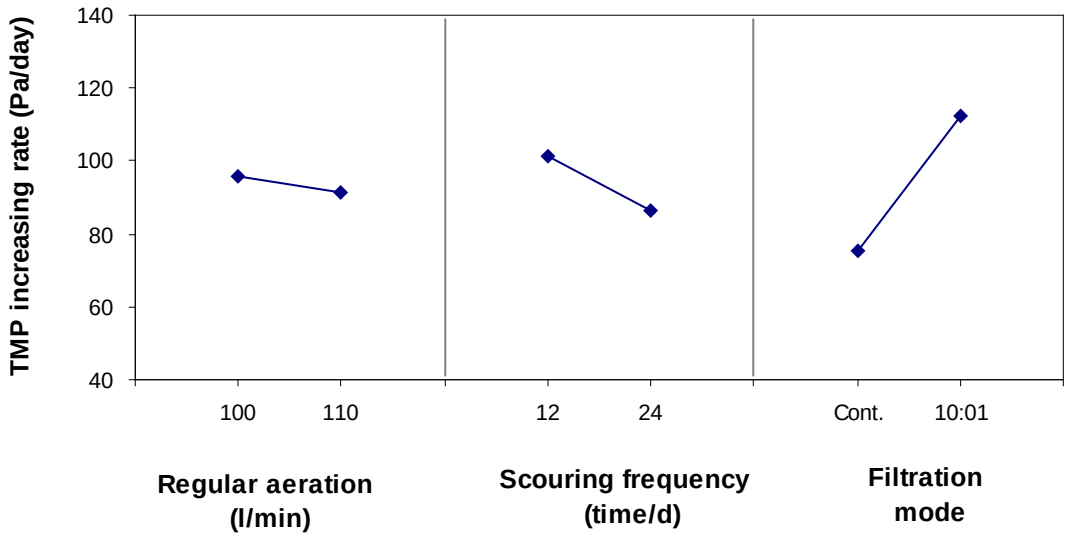

Fig. 6.21 Total comparison of mean fouling responses

6.3.4 Confirmation experiments

In general, if the optimum setting is not one of the trial run experiments, confirmation testing is a necessary and important step in the Taguchi method, as it is a

direct proof of the methodology. A confirmation experiment consists of adopting the recommended levels of the significant factors and the most favorable setting of all remaining factors investigated in the experiment (Idris *et al.* 2002). In this study, a confirmation experiment at the optimum condition is not really necessary because it was one of the trial tests. However, long term operation at the two reference levels (120 L/min aeration, intermittent (10 min on: 2 min off) and continuous filtration) and the optimum operating condition (110 L/min aeration, continuous filtration and 24 times/d scouring) were performed to observe the validity of this approach. The results are presented in Fig. 6.23.

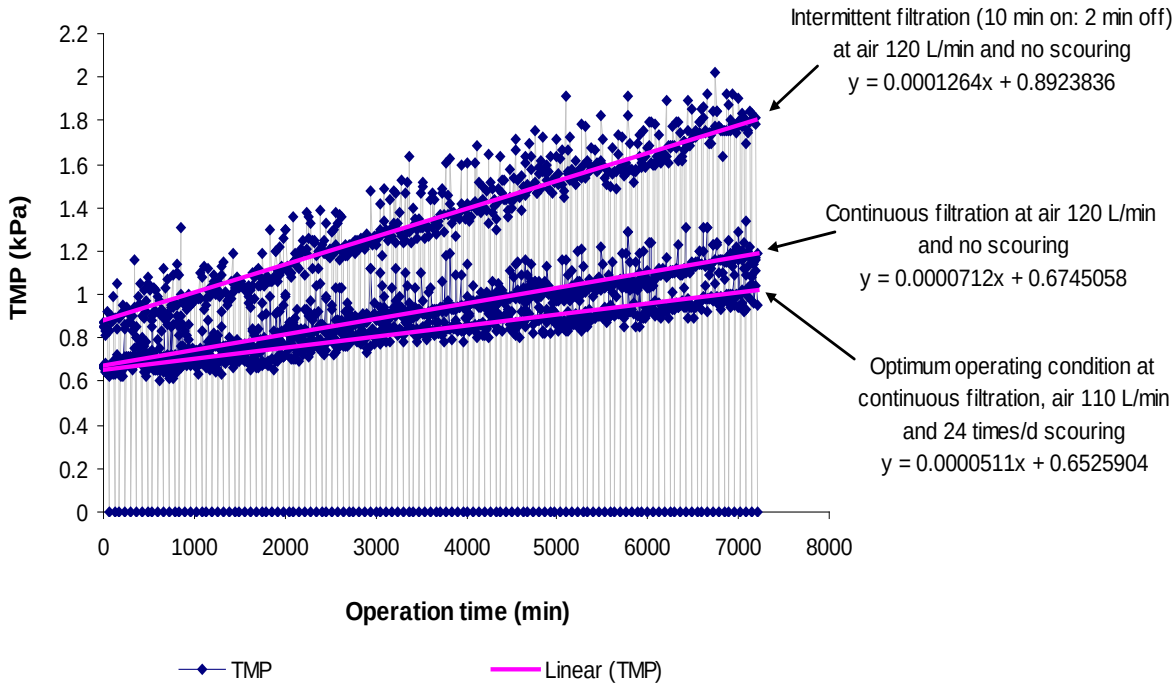

Fig. 6.22 The changing TMP over long term operation

With optimum operating conditions, the fouling rate in the SMBR system can be reduced up to 28% and 57% of fouling propensity compared to the reference

levels, which run with no scouring at continuous and intermittent filtration modes, respectively. Therefore, operation at an optimum condition can be considered as one of the most effective fouling reduction technique.

6.4 CONCLUSION

Based on the equivalent flux and air volume, the influence of variation of aeration intensity, scouring frequency and filtration modes on the rate of fouling increase were investigated. The orthogonal designed experiment was adopted to investigate the influences of these three factors on membrane fouling performance. Filtration mode was a key factor influencing the membrane fouling process, followed by scouring frequency and aeration mode in decreasing order of impact.

To avoid encountering only a local optimal solution, the sequential elimination of level (SEL) method was used to optimize the operating parameters of the system under study. One level of each factor that gave the largest fouling trend is eliminated and a new orthogonal experiment is performed. Similarly, in the second round experiment, the filtration mode and scouring frequency still played the most and second-most influence on the increase of membrane fouling rate. Once more, the worst level of each factor is eliminated and the optimum operating condition for the lowest membrane fouling profile is suggested at 110 L/min aeration with continuous filtration and 24 times scouring per day. Long term experiments (120 hour) are also carried out. With optimum operating strategy, fouling propensity in the SMBR system can be reduced up to 28% and 57% compared to the reference levels that run with no scouring filtrations at continuous and intermittent filtration modes, respectively.

CHAPTER 7

CONCLUSIONS AND RECOMMENDATIONS

7.1 CONCLUSION

This thesis aims to understand biofouling performances in a pilot scale SMBR for municipal wastewater treatment. A number of conclusions can be made from the results obtained in this thesis.

- Based on design and construction shown in chapter 3, the SMBR pilot scale presented excellent removal of ammonia and COD but not well achieved in nitrate and phosphate removal due to high DO concentration interrupting the anaerobic and anoxic stages.

- With the SMBR pilot plant, critical flux determinations based on different proposed concepts were tested in chapter 4. Slightly variations of the critical flux values were obtained from various determination methods. However, the two-third limiting flux and the flux hysteresis concepts are likely to indicate upper and lower border of the transient critical zone. Compared with step-height variable, the step-length variable has no obvious effect on the critical flux assessment. An increase in aeration could enhance the critical flux while the higher MLSS gave negative results on critical flux.

- In chapter 5, membrane fouling mechanisms were examined. Under supra-critical flux operation, cake fouling accounted for the largest fouling contribution while pore fouling were marginal for both under sub-critical flux

and supra-critical flux operations. EPS and colloids appeared to have dominant fouling potential on membrane pore plugging regardless of MLSS concentration. EPS carbohydrate in soluble and bound form has greater impact on both pore fouling and cake fouling than would EPS protein

- In chapter 6, the optimization of the SMBR operation was investigated based on similar yield of permeate and similar quantity of energy consumption. The results showed that operating variables were influential in the fouling increase rate but in the order of filtration mode > scouring frequency > regular aeration. With the Sequential Elimination of Level (SEL) technique, the optimum operating condition for the SMBR was suggested at 110 L/min aeration with continuous filtration and 24 times scouring per day.

7.2 RECOMMENDATION FOR FUTURE WORK

- The poor performance of nitrate and phosphorous removal should be improved by adjusting the system configuration such as extension of the anaerobic hydraulic retention time (HRT) or adding some more treatment units to create the anaerobic stage in the SMBR system etc.
- Actual feeds with high fluctuation of inlet matters from real municipal wastewater obtained from Townsville Mt St John treatment plant may cause different fouling behavior in each experimental period. Therefore, this should be more controlled.
- More modeling and simulation to predict the SMBR performance should be further studied.

- Experiments based on different critical flux suggested in chapter 4 should be tested in long term runs.
- Colloidal TOC is strongly related with soluble EPS as shown in chapter 5 based on two aerations and different filtration phases. It is suggested that more variation of aeration and colloidal TOC should be broaden studied.
- Fouling propensity may be different at different duration of filtration. Therefore, long term operation on the optimum condition suggested in chapter 6 should be further examined.
- Other fouling mitigation techniques such as back-flushing and external cleaning are interesting to be added in the future studies because it can represent the real applicable conditions been used in the industrial SMBR.
- For the establishment of the complete picture of submerged membrane fouling, more works are needed to evaluate the correlation among critical flux, EPS, pore fouling and cake fouling.

REFERENCES

Ahmed, Z., J. Cho, *et al.* (2006). "Effects of sludge retention time on membrane fouling and microbial community structure in a membrane bioreactor." Journal of Membrane Science 287 211–218.

Ahn, K.-H., H.-Y. Cha, *et al.* (1998). Application of nanofiltration for recycling of paper regeneration wastewater and characterization of filtration resistance Desalination Conference, Amsterdam.

Ahn, K.-H. and K.-G. Song (2000). "Application of microfiltration with a novel fouling control method for reuse of wastewater from a large-scale resort complex." Desalination 129(3): 207-216.

Al Ahmed, M., F. A. Abdul Aleem, *et al.* (2000). "Biofuoling in RO membrane systems Part 1: Fundamentals and control." Desalination 132(1-3): 173-179.

APHA, A. a. W. (2005). Standard Methods for the Examination of Water and Wastewater. 21st ed. Washington DC, USA, APHA.

Bacchin, P. (2004). "A possible link between critical and limiting flux for colloidal systems: consideration of critical deposit formation along a membrane." Journal of Membrane Science 228 237–241.

Bacchin, P., P. Aimar, *et al.* (2006). "Critical and sustainable fluxes: Theory, experiments and applications." Journal of Membrane Science 281(1-2): 42-69.

Bae, T.-H. and T.-M. Tak (2005). "Interpretation of fouling characteristics of ultrafiltration membranes during the filtration of membrane bioreactor mixed liquor." Journal of Membrane Science 264(1-2): 151-160.

Bai, R. B. and H. F. Leow (2002). "Microfiltration of activated sludge wastewater - the effect of system operation parameters." Sep. Purif. Technol. 29 189.

Bailey, A. D., G. S. Hansford, *et al.* (1994). "The use of microfiltration to enhance the performance of an activated sludge reactor." Water. Res. 28: 197-301.

Bailey, J. E. and D. F. Ollis (1986). Biochemical Engineering Fundamentals. New York, McGraw-Hill Book Company.

Baker, R. W. (2004). Membrane technology and applications. England, McGraw-Hill.

Belfort, G., R. H. Davis, *et al.* (1994). "The behavior of suspensions and macromolecular solutions in crossflow microfiltration." Journal of Membrane Science 96(1-2): 1-58.

Benefield, L. D. and C. W. Randall (1980). Biological Process Design for Wastewater Treatment. Englewood Cliffs, NJ, Prentice-Hall.

Beranek, D. A. (2001). Biological nutrient removal Washington, DC., U.S. Army Corps of Engineers.

Beril, A. S. and A. Ugurlu (2004). "The effect of an anoxic zone on biological phosphorus removal by a sequential batch reactor." Bioresour. Technol. 94(1): 1-7.

Bouhabila, E. H., R. B. Aïm, *et al.* (1998). "Microfiltration of activated sludge using submerged membrane with air bubbling (application to wastewater treatment)." Desalination 118(1-3): 315-322.

Bouhabila, E. H., R. B. Aïm, *et al.* (2001). "Fouling characterisation in membrane bioreactors." Separation and Purification Technology 22-23: 123-132.

Brdjanovic, D., S. Logemann, *et al.* (1998). "Influence of temperature on biological phosphorus removal: process and ecological studies " Wat. Res. 32(4): 1035-1048.

Brdjanovic, D., M. C. M. van Loosdrecht, *et al.* (2000). "Modeling COD, N and P removal in a full-scale wwtp Haarlem Waarderpolder." Wat. Res. 34(3): 846-858.

Brindle, K. and T. Stephenson (1996). "The application of membrane biological reactors for the treatment of wastewaters." Biotechnol. Bioeng. 49: 601.

Buchanan, C. M., R. M. Gardner, *et al.* (1993). "Aerobic biodegradation of cellulose acetate,." J. Appl. Polym. Sci. 47: 1709.

Cabassaud, C., S. Laborie, *et al.* (2001). "Air sparging in ultrafiltration hollow fiber: relationship between flux enhancement, cake characteristics and hydrodynamic parameters." Journal of Membrane Science 181(57-69).

Cabassud, C., S. Labotie, *et al.* (1997). "How slug flow can enhance the ultrafiltration flux in organic hollow fibres " Journal of Membrane Science 128: 93-101.

Chan, R. and V. Chen (2001). "The effects of electrolyte concentration and pH on protein aggregation and deposition: critical flux and constant flux membrane filtration." Journal of Membrane Science 185(2): 177-192.

Chan, R., V. Chen, *et al.* (2004). "Quantitative analysis of membrane fouling by protein mixtures using MALDI-MS." Biotechnol.Bioeng. 85: 190-201.

Chang, I. S. and S. J. Judd (2002). "Air sparging of a submerged MBR for municipal wastewater treatment." Process Biochem 37: 915–920.

Chang, I. S. and C. H. Lee (1998). "Membrane filtration characteristics in membranecoupled activated sludge system—the effect of physiological states of activated sludge on membrane fouling." Desalination 120 221–233.

Chang, I.-S., S.-O. Bag, *et al.* (2001). "Effects of membrane fouling on solute rejection during membrane filtration of activated sludge." Process Biochem. 36 855-860.

Chang, I.-S., P. Le Clech, *et al.* (2002). "Membrane Fouling in Membrane Bioreactors for Wastewater Treatment." Journal of Environmental Engineering (Reston, VA, United States) 128, : 1018-1029.

Chang, S., A. G. Fane, *et al.* (2002). "Experimental assessment of filtration of biomass with transverse and axial fibres." Chemical Engineering Journal 87(1): 121-127.

Characklis, W. G. and K. C. Marshall (1990). "Microbial fouling control " Biofilms: 585–634.

Chellam, S. and M. R. Wiesner (1998). "Evaluation of crossflow filtration models based on shear-induced diffusion and particle adhesion: Complications induced by feed suspension polydispersivity." Journal of Membrane Science 138(1): 83-97.

Chen, V. (1998). "Performance of partially permeable microfiltration membranes under low fouling conditions." Journal of Membrane Science 147(2): 265-278.

Chen, V., A. G. Fane, *et al.* (1997). "Particle deposition during membrane filtration of colloids: Transition between concentration pola rization and cake formation." Journal of Membrane Science 125: 109-122.

Chen, V., H. Li, *et al.* (2004). "Non-invasive observation of synthetic membrane processes - a review of methods." Journal of Membrane Science 241(1): 23-44.

Cheryan, M. (1998). Ultrafiltration and microfiltration handbook. Lancaster, Technomic Pubishing company, Inc.

Cho, B. D. and A. G. Fane (2002). "Fouling transients in nominally sub-critical flux operation of a membrane bioreactor." Journal of Membrane Science 209(2): 391-403.

Cho, D. and A. G. Fane (1999). Biological waste water treatment and membranes. Proceedings of Membrane Technology in Environmental Management, Tokyo.

Cho, J., K. G. Song, *et al.* (2005). "Quantitative analysis of biological effect on membrane fouling in submerged membrane bioreactor." Water Science and Technology 51: 9-18.

Chu, H. P. and X. Li (2005). "Membrane fouling in a membrane bioreactor (MBR): sludge cake formation and fouling characteristics." Biotechnol. Bioeng. 90: 323-331.

Chua, H. C., T. C. Arnot, *et al.* (2002). "Controlling fouling in membrane bioreactors operated with a variable throughput " Desalination 149(1-3): 225-229.

Churchouse, S. and D. Wildgoose (1999). "Membrane bioreactors progress from the laboratory to full-scale use." Membrane Technology 1999(111): 4-8.

Cicek, N., H. Winnen, *et al.* (1998). "Effectiveness of the membrane bioreactor in the biodegradation of high molecular weight compounds." Water Research 32: 1553-1563.

Combe, C., *et al.*, (1999). “The effect of CA membrane properties on adsorptive fouling by humic acid”. Journal of Membrane Science 154(1): 73-87.

Cote, P., H. Buisson, *et al.* (1997). "Immersed membrane activated sludge for the reuse of municipal wastewater " Desalination 113 (2–3): 189–196.

Couvert, A., D. Bastoul, *et al.* (2001). "Prediction of liquid velocity and gas hold-up in rectangular air-lift reactors of different scales." Chemical Engineering and Processing 40 (2001) 113–119 40: 113-119.

Cui, Z., S. Chang, *et al.* (2003). "The use of gas bubbling to enhance membrane processes-a review." J.Memb. Sci. 221: 1–35.

Decarolis, J., S. Hong, *et al.* (2001). "Fouling behavior of a pilot scale inside-out hollow fiber UF membrane during dead-end filtration of tertiary wastewater." Journal of Membrane Science 191(1-2): 165-178.

Defrance, L. and M. Y. Jaffrin (1999). "Comparison between filtrations at fixed transmembrane pressure and fixed permeate flux: application to a membrane bioreactor used for wastewater treatment." Journal of Membrane Science 152(2): 203-210.

Defrance, L. and M. Y. Jaffrin (1999). "Reversibility of fouling formed in activated sludge filtration." Journal of Membrane Science 157(1): 73-84.

Defrance, L., M. Y. Jaffrin, *et al.* (2000). "Contribution of various constituents of activated sludge to membrane bioreactor fouling. ." Bioresour. Technol. 73(105-112).

Dische, Z. (1962). "Colour reactions of hexoses." Methods Carbohydr. Chem. 1: 488–494.

Ducom, G., F. P. Puech, *et al.* (2002). "Air sparging with flat sheet nanofiltration: a link between wall shear stresses and flux enhancement." Desalination 145(1-3): 97-102.

Dunham, S. R. and D. L. Kronmiller. (1995). "Membrane Cleaning Under the Microscope Successful Cleaning Means Knowing the Foulan." Water Technology, from http://www.pwtinc.com/membrane_cleaning_under_the_micr.htm.

Duranceau, S. J. (2001). Membrane practice for water treatment, American Water Works Association, Denver CO.

Elarde, J. R. and R. A. Bergman (2001). The cost of membrane filtration for municipal water supplies in:. Membrane practices for Water treatment. S. J. Duraceau. Denver, American Water Works Association.

Escher, A. and W. G. Characklis (1990). Modeling the initial events in biofilm accumulation. Biofilms. New York, John Wiley & Sons, Inc.: 445-486.

Espinasse, B., P. Bacchin, *et al.* (2002). "On an experimental method to measure critical flux in ultrafiltration." Desalination 146(1-3): 91-96.

Evans, L. R. and J. E. Miller (2002). Sweeping gas membrane desalination using commercial hydrophobic hollow fiber membranes. California, Sandia National Laboratory.

Fan, F. (2005). Fouling mechanism and control strategies for improving membrane bioreactor process. Canada, The University of Guelph. PhD Thesis.

Fan, F., H. Zhou, *et al.* (2006). "Identification of wastewater sludge characteristics to predict critical flux for membrane bioreactor processes." Water Research 40(2): 205-212.

Fan, X. J., V. Urbain, *et al.* (2000). "Ultrafiltration of activated sludge with ceramic membranes in a cross-flow membrane bioreactor process." Water Sci. Technol. 41: 243.

Fane, A. G. (2002). "Membrane bioreactors: design and operational options." " Filtration and Separation 39(5): 26-29.

Fane, A. G. (2005). Towards sustainability in membrane processes for water and wastewater processing. Proceedings of the International Congress on Membranes and Membrane Processes (ICOM), Seoul, Korea.

Fane, A. G., S. Chang, *et al.* (2002). "Submerged hollow fibre membrane module - design options and operational considerations." Desalination 146(1-3): 231-236.

Fane, A. G. and C. J. D. Fell (1981). "Ultrafiltration/activated sludge system—development of a predictive model." Polym.Sci. Technol 13: 631-658.

Fane, A. G., A. Yeo, *et al.* (2005). "Low pressure membrane processes ~ doing more with less energy." Desalination 185(1-3): 159-165.

Fang, H. H. P. and X. Shi (2005). "Pore fouling of microfiltration membranes by activated sludge." Journal of Membrane Science 264: 161-166.

Field, R. W., D. Wu, *et al.* (1995). "Critical flux concepts for microfiltration fouling." Journal of Membrane Science 100(3): 259-272.

Flemming, H. C., G. Schaule, *et al.* (1997). "Biofouling--the Achilles heel of membrane processes." Desalination 113(2-3): 215-225.

Flemming, H. C. and J. Wingender (2001). "Relevance of micribial extracellular plymeric substances (EPSs)-Part I: Structural and ecological aspects." Water Science and Technology 43(6): 1-8.

Fradin, B. and R. W. Field (1999). "Crossflow microfiltration of magnesium hydroxide suspensions: determination of critical fluxes, measurement and modelling of fouling." Separation and Purification Technology 16(1): 25-45.

Frederickson, K. C. (2005). The Application of a Membrane Bioreactor for Wastewater Treatment on a Northern Manitoban Aboriginal Community. Department of Biosystems Engineering. Winnipeg, Manitoba, Canada, University of Manitoba. Master of Science.

Frey, J. M. and P. Schmitz (2000). "Particle transport and capture at the membrane surface in cross-flow microfiltration." Chemical Engineering Science 55(19): 4053-4065.

Frolund, B., R. Palmgren, *et al.* (1996). "Extraction of extracellular polymers from activated sludge using a cation exchange resin." Water Research 30(8): 1749-1758.

Gander, M., B. Jefferson, *et al.* (2000). "Aerobic MBRs for domestic wastewater treatment: a review with cost considerations." Separ. Purif. Technol. 18 (2): 119–130.

Gander, M., B. Jefferson, *et al.* (2000). "TechnologyAerobic MBRs for domestic wastewater treatment: a review with cost considerations." Separation and Purification 18: 119-130.

Geesay, G. G., M. W. Stupy, *et al.* (1992). "The dynamics of biofilms, ." Int. Biodeterior. Biodegrad. 30 (135).

Geng, Z. and E. R. Hall (2007). "A comparative study of fouling-related properties of sludge from conventional and membrane enhanced biological phosphorus removal processes." 2007 41(19): 4329-43338.

Genkin, G., T. D. Waite, *et al.* (2005). The effet of axial vibratins on the filtration performance of submerged hollow fibre membranes. Proceedings of the International Congress on Membranes and Membrane Processes (ICOM), Seoul, Korea.

Gesan-Guiziou, G., E. Boyaval, *et al.* (1999). "Critical stability conditions in crossflow microfiltration of skimmed milk: Transition to irreversible deposition." Journal of Colloid and Interface Science 158: 211-222.

Ghaffour, N., R. Jassim, *et al.* (2004). "Flux enhancement by using helical baffles in ultrafiltration of suspended solids." Desalination 167 201–207.

Ghosh, R. and Z. F. Cui (1998). "Fractionation of BSA and lysozyme using ultrafiltration: effect of pH and membrane pretreatment." Journal of Membrane Science 139(1): 17-28.

Globe-Inc. (2003). "Dissolved oxygen protocol: http://archive.globe.gov/tctg/sectionpdf.jsp?sectionId=151&rg=n%E2%8C%A9=en."

Gottenbos, B., H. C. van der Mei, *et al.* (1999). Models for studying initial adhesion and surface growth in biofilm formation on surfaces. Methods in Enzymology, Academic Press. Volume 310: 523-534.

Grima, E. M., Y. Chisti, *et al.* (1997). "Characterization of shear rates in airlift bioreactors for animal cell culture." Jounal of Biotechnology 54: 195-210.

GSEE-Inc. (2001). "ASCE oxygen transfer determination: www.aerationsolutions.com/ASIO2a.pdf."

Guglielmi, G., D. Chiarani, *et al.* (2007). "Flux criticality and sustainability in a hollow fibre submerged membrane bioreactor for municipal wastewater treatment." Journal of Membrane Science 289(1-2): 241-248.

Gui, P., X. Huang, *et al.* (2002). "Effect of operational parameters on sludge accumulation on membrane surfaces in a submerged membrane bioreactor." Desalination 151: 185-194.

Guibert, D., R. B. Aim, *et al.* (2002). "Aeration performance of immersed hollow-fibre membranes in a bentonite suspension." Desalination 148(1-3): 395-400.

Gujer, W., M. Henze, *et al.* (1999). "Activated Sludge Model No. 3." Water Sci. Technol. 39(1): 183-193.

Guo, W. S., S. Vigneswaran, *et al.* (2004). A rational approach in controlling membrane fouling problems: pretreatments to a submerged hollow fiber membrane system, . Proceedings of theWater Environment-Membrane Technology Conference, Seoul, Korea.

Guo, W. S., S. Vigneswaran, *et al.* (2005). "Effect of flocculation and/or adsorption as pretreatment on thecritical flux of crossflow microfiltration." Desalination 172(1): 53-62.

Han, S.-S., T.-H. Bae, *et al.* (2005). "Influence of sludge retention time on membrane fouling and bioactivities in membrane bioreactor system." Process Biochemistry 40(7): 2393-2400.

Hartree, E. F. (1972). "Determination of protein: a modification of the lowry method that gives a linear photometric response." Anal. Biochem. 48(2): 422–427.

He, Z., A. Petiraksakul, *et al.* (2003). "Oxygen transfer measurement in clean water." Journal of KMITNB 13(1): 14-19.

Henze, M., W. Gujer, *et al.* (2000). Activated sludge models ASM1, ASM2, ASM2d and ASM3, scientific and technical reports. London, IWA Publishing.

Henze, M., W. Gujer, *et al.* (1999). "Activated Sludge Model No. 2d, ASM2d. ." Water Sci. Technol 39(1): 165-182.

Hernandez Rojas, M. E., R. Van Kaam, *et al.* (2005). "Role and variations of supernatant compounds in submerged membrane bioreactor fouling." Desalination 179(1-3): 95-107.

Hiu-Man, W. (2004). Removal of Pathogens by Membrane Bioreactor: Removal Efficiency, Mechanisms and Influencing Factors: M.Phil. Thesis. Civil Engineering

Department. Hong Kong, The Hong Kong University of Science and Technology. Master of Philosophy: 103.

Holmes-Farley (2002). ORP and the reef Aquarium: www.reefkeeping.com /issues/2003-12/rhf/feature/index.php Reefkeeping.

Hong, S., R. S. Faibish, *et al.* (1997). "Kinetics of Permeate Flux Decline in Crossflow Membrane Filtration of Colloidal Suspensions." Journal of Colloid and Interface Science 196(2): 267-277.

Hong, S. P., T. H. Bae, *et al.* (2002). "Fouling control in activated sludge submerged hollow fiber membrane bioreactors." Desalination 143 219-228.

Howell, J. A. (1995). "Sub-critical flux operation of microfiltration." Journal of Membrane Science 107: 165-171.

Howell, J. A., H. C. Chua, *et al.* (2004). "In situ manipulation of critical flux in a submerged membrane bioreactor using variable aeration rates, and effects of membrane history." Journal of Membrane Science 242(1-2): 13-19.

Hsieh, K. M., G. A. Murgel, *et al.* (1994). "Interactions of microbial biofilms with toxic trace metals. Observation and modeling of cell growth, attachment, and production of extracellular protein, ." Biotechnol. Bioeng. 44 219–231.

Huang, X., R. Liu, *et al.* (2000). "Behaviour of soluble microbial products in a membrane bioreactor." Process. Biochem. 36 401–406.

Huisman, I. H., E. Vellenga, *et al.* (1999). "The influence of the membrane zeta potential on the critical flux for crossflow microfiltration of particle suspensions." Journal of Membrane Science 156(1): 153-158.

Idris, A., A. F. Ismail, *et al.* (2002). "Optimization of cellulose acetate hollow fiber reverse osmosis membrane production using Taguchi method." Journal of Membrane Science 205 223–237.

Itonaga, T., K. Kimura, *et al.* (2004). "Influence of suspension viscosity and colloidal particles on permeability of membrane used in membrane
bioreactor (MBR) " Water Sci. Technol. 50 301–309.

Janga, N., X. Ren, *et al.* (2007). "Characteristics of soluble microbial products and extracellular polymeric substances in the membrane bioreactor for water reuse." Desalination 202(1-3): 90-98.

Ji, L. and J. Zhou (2006). "Influence of aeration on microbial polymers and membrane fouling in submerged membrane bioreactors." Journal of Membrane Science 276(1-2): 168-177.

Jiang, T., M. D. Kennedy, *et al.* (2005). "Optimising the operation of a MBR pilot plant by quantitative analysis of the membrane fouling mechanism." Water Sci. Technol. 51: 19–25.

Jorand, F. (1995). Structure et proprieÂteÂs hydrophobes des agreÂgats bacteÂriens de boues activeÂes. France, Nancy I University,. Ph.D. Thesis.

Joshi, J. B., C. B. Elias, *et al.* (1996). "Role of hydrodynamic shear in the cultivation of animal, plant and microbial cells." The Chemical Engineering Journal and the Biochemical Engineering Journal 62(2): 121-141.

Judd, S., H. Alvarez-Vazquez, *et al.* (2006). "The impact of intermittent aeration on the operation of air-lift tubular membrane bioreactors under sub-critical conditions." Sep. Sci. Technol. 41 1293–1302.

Kang, S.-T., A. Subramani, *et al.* (2004). "Direct observation of biofouling in cross-flow microfiltration: mechanisms of deposition and release." Journal of Membrane Science 244(1-2): 151-165.

Kargi, F. and A. Uygur (2002). "Nutrient removal performance of a sequencing batch reactor as a function of the sludge age." Enzyme and Microbial Technology 31(6): 842-847.

Khongnakorn, W., C. Wisniewski, *et al.* (2007). "Physical properties of activated sludge in a submerged membrane bioreactor and relation with membrane fouling." Separation and Purification Technology 55(1): 125-131.

Kim, J., M. Jang, *et al.* (2004). Characteristics of membrane and module affecting membrane fouling. Proceedings of the Water Environment-Membrane Technology Conference, Seoul, Korea.

Kim, J.-S., S. Akeprathumchai, *et al.* (2001). "Flocculation to enhance microfiltration." Journal of Membrane Science 182(1-2): 161-172.

Kimura, K., Y. Watanabe, *et al.* (1998). "Filtration resistance induced by ammonia oxidizers accumulating on the rotating membrane disk." Water Science and Technology 38(4-5): 443-452.

Knyazkova, T. V. and A. A. Maynarovich (1999). "Recognition of membrane fouling: testing of theoretical approaches with data on NF of salt solutions containing a low molecular weight surfactant as a foulant." Desalination 126(1-3): 163-169.

Koch, G., M. Kühni, *et al.* (2000). "Calibration and validation of Activated Sludge Model No. 3 for Swiss municipal wastewater." Wat. Res. 34(14): 3580-3590.

Kouakou, E., T. Salmon, *et al.* (2005). "Gas-liquid mass transfer in a circulating jet-loop nitrifying MBR." Chemical Engineering Science 60(22): 6346-6353.

Kraume, M., U. Bracklow, *et al.* (2004). Nutrient removal in MBRs for municipal wastewtaer treatment. Keynote, IWA Special, WEMT Seoul, Korea.

Kubota-Corporation (2004). Instruction manual for submerged membrane unit.

Kwon, D. Y. and S. Vigneswaran (1998). "Influence of particle size and surface charge on critical flux of crossflow microfiltration." Water Science and Technology 38(4-5): 481-488.

Kwon, D. Y., S. Vigneswaran, *et al.* (2000). "Experimental determination of critical flux in cross-flow microfiltration." Separation and Purification Technology 19(3): 169-181.

Lahoussine-Turcaud, M., R. Wiesner, *et al.* (1990). "Fouling in tangential-flow ultrafiltration: The effect of colloid size and coagulation pretreatment." J.of Membrane Science 52: 173-190.

Laspidou, C. S. and B. E. Rittmann (2002). "A unified theory for extracellular polymeric substances, soluble microbial products, and active and inert biomass." Water Research 36(11): 2711-2720.

Le Clech, P. (2002). Process configuration and fouling in membrane bioreactors. UK, Cranfield University. PhD Thesis.

Le Clech, P., V. Chen, *et al.* (2006). "Fouling in membrane bioreactors used in wastewater treatment." Journal of Membrane Science 284(1-2): 17-53.

Le Clech, P., V. Chen, *et al.* (2006). "Review: Fouling in membrane bioreactors used in wastewater treatment." Journal of Membrane Science 284: 17–53.

Le Clech, P., B. Jefferson, *et al.* (2003). "Critical flux determination by the flux-step method in a submerged membrane bioreactor." Journal of Membrane Science 227(1-2): 81-93.

Le Clech, P., B. Jefferson, *et al.* (2003). "Impact of aeration, solids concentration and membrane characteristics on the hydraulic performance of a membrane bioreactor." Journal of Membrane Science 218(1-2): 117-129.

Lee, C.-K., W.-G. Chang, *et al.* (1993). "Air slugs entrapped cross-flow filtration of bacterial suspensions." Biotechnology and Bioengineering 41(5): 525-530.

Lee, J., W.-Y. Ahn, *et al.* (2001). "Comparison of the filtration characteristics between attached and suspended growth microorganisms in submerged membrane bioreactor. ." Water Research 35(10): 2435-2445.

Lee, H.-I., *et al.* (2002). “Characterization of anion exchange membranes fouled with humate during electrodialysis”. Journal of Membrane Science 203(1-2): 115-126.

Lee, W., S. Kang, *et al.* (2003). "Sludge characteristics and their contribution to microfiltration in submerged membrane bioreactors." J. Membr. Sci. 216(1-2): 217–227.

Lee, W.-N., I.-S. Chang, *et al.* (2007). "Changes in biofilm architecture with addition of membrane fouling reducer in a membrane bioreactor " Process Biochemistry 42: 655-661.

Lee, Y., J. Cho, *et al.* (2002). "Modeling of submerged membrane bioreactor process for wastewater treatment." Desalination 146: 451-457.

Lesjean, B. and F. Luck (2006) Assessment of the membrane bioreactor technology and European market outlook Volume, DOI:

Leslie, G. L., R. P. Schneider, *et al.* (1993). "Fouling of a microfiltration membrane by two Gram-negative bacteria." Colloids Surf. A 73(165).

Levine, A. D., G. Tchobanoglous, *et al.* (1991). "Size distributions of particulate contaminants in wastewater and their impact on treatability." water Research 25(911-922).

Li, H., A. G. Fane, *et al.* (1998). "Direct observation of particle deposition on the membrane surface during crossflow microfiltration." Journal of Membrane Science 149(1): 83-97.

Li, H., A. G. Fane, *et al.* (2000). "An assessment of depolarisation models of crossflow microfiltration by direct observation through the membrane." Journal of Membrane Science 172(1-2): 135-147.

Li, H., A. G. Fane, *et al.* (2003). "Observation of deposition and removal behaviour of submicron bacteria on the membrane surface during crossflow microfiltration." Journal of Membrane Science 217(1-2): 29-41.

Li, J., Y. Li, *et al.* (2007). "Impact of filamentous bacteria on properties of activated sludge and membrane-fouling rate in a submerged MBR." Separation and Purification Technology In Press, Corrected Proof.

Li, Q. Y., Z. F. Cui, *et al.* (1997). "Effect of bubble size and frequency on the permeate flux of gas sparged ultrafiltration with tubular membranes." Chemical Engineering 67: 71-75.

Li, Q. Y., R. Ghosh, *et al.* (1998). "Enhancement of ultrafiltration by gas sparging with flat sheet membrane modules." Separation and Purification Technology 14(1-3): 79-83.

Li, X.-y. and X.-m. Wang (2005). "Modelling of membrane fouling in a submerged membrane bioreactor." Journal of Membrane Science In Press, Corrected Proof.

Li, Y.-Z., Y.-L. He, *et al.* (2005). "Comparison of the filtration characteristics between biological powdered activated carbon sludge and activated sludge in submerged membrane bioreactors." Desalination 174: 305-314.

Liao, B. (2000). Physiochemial studies of microbial flocs. Toronto, The University of Toronto.

Lim, A. L. and R. Bai (2003). "Membrane fouling and cleaning in microfiltration of activated sludge wastewater." Journal of Membrane Science 216: 279–290.

Lim, B. S., B. C. Choi, *et al.* (2007). "Effects of operational parameters on aeration on/off time in an intermittent aeration membrane bioreactor." Desalination 202(1-3): 77-82.

Lin, Y.-H., Y.-Y. Tyan, *et al.* (2004). "An assessment of optimal mixture for concrete made with recycled concrete aggregates." Cement and Concrete Research 34 1373–1380.

Liu, C., S. Caothien, *et al.* (2001). Membrane Cleaning: from Art to Science. Membrane Technology Conference, SanAntonio, TX.

Liu, R., X. Huang, *et al.* (2003). "Hydrodynamic effect on sludge accumulation over membrane surfaces in a submerged membrane bioreactor." Process Biochemistry 39(2): 157-163.

Liu, R., X. Huang, *et al.* (2000). "Study on hydraulic characteristics in a submerged membrane bioreactor process." Process Biochem. 36(3): 249-254.

Lubbecke, S., A. Vogelpohl, *et al.* (1995). "Wastewater treatment in a biological high-performance system with high biomass concentration." Water Research 29(3): 793-802.

M.R. Wiesner, S. V., D. Brejchova, (1992). Improvement in microfiltration using coagulation pretreatment, . Proceedings of the Fifth Gothenburg Symposium on Chemical Water and Wastewater Treatment II,, Nice, France, Springer, New York.

Madaeni, S. S. (1997). "The effect of operating conditions on critical flux in membrane filtration of latexes, ." Process Saf. Environ. Prot. 75 266-269.

Madaeni, S. S., A. G. Fane, *et al.* (1999). "Factors influencing critical flux in membrane filtration of activated sludge." J.Chem. Technol. Biotechnol 74: 539-543.

Madec, A., H. Buisson, *et al.* (2000). Aeration to enhance membrane critical flux. Proceeding of World Filtration Congress, Brighton, UK.

Magara, Y. and M. Itoh (1991). "The effect of operational factors on solid/liquid separation by ultramembrane filtration in a biological denitrification system for collected human excreta treatment plants." Water Sci. Technol. 23 1583–1590.

Mallevialle, J., C. Anselme, *et al.*, Eds. (1989). Effects of Humic Substances on Membrane Processes. Advances in chemistry Denver, Colorado, American Chemical Society.

Mandal, A., C. F. J. Wu, *et al.* (2006). "SELC: Sequential Elimination of Level Combinations by means of modified Genetic Algorithms." Technometrics 48(273-283).

Manem, J. and R. Sanderson (1996). Chapter 17 Membrane bioreactors in water treatment. Water Treatment Membrane Process. A. R. Foundation. New York, McGraw-Hill.

Manem, J. and R. Sanderson (1996). Water Treatment Membrane Processes (Chapter 17). New York, AWWA Research Foundation, McGraw-Hill.

Marcier, M., C. Fonade, *et al.* (1997). "How slug flow can enhance the ultrafiltration flux in mineral tubular membranes." Journal Membrane Science 128: 103-113.

Masciola, D. A., R. C. Viadero, *et al.* (2001). "Tubular ultrafiltration flux prediction for oil-in-water emulsions: analysis of series resistances." Journal of Membrane Science 184(2): 197-208.

Masse, A., M. Sperandio, *et al.* (2006). "Comparison of sludge characteristics and performance of a submerged membrane bioreactor and an activated sludge process at high solids retention time." Water Research 40(12): 2405-2415.

McAdam, E., S. J. Judd, *et al.* (2005). "Critical analysis of submerged membrane sequencing batch reactor operating conditions • ARTICLE." Water Research 39(16): 4011-4019.

Meijer, S. C. F. (2004). Theoretical and practical aspects of modeling activated sludge processes. Biotechnological Engineering. the Netherlands, The Delft University of Technology.

Meng, F. and F. Yang (2008). "Fouling mechanisms of deflocculated sludge, normal sludge, and bulking sludge in membrane bioreactor." Journal of Membrane Science In Press, Corrected Proof.

Meng, F., H. Zhang, *et al.* (2006). "Identification of activated sludge properties affecting membrane fouling in submerged membrane bioreactors." Separation and Purification Technology 51(1): 95-103.

Meng, F. G., H. M. Zhang, *et al.* (2005). "Cake layer morphology in microfiltration of activated sludge wastewater based on fractal analysis." Separation and Purification Technology 44: 250-257.

Mercier, M., Fonade, C. and Lafforgue-Delmorme, C. (1997). "How slug flow can enhance the ultrafiltration flux of mineral tubular membranes." Journal of Membrane Science 128: 103-113.

Mercier-Bonin, M., C. Lagane, *et al.* (2000). "Influence of a gas/liquid two-phase flow on the ultrafiltration and microfiltration performances: case of a ceramic flat sheet membrane." Journal of Membrane Science 180: 93–102.

Merlo, R. P., R. S. Trussell, *et al.* (2004). "Physical, chemical and biological properties of submerged membrane bioreactor and conventional activated sludges."

Metsämuuronen, S., J. A. Howell, *et al.* (2002). "Critical flux in ultrafiltration of myoglobin and baker's yeast." Journal of Membrane Science
196: 13-25.

Metzger, U., P. Le Clech, *et al.* (2007). "Characterisation of polymeric fouling in membrane bioreactors and the effect of different filtration modes." Journal of Membrane Science 301(1-2): 180-189.

Mikkelsen, L. H. and K. Keiding (2002). "The shear sensitivity of activated sludge: an evaluation of the possibility for a standardised floc strength test." Water Research 36(12): 2931-2940.

Mulder, M. (1996). Basic Principles of Membrane Technology, Kluwer Academic Publisher

Mulder, M. (2000). Basic principles of memnrane technology, Dordecht, Kluwer Academic Publishers.

Muller, E. B., A. H. Stouthamer, *et al.* (1995). "Aerobic domestic wastewater treatment in a pilot plant with complete sludge retention by crossflow filtration." Water research 29: 1179-1189.

Murnleitner, E., T. Kuba, *et al.* (1997). "An integrated metabolic model for the aerobic and denitrifying biological phosphorous removal." Biotechnol. Bioeng. 54: 434-450.

Nagaoka, H., S. Ueda, *et al.* (1996). "Influence of bacterial extracellular polymers on the membrane separation activated sludge process." Water Science and Technology 34(9): 165-172.

Nagaoka, H., S. Yamanishi, *et al.* (1998). "Modeling of biofouling by extracellular polymers in a membrane separation activated sludge system." Water Science and Technology 38(4-5): 497-504.

Nagaoka, H., S. Yamanishi, *et al.* (1998). "Modeling of biofouling by extracellular polymers in a membrane separation activated sludge system." Water Science and Technology 38(4-5): 497-504.

Negaresh, E. (2007). Particle and macromolecular fouling in submerged membrane. School of Chemical Science and Engineering. Sydney, Australia, The University of New South Wales. M. Eng Thesis.

Ng, C. A., D. Sun, *et al*. (2005). Strategies to improve the sustainable operation of membrane bioreactors. Proceedings of the International Desalination Association Conference, Singapore.

Ng, H. and W. Hermanowics (2004). Membrane bioreactor at short term cell residence times - a new mode of operation. IWA Special. Conf. WEMT, Seoul, Korea.

Ng, H. Y. and S. W. Hermanowicz (2005). "Specific resistance to filtration of biomass from membrane bioreactor reactor and activated sludge: effects of exocellular polymeric substances and dispersed microorganisms. ." Water Environ. Res. 77 (2): 187–192.

.

Nuengjamnong, C., J. H. Kweon, *et al.* (2005). "Membrane fouling caused by extracellular polymeric substances during microfiltration processes." Desalination 179: 117-124.

Ognier, B. S., C. Wisniewski, *et al.* (2002). "Membrane fouling during constant flux filtration in membrane bioreactors,." Membr. Technol. 7: 1-10.

Ognier, S., C. Wisniewski, *et al.* (2001). "Biofouling in membrane bioreactors: phenomenon analysis and modelling in: MBR." Cranfield University: 29-43.

Ognier, S., C. Wisniewski, *et al.* (2002). "Characterisation and modelling of fouling in membrane bioreactors." Desalination 146(1-3): 141-147.

Ognier, S., C. Wisniewski, *et al.* (2004). "Membrane bioreactor fouling in sub-critical filtration conditions: a local critical flux concept." Journal of Membrane Science 229: 171-177.

Orantes, J., C. Wisniewski, *et al.* (2006). "The influence of operating conditions on permeability changes in a submerged membrane bioreactor." Separation and Purification Technology 52: 60-66.

Osmonics. (1996). "The filtration spectrum." from http://www.osmonics.com /library/zoom-spold.htm.

Ozaki, N. and K. Yamamoto (2001). "Hydraulic effects on sludge accumulation on membrane surface in crossflow filtration." Water Research 35(13): 3137-3146.

Park, D., D. S. Lee, *et al.* (2005). "Continuous biological ferrous iron oxidation in a submerged membrane bioreactor,." Water Sci. Technol. 51 59–68.

Persson, A., A.-S. Jonsson, *et al.* (2001). "Separation of lactic acid-producing bacteria from fermentation broth using a ceramic microfiltration membrane with constant permeate flow " Biotechnol.Bioeng. 75: 233-238.

Pierre, L.-C., V. Chen, *et al.* (2006). "L.-C. Pierre, V. Chen, T.A.G. Fane, Fouling in membrane bioreactors used in wastewater treatment, J. Membr. Sci. 284 (2006) 17–53." Journal of Membrane
Science 284 17-53.

Pinnua, I. (2004). Workshop organized by the NAMS: Polymeric and inorganic membrane material and membrane formation, Jackson Hole.

Pollice, A., A. Brookes, *et al.* (2005). "Sub-critical flux fouling in membrane bioreactors — a review of recent literature " Desalination 174(3): 221-230.

Psoch, C. (2005). Improved membrane filtration for water and wastewater using air sparging and backflushing. Fairbanks, Alaska, The University of Alaska Fairbanks. PhD Thesis.

Psoch, C. and S. Schiewer (2005). "Critical flux aspect of air sparging and backflushing on membrane bioreactors." Desalination 175(1): 61-71.

Psoch, C. and S. Schiewer (2005). "Long-term study of an intermittent air sparged MBR for synthetic wastewater treatment." Journal of Membrane Science 260(1-2): 56-65.

Qiu, S. (2005). Nanofiber as flocculant or modifier in membrane bioreactors for wastewater treatment The University of Akron. M.Sc. Thesis: 110.

Ramphao, M., M. C. Wentzel, *et al.* (2005). "Impact of membrane solid-liquid separation on design of biological nutrient removal activated sludge systems." Biotechnology and Bioengineering 89(6): 630-646.

Reicherter (1999). Kosten und Betriebsdaten von Kleinkläranlagen. Seminar des Bayerischen Industrieverbands Steine und Erden e.V., 6 October 1999, Hirschaid, Germany.

Ridgeway, H. F. and H.-C. Flemming (1996). Membrane biofouling in:. Water Treatment Membrane Processes. J. Mallevialle, P. E. Odendaal and M. R. Wiesner. New York, McGraw-Hill: pp. 6.1–6.62.

Roest, H. F. v. d., D. P. Lawrence, *et al.* (2002). Membrane bioreactors for municipal wastewater treatment IWA Publishing.

Rosenberger, S. and M. Kraume (2002). "Filterability of activated sludge in membrane bioreactors." Desalination 151: 195-200.

Rosenberger, S. and M. Kraume (2003). Parameters influencing filterability of activated sludge in membrane bioreactors Proc. AWWA Membrane Technology, Atlanta.

Ross, W. R., J. P. Barnard, *et al.* (1990). "Application of ultrafiltration membranes for solid-liquid separation in anaerobic digestion systems: the ADUF process." WAter SA 16(2): 85-91.

Ruiz, G., D. Jeison, *et al.* (2006). "Nitrification-denitrification via nitrite accumulation for nitrogen removal from wastewaters " Bioresource Technology 97(2): 330-335.

Rushton, A., A. S. Ward, *et al.* (2000). Solid-liquid filtration and separation technology, Wiley VCH.

Saito, T., D. Brdjanovic, *et al.* (2004). "Effect of nitrite on phosphate uptake by phosphate accumulating organisms." Water Res. 38(17): 3760–3768.

Sato, T. and Y. Ishii (1991). "Effects of activated sludge properties on water flux of ultrafiltration membrane used for human excrement treatment." Water Sci. Technol. 23: 1601.

Schoeberl, P., M. Brik, *et al.* (2005). "Optimization of operational parameters for a submerged membrane bioreactor treating dyehouse wastewater." Separation and Purification Technology 44 61–68.

Semmens, M. and D. Hanus (1999). "Studies of a membrane aerated bioreactor for wastewater treatment." Membrane Technology 1999(111): 9-13.

Shimizu, Y., Y. I. Okuno, *et al.* (1996). "Filtration characteristics of hollow fiber microfiltration membranes used in membrane bioreactor for domestic wastewater treatment." Water Research 30: 2385.

Shimizu, Y., K. I. Shimodera, *et al.* (1993). "Cross flow microfiltration of bacterial cells." Journal of Ferment Buiengineering: 493-500.

Shin, H.-S., W.-T. Lee, *et al.* (2002). Contribution of solids and soluble materials of sludge to UF behavior under starvation Proceedings IMSTEC 2002, Melbourne, Australia.

Silva, C. M., D. W. Reeve, *et al.* (2000). "Model for flux prediction in high-shear microfiltration systems." Journal of Membrane Science 173(1): 87-98.

Smith, C. W., D. Di Gregorio, *et al.* (1967). The use of ultrafiltration membrane for activated sludge separation. The 24th Annual Purdue industrial waste conference, Purdue University, West Lafayette.

Smolders, G. L. F., J. M. Klop, *et al.* (1995). "A metabolic model for the biological phosphorus removal process: Effect of the sludge retention time." Biotechnol. Bioeng. 48: 222-233.

Smolders, G. L. F., J. van der Meij, *et al.* (1994). "Stoichiometric model of the aerobic metabolism of the biological phosphorus removal process." Biotechnol.Bioeng. 44(7): 837-848.

Sofia, A., W. J. Ng, *et al.* (2004). "Engineering design approaches for minimum fouling in submerged MBR." Desalination 160(1): 67-74.

Sommariva, C., A. Converti, *et al.* (1997). "Increase in phosphate removal from wastewater by alternating aerobic and anaerobic conditions." Desalination 108(1-3): 255–260.

Song, L. (1998). "Flux decline in crossflow microfiltration and ultrafiltration: mechanisms and modeling of membrane fouling." Journal of Membrane Science 139(2): 183-200.

Sponza, D. T. (2002). "Extracellular polymer substances and physicochemical properties of flocs in steady and unsteady-state activated sludge systems." Process Biochem. 37 (983).

Stephenson, T. S. Judd, *et al.* (2000). Membrane bioreactor for wastewater treatment. London, IWA Publishing.

Strathmann, M., J. Wingender, *et al.* (2002). "Application of fluorescently labelled lectins for the visualization and biochemical characterization of polysaccharides in biofilms of Pseudomonas aeruginosa." Journal of Microbiological Methods 50(3): 237-248.

Sun, L.-X., F. Xu, *et al.* (1998). "Studies on optimization of a platinum catalyst and porphine modified, pyrolytic graphite, amperometric, glucose sensor by sequential level elimination experimental design." Talanta 47: 1165–1174.

Taguchi, G. (1987). System of experimental design. New York, Kraus.

Tao, G., K. Kekre, *et al.* (2005). "Membrane bioreactors forwater reclamation." Water Sci.Technol. 51 431–440.

Tardieu, E., A. Grasmick, *et al.* (1998). "Hydrodynamic control of bioparticle deposition in a MBR applied to wastewater treatment." Journal of Membrane Science 147(1): 1-12.

Tardieu, E., A. Grasmick, *et al.* (1999). "Influence of hydrodynamics on fouling velocity in a recirculated MBR for wastewater treatment." Journal of Membrane Science 156(1): 131-140.

Tay, J.-H., Q. S. Liu, *et al.* (2004). "The effect of upflow air velocity on the structure of aerobic granules cultivated in a sequencing batch reactor." Water Sci. Technol 49: 35-40.

Tchobanoglous, G., F. Burton, *et al.* (2003). Wastewater Engineering: Treatment and Reuse. New York, Metcalf and Eddy, McGraw-Hill Company.

Tchobanoglous, G. and F. L. Burton, Eds. (1991). Wastewater engineering : treatment, disposal, and reuse. New York, Metcalf and Eddy, McGraw-Hill Company.

Tiranuntakul, M., V. Jegatheesan, *et al.* (2005). "Performance of an oxidation ditch retrofitted with a membrane bioreactor during the start-up." Desalination 183(1-3): 417-424.

Ueda, T., K. Hata, *et al.* (1997). "Effects of aeration on suction pressure in a submerged membrane bioreactor." Water Research 31 (3): 489–494.

Vallero, M. V. G., G. Lettinga, *et al.* (2005). "High rate sulfate reduction in a submerged anaerobic membrane bioreactor (SAMBaR) at high salinity." J. Membr. Sci. 253 217–232.

van Veldhuizen, H. M., M. C. M. van Loosdrecht, *et al.* (1999). "Modelling biological phosphorus and nitrogen removal in a full scale activated sludge process." Wat. Res. 33(16): 3459-3468.

Vieira, M. J., L. F. Melo, *et al.* (1993). "Biofilm formation: hydrodynamic effects on internal diffusion and structure." Biofouling 7: 67.

Wagner, J. (2001). Membrane filtration handbook-Practical tips and hints. 2nd, Osmonics, Inc.

Wentzel, M. C., P. L. Dold, *et al.* (1989). "Enhanced polyphosphate organism cultures in activated sludge. Part III: Kinetic Model " Water SA 15: 89-102.

Wicaksana, F. (2006). Submerged hollow fibre membrane in bubbling systems. School of Chemical engineering and Industrial chemistry. Sydney, Australia, The University of New South Wales. PhD thesis.

Wicaksana, F., A. G. Fane, *et al.* (2006). "Fibre movement induced by bubbling using submerged hollow fibre membranes." Journal of Membrane Science 271(1-2): 186-195.

Wiesner, M. R. and S. Chellam (1999). "The promise of membrane technology." Environmental Science and Technology 33: 360-366.

Wingender, J., T. Neu, *et al.* (1999). Bacterial extracellular polymeric substances. Berlin, Springer.

Wingender, T. R. N. and H. C. Flemming (1999). Microbial extracellular polymeric substances. Berlin Sprinter.

Wisniewski, C. and A. Grasmick (1998). "Floc size distribution in a membrane bioreactor and consequences for membrane fouling." Colloids and Surfaces A: Physicochemical and Engineering Aspects 138(2-3): 403-411.

Wu, C. F. J., S. S. Mao, *et al.*, Eds. (1990). SEL: A search method based on orthogonal arrays. Statistical Design and Analysis of Industrial Experiments. New York, Marcel Dekker, Inc.

Wu, D., J. A. Howell, *et al.* (1999). "Critical flux measurement for model colloids." Journal of Membrane Science 152(1): 89-98.

Wu, Z., Z. Wang, *et al.* (2008). "Effects of various factors on critical flux in submerged membrane bioreactors for municipal wastewater treatment." Separation and Purification Technology 62: 56-63.

Xu, J. L., P. Cheng, *et al.* (1999). "Gas-liquid two-phase flow regimes in rectangular channels with mini/micro gaps." International Journal of Multiphase Flow 25: 411-432.

Yamamoto, K., M. Hiasa, *et al.* (1999). "Direct solid-liquid separation using hollow fiber membrane in an activated sludge aeration tank." Water Sci. Technol. 21: 43-54.

Yamamoto, K. and K. A. Win (1991). "Tannery wastewater treatment using sequencing batch membrane reactor." Water Sci. Technol. 22 1639.

Yang, Q., J. Chen, *et al.* (2006). "Membrane fouling control in a submerged membrane bioreactor with porous, flexible suspended carriers." Desalination 189: 292–302.

Yang, W., N. Cicek, *et al.* (2006). "State-of-the-art of membrane bioreactors: Worldwide research and commercial applications in North America." Journal of Membrane Science 270(1-2): 201-211.

Ye, Y. (2005). Macromolecular fouling during membrane filtration of complex fluids. Sydney, The University of New South Wales. PhD Thesis.

Yeom, I.-T., Y.-M. Nah, *et al.* (1999). "Treatment of household wastewater using an intermittently aerated membrane bioreactor." Desalination 124(1-3): 193-203.

Yeon, K. M., J. S. Parka, *et al.* (2005). "Membrane coupled highperformance compact reactor: a new MBR system for advanced wastewater treatment." Water Res. 39 1954–1961.

Yoon, S. H., J. H. Collins, *et al.* (2005). "Effects of flux enhancing polymer on the characteristics of sludge in membrane bioreactor process." Water Sci. Technol. 51 (151–157.).

Yu, H. Y., M. X. Hu, *et al.* (2005). "Surface modification of polypropylene microporous membranes to improve their antifouling property in MBR: NH3 plasma treatment." Sep. Purif. Technol. 45 8–15.

Yu, K., X. Wen, *et al.* (2003). "Critical flux enhancements with air sparging in axial hollow fibers cross-flow microfiltration of biologically treated wastewater." ournal of Membrane Science 224: 69–79.

Zeman, L. and A. L. Zydney (1996). Microfiltration and ultrafiltration: Principle and applications. New York, Marcel Dekker Inc.

Zhang, H.-M., J.-N. Xiao, *et al.* (2006). Comparison between a sequencing batch membrane bioreactor and a conventional membrane bioreactor. Process Biochem.

Zhang, J., H. C. Chuaa, *et al.* (2006). "Factors affecting the membrane performance in submerged membrane bioreactors." Journal of Membrane Science 284 54-66.

Zhang, S. T., Y. B. Qu, *et al.* (2005). "Experimental study of domestic sewage treatment with a metal membrane bioreactor." Desalination 177 83–93.

Zhang, Y., D. Bu, *et al.* (2004). Study on retarding membrane fouling by ferric salts dosing in membrane bioreactors. Proceeding of the Water Environment-Membrane Technology Conference, Seoul, Korea.

Zhao, Y., W. Xing, *et al.* (2003). "Hydraulic resistance in microfiltration of titanium white waste acid through ceramic membranes." Separation and Purification Technology 32(1-3): 99-104.

Zhou, H. and D. W. Smith (2001). "Advanced treatment technologies in wastewater treatment." Canadian Journal of Civil Engineering 28 (S1): 49-66.

APPENDICES

APPENDIX A

CALCULATION DETAILS FOR CHAPTER 3

A.1 MODELS AND SIMULATION FOR MBR DESIGN

A.1.1 Biological model for microorganism activities

For the wastewater treatment part, one of the activated sludge family models named TUDP model (developed by the Delft University of Technology Netherlands) is applied in this study to simulate treatment characteristics of a combined nitrogen and phosphorous biological removal. Study from some research shows that TUDP model is capable of describing full-scale conditions of wastewater treatment, without significant adjustment (van Veldhuizen *et al.* 1999; Brdjanovic *et al.* 2000). The TUDP model used in this study follows the last updated version of TUDP model (Meijer, 2004) but neglect the effect of substrate competition.

From Fig. A.1, AMOs grow by oxidizing the external ammonium substrate (SNH) and release the soluble nitrate (SNO) to the system. Decay of AMOs separate in two parts: inert non-biodegradable particulate biomass (XI) and slowly biodegradable microorgnisms (XS). XS may be a part of the up-taken influent for HMOs whereas it also may be formed in the process from lysis of HMOs and AMOs resulting in endogenous oxygen consumption and an internal recycle of substrate (XS). XS is assumed to contain not only carbon substance but also a fraction of ammonium and phosphate. Heterotrophic microorganisms (XH) grow aerobically by up-taking both a volatile fatty acid substance (SA) and a readily biodegradable substance (SF) and also decay to become XI and XS. No cell-internal storage is

modeled in this stage. XH is also assumed to contain a fraction of ammonium and phosphate. These fractions are equal for all biomass fractions (i.e. XH, XPAO and XA). In the metabolic Bio-P model, SA is readily available stored in the form of cell-internal storage of poly-hydroxyalkanoates (XPHA). This facilitates is the more straightforward maintenance concept, which also is used in ASM3-bio-P model (Koch *et al.* 2000). XPHA is directly oxidized for maintenance purposes. Hereby, no particulate inert matter (XI) and particulate substrate (XS) are formed, and therefore XS recycle is avoided. All Equations used in the simulation of biological activities (Meijer 2004) are shown in Table A.1.

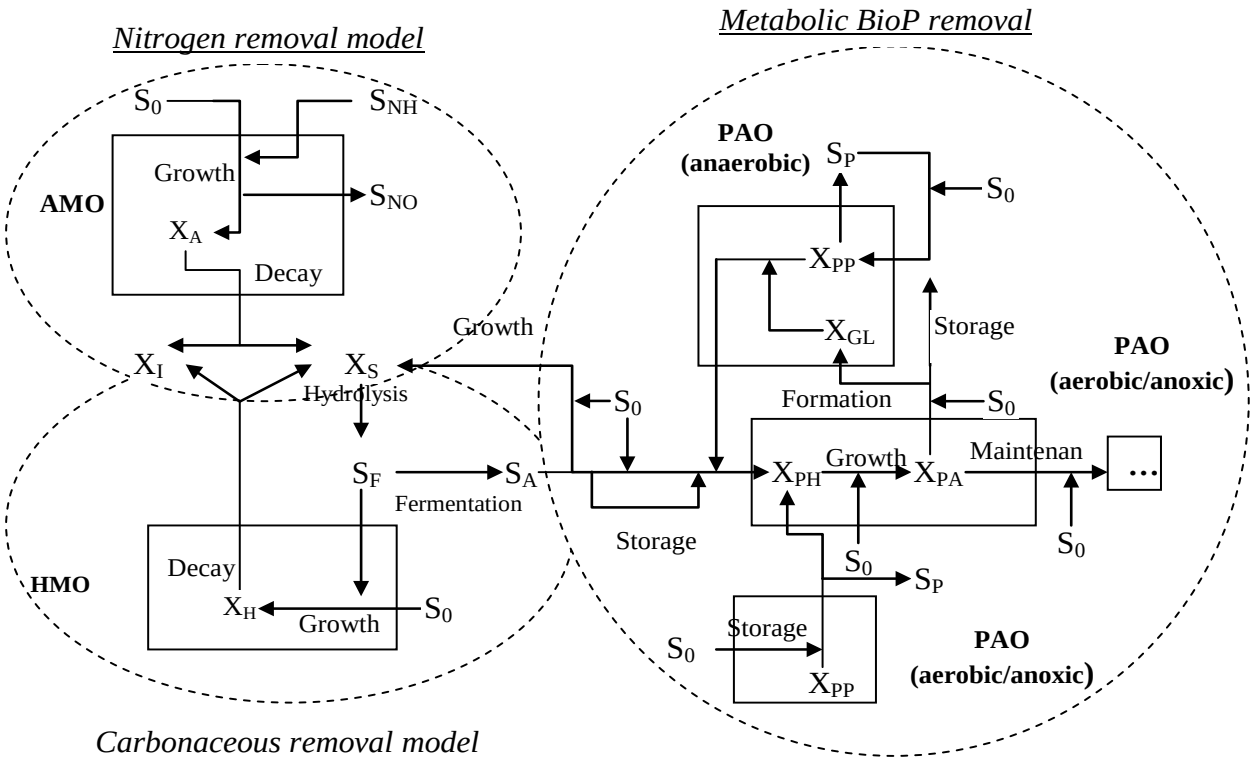

Fig. A.1 Schematic diagram of substrate flow in TUDP model

Fig A.1 showed a complete substrate flow diagram of TUDP model, the dash circle areas represent the nutrient removal model of different substances including carbon, nitrogen and phosphorous. The block areas distinguished between different microorganisms and processes where: AMO = active autotrophic nitrifying microorganisms, HMO = active heterotrophic microorganisms and PAO = phosphate accumulating microorganisms. The decay of AMOs triggered the growth of HMOs. Both anaerobic and aerobic storage of PHAs by PAOs were modeled.

These simulation models will be used to predict performances of the pilot scale MBR fed with real municipal wastewater from Townsville Mt St John treatment plant. Therefore, the nutrient effluent information from this treatment plant is considered as the simulation influent parameters shown in Table A.2.

Table A.1 Kinetic Equations of the TUDP model (Meijer 2004)

Process			Kinetic rate Equation	Equation
(1) Aerobic hydrolysis $gCOD_{XS}/d$)	r_h^O	=	$k_h \cdot \frac{X_S/(X_H+X_{PAO})}{K_X+X_S/(X_H+X_{PAO})}$	A.1
(2) Anoxic hydrolysis ($gCOD_{XS}/d$)	r_h^{NO}	=	$\eta_{NO} \cdot k_h \cdot \frac{X_S/(X_H+X_{PAO})}{K_X+X_S/(X_H+X_{PAO})} \cdot \frac{S_{NO}}{K_{NO}+S_{NO}}$	A.2
(3) Anaerobic hydrolysis ($gCOD_{XS}/d$)	r_h^{AN}	=	$\eta_{fe} \cdot k_h \cdot \frac{X_S/(X_H+X_{PAO})}{K_X+X_S/(X_H+X_{PAO})} \cdot (X_H+X_{PAO})$	A.3
(4) Aerobic growth on SF (gCODXH/d)	r_{SFO}	=	$\mu_H \frac{S_F}{S_A+S_F} \frac{S_F}{K_F+S_F} \frac{S_O}{K_O+S_O} \cdot X_H$	A.4
(5) Aerobic growth on SA (gCODXH/d)	r_{SAO}	=	$\mu_H \frac{S_A}{S_A+S_F} \frac{S_F}{K_F+S_F} \frac{S_O}{K_O+S_O} \cdot X_H$	A.5

Table A.1 Kinetic Equations of the TUDP model (continued)

Process			Kinetic rate Equation	Equation
(6) Anoxic growth on SF ($gCODXH/d$)	r_{SFNO}	=	$\eta\,\mu_H \frac{S_F}{S_A+S_F}\frac{S_F}{K_F+S_F}\frac{S_{NO}}{K_{NO}+S_{NO}}\cdot X_H$	A.6
(7) Anoxic growth on SA ($gCODXH/d$)	r_{SANO}	=	$\eta_{NO}\,\mu_H \frac{S_A}{S_A+S_F}\frac{S_F}{K_F+S_F}\frac{S_{NO}}{K_{NO}+S_{NO}}\cdot X_H$	A.7
(8)Fermentation of S_F ($gCOD_{SF}/d$)	r_{fe}^{AN}	=	$q_{fe}\cdot\left(S_F/(K_{fe}+S_F)\right)\cdot X_H$	A.8
(9) Heterotrophic lysis ($gCOD_{XH}/d$)	r_{HL}	=	$b_H\cdot X_H\sqrt{2}$	A.9
(10) Anaerobic storage S_A ($gCOD_{SA}/d$)	r_{SA}^{AN}	=	$q_{Ac}\cdot\left(S_A/(K_A+S_F)\right)\cdot X_{PAO}$	A.10
(11) Anaerobic maintenance (gP/d)	r_M^{AN}	=	$m_{AN}\cdot X_{PAO}$	A.11
(12) Anoxic storage of SA ($gCOD_{SA}/d$)	r_{SA}^{NO}	=	$q_{Ac}^{NO}\cdot\frac{S_A}{K_A+S_A}\cdot\frac{S_{NO}}{K_{NO}+S_{NO}}\cdot X_{PAO}$	A.12
(13) Anoxic PHA consumption ($gCOD_{XPHA}/d$)	r_{PHA}^{NO}	=	$\eta_{NO}\,k_{PHA}\cdot\frac{X_{PHA}/X_{PAO}}{K_{PHA}+(X_{PHA}/X_{PAO})}\cdot\frac{S_{NO}}{K_{NO}+S_{NO}}\cdot X_{PAO}$	A.13
(14) Anoxic storage of PP (gP/d)	r_{Pp}^{NO}	=	$\eta_{NO}\,k_{PP}\frac{X_{PAO}}{X_{PP}}\cdot\frac{S_{PO}}{K_{PO}+S_{PO}}\cdot\frac{S_{NO}}{K_{NO}+S_{NO}}\cdot X_{PAO}$	A.14
(15)Anoxic glycogen formation ($gCOD_{XGLY}/d$)	r_{GLY}^{NO}	=	$\eta_{NO}\,k_{GLY}\frac{X_{PHA}}{X_{GLY}}\cdot\frac{S_{NO}}{K_{NO}+S_{NO}}\cdot X_{PAO}$	A.15
(16) Anoxic maintenance ($gCOD_{XPA}/d$)	r_M^{NO}	=	$m_{NO}\cdot\left(S_{NO}/(K_{NO}+S_{NO})\right)\cdot X_{PAO}$	A.16
(17)Aerobic PHA consumption ($gCOD_{XPHA}/d$)	r_{PHA}^{O}	=	$k_{PHA}\cdot\frac{X_{PHA}/X_{PAO}}{K_{FPHA}+(X_{PHA}/X_{PAO})}\cdot\frac{S_O}{K_O+S_O}\cdot X_{PAO}$	A.17

Table A.1 Kinetic Equations of the TUDP model (continued)

Process			Kinetic rate Equation	Equation
(18) Aerobic storage of PP (gP/d)	r_{PP}^{O}	=	$k_{PP}\frac{X_{PAO}}{X_{PP}}\cdot\frac{S_{PO}}{K_{PO}+S_{PO}}\cdot\frac{S_O}{K_O+S_O}\cdot X_{PAO}$	A.18
(19)Aerobic glycogen formation($gCOD_{XGLY}$/d)	r_{GLY}^{O}	=	$k_{GLY}\frac{X_{PHA}}{X_{GLY}}\cdot\frac{S_O}{K_O+S_O}\cdot X_{PAO}$	A.19
(20) Aerobic maintenance ($gCOD_{XPAO}$/d)	r_M^{O}	=	$m_O\cdot(S_O/(K_O+S_O))\cdot X_{PAO}$	A.20
(21) Autotrophic growth ($gCOD_{XA}$/d)	r_A^{O}	=	$\mu_A\frac{S_{NH}}{K_{NH}+S_{NH}}\cdot\frac{S_O}{K_O+S_O}\cdot X_A$	A.21
(22) autotrophic lysis ($gCOD_{XA}$/d)	r_{AL}^{O}	=	$b_A\cdot X_A$	A.22

Table A.2 Influent characteristics and initial state of simulation of the MBR

Influent							
DO*	So	2.1 ± 0.24	gO_2/m^3	Nitrate*	S_{NO}	0	gN/m^3
COD*	S_F	739 ± 426	$gCOD/m^3$	Inert COD [a]	S_I	40	$gCOD/m^3$
Ortho-phosphate*	S_{PO}	10.5 ± 6	gP/m^3	Fatty acid [a]	S_A	91	$gCOD/m^3$
Ammonium*	S_{NH}	29 ± 4	gN/m^3				
Initial state of simulation							
Autotrophic cells [b]	X_A	75	$gCOD/m^3$	Inert COD	X_I	1500	$gCOD/m^3$
Heterotrophic cells	X_H	2500	$gCOD/m^3$	Solid COD [b]	X_S	63	$gCOD/m^3$
P-accumulating cells [b]	X_{PAO}	32.9	$gCOD/m^3$	Glycogen [b]	X_{GLY}	12.5	$gCOD/m^3$
Poly-hydroxybuterate [b]	X_{PHA}	0.7	$gCOD/m^3$	Poly phosphate	X_{PP}	5.7	$gCOD/m^3$
Flow							
Recycle I (0.2 Q_{in})	Q_{RI}	30	l/h	Influent	Q_{in}	150	l/h
Recycle II (3Q_{in})	Q_{RII}	450	l/h	Permeate	Q_p	150	l/h

* Average nutrient from Mt St John treatment plant (Table 3.1 of chapter 3 of this thesis)

[a] values from Table 3.2 in Meijer 2004, [b] values from Table 4.4 in Meijer 2004

A.1.2 EPS and membrane fouling model

The accumulation and consolidation of EPS on membrane surface coupling with a shear biofouling detachment follow the concept of Nagaoka *et al.* (1998). However, in this study, EPS concentration model from Nagaoka's work is modified to be produce from heterotrophic biomass instead of total biomass at the certain rate and to be decomposed obeying first order kinetics (A.23) (Lee, Cho *et al.* 2002). Soluble EPS accumulates on the membrane surface (A.24) due to the effect of advective pressure and will be detached by the bubble aeration shear stress (A.25). The accumulated EPS on the membrane consolidates itself slowly by suction pressure (A.26) that increases the specific resistance of filtration approaching to the ultimate value (A.27). The total filtration resistance (A.28) which is sum of biofouling resistance depositing on membrane and membrane itself resistance affects on the filtration performance as shown in A.29. All parameters in equation A.23-A.29 were addressed in appendix E.

EPS concentration in the mixed liquor:	$\frac{dEPS}{dt}$	=	$\beta \cdot X_t - k_{dEPS} \cdot EPS$	**A.23**
EPS density on the membrane surface:	$\frac{dm}{dt}$	=	$J \cdot EPS - k_{dm} \cdot m$	**A.24**
Detachment rate of EPS:	k_{dm}	=	$\gamma(\tau_m - \lambda_m \cdot P)$, $(k_{dm} \geq 0)$	**A.25**
Consolidation of the accumulated EPS:	$\frac{d\alpha}{dt}$	=	$k_\alpha(\alpha_\infty - \alpha)$	**A.26**
Ultimate vale of specific resistance	α_∞	=	$\alpha_0 + \alpha_p \cdot P$	**A.27**
Total membrane resistance:	R	=	$\alpha \cdot m + R_m$	**A.28**
Membrane filtration model:	J	=	$\frac{P}{\mu \cdot R}$	**A.29**

A.1.3 Air supply and oxygen transfer rate

The dissolved oxygen concentration in wastewater system is the residual of oxygen transfer from gas phase to wastewater and up-taken by sludge microorganisms. The oxygen transfer rate from air to become dissolved oxygen can be written as (Tchobanoglous and Burton 1991):

$$r_C = \frac{dC}{dt} = K_L a(C_s - C) - \text{OUR} \qquad \textbf{A.30}$$

$$\text{Or} \quad \frac{dC}{dt} = \text{OTR / V} = \frac{SOTR}{V}\left(\frac{\beta C_s - C}{C_{s20}}\right)\theta^{T-20}(\alpha) \qquad \textbf{A.31}$$

All parameters in equation A.30-A.31 were addressed in appendix E.

A.1.4 Shear intensity model

The turbulent shear intensity model was used to calculate the apparent shear for the submerged hollow fiber membrane in activated sludge reactor. For a given aeration intensity, the apparent shear intensity of fluid turbulence can be estimated by

$$G_0 = \sqrt{\frac{\rho_{LS}\, g\, q_{air}}{\mu_s}} \quad \text{(Li \&Wang, 2005)}$$

$$= \sqrt{\frac{Q_{air}\, H\, \gamma_w}{V \mu}} \quad \text{(Merlo, 2004)} \qquad \textbf{A.34}$$

shear stress (τ) can be written as:

$$\tau = G0 \times \mu = \gamma x \mu \qquad \textbf{A.35}$$

All parameters in equation A.34-A.35 were addressed in appendix E.

A.1.5 Arrangement of models for simulation

The performances of treatment process and membrane filtration are simulated with AQUASIM 2.0 software. By giving the value of air supply, the oxygen transfer rate will be calculated and influences on the activities of biomass activated sludge including EPS production and attachment of EPS on the membrane surface, meanwhile the shear aeration value will also be estimated to present the detachment of EPS biofilm. Finally, the membrane fouling manner as well as the treatment efficiency can be evaluated (see Fig. A.2).

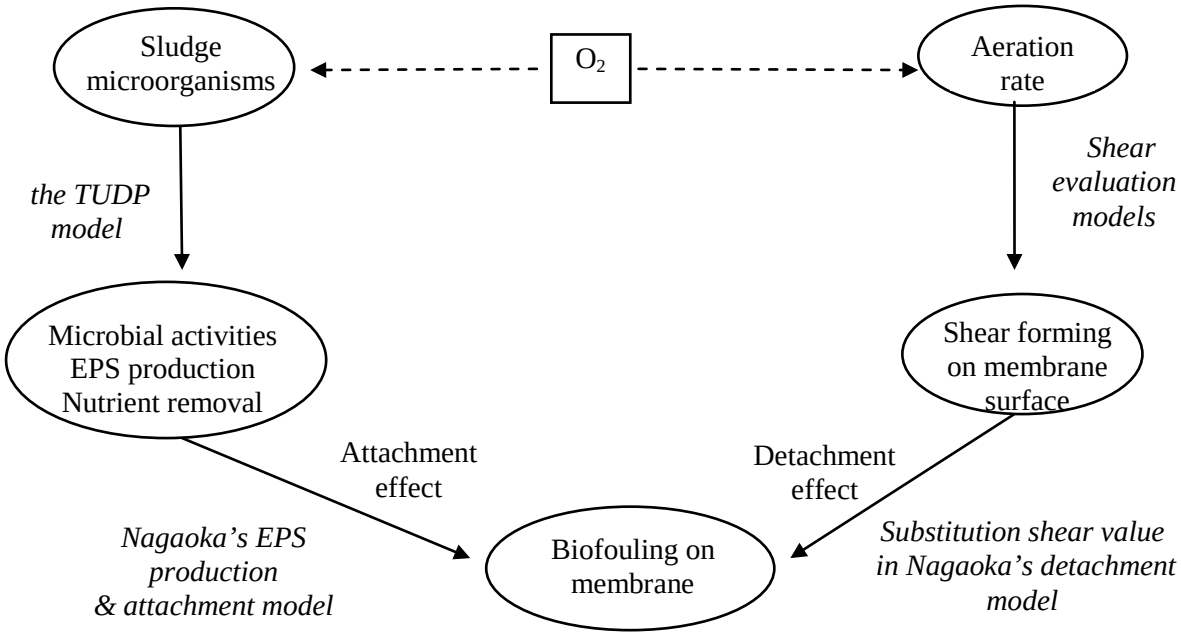

Fig. A.2 Schematic diagram of model arrangement for simulation

A.2 CALCULATION OF SOME SMBR CONSIDERATIONS

A.2.1 Calculation of sludge production and nutrient requirements

Sludge production indicates the transformation between BOD (and/or COD) up-taken and the amount of particulate biomass increase in the system (Tchobanoglous *et al.* 2003). Sludge production can be calculated by the following:

Sludge production: $P_x = Y_{obs}\,(Q_{in})(S_o - S)$ **A.36**

All parameters in equation A.36 were addressed in appendix E.

Observed yield values (Y_{obs}), based on BOD, are illustrated on Fig. A.3. A temperature range 20 - 30 ^{0}C based on tropical Townsville region is used for the graph reading in Fig. A.3, and a long SRT is planned for the MBR treatment configuration in order to increase sludge building-up. In fact, for the conventional activated sludge (CAS) process for treating domestic wastewater, sludge yield is normally in the range 0.30–0.50 gVSS/gCOD (Tchobanoglous *et al.* 2003) and the observed yield in MBR system is normally lower than the observed yield occurring in CAS process for the same type of influent (Khongnakorn *et al.* 2007).

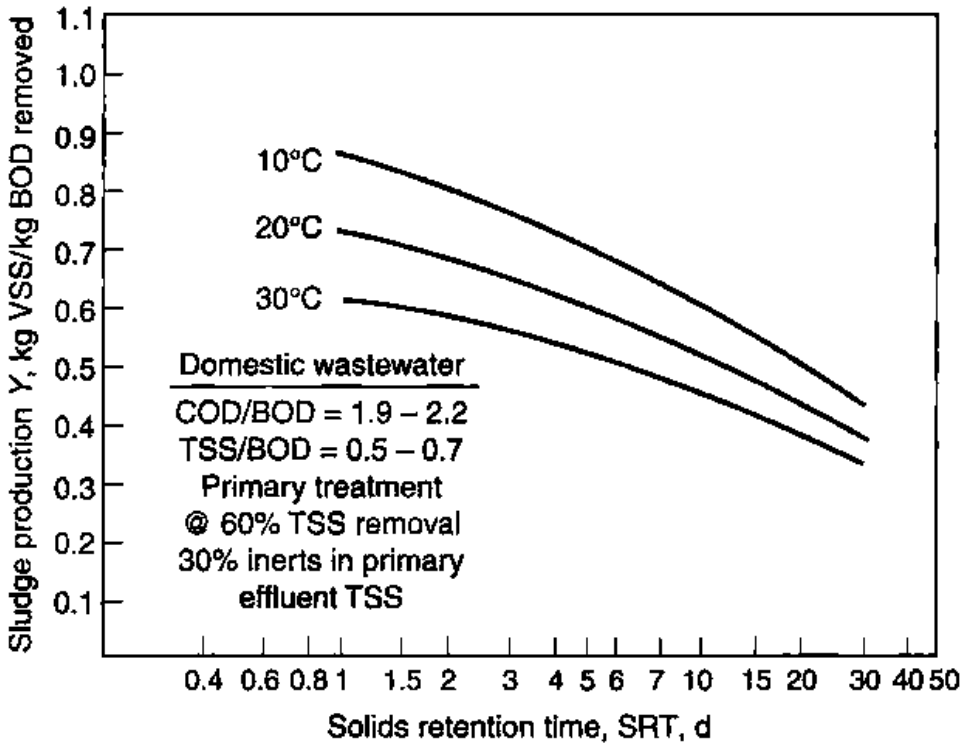

Fig. A.3 Net solid production, SRT and temperature with primary treatment (Tchobanoglous, Burton *et al.* 2003)

Therefore, observed yields of no more than 0.5 (kgVSS/kg BOD removal) can be assumed in the design calculation and nearly complete of BOD removal is expected for the process. Also, an influent 150 L/h or 3.6 m^3/d (Q_{in}) is the recommended operating point for the membranes used in this study (Kubota-Corporation 2004).

The estimation of sludge production can be calculated based on Equation A.36:

Sludge production: $P_x = Y_{obs}\,(Q_{in})(S_o - S)$

$P_x = (0.5\ g/g) \times (3.6\ m^3/d) \times (309.6 - 0\ mg/l)$

$$P_x = 0.557 \text{ kg VSS/d}$$

The calculation details of the nutrient requirement based on Equation A.37-A.40 as following:

$$\text{Nitrogen (N) requirement} = 0.122 \times P_x \quad \textbf{A.37}$$
$$= 0.122 \times (0.557 \text{ kg/d})$$
$$= 0.0679 \text{ kg/d}$$

$$\text{Nitrogen - loading} = Q_{in} \times \text{influent TKN} \quad \textbf{A.38}$$
$$= (3.6 \text{ m}^3\text{/d}) \times (24.6/1000 \text{ kg/m}^3)$$
$$= 0.0886 \text{ kg/d}$$

$$\text{Phosphorous (P) requirement} = 0.023 \times P_x \quad \textbf{A.39}$$
$$= 0.023 \times (0.557 \text{ kg/d})$$
$$= 0.0128 \text{ kg/d}$$

$$\text{Phosphorous - loading} = 8.34 \times Q_{in} \times \text{influent P} \quad \textbf{A.40}$$
$$= 8.34 \times (3.6 \text{ m}^3\text{/d}) \times (11.8/1000 \text{ kg/m}^3)$$
$$= 0.0427 \text{ kg/d}$$

From calculation details of Equation A.37 - A.40 shown above, there is sufficient nutrient in the influent supplied to the MBR pilot plant.

A.2.2 Calculation of oxygen requirement

Oxygen requirement for carbonaceous organic matter

Oxygen required to oxidize a unit of biomass can be written as (Benefield and Randall 1980):

$$C_5H_7NO_2 \quad + \quad 5\,O_2 \quad \rightarrow \quad 5\,CO_2 \; + \; 2\,H_2O \; + \; NH_3$$

113 : 1 cell (5x32)

= 1.42 where 5 x32/113 = 1.42 units O_2 / unit biomass oxidized

To remove the carbonaceous organic, oxygen requirement can be (Tchobanoglous *et al.* 2003):

$$\begin{pmatrix} actual\ O_2 \\ required/day \end{pmatrix} = \begin{pmatrix} total\ amount\ of \\ substrate\ removed/day \\ given\ as\ ultimate\ BOD \end{pmatrix} - 1.42 \begin{pmatrix} total\ active\ mass\ of \\ organisms\ waste/day \end{pmatrix}$$

$$\therefore O_2\ requirement\ (kg/d)\ for\ BOD\ removal = \frac{Q_{in}\,(S_o - S)}{f} - 1.42\,(P_x) \quad \textbf{A.41}$$

where: f = converting factor of BOD_5 and ultimate BOD (*UBOD*)

The BOD exerted up to time (t) is given by:

$$BOD_t = UBOD\,(1 - e^{-kt}) \quad \textbf{A.42}$$

$$k = k_{20}\,\theta^{T-20} \quad \textbf{A.43}$$

All parameters in equation A.42-A.43 were addressed in appendix E.

Oxygen requirement for nitrification (Tchobanoglous *et al.* 2003):

Step I: $$2\,NH_4^+ + 3O_2 \xrightarrow{Nitrosomonas} 2\,NO_2^- + 2\,H_2O + 4H^+$$

where O_2 required = 3.43 g/g-N oxidized

alkalinity = 7.14 g CaCO3/g N-oxidized

Step II: $2\,NO_2^- + O_2 \xrightarrow{Nitrobacter} 2\,NO_3^-$

where O_2 required = 1.14 g/ g N-oxidized

Thus, O_2 requirement for step I and II is (3.43+1.14) = 4.57 g O2/g N-oxidized

$$\therefore O_2 \text{ requirement } (kg/d) \text{ for nitrogen removal} = 4.57 \times Q_{in}\,(N_o - N) \quad \textbf{A.44}$$

where N_o = influent TKN (mg/L)

N = effluent TKN (mg/L)

Therefore, total oxygen requirement for both carbonaceous and nitrogen removal can be calculated using Equation below:

$$\therefore \text{Total } O_2 \text{ requirement } (kg/d) = \frac{Q_{in}(S_o - S)}{f} - 1.42(P_x) + 4.57\,Q_{in}(N_o - N) \quad \textbf{A.45}$$

Substituting all parameter values from TableA.3 in the Equation A.45 can be calculated as below:

$$\therefore \text{Total } O_2 \text{ requirement} = \frac{Q(S_o - S)}{f} - 1.42(P_x) + 4.57.\,Q(N_o - N) \quad \textbf{A.45}$$

= [(3.6 m^3/d) x (309.6 – 0 mg/L) / 0.764]

- (1.42 x 0.557 kg/d)

+ [4.57 x (3.6 m^3/d) x (60.26 – 0 mg/L)]

Therefore, total O_2 requirement = 1.66 kg/d

Based on Equation A.45 and calculation shown above, total oxygen requirement is 1.66 kg/d.

Table A.3 Parameter values for calculation of oxygen requirement

Parameters	Definition	Value	Source
Q_{in}	influent flow rate	3.6 m^3/d	recommended flow for Kubota LF-10
$S_o - S$	BOD removal (assumed 100%)	309.6 mg/L	Table3.1 (data from CitiWater)
P_x	sludge production	0.557 kgVSS/d	determined using Equation 3.1
f	BOD conversion factor	0.764	determined using Equation A.42-43
BOD_5	concentration of BOD	309.6 mg/L	Table3.1 (data from CitiWater)
k_{25}	reaction rate constant at 25 ^{0}C	0.289 1/d	determined using Equation 3.8
$UBOD$	ultimate BOD	405 mg/L	determined using Equation 3.7
$N_o - N$	nitrogen removal (assumed 100%)	60.26 mg/L	Table3.1 (data from CitiWater)

A.2.3 Calculation of air flow rate requirement

Aeration can be estimated using Equation below (Tchobanoglous *et al.* 2003):

$$\textit{Air flow rate } (m^3/min) = \frac{(SOTR\ kg/h)}{[(E)(60min/h)(kg\ O_2/m^3\ air)]} \qquad \textbf{A.46}$$

where $SOTR$ = a standard oxygen transfer rate in tap water at 20 ^{0}C and zero dissolved oxygen which can be calculated as:

$$= AOTR \left[\frac{C_{s,20}}{\alpha F(\beta C_{\bar{S},T,H} - C_L)}\right](1.024^{T-20}) \qquad \textbf{A.47}$$

$C_{\bar{S},T,H}$ = the saturation average dissolved O2 in clean water aeration tank

$$= \quad (C_{S,T,H}) \frac{1}{2} \left(\frac{P_{atm,H} + P_{w,depth}}{P_{atm,H}} + \frac{O_t}{21} \right) \qquad \textbf{A.48}$$

All parameter used in Equation A.46-A.48 are shown in Table A.4

Table A.4 Parameters used for calculation in Equation A.46-A.48

Parameters	Definition	Value	Source
E	oxygen transfer efficiency	30%	assumed
α	mixing correction factor	0.4 to 0.8	source [a]
F	fouling factor	0.9	assumed
β	salinity-surface tension correction factor	0.95 to 0.98	source [a]
C_L	operating oxygen concentration	2 mg/L	assumed
$C_{s,20}$	dissolved O_2 in water as a function of temperature	9.08 mg/L	appendix D.1[a]
T	Temperature (average in Townsville)	25 ^{0}C	-
$AOTR$	actual O_2 transfer rate under field conditions	1.66 kg/d	O_2 requirement [b]
O_t	percent oxygen leaving the aeration	19-21%	source [a]
$C_{S,T,H}$	saturated O2 in water $C_{S,25,1atm}$	8.24 mg/L	appendix D.2a
$P_{w,depth}$	pressure at the depth of air release	1.8 m	water level
$P_{atm,H}$	atmospheric pressure at altitude H	1.7 m	$P_{atm,H} = P_{atm} / \gamma$
γ	specific weight of air	59.4 kN/m3	$\gamma = P/(RT)$
P	atmospheric pressure	14.7 lb/in2	-
R	universal gas constant (ft.lb/ lb-air.0R)	53.3	source a

Note: a = from (Tchobanoglous *et al.* 2003), b = from Equation A.45

Substituting all parameter values in Equation A.48 below to get $C_{S,T,H}^{-}$ value

$$C_{\bar{S},T,H} = (C_{S,T,H})\frac{1}{2}\left(\frac{P_{atm,H}+P_{w,depth}}{P_{atm,H}}+\frac{O_t}{21}\right)$$

$$= (8.24 \text{ mg/L})\ (1/2)\ [((1.7 + 1.8)/1.7) + (19/21)] = 12.2 \text{ mg/L}$$

Then, substituting all parameter values in Equation (A.47) to get SOTR value, assuming α = 0.5, F = 0.9, β = 0.95;

$$\text{SOTR} = \text{AOTR}\left[\frac{C_{s,20}}{\alpha F(\beta C_{\bar{S},T,H}-C_L)}\right](1.024^{T-20})$$

$$= \frac{(1.66\ kg/d)\ (9.08\ g/m^3)\ (1.024)^{20-25}}{(0.5)\ (0.9)\ [(0.95)(12.2\ g/m^3)-2\ g/m^3]}$$

$$= 3.12 \text{ kg/d} = 0.13 \text{ kg/hr}$$

The air density at 25 ^{0}C and pressure 1 atm is 1.184 kg/m^3 (from appendix B Tchobanoglous *et al.* 2003). The corresponding amount of oxygen by weight is 0.2744 (0.2318; from 23.18 % of O_2 in air, x 1.184 kg/m^3) and air flow rate are ready to be calculated using Equation A.46 as following:

$$\text{Air flow rate (m}^3\text{/min)} = \frac{(SOTR\ kg/h)}{[(E)(60\,\text{min}/h)(kg\,O_2/m^3 air)]}$$

$$= \frac{0.13\ kg/h}{[(0.35)(60\,\text{min}/h)(0.2744\ kgO_2/m^3 air)}$$

$$= 0.02256 \text{ m}^3\text{/min} = 22.56 \text{ l/min}$$

Based on Equation 3.11 and calculation shown above, necessary air flow rate is 22.56 l/min. Therefore, the blower used in the pilot MBR has to cover at least 22.56 l/min of aeration due to oxygen requirement.

A.2.4 Calculation of head loss

Head loss can be calculated using Bernoulli Equation, shown below.

Energy Equation for fluid flow:

$$Z_1 + \frac{P_1}{\rho g} + \frac{V_1^2}{2g} = Z_2 + \frac{P_2}{\rho g} + \frac{V_2^2}{2g} + h_L$$

$$h_L = \left(\sum f \frac{L}{D}\frac{V_i^2}{2g}\right) + \left(\sum K_L \frac{V_i^2}{2g}\right)$$

where $\sum f \frac{L}{D}\frac{V_i^2}{2g}$ = major head loss depends on pipe diameter and flow pattern

$\sum K_L \frac{V_i^2}{2g}$ = minor head loss depends on pipe connection (e.g. bend, valve)

In this case, only major head loss is considered, therefore;

$$Z_1 + \frac{P_1}{\rho g} + \frac{V_1^2}{2g} = Z_2 + \frac{P_2}{\rho g} + \frac{V_2^2}{2g} + \left(\Sigma f \frac{L}{D}\frac{V_i^2}{2g}\right) \qquad \textbf{A.49}$$

where L, D = length an diameter of pipe (m), respectively

f = friction factor: for laminar flow f = 64/Re for Re $\leq$ 2000;

for turbulent flow using Swamee-Jain Equation (error 2-5%):

$$f = \frac{0.25}{\left[\log\left(\frac{k/d}{3.7} + \frac{5.74}{\mathrm{Re}^{0.9}}\right)\right]^2}$$

A summary of head loss calculation is presented in TableA.5.

Table A.5 Head loss calculation of the MBR (see flow diagram Fig. 3.2 in chapter 3)

Section of flowing	di (in)	area (m^2)	flow (m^3/s)	velocity (m/s)	Re	Friction factor	hf (m)
Section I : Inlet flow to anaerobic unit, Flow 1Qin (Qin =150l/h), pipe length 20 m	1.5	0.001268	4.17E-05	0.0515	1565.86	0.046	0.00221
Section II : Overflow from anaerobic unit to anoxic unit, Flow 1.2Qin, pipe length 2 m	2	0.002028	5.00E-05	0.025	1252.68	0.051	0.00006
Section III : Overflow from anoxic to aerobic-membrane unit, Flow 4.2Qin, pipe 2 m	2	0.002028	1.75E-04	0.086	4384.39	0.015	0.000218
Section IV : Return flow from aerobic-membrane to anaerobic unit, Flow 0.2Qin , pipe 10 m	0.5	0.000127	8.33E-06	0.066	835.123	0.077	0.013313
Section V : Return flow from aerobic-membrane to anoxic unit, Flow 3Qin, pipe 6 m	1	0.000507	1.25E-04	0.247	6263.422	0.010	0.007591

APPENDIX B

EXPERIMENTAL DATA FOR CHAPTER 4

B.1 FILTRATION PROFILES USING FLUX STEPPING TECHNIQUE

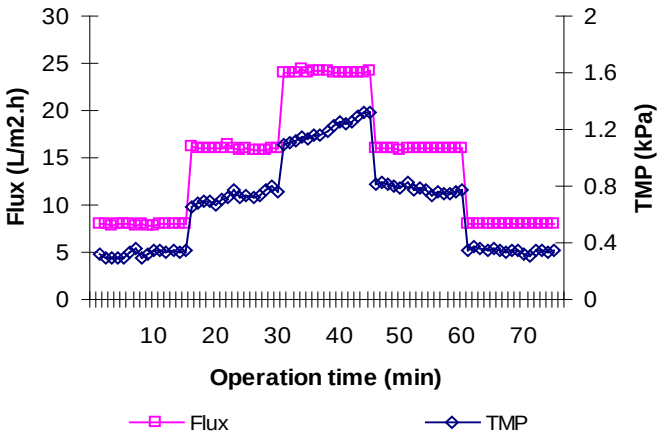

Fig. B.1 Flux and TMP profile at step height 8 L/m^2h and step length 15 min using flux stepping technique

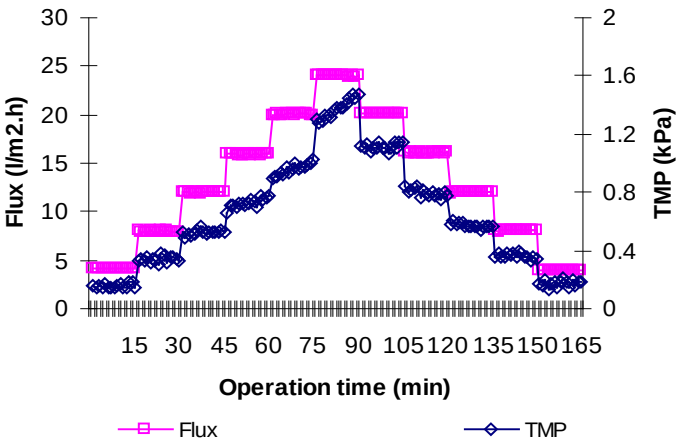

Fig. B.2 Flux and TMP profile at step height 4 L/m^2h and step length 15 min using flux stepping technique

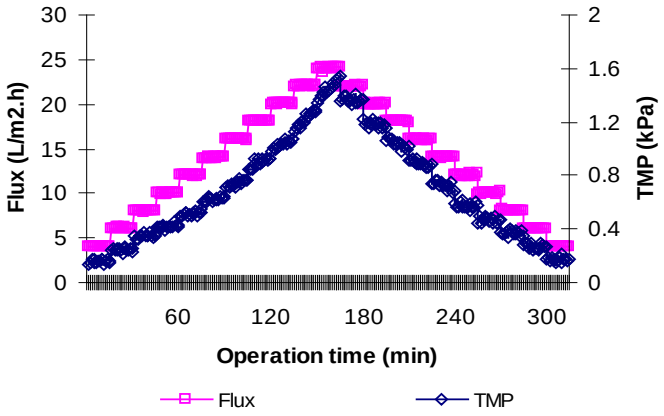

Fig. B.3 Flux and TMP profile at step height 2 L/m^2h and step length 15 min using flux stepping technique

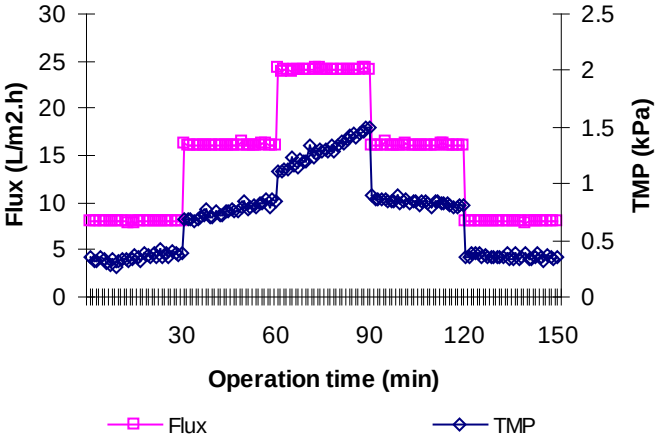

Fig. B.4 Flux and TMP profile at step height 8 L/m^2h and step length 30 min using flux stepping technique

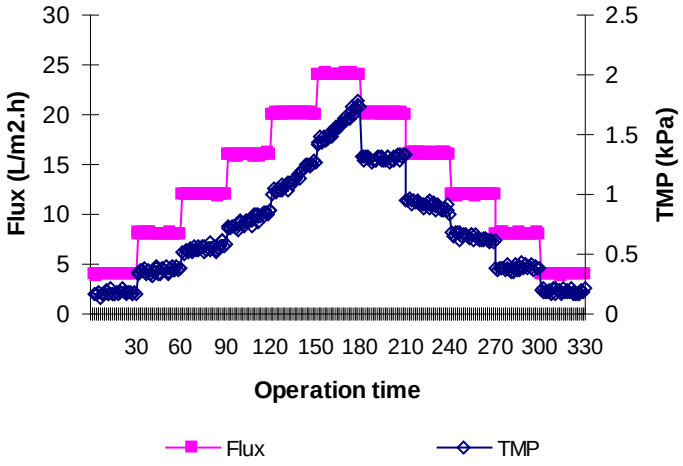

Fig. B.5 Flux and TMP profile at step height 4 L/m^2h and step length 30 min using flux stepping technique

Fig. B.6 Flux and TMP profile at step height 2

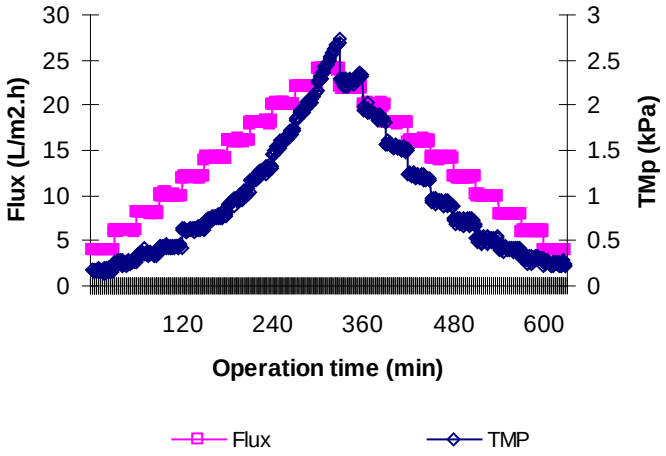

L/m^2h and step length 30 min using flux stepping technique

B.2 FILTRATION PROFILES USING FLUX CYCLING TECHNIQUE

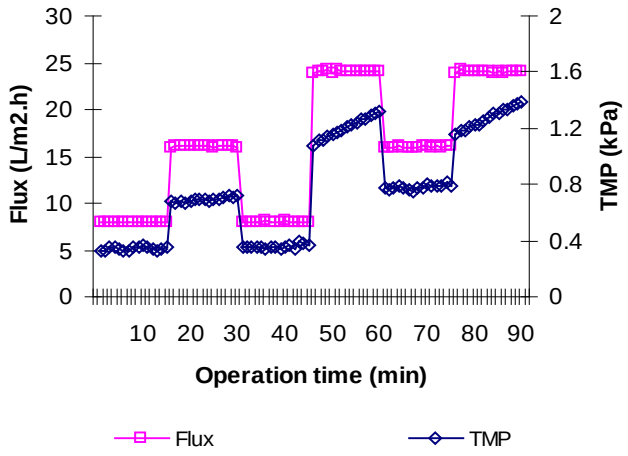

Fig. B.7 Flux and TMP profile at step height 8 L/m^2h and step length 15 min using flux cycling technique

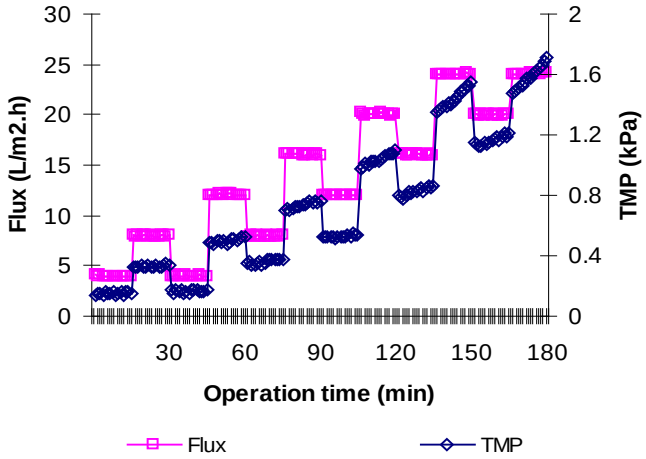

Fig. B.8 Flux and TMP profile at step height 4 L/m^2h and step length 15 min using flux cycling technique

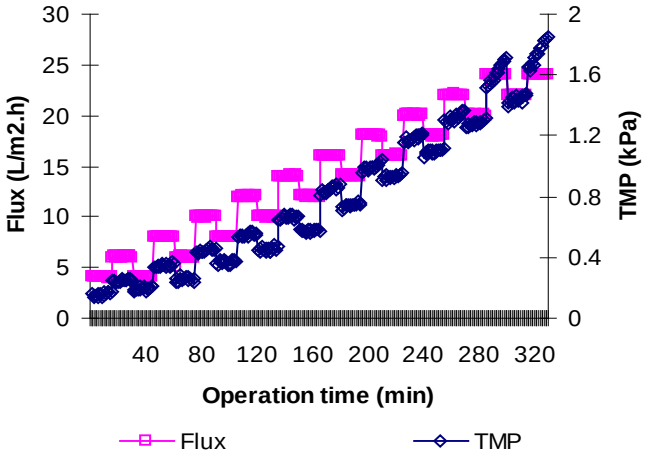

Fig. B.9 Flux and TMP profile at step height 2 L/m^2h and step length 15 min using flux cycling technique

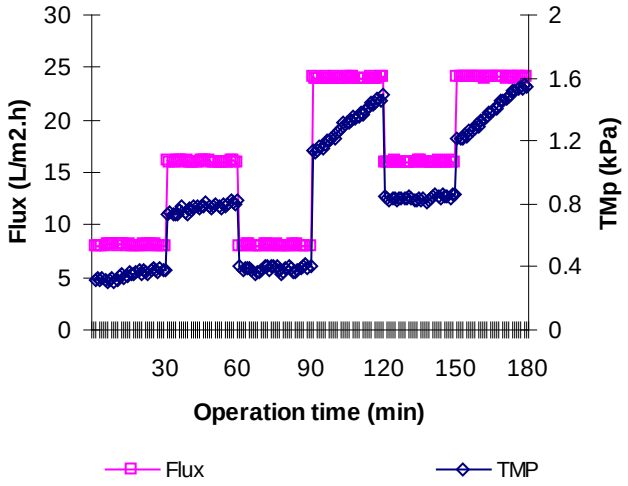

Fig. B.10 Flux and TMP profile at step height 8 L/m^2h and step length 30 min using flux cycling technique

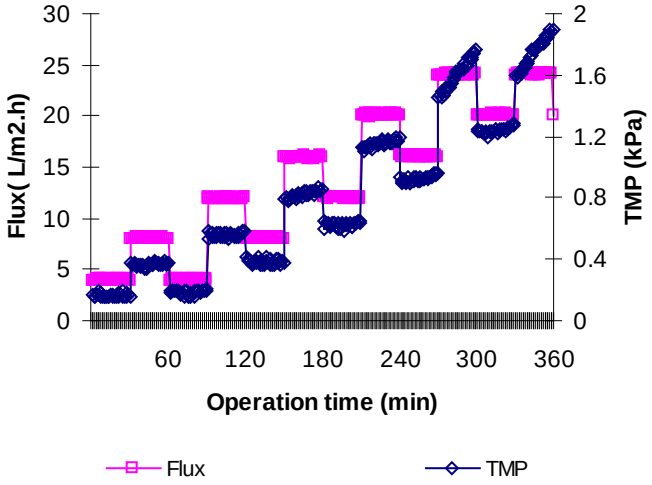

Fig. B.11 Flux and TMP profile at step height 4 L/m^2h and step length 30 min using flux cycling technique

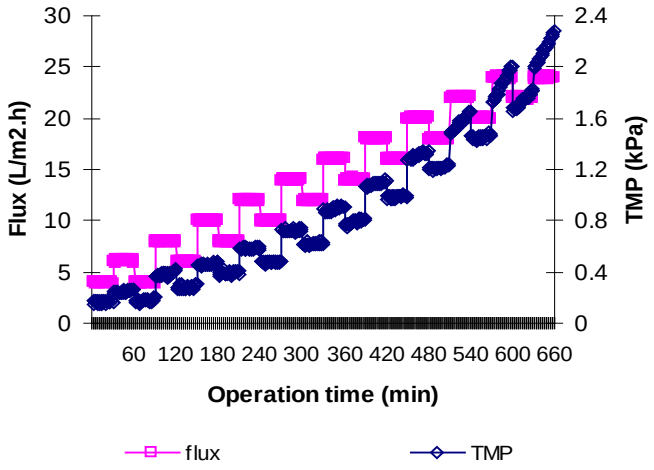

Fig. B.12 Flux and TMP profile at step height 2 L/m^2h and step length 30 min using flux cycling technique

B.3 CRITICAL FLUX BASED ON FLUX LINEARITY

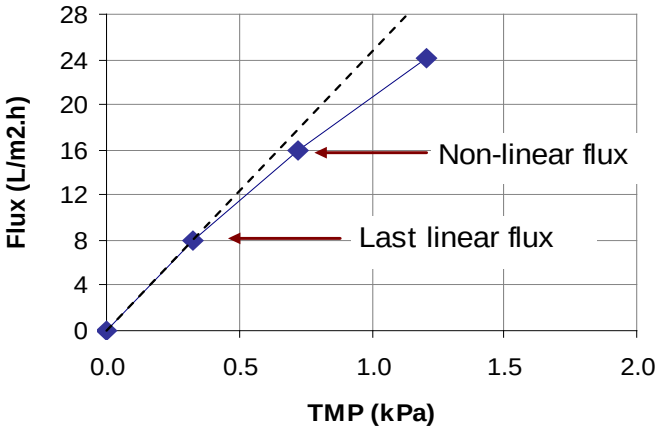

Fig. B.13 Critical flux based on flux linearity at step height 8 L/m^2h and step length 15 min using flux stepping technique

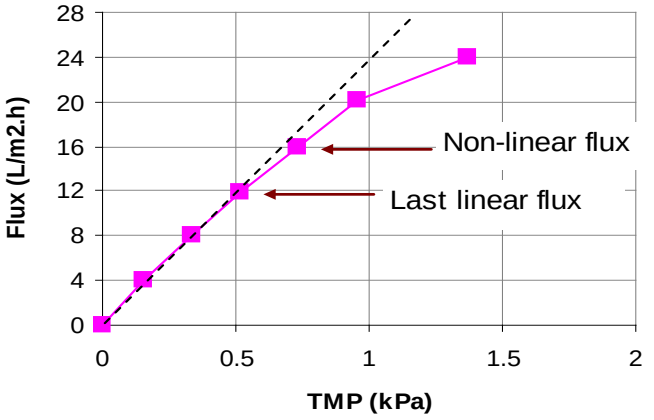

Fig. B.14 Critical flux based on flux linearity at step height 4 L/m^2h and step length 15 min using flux stepping technique

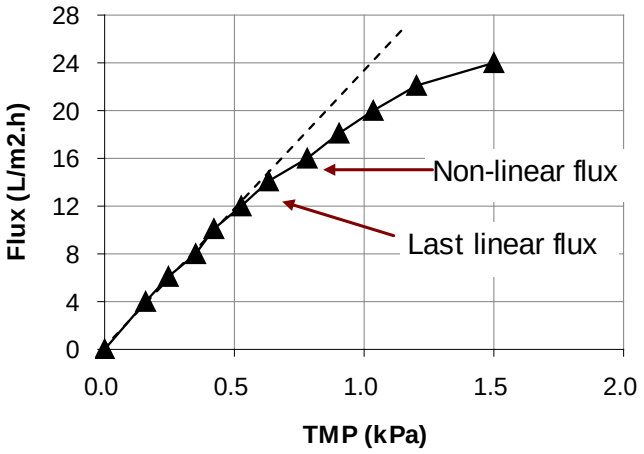

Fig. B.15 Critical flux based on flux linearity at step height 2 L/m^2h and step length 15 min using flux stepping technique

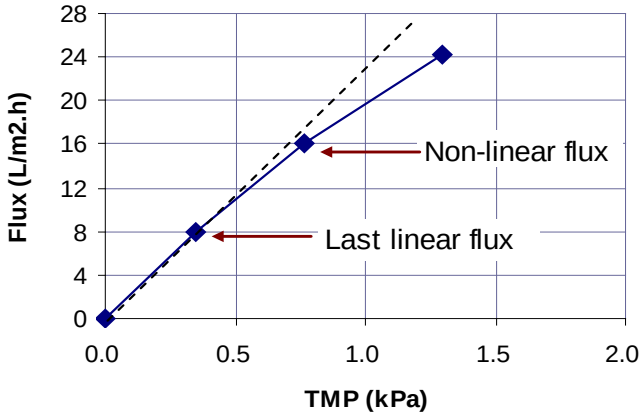

Fig. B.16 Critical flux based on flux linearity at step height 8 L/m^2h and step length 30 min using flux stepping technique

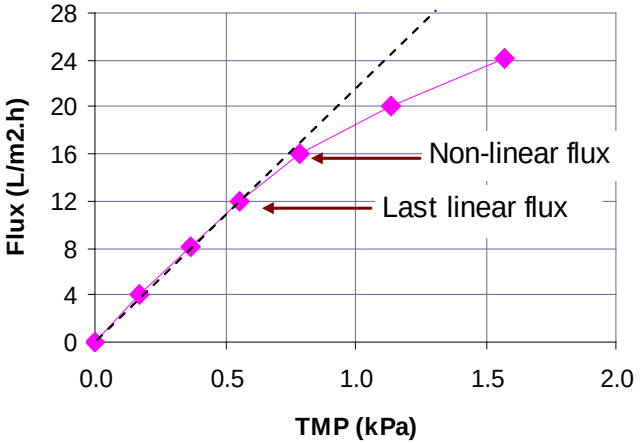

Fig. B.17 Critical flux based on flux linearity at step height 4 L/m^2h and step length 30 min using flux stepping technique

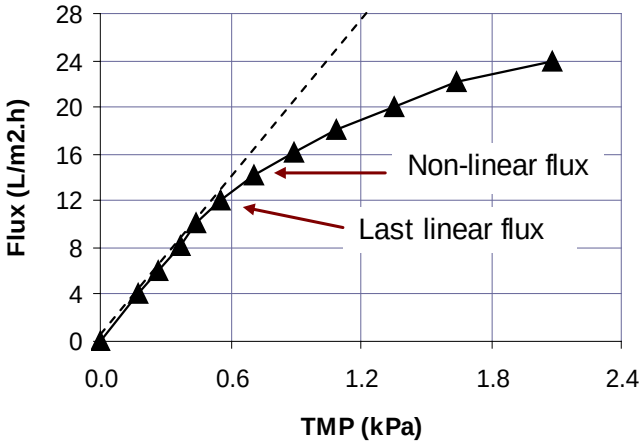

Fig. B.18 Critical flux based on flux linearity at step height 2 L/m^2h and step length 30 min using flux stepping technique

B.4 CRITICAL FLUX BASED ON 90% PERMEABILITY

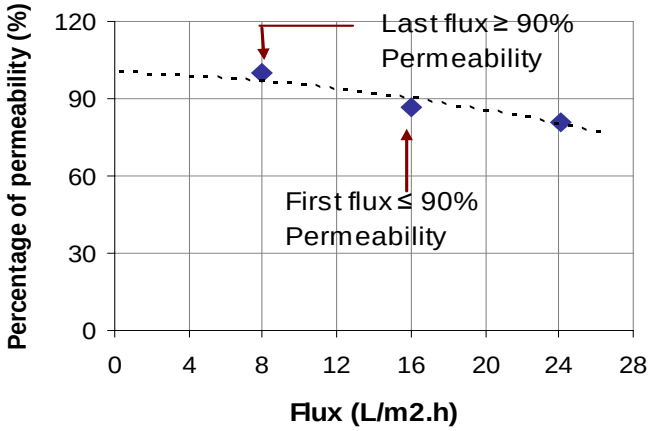

Fig. B.19 Critical flux based on 90% permeability at step height 8 L/m^2h and step length 15 min using flux stepping technique

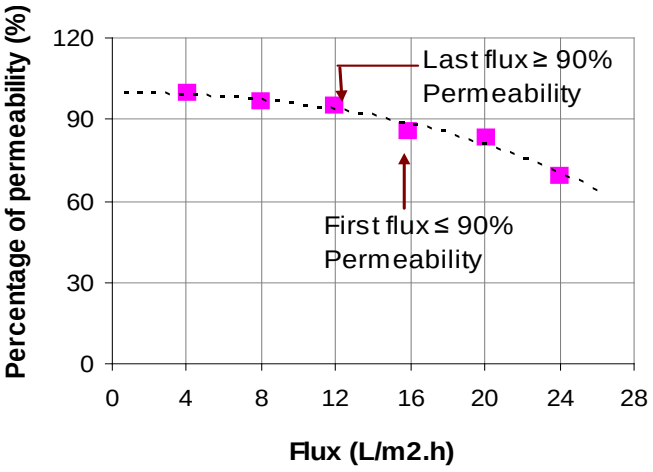

Fig. B.20 Critical flux based on 90% permeability at step height 4 L/m^2h and step length 15 min using flux stepping technique

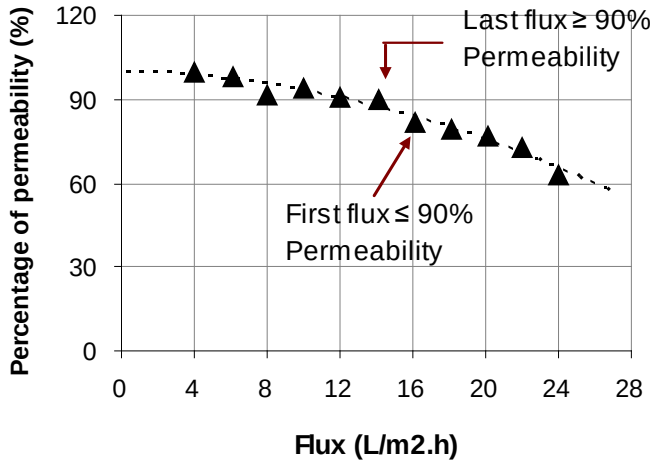

Fig. B.21 Critical flux based on 90% permeability at step height 2 L/m^2h and step length 15 min using flux stepping technique

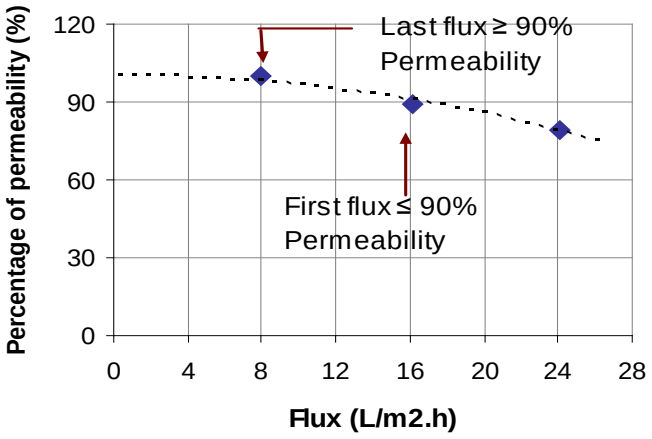

Fig. B.22 Critical flux based on 90% permeability at step height 8 L/m^2h and step length 30 min using flux stepping technique

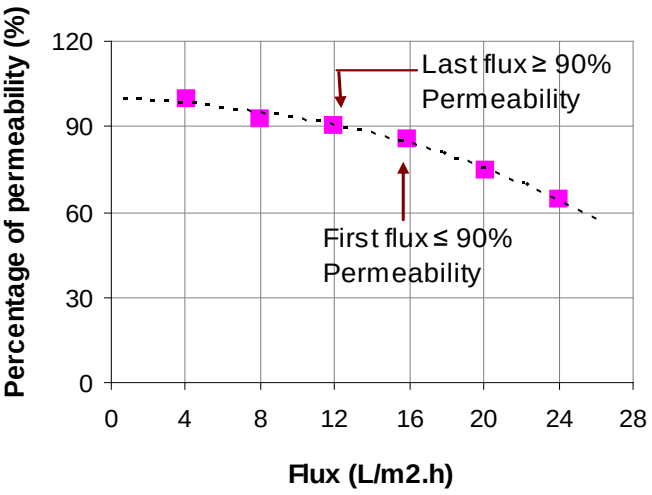

Fig. B.23 Critical flux based on 90% permeability at step height 4 L/m^2h and step length 30 min using flux stepping technique

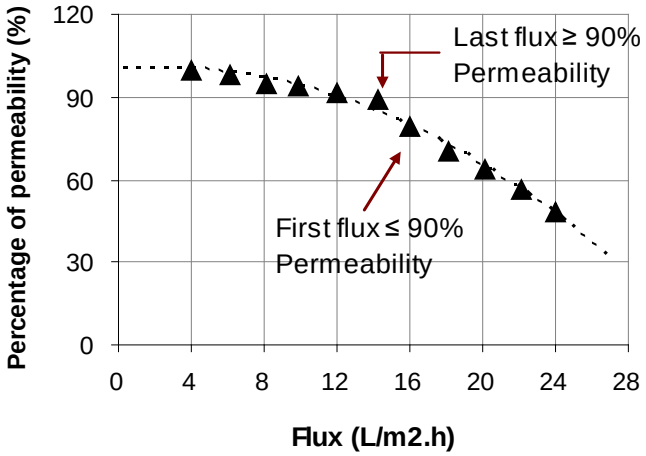

Fig. B.24 Critical flux based on 90% permeability at step height 2 L/m^2h and step length 30 min using flux stepping technique

B.5.1 CRITICAL FLUX BASED ON FOULING REVERSIBILITY FROM HYSTERESIS LOOP

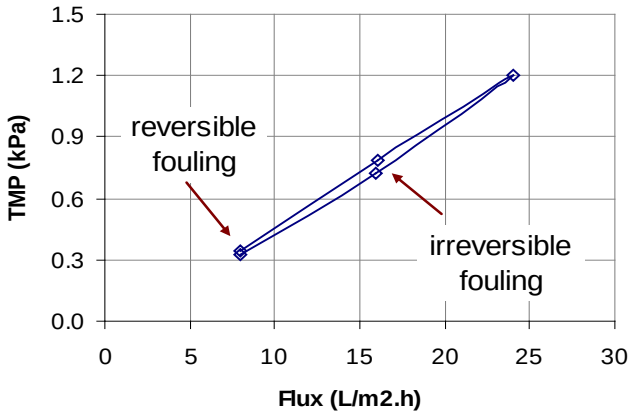

Fig. B.25 Critical flux based on fouling reversibility at step height 8 L/m^2h and step length 15 min from hysteresis loop of flux stepping technique

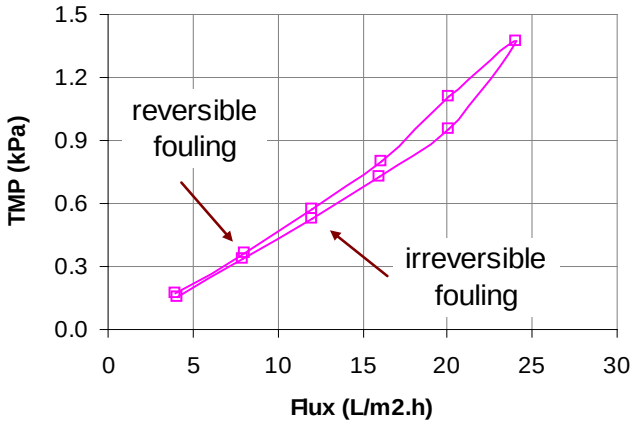

Fig. B.26 Critical flux based on fouling reversibility at step height 4 L/m^2h and step length 15 min from hysteresis loop of flux stepping technique

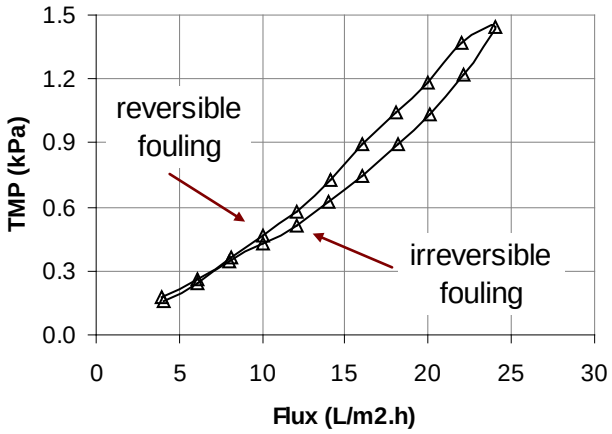

Fig. B.27 Critical flux based on fouling reversibility at step height 2 L/m^2h and step length 15 min from hysteresis loop of flux stepping technique

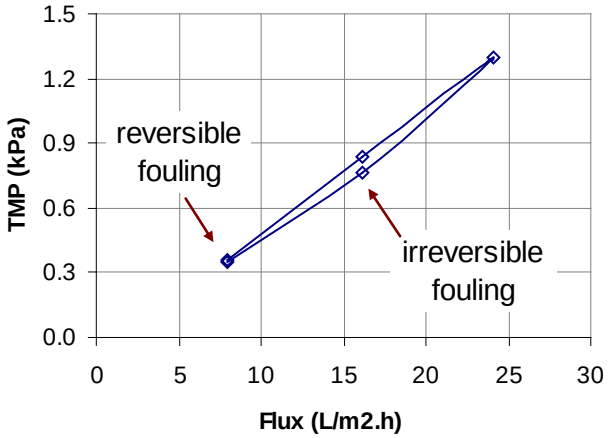

Fig. B.28 Critical flux based on fouling reversibility at step height 8 L/m^2h and step length 30 min from hysteresis loop of flux stepping technique

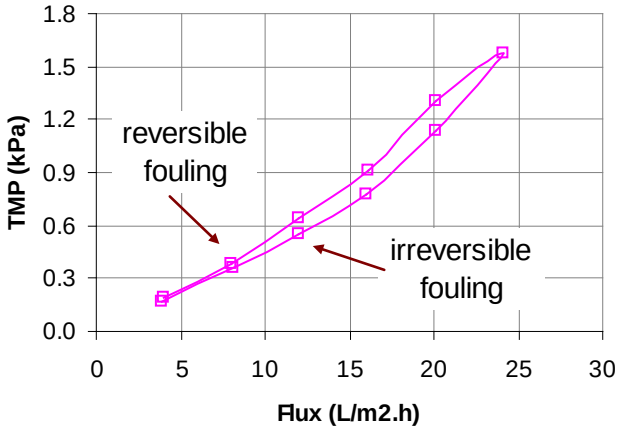

Fig. B.29 Critical flux based on fouling reversibility at step height 4 L/m^2h and step length 30 min from hysteresis loop of flux stepping technique

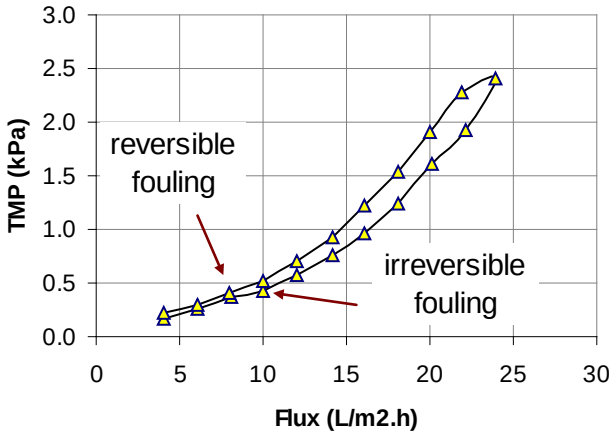

Fig. B.30 Critical flux based on fouling reversibility at step height 2 L/m^2h and step length 30 min from hysteresis loop of flux stepping technique

B.5.2 CRITICAL FLUX BASED ON FOULING REVERSIBILITY FROM FLUX CYCLING

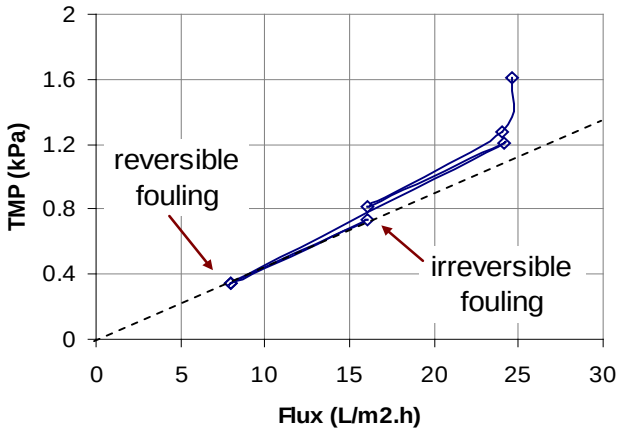

Fig. B.31 Critical flux based on fouling reversibility at step height 8 L/m^2h and step length 15 min using flux cycling technique

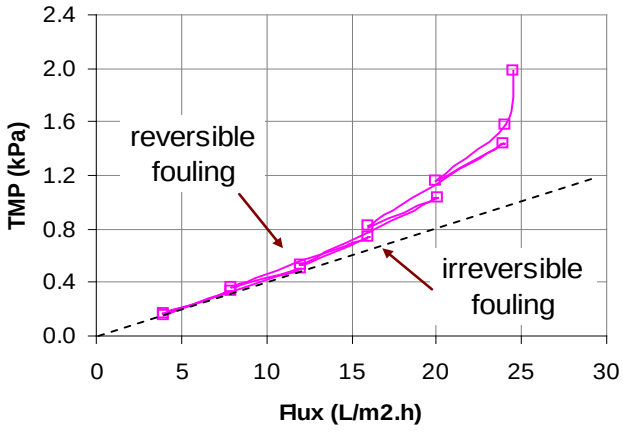

Fig. B.32 Critical flux based on fouling reversibility at step height 4 L/m^2h and step length 15 min using flux cycling technique

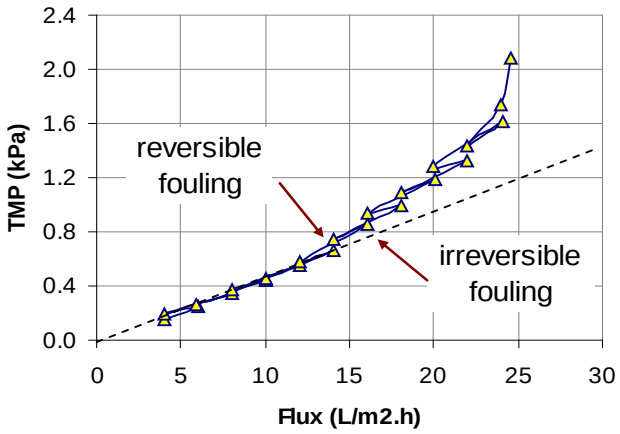

Fig. B.33 Critical flux based on fouling reversibility at step height 2 L/m^2h and step length 15 min using flux cycling technique

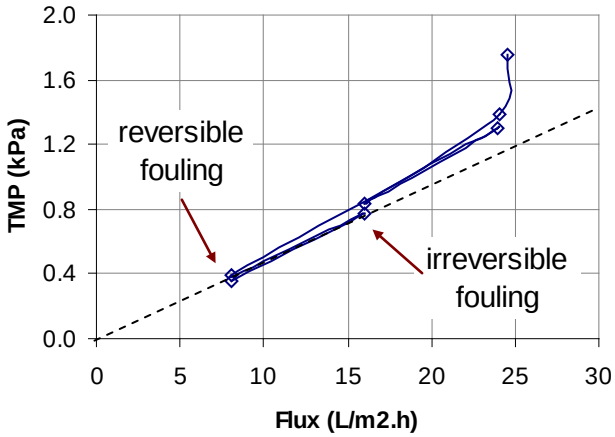

Fig. B.34 Critical flux based on fouling reversibility at step height 8 L/m^2h and step length 30 min using flux cycling technique

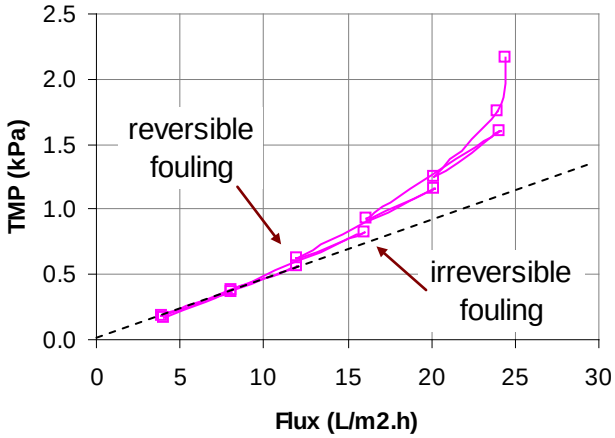

Fig. B.35 Critical flux based on fouling reversibility at step height 4 L/m^2h and step length 30 min using flux cycling technique

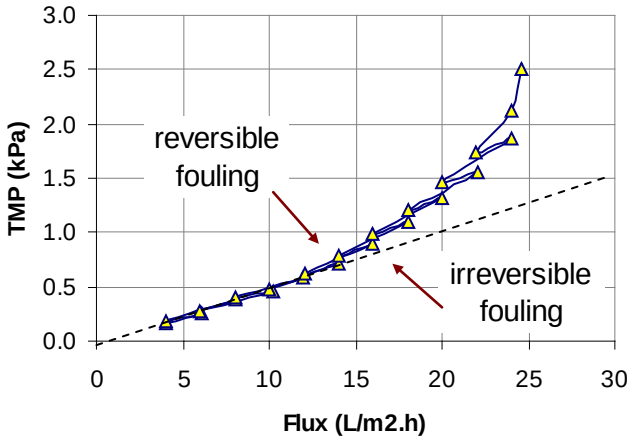

Fig. B.36 Critical flux based on fouling reversibility at step height 2 L/m^2h and step length 30 min using flux cycling technique

B.6 SUSTAINABLE FLUX BASED ON FOULING RATE

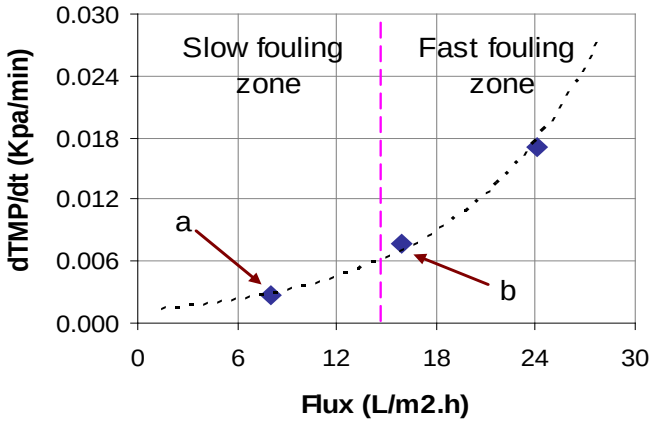

Fig. B.37 Sustainable flux based on fouling rate at step height 8 L/m^2h and step length 15 min using flux stepping technique

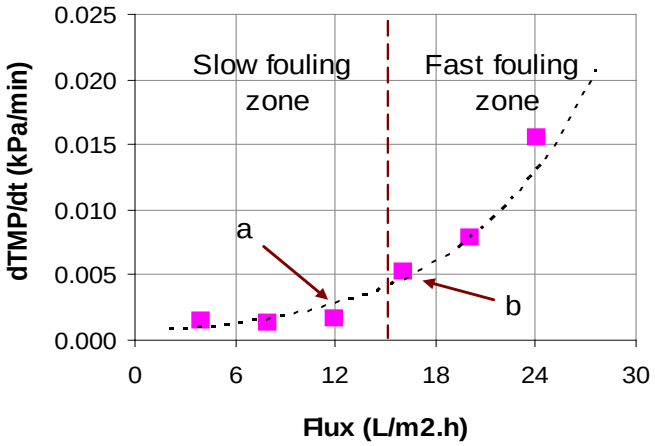

Fig. B.38 Sustainable flux based on fouling rate at step height 4 L/m^2h and step length 15 min using flux stepping technique

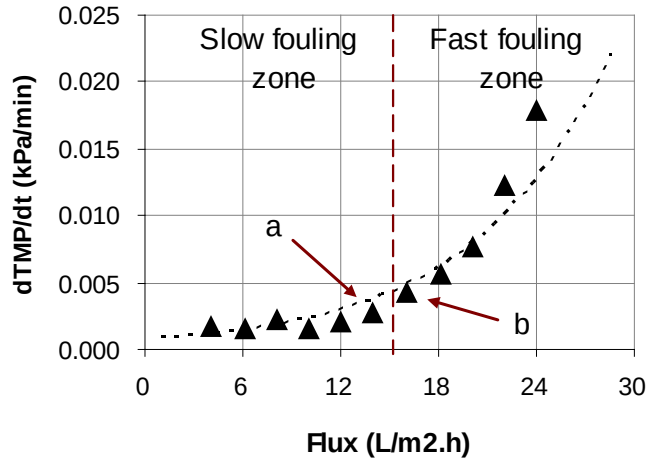

Fig. B.39 Sustainable flux based on fouling rate at step height 2 L/m^2h and step length 15 min using flux stepping technique

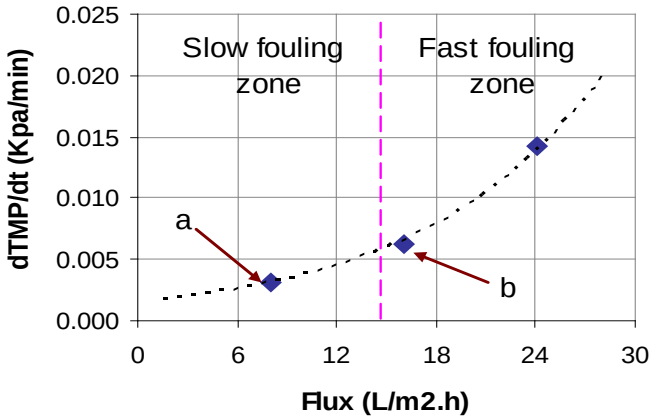

Fig. B.40 Sustainable flux based on fouling rate at step height 8 L/m^2h and step length 30 min using flux stepping technique

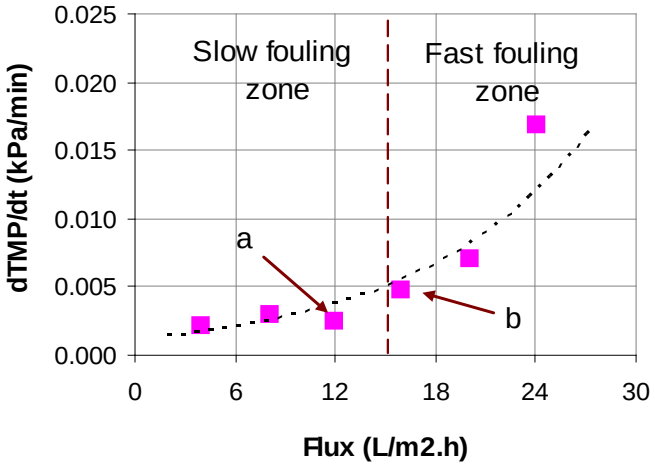

Fig. B.41 Sustainable flux based on fouling rate at step height 4 L/m^2h and step length 30 min using flux stepping technique

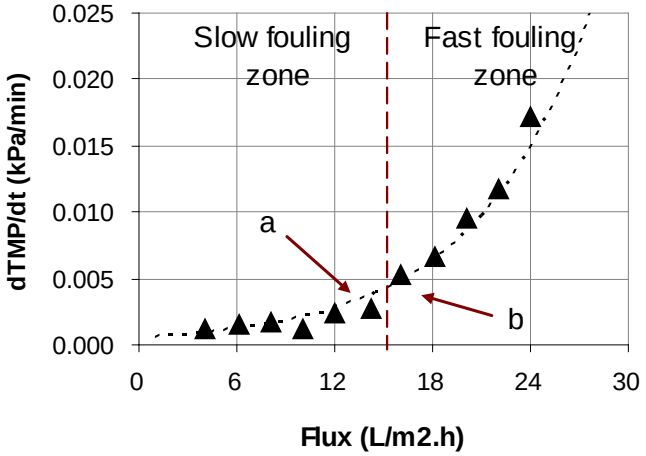

Fig. B.42 Sustainable flux based on fouling rate at step height 2 L/m^2h and step length 30 min using flux stepping technique

APPENDIX C

EXPERIMENTAL DATA FOR CHAPTER 5

C.1 CRITICAL FLUX DETERMINATION FOR CHAPTER 5

Critical flux (J_{crit}) was tested under constant permeate flux condition and it indicates the flux below which TMP rises moderately and then can stabilize, but above which rapid rise in TMP will be observed. Flux-stepping experiment with 15 min step

duration and 2 L/m^2.h flux step height was carried out to determine the critical flux. Table C.1 showed the percentage of permeability of different filtrations at MLSS 4 g/L with 90 l/min aeration and at MLSS 8 g/L with 170 l/min aeration.

Table C.1 Permeability of flux stepping filtrations at MLSS 4 g/L and 90 l/min aeration and MLSS 8 g/L and 170 L/min aeration

Flux stepping filtration at 8 g/L MLSS and 170 l/min aeration				Flux stepping filtration at 4 g/L MLSS and 90 l/min aeration			
Time (min)	TMP (kPa)	Flux (L/m^2.h)	Percentage of Permeability	Time (min)	TMP (kPa)	Flux (L/m^2.h)	Percentage of Permeability
15	0.26	6.12	100.00	15	0.24	6.16	100.00
30	0.35	8.06	99.84	30	0.33	8.16	98.76
45	0.45	9.99	95.26	45	0.40	10.01	98.19
60	0.56	12.03	92.98	60	0.50	12.05	96.13
75	0.66	14.09	91.87	75	0.59	14.08	94.77
90	0.77	16.17	90.12 ←A*	90	0.68	16.09	93.65 ←A*
105	0.92	18.19	84.56 ←B*	105	0.81	18.20	89.43 ←B*
120	1.18	20.04	73.14	120	0.95	20.06	83.99
Flux stepping filtration at 8 g/L MLSS and 170 l/min aeration				Flux stepping filtration at 4 g/L MLSS and 90 l/min aeration			
Time (min)	TMP (kPa)	Flux (L/m^2.h)	Percentage of Permeability	Time (min)	TMP (kPa)	Flux (L/m^2.h)	Percentage of Permeability
135	1.42	22.08	66.84	135	1.14	22.10	76.73
150	1.90	24.03	54.17	150	1.45	24.05	65.81

Hint: based on 90% permeability; A* = sub-critical flux and B* = supra-critical flux

From Table C.1, it can be seen that the decline in percentage of permeability of each filtration step from flux 6 L/m^{2}h up to flux 16 L/m^{2}h was small, while a decrease of permeability since flux 18 L/m^{2}h and above were clearly major. The change of percentage of permeability above 90% and lower at the 16 and 18 L/m^{2}h flux, was selected as the indicative of sub and supra critical flux border based on the 90% permeability critical flux concept. The average value (17 L/m^{2}h) between these two fluxes was then considered in this study as the critical flux value which will provide a practical criterion for comparing the effect of filtration stages on the various parameters.

C.2 CARBOHYDRATE AND PROTEIN CALIBRATION CURVES

The carbohydrate concentration was determined from a calibration curve based on glucose as a standard solution (see Fig. C.1). The protein concentration was determined from a calibration curve based on bovine serum albumin (BSA) as a standard solution (see Fig. C.2).

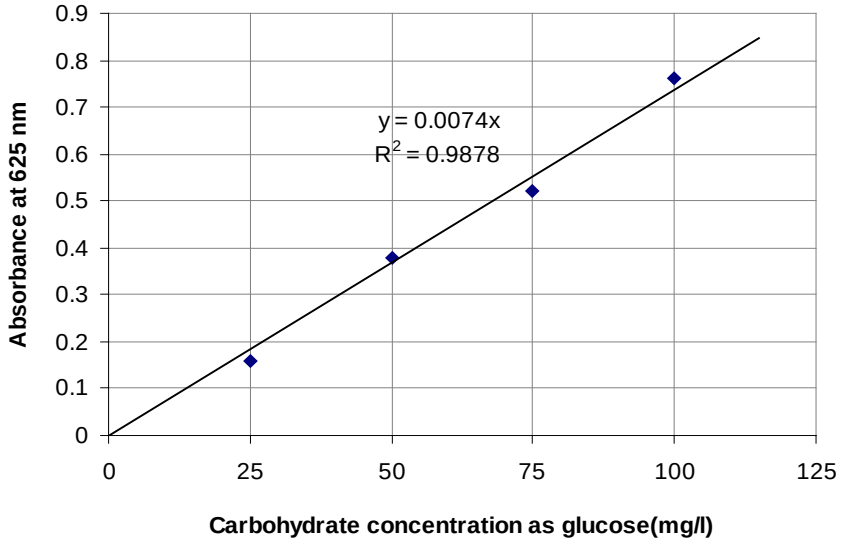

Fig. C.1 Carbohydrate calibration curve

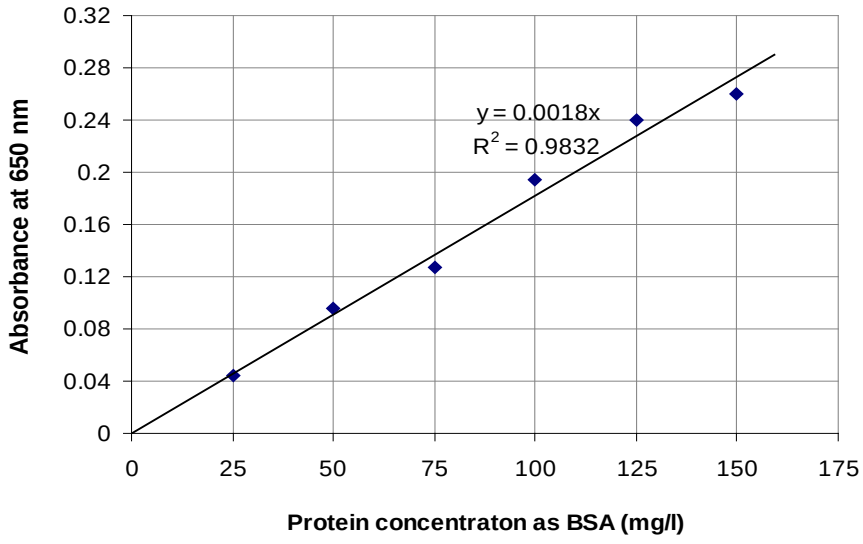

Fig. C.2 Protein calibration curve

C.3 FILTRATION PROFILES UNDER DIFFERENT FLUX STAGES AND DIFFERENT SLUGDE COMPOSITIONS

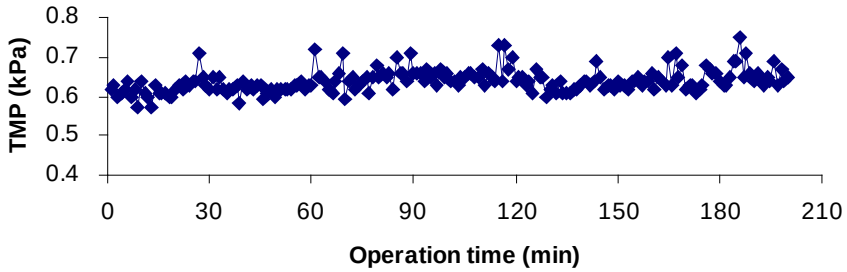

Fig. C.3 TMP under sub-critical flux operation of sludge 8 g/L and high soluble EPS

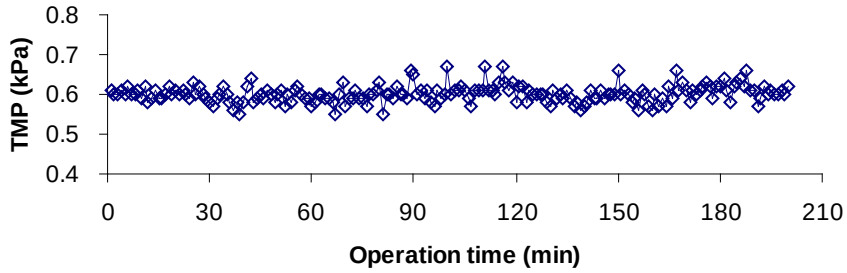

Fig. C.4 TMP under sub-critical flux operation of sludge 8 g/L and low soluble EPS

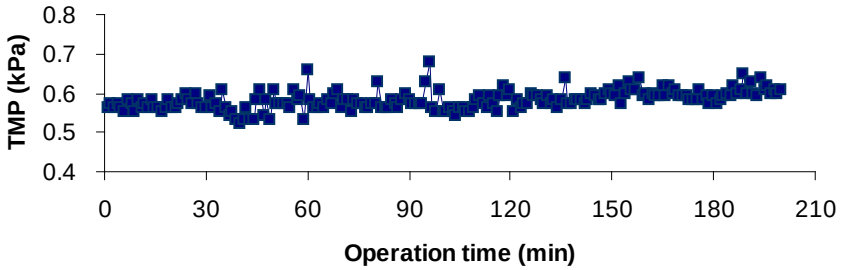

Fig. C.5 TMP under sub-critical flux operation of sludge 4 g/L and high soluble EPS

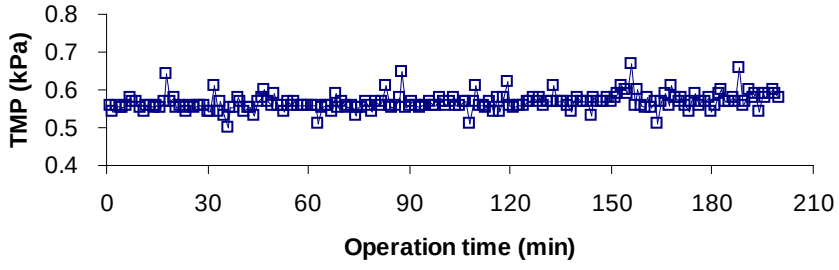

Fig. C.6 TMP under sub-critical flux operation of sludge 4 g/L and low soluble EPS

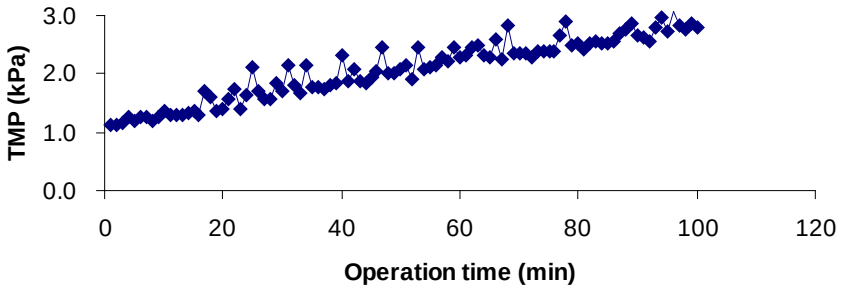

Fig. C.7 TMP under supra-critical flux operation of sludge 8 g/L and high soluble EPS

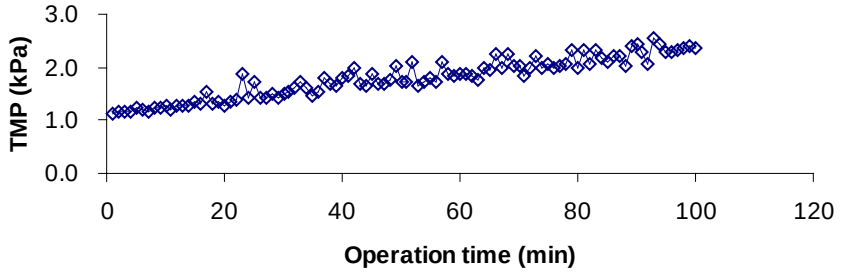

Fig. C.8 TMP under supra-critical flux operation of sludge 8 g/L and low soluble EPS

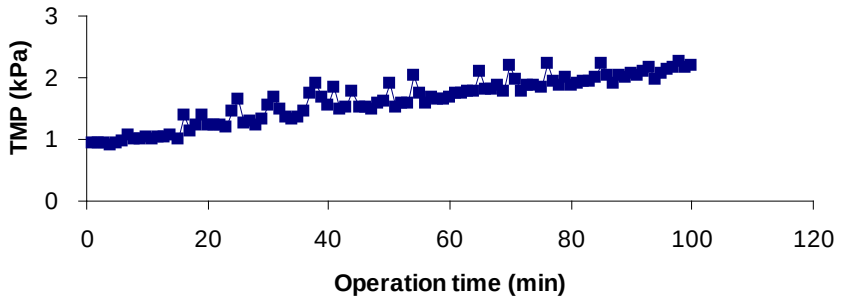

Fig. C.9 TMP under supra-critical flux operation of sludge 4 g/L and high soluble EPS

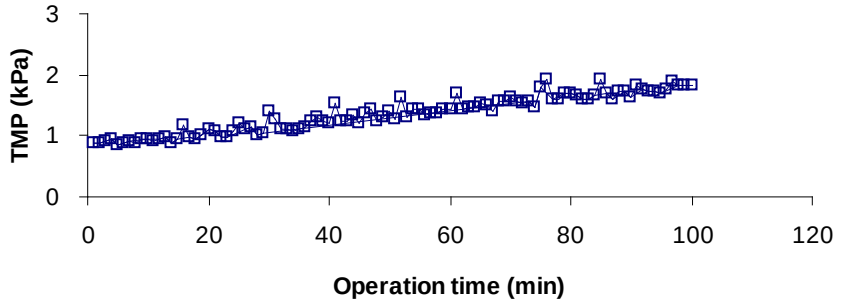

Fig. C.10 TMP under supra-critical flux operation of sludge 4 g/L and lowsoluble EPS

APPENDIX D

ANALYSIS OF VARIANCE (ANOVA) FOR CHAPTER 6

The quantitative measure of the influence of individual factors is obtained from the analysis of variance (ANOVA). An important purpose of ANOVA is for determining the relative importance of the various factors. A portion of the total variance observed in the experiment attributed to each significant factor is reflected in the percent contribution. The percent contribution is a function of the sum of squares for each significant item. The sums of squares for factor A (SS_A) is defined by

$$SS_A = (A_1 - A_m)^2 \quad \textbf{D.1}$$

The values of A_1 and A_m can be calculated using eq C.2 and C.3 below (Idris, 2002). The sums of squares for the rest of the factors are determined in a similar manner.

$$A_1 = \sum_{i=1} X_i = X_1 + X_2 + X_3 + \ldots \quad \textbf{D.2}$$

$$A_m = \frac{1}{n}\sum_{i=1}^{n} X_i = (1/n).(X_1 + X_2 + X_3 + \ldots + X_n) \quad \textbf{D.3}$$

The F-ratio also called the variance ratio is the ratio of variance due to the effect of a factor and variance due to the error term. This ratio is used to measure the significance of the factor under investigation with respect to the variance of all the factors included in the error term (Idris, 2002).

The error sum of squares: $S_e = S_T - S_m$ **D.4**

where $S_m = SS_A + SS_B + SS_C + SS_D + SS_E$ **D.5**

$$S_T = \sum_{i=1}^{9}(X_i)^2 - CF \quad \textbf{D.6}$$

$$CF = \frac{1}{9}\left(\sum_{i=1}^{9}(X_i)\right)^2 \quad \textbf{D.7}$$

The *F*-ratio for factor *A* is given by: $F\text{-ratio} = \frac{V_A}{V_e}$ **D.8**

where V_A and V_e are variance due to factor *A* and error, respectively is given by eq D.9 and C.10 as shown below.

$$V_A = \frac{SS_A}{f_A} \quad \textbf{D.9}$$

$$V_e = \frac{SS_e}{f_e} \quad \textbf{D.10}$$

where f_A and f_e are defined as the degree of freedom for factor *A* and error. Similarly, the *F*-ratios for the other factors are worked out in a similar manner.

APPENDIX E

NOMENCLATURE

A_m	=	surface area (m^2)
BOD_t	=	amount of BOD exerted up to time t (mg/L)
C	=	sludge concentration
C_b	=	the biosolids concentration (kg/m^3)
Cs	=	Saturation oxygen concentration
Cs_{20}	=	saturation O_2 concentration for clean water at 20ºC (9.08 mg/L)
EPS	=	EPS concentration (mg/L)
g	=	gravitational constant (9.81 m/s^2)
H	=	depth of membrane tank (1.75 m)
h_L	=	head loss (m)
J	=	the permeate flux ($L/m^2.hr$)
J_{sludge}	=	flux of activated sludge filtration ($L/m^2.hr$)
J_w	=	flux of initial water flux
$J_{w,\ final}$	=	flux of final water flux after removing cake layer on the membrane
k	=	first order reaction rate constant (1/d) which can be calculated
k_{20}	=	a typical k value base at 20 ^{0}C = 0.23 1/d
k_{dEPS}	=	decay rate of EPS = 0.018 (1/d)
k_{dm}	=	detachment rate of EPS off the membrane surface (1/d)
K_La	=	overall mass transfer coefficient
k_α	=	rate constant concerning the consolidation process, k_α = 0.015 (1/d)

m = EPS density on membrane surface (g/m^2)

OTR = actual oxygen transfer rate under field condition (kg O_2/h),

OUR = oxygen consumption rate

P = trans-membrane pressure (Pa)

P_x = net waste activated sludge produced each day, kg VSS/d

ΔP_{sludge} = TMP of activated sludge filtration (Pa)

ΔP_w = TMP of initial water flux,

$\Delta P_{w,\,final}$ = TMP of final water flux after removing cake layer on the membrane

$Qair$ = air flow (1.157 x 10-3 m^3/s)

Q_{in} = influent flow, l/d

r_c = change in oxygen solution concentration (mg/L .s),

R_t = total fouling resistance (1/m)

R_m = intrinsic membrane resistance (1/m)

R_f = resistance induced by membrane fouling (1/m)

R_c = cake layer resistance (1/m)

R_p = the pore fouling resistance (1/m)

S = effluent substrate concentration, mg/L

S_o = influent substrate (BOD) concentration, mg/L

$SOTE$ = standard oxygen transfer efficiency, referred to the fraction of oxygen in the input gas dissolved under the standard condition, in this case 6.9 (estimated from diffuser data for tank volume 1.9 m^3, depth 1.5 m, and aeration 1.85 ft^3/min, (GSEE-Inc 2001)

$SOTR$ = standard oxygen transfer rate at 20 ^oC and zero DO (kg O_2/h),

t = time, d

T = actual temperature, ^{0}C = 25 ^{0}C

$UBOD$ = total or ultimate carbonaceous BOD, mg/L

V = aerobic reactor volume (m3) (1.35 $m^{3)}$

V_{perm} = a permeate volume (m^3)

v = velocity (m/s)

VSS = volatile suspended solid

w = a mass of dry solids per unit area (kg/m^2).

X_t = biomass concentration (mg/L)

Y_{obs} = observed yield (gVSS/g substrate removal)

Z = elevation above datum (m)

β = ratio of produced EPS to increased MLSS = 0.012 (g EPS/g MLSS)

θ = correction factor above 20 ^{0}C = 1.056

γ_w = specific weight of water (9800 $N/m^{3)}$

μ = the viscosity (Pa.s)

μ_L = viscosity of the sludge mixture concentration:

μ_w = viscosity of water

ρ_{LS} = density of sludge mixture

α = specific resistance of EPS (m/g) and

α_∞ = ultimate value of α (m/g)

α_0 = α value at (P = 0) = $5x10^{13}$ (m/g),

α_P = a constant = 2.5 x 10^{10} (m/g.Pa)

γ = constant = 0.1 (1/Pa.d)

λ_m = static friction coefficient = 0.001

τ_m = shear stress (Pa)